RCA Engineer

19th Anniversary Issue

Vol 20 No 1
Jun Jul
1974

Nineteenth anniversary issue

With the exception of its annual anniversary issue, the *RCA Engineer* develops each issue around a central technological theme, with a number of articles coming from the RCA organizations primarily concerned with that specific technology.

Since the anniversary issue includes contributions from most divisions and on a broad range of subjects, it seems fitting that RCA Laboratories has been asked to provide its foreword. As the central research organization for the RCA Corporation, we at RCA Laboratories feel that we must cover the entire electronics spectrum, rather than being limited to a few specific themes, to accomplish our objective.

Stated simply, that objective is the development of new RCA products and services plus assisting the RCA product divisions in improving existing products and services.

Obviously, we can achieve our objective only when we have good two-way communications with the product divisions. And the *RCA Engineer* is one of the Laboratories' and the Corporation's communications tools.

As the *RCA Engineer* starts its 20th year with this issue, Bill Hadlock, the Editor, and his colleagues are to be congratulated for the fine work they have done in providing an outstanding channel for RCA's scientists and engineers to exchange ideas. Although it probably has not eliminated the process, the *Engineer* certainly has reduced the number of times RCA engineers have "re-invented the wheel"!

In recent years, we feel that two-way communications between the Laboratories and the RCA product divisions have been improved. Yet, I cannot let this opportunity pass without acknowledging that they could be better. Therefore, I'm inviting readers of the *RCA Engineer* to send me their suggestions on how the Laboratories can better serve the product divisions. Reasoned letters on this subject will be beneficial to the Laboratories, the RCA product divisions, and the Corporation.

Wm Webster

William M. Webster
Vice President
RCA Laboratories
Princeton, N.J.

Our cover

symbolizes the improved performance delivered by transistorized ignition systems developed by RCA The power transistor in the foreground is used on most 1974 Chrysler Corporation cars The engineers in the photo — Wil Bennett (right) and Gil Lang — are two members of the team that won a 1974 David Sarnoff Award for Outstanding Technical Achievement for "development of high voltage power transistors for automotive ignition and other applications "

Cover concept: Joan Dunn **Photography:** John Semonish, Electronic Components, Clark, NJ Automobile courtesy of Liccardi Motors, Inc ; Route 22. Greenbrook, NJ

Contents

Emphasis — Nineteenth anniversary

ex-RCA'ers

—an update

F. J. Strobl*

Over a year ago, we reported on "the ex-RCA'ers"—an organization of RCA retirees who gather monthly to chat and reminisce. And we noted that this Delaware Valley group is unique in that it has no official name, by-laws, charter, elected officers, dues, or formal agenda.

Today, these "non-organizational attributes" remain unchanged. But the size of the membership roster has jumped from 150 (at our last report) to more than 300 members, collectively representing past ties to almost every RCA activity. Through the various stages of their growth, the ex-RCA'ers were forced to find larger and larger facilities for their monthly meetings. A banquet room at the Mallard Inn in Mount Laurel, N.J., presently serves as their rendezvous point.

Meetings are held the second Monday of each month (except July and August). When meeting at the Mallard Inn, the group assembles at 11:30 a.m. for some preliminary socializing before lunch. Luncheons are paid for in the club's traditional way: each member pays a set amount, which covers the meal and gratuity and tax.

Occasionally, the club has a guest speaker. At one meeting, Anthony L. Conrad, RCA President and Chief Operating Officer addressed the group. Dr. George H. Brown, formerly Executive Vice President, RCA Patents and Licensing, was the speaker at another.

Far left: Ted Smith, unofficial president of the ex-RCA'ers welcomes the members to AED and expresses appreciation to his hosts at AED for the fine reception extended to the group.
Left: C. S. Constantino, Division Vice President and General Manager, of AED welcomed the ex-RCA'ers, and many former associates among them, to the Space Center and gave a slide presentation of the facility's history.
Below left: After lunch in the AED cafeteria, the ex-RCA'ers listen to a briefing of the projects and activities at the RCA Space Center.
Below: Barton Kreuzer, former Division Vice President and General Manager of the Astro-Electronics Division (1960-1967) and recently retired as Executive Vice President, is introduced as one of the new, distinguished ex-RCA'ers.

Above left: George K. Martch, Program Manager, Atmosphere Explorer, explains the design features of one of AED's spacecraft.
Above: Hank Hurlburt, Manager, Operations Engineering, Advanced Technology, explains the workings of AED's 28,000-force-pound vibration test facility to the ex-RCA'ers.

2

The ex-RCA'ers have also held meetings at RCA facilities. May is the traditional month for such visits. For example, in May 1972 and in May 1973, the group traveled to the David Sarnoff Research Center in Princeton for their meeting.

In May of this year, the club visited the Astro-Electronics Division. Three bus loads of ex-RCA'ers were joined by others arriving in autos from surrounding areas. Gathering in the AED lobby, this was the largest turnout yet in the club's three and one-half-year history — approximately 175 members. The following is a short account of their day at RCA's Space Center.

First on the agenda, after an informal welcome, was a trip to the AED cafeteria for lunch, where an official welcome was extended by C.S. (Gus) Constantino, Division Vice President and General Manager, and Warren Wagner, Manager, Industrial Relations. Mr. Constantino then provided an overview of activities at AED and touched on past, present, and future spacecraft projects at the Space Center.

Ted Smith, "unofficial president" of the club, thanked Mr. Constantino and Mr. Wagner for the reception accorded to the club by AED and thanked Wally Poch, formerly with AED, for initiating the visit to the Space Center. Ted also introduced two new, distinguished members of the ex-RCA'ers: Barton Kreuzer, who headed AED from 1960-1967, and Dr. George H. Brown. Ted also noted the presence of Otto Schairer "one of the real veterans of the company," who was the senior attendee at 94. Dr. Schairer was Vice President in charge of the RCA Patent Department in the 30's.

The retirees then toured AED's facilities. The visitors were treated to views of the ITOS integration area, Atmosphere Explorer integration area, environmental test facility, computer room, manufacturing clean room, and high-resolution lab.

After this look at the sophisticated systems in AED's bailiwick, the ex-RCA'ers reassembled in the lobby

and by 4 p.m. boarded the buses for the return trip. Afterwards, Merrill Trainer, "unofficial vice president" of the club, said he received many calls commenting on the day's program; "it was very well received, and the callers were delighted to have had the opportunity to make the tour; and they were amazed at the size of the facility."

These meetings of the ex-RCA'ers take but one day a month of their time. What happens to the other days? Well, as we found in our last report, if Satan is looking for idle hands, he won't find them among the ex-RCA'ers.

A specific example is Wally Poch, formerly at AED and Broadcast Systems. In past years, Wally had made several business trips to Russia and found he "knew enough of the language so I could do translations." Wally continued, "So I'm now doing translations of technical articles from Russian to English for an outfit headquartered in Washington. I've also done a little of it for the SMPTE. Apparently there is a need for this kind of thing, and as fast as I get these done they send me some more."

According to Wally, this type of work "doesn't pay very much, but in a way it uses all my past experience because the articles that come in cover a pretty wide spectrum. And it's another way of keeping me up to date with what's going on too. I find I learn things from the material they send me. And it's rewarding in that respect."

In discussing retirement with others, the response from Tony Maugeri, formerly with Broadcast Audio Products, Camden, N.J., was a typical one: "I've retired from RCA, but not from life. It's amazing, I'm busier now than I ever was."

And Sam Watson, formerly Manager, Corporate Standards Engineering, Cherry Hill, N.J., observed, "One thing that becomes immediately obvious, when you retire, is that there are no end of opportunities available to you on a no-fee basis."

Many of the ex-RCA'ers are in business for themselves or are planning to be in a business of some sort.

And mostly it's for fun. It's something they like to do and do it just for that reason.

It is also apparent that with all their activities, they still value their relationship with the corporation and are interested in its various business endeavors and the people behind them. Through such spontaneous and voluntary support, this non-organization demonstrates the drive and spirit that has made RCA and the electronics industry a primary force in this country's development over the past half century.

(**Ed. note:** For details on the ex-RCA'ers club, contact either **T.A. Smith,** 125 Coulter Ave., Ardmore, Pa., 19003 or **M.A. Trainer,** 112 Colonial Ridge, Moorestown, N.J. 08057.)

3

History and development of the color picture tube

E. W. Herold

This paper covers the early history of the shadow-mask color picture tube and its development up to approximately 1973. The shadow-mask tube by then was almost 25 years old and had established itself as the only successful color display for home television. Other color tube types that have been under laboratory investigation, but have not achieved commercialization, will not be described; for a more complete discussion that includes these types, the reader is referred to the Academic Press book, *Color Television Picture Tubes*, **by Morrell, Law, Ramberg, and Herold.**[1]

Fig. 1 — Picture of one of the first shadow-mask tubes.

SHADOW-MASK development started in September 1949. For anyone who was not involved, it is difficult to appreciate the inadequacy of color displays at that time. Black-and-white television was well established, with excellent pictures via the cathode-ray tube. For color, there were only three ways to display a picture. The first was the rotating color disc in front of a black-and-white picture tube. The method was severely limited in picture size and required scanning standards that were not compatible with black-and-white transmissions. A second method used three Schmidt-optics projection systems with images superimposed on the screen; this was too expensive for a consumer product. Finally, there was the most awkward of all — a combination of three orthogonal cathode-ray tubes viewed in superposition through large dichroic mirrors. This arrangement produced a direct-view picture of about 12-inch diagonal in a cabinet occupying the volume of two upright pianos!

In spite of these inadequate systems, work on color television in early 1949

went on at a feverish pace, with many predictions that some day soon a simple and low-cost color display would become available. To many experts in the electron-device field, these predictions seemed irrational, with no basis in reality. Yet, six months after starting work, some of these same skeptics (the writer included) were able to take to Washington four color receivers with a half-dozen spare tubes and put on a demonstration in which the performance achieved startled the entire industry. Color pictures were displayed on the shadow-mask color tube, using a compatible-color system essentially the same as the one now used throughout the world.

The mobilization of corporate resources

It all started at RCA Laboratories one day that September, 1949, when Dr. Elmer Engstrom, who then headed the Laboratories, asked the writer to organize and coordinate a company-wide program to develop a color tube. We were promised unlimited funds, top priority,

and freedom to use all the technical expertise that RCA had available. There was only one catch: Feasibility was to be demonstrated in three months and a final result in six months. It seemed impossible because, although we had some ideas, none were technologically practicable. But research teams were set up to explore five different approaches that have been described elsewhere.[2] One available idea had been described some years before in an invention by a German named Flechsig.[3] He proposed the shadow effect of a grill of wires, with three electron beams, one for each color. It seemed clear to many that Flechsig had never tried to make such a tube, or he would have been embarrassed to put his name on the idea. What appeared to be equally impractical

Dr. Edward W. Herold, was Director, Technology, Research and Engineering at the time of his retirement in November 1972. Dr Herold joined RCA in 1930 in Harrison, N.J., where he engaged in tube research. In 1942 he transferred to the newly established RCA Laboratories where he served as Director of the Radio Tube Laboratory and, later, the Electronics Research Laboratory. In 1957, he was placed in charge of the RCA group working on Princeton University's C Stellarator project for research on controlled thermonuclear fusion. In 1959 he was appointed Vice President, Research, for Varian Associates, returning to RCA in 1965, where he was a member of the Corporate Engineering Staff for the past seven years. Dr. Herold received the B.S. in Physics in 1930 from the University of Virginia and the M.S. in Physics in 1942, from the Polytechnic Institute of Brooklyn. That institution honored him with a Doctor of Science degree in 1961 for his "distinguished accomplishments in the fields of electron tubes and solid state devices." A Fellow and former Director of the IEEE, Dr. Herold is a member of the American Physical Society, the American Association for the Advancement of Science, the Society of Motion Picture and Television Engineers, Phi Beta Kappa and Sigma Xi.
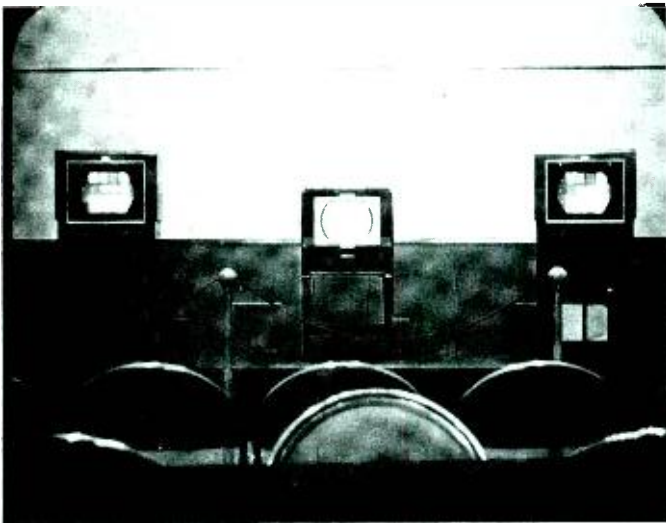
4

Fig. 2 — Picture of color receivers at the first demonstration, March 1950.

Fig. 3 — Picture taken of "ski girl" slide at time of first demonstration (original in color).

was modification suggested by Dr. A.N. Goldsmith[4]: thousands of tiny holes in a mask instead of wires, with three electron guns spaced 120° apart and separate deflection systems corrected for "keystoning". In our own laboratory, Mr. A. C. Schroeder[5] had proposed putting the three guns so close together that they would pass through the same deflection yoke. Even this seemed out of reach because no one saw how to line up several hundred-thousand tiny holes with an equal number of phosphor-dot triplets.

Nevertheless, in our crash program, Dr. Harold B. Law selected the Schroeder idea for exploitation. Law was skilled as well as tenacious, and he then made the key invention, called the "lighthouse"[6] With this device, Law used light to simulate the shadowing of electrons. The light permitted use of photographic and lithographic processes to locate the phosphor dots in the desired positions back of the mask. The lighthouse is still the basis of today's manufacture of color tubes, and it still goes by the same name. The method worked so well that, in less than the prescribed three months, Law had a few square inches of color picture that proved feasibility, and he had built a first tube with a 7-in. diagonal screen. In three more months, a few hundred other people, working seven days a week, had helped produce a dozen or so tubes with a 12-in. diagonal picture of remarkable quality[7,8,9]. A picture of one of these first tubes is shown in Fig. 1. It used a 16-in. metal bulb and had a flat color screen and shadow mask mounted inside.

A one-gun variation of the shadow-mask tube [10] was devised by Dr. Russell R. Law

(unrelated to Harold Law), who was part of the RCA group that worked so hard to make the shadow-mask tube a reality. However, the three-gun tube had so many advantages that the one-gun version is no longer of interest. In March 1950, two receivers of each type were taken to Washington to demonstrate to the F.C.C.[11]

In Fig. 2 there are three receivers: A black-and-white one in the center, the three-gun shadow mask at the right, and the one-gun shadow-mask receiver at the left. The picture was taken in March 1950 at the time of the demonstration. The picture quality of the three-gun tube is shown by Fig. 3 taken at the same time. Compared with today's tubes, the pictures were smaller, had only 7-fl highlight brightness and required an almost fully darkened room for satisfactory viewing. However, the industry reaction was overwhelming. A typical comment from the April 1, 1950 *TV Digest* is quoted as follows:

"Tri-color tube has what it takes: RCA shot the works with its tri-color tube demonstration this week, got full reaction it was looking for....not only from....FCC...and newsmen, but from some 50 patent licensees...." "So impressed was just about everybody by remarkable performance, that it looks...as if RCA deliberately restrained its pre-demonstration enthusiasm to gain full impact."

This early experience deserves attention both because it was so dramatic, and because there's a lesson for all of us. This project was an example of how an apparently unattainable result can be achieved by use of unlimited effort. In fact, of course, there's no such thing as unlimited effort; yet, when a group of

competent people are told that the sky's the limit — forget money, forget red tape, forget lines of authority — their enthusiasm has no bounds and even the unattainable becomes possible. If the shadow-mask idea had not worked out, at least two other ideas could have been brought to fruition. Unfortunately, there are far too few corporate or government executives who have the foresight and the nerve to authorize this kind of project. They usually insist on budgets, cost controls, cost/effectiveness analysis and, in the end, they may spend much more than would the "crash" program while often failing to achieve the desired result.

The 1950 tube was, of course, only a start. Most of the RCA group had what proved to be an erroneous idea. We believed there was one way only to achieve low enough cost to make the color tube practical, and that was to make every shadow mask exactly alike, and every phosphor screen identical with every other. We thought that they could then be mass-produced and any mask would work with any phosphor screen. Although the RCA group was making progress toward that goal, the accuracy required in construction of the screen and mask made this approach very difficult to carry out.

Another approach to mass production, which abandoned the interchangeability feature, was the result of the ingenuity of Mr. Norman Fyler[12], in late 1953, at CBS Hytron. Instead of the screen being placed on an internal flat glass plate as in the RCA approach, Fyler and his associates built a shadow-mask tube with a curved mask and direct photo-

5

deposition of phosphors on the curved inside face of the tube. A crucial aspect of the system was that the mask was destined for use with that screen only. Exact duplication of parts was not necessary and the picture was larger and more appealing on the face of the tube than on the internal flat-screen plate in use by the RCA group. Fyler's design is now the standard way of making color tubes. It is interesting that, although Harold Law made his first screen by a settling process, he had also invented the direct photo-deposition of phosphors[13] and mentions it in his original paper.[6]

RCA technological advances

Although not the first with the curved mask, the RCA group had its own set of successes in the early 1950-1954 period. Several of their developments must be mentioned because they have remained in use ever since; without them there is some question whether the shadow-mask principle would have reached its present predominance. The first has to do with the convergence or coincidence of the three beams. Obviously, unless the red, green, and blue pictures coincide, *i.e.*, converge over the entire screen, a poor picture would result. The solution involved pointing the three guns to the center of the screen and providing both static and dynamic adjustments, via static and alternating magnetic fields. The important invention here was the incorporation in the three electron guns of internal pole pieces that permitted each beam to be independently adjusted.[14] The earliest shadow-mask tubes were easier to converge because they used only a 45° deflection, but this made the tubes awkwardly long. By devising the internal-pole-piece gun, it became possible to go to 70° deflection and ultimately to 90° and more.

A second RCA development that remains in use to this day relates to the curved mask principle employing photographic deposition of the three color phosphors; such deposition requires three separate exposures. The shadow-mask must be mounted and removed again for each exposure, without any shift in alignment when it is remounted. This is an exacting requirement, but a solution was found by mounting tapered metal studs at the sides of the faceplate cap.[15] The studs are engaged by circumferential springs on the light-weight frame that holds the curved shadow mask.

These two important technological ad-

vances were incorporated in the first large-scale production type introduced by RCA in 1954.[14] The tube had 70° deflection, with a 21-in.-diameter round metal bulb and the phosphors were photo-deposited on the curved glass faceplate. This type was used in most of the early color sets that established the NTSC color system as a commercial success. A few years later, 1958, the metal envelope was replaced by a glass one,[16] made possible by the development of a new frit-glass seal by Corning Glass: This frit fuses at a low temperature to make the seal. Upon further heating it converts to a crystalline material which provides a ceramic-like bond that cannot again be parted. As with some of the other early developments, the frit seal remains to the present day.

Other important developments that are only touched upon here were the slurry process that mixes the phosphors with the photoresist and the correction lens that is used in the lighthouse to preserve the match of phosphor dots with electron beam landing positions, particularly under large-angle beam deflection conditions. But beyond even these items, the period of 1954 to 1968 led to almost unbelievable advances in manufacturing technology; costs were reduced, quality and performance were greatly increased, and picture size, deflection angle, and brightness became comparable to those of black-and-white tubes. There were hundreds of other detailed improvements in guns, compensation for thermal expansion of the mask, phosphor deposition and mask making. Major advances were made in color phosphors, notably by use of rare-earth elements in the red phosphor. The shape of the picture tube face was made rectangular, and the tubes became much shorter by increasing the deflection angle to 90°. From a slow start, when few programs were broadcast in color, receiver sales and color broadcasts progressively increased, and many manufacturers entered the field of color tube manufacture. By 1967, about 15-million color tubes had already been produced and the shadow-mask tube was finally established as a commercial as well as a technical success.

In the most recent period, from 1968 to 1973, design changes continued but there were four dramatic developments that deserve more detailed scrutiny. These four are the Trinitron, the black-matrix phosphor screen, 110° deflection, and the self-converging Precision In-Line system. These are taken up in turn.

The Trinitron

About 1968, as a result of work at the Sony Corporation in Japan, a different design of shadow-mask tube was introduced under the name Trinitron.[17,18] As with many other color tube developments, the Trinitron was also the result of a team effort, in this case by S. Miyaoka, A. Ohkoshi and S. Yoshida. In Fig. 4, at the left, is shown the traditional round-hole shadow-mask arrangement. It uses three essentially separate electron guns in a delta configuration pointed at the center of the screen. Shown schematically at the right in Fig. 4 is the Trinitron gun which uses a single large-diameter lens with three in-line electron beams from the one gun. The shadow mask now consists of vertical strips, and the phosphors are deposited in vertical lines.

The Trinitron has three advantages over the traditional design. The large lens diameter reduces aberrations, so that the electron spot is more easily kept small. Secondly, the vertical apertures in the mask have no horizontal cross ties or structure, so that the vertical resolution is totally unaffected. A third advantage is that convergence of three in-line beams is simpler than with the delta-gun arrangement. Convergence of in-line beams is discussed in more detail later. Pictures produced by the Trinitron are reputed to be excellent.

Along with the advantages, there are some shortcomings. Because the mask has continuous vertical apertures, it cannot be spherically curved and be self-supporting, as with the round-hole mask. Thus, it is curved cylindrically and stretched on a relatively heavy frame. Trinitron designs are often longer than traditional ones of the same screen diagonal and deflection angle. In summary, the good technical performance is accompanied by a higher cost of manufacture and a less flexible receiver configuration.

The matrix screen

It has long been recognized that the "whiteness" of phosphor materials is a disadvantage in that it diffuses back any ambient light and reduces contrast. Transparent phosphors were tried in an attempt to reduce the back-scattered light but were far too inefficient. For a long time, the only low-cost solution was the use of a light-absorbing glass faceplate —
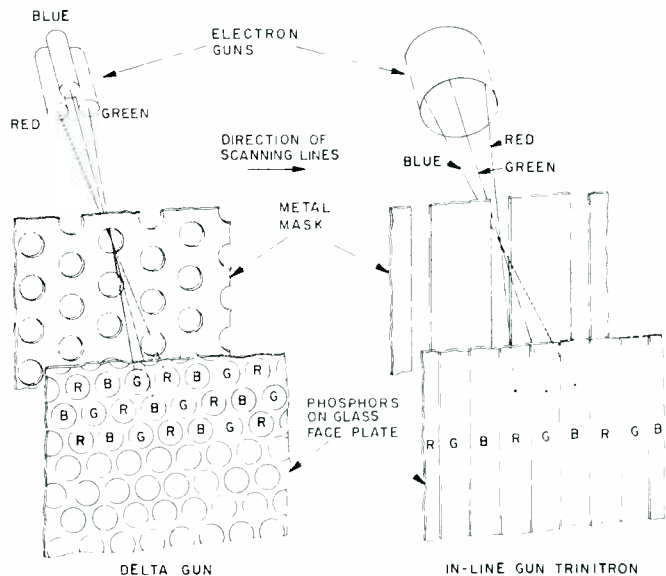
6

Fig. 4 — Trinitron system, compared with conventional delta-gun system.

Fig. 5 — Grey-glass action and comparison with matrix screen.

the so-called "grey" glass. Grey glass works because the ambient light passes through the grey glass twice, but the phosphor-emitted light goes through only once. In Fig. 5 it is shown that, if the faceplate has a transmission T of the order of 0.5, the phosphor light output is cut in half; the diffused ambient goes down to T^2, *i.e.*, to one-quarter. Thus, by losing half the brightness, the contrast is doubled. Up to 1969, this was the only method in use to enhance contrast in color tubes.

Fig. 5 also shows one of the hundreds of thousands of phosphor-element triplets as they are located on the faceplate. In practical tubes, the mask openings must be made smaller than the phosphor dots so that slight inaccuracy of position will not change the color. The tolerance required can be as much as 25% of the diameter, so that the useful part of the phosphor covers only about 50% of the screen area. Color-tube workers had long recognized that it would be desirable to use black on any portion of the screen not needed for phosphor. This was first applied on a different type of color tube, called the line-screen index tube, developed by Philco but never put into production. About 1969, both RCA and Zenith announced shadow-mask tubes that used a black matrix on the faceplate, with round openings that permitted the phosphor dots to be seen. Only the Zenith version, published in 1969 by J. P. Fiore and S. H. Kaplan[19] is described, because it gives the largest improvement and is now available from most manufacturers, including RCA.

The matrix used by Fiore and Kaplan had round openings defining only the central useful area of the phosphor dots. This means that the maximum possible area of black is provided. However, to provide tolerance for possible beam position inaccuracy, it is now necessary to make the beam areas *larger* than the matrix openings, and this is done by opening up the mask holes to be larger than the holes in the traditional non-matrix mask. In the first RCA matrix tube, the beam spots, and therefore the mask holes, are smaller than the phosphor dots as defined by the matrix; and the system is said to have "positive" tolerance. With the Fiore-Kaplan matrix, the mask holes are larger than the useful size of the phosphor dots and the system is said to have "negative" tolerance. Tubes with this system are often loosely called "negative matrix" types.

The manufacturing procedure for the negative-tolerance matrix screen is considerably more complex than for the traditional non-matrix type, or for the positive tolerance type, but the result is most gratifying. Because the screen now has about 50% of its area covered by black, the back-scattered ambient light is cut in half just as with 50% grey glass, *but there is now no reduction in brightness.* In other words, the picture is twice as bright as the grey-glass tube for the same contrast.

The numbers used are illustrative only. In practice, there are many tradeoffs between the permissible tolerances, the matrix open area, and the glass faceplate transmission, which result in tradeoffs between brightness and contrast. Usually the tube designer uses both grey glass and
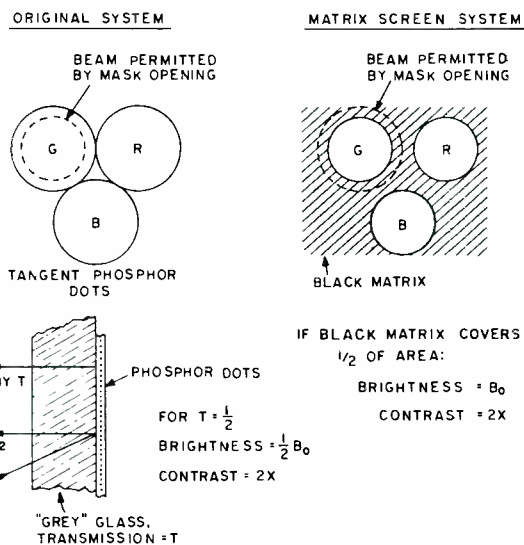
matrix methods to achieve what he believes to be a best compromise. The matrix screen made a major advance in picture-tube performance and is now in extensive use in the United States. In Europe, matrix screens have not yet taken over. One reason may be that, with their 50-Hz standards, high brightness makes flicker more noticeable.

Large-angle deflection

One of the disadvantages of the standard cathode-ray tube when designed into a display console has always been its front-to-back length. It has been desirable to increase the deflection angle as much as possible to reduce this length. However, a large angle makes convergence of the three beams more difficult and requires high deflection power unless the neck diameter is reduced in inverse proportion, which produces a new set of problems. Fortunately, there is also a performance advantage in a wider deflection angle in that the beam has a shorter throw and the spot remains small for a higher current, so that the picture can be made brighter. Conversely, the picture can be sharper for the same brightness when the deflection angle is increased. The advance from the original 45° angle tube to 70° and then to 90° has been mentioned. In no way should achievement of these angle increases be considered easy; they were all difficult. But the goal remained even higher, and it was first achieved in 1970 by an RCA tube of 18-inch diagonal and 110° deflection[20]. The same year, a 25-inch tube with 110° deflection was announced by Philips[21]

ELECTRON
GUNS

BLUE RED GREEN

DIRECTION OF
SCANNING LINES

METAL
MASK

PHOSPHORS
ON GLASS
FACE PLATE

G R B G R B G R B

GUNS AND SCREEN

Fig. 6 — Precision in-line system.

ACTION OF ASTIGMATIC TOROIDAL
DEFLECTION YOKE

GUN PLANE   DEFLECTION PLANE   SCREEN

Fig. 7 — Astigmatic yoke action.

ϵ 0.17N

LIGHT OUTPUT OF SHADOW-MASK
COLOR PICTURE TUBES

AVERAGE BRIGHTNESS, FT. LAMBERTS
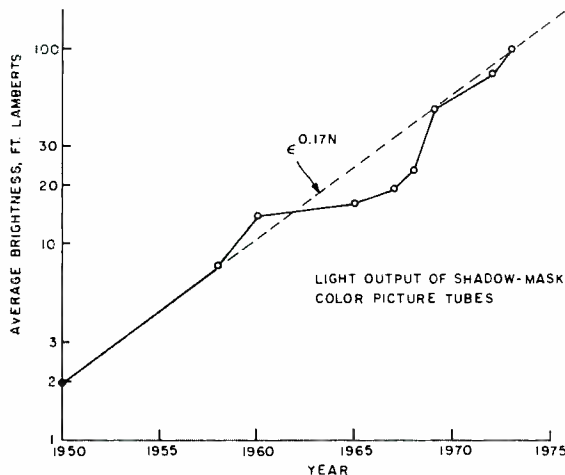
YEAR

Fig. 8 — Plot of brightness increase from 1950 to 1973.

and one year later in a different form, by RCA[22]. The Sony engineers went just a little further, to a 114° Trinitron[23]. In all these cases, the deflection problem was aided by new yoke designs and by new solid state devices for horizontal deflection. The reduced cabinet depth permitted by these large-angle systems is considered highly desirable and, fortunately, the picture is improved as well.

The Precision In-Line system

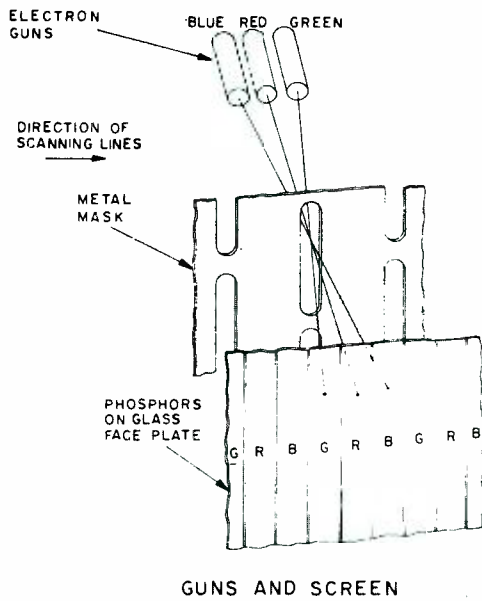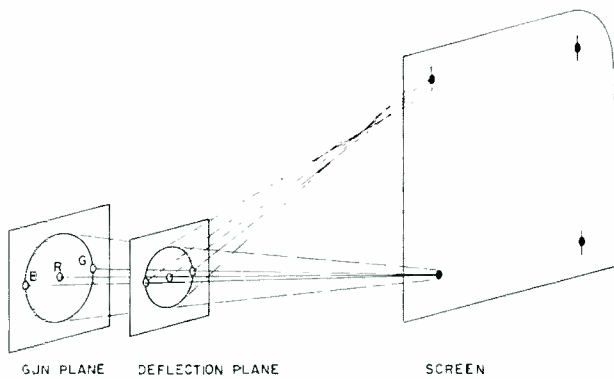The most recent advance in color tubes covered in this paper is known as the Precision In-Line system, announced in 1972 by RCA[24] This system is also a radical departure from the traditional shadow-mask design. As with the Trinitron, the beams are in a horizontal line, as shown in Fig. 6, and the phosphors are in the form of vertical stripes. The mask, however, in distinction to that of the Trinitron, uses slits with horizontal supporting ties or webs. These webs are sufficient to provide overall rigidity to the mask so that it can be self-supporting and can be curved spherically. Thus, the manufacturing technology retains the low cost of the round-hole mask. In addition, the system solved one of the major problems of shadow-mask tubes, namely the convergence of the three beams over the entire screen.

With the traditional delta gun and round-hole mask, it is necessary to add special dynamic convergence hardware and appropriate adjustable ac signals in order to converge the three beams. The adjustments are made by the receiver manufacturer for each individual tube and sometimes must be touched up in the home. Replacement of the picture tube requires complete readjustment. In the typical traditional system, there are 12 such adjustments needed to obtain red, green, and blue pictures that are properly superimposed all over the screen. It is remarkable that a skilled technician, using a video dot pattern and a cross-hatch pattern, can get good convergence in a matter of minutes. Even so, convergence has always been an annoying difference between the simple black-and-white picture tube and the three-gun shadow-mask tube.

Use of an in-line gun, as has already been mentioned, simplifies convergence somewhat, but the ultimate in simplification came about by designing a special deflection yoke to complement the in-line gun and the line-screen system. When the yoke is aligned with the gun in the

8

Precision-In-Line system, no dynamic convergence adjustment is needed and none is provided. The yoke is aligned on the tube neck and can be permanently affixed in the tube factory. The combined tube and yoke can then be plugged into a receiver with almost the same simplicity as with a black-and-white tube. The principle employed is shown in Fig. 7. The yoke is purposely made astigmatic. An astigmatic system, as we know, produces an image that is distorted from that of the object. In this instance, a circular object is distorted into a vertical line. If the three beams lie on a horizontal diameter of the object circle, they then converge to the center of the vertical line. The only trick is to assure accuracy in the yoke field pattern so that the astigmatism occurs uniformly over the entire screen. Precision yoke fields were obtained by a ferrite core with slotted end pieces and toroidal windings in which every turn is exactly positioned in its correct slot. With this construction, the yokes are all essentially identical. In the tube factory, the yoke is positioned and then permanently attached to the tube neck. Center-screen static convergence is built into the gun and is touched up with small external magnets, also in the tube factory. Thereafter, the tube is ready for shipment and has eliminated the 12 dynamic convergence adjustments required by the traditional shadow-mask tube.

The Precision In-Line system can be thought of as an example of integration, not as complex as an integrated circuit, but sharing the advantage of a factory-designed system that greatly simplifies color receiver production and maintenance. In this system, we see a portent of the future, in which color tubes are no more difficult to use and install than is the ordinary single-beam cathode-ray tube.

Conclusion

The progress that has been made in the 24 years since 1950 is remarkable. Cost and picture quality have been tremendously improved. A large range of picture sizes, from 25-in. diagonal on down, were made available, and the length of tubes has been greatly reduced. Each year, approximately 20 million tubes are being manufactured, worldwide, representing a $2-billion part of the consumer electronics industry.

Perhaps the simplest factor for showing the improvement in picture performance

is the screen brightness. In Fig. 8, the average brightness in a picture is plotted against the calendar year. The first tubes of 1950 had about 2 fl, average, and 7 fl in the highlights. By 1973, 100 fl average was obtainable, with several times as much in highlights. The dotted line on the exponential plot shows that the brightness has been increasing at a rate of 17% per year. It is small wonder that other color-tube concepts have failed to compete in the commercial market, even though they are technically feasible and much laboratory work has been done on them.

In Table I the milestones in the history of the shadow-mask tube are listed. What appeared as an impossibility in 1949 has evolved as one of the most remarkable and successful developments ever made in the history of the electron tube. It is also interesting that two of the major developments in recent years, the integrated circuit and the shadow-mask tube, have both come about through applications of photolithography. Those of us in the field of science and engineering tend to credit ourselves with the brains, the ingenuity, and the foresight to propose and carry out our new developments. In the case of the shadow-mask tube, much credit must go to the executives and financial entrepreneurs who were willing to take the risk in supporting the tremendous investment in manufacturing technology that was required. Without such an investment, color television as we know it today would not have been possible. The two men to whom the greatest credit in this respect must be given are David Sarnoff and Elmer Engstrom, the two RCA executives who steadily and consistently pushed ahead on the shadow-mask tube at a time when it looked as though it would never become profitable.

In this brief space, it is impossible to adequately acknowledge the many other

technical and management contributors to this development. As the history of the past two decades is being studied, perhaps others will record their experiences so that the whole story will become known.

References

1. Morrell, A.M.; Law, H.B.; Ramberg, E.G.; Herold, E.W., *Color Television Picture Tubes* (Academic Press; N.Y.; 1974)

2. See a series of 11 papers in *Proc. IRE*, Vol. 39 (Oct. 1951) pp. 1177-1263; also in *RCA Review*, Vol. 12 (Sept. 1951) pp. 445-644.

3. Flechsig, W.; "Cathode Ray Tube for the Production of Multicolored Pictures on a Luminescent Screen," German Patent 736,575 (filed 1938); see also the corresponding French Patent 866,065 (issued 1941).

4. Goldsmith, A. N.; U.S. Patent 2,431,115 (filed 1944, issued 1947).

5. Schroeder, A. C.; "Picture Reproducing Apparatus," U.S. Patent 2, 595, 548 (filed 1947, issued 1952).

6. Law, H.B.; "A three-gun shadow-mask color kinescope," *Proc. IRE*, Vol. 39 (Oct. 1951) pp. 1186-1194. See also Law, H.B.; "Art of Making Color Kinescopes," U.S. Patent 2, 625, 734 (filed 1950, issued 1953).

7. Freedman, N. S. and McLaughlin, K. M.; "Phosphor-Screen Application in Color Kinescopes," *Proc. IRE*, Vol. 39 (Oct. 1951) pp. 1230-1236.

8. Moody, H.C. and Van Ormer, D. D.; "Three-Beam Guns for Color Kinescopes," *Proc. IRE*, Vol. 39 (Oct. 1951) pp. 1236-1240.

9. Barnes, B. E. and Faulkner, R. D.; "Mechanical Design of Aperture-Mask Tri-Color Kinescopes," *Proc. IRE*, Vol. 39 (Oct. 1951) pp. 1241-1245.

10. Law, R. R.; "A One-Gun Shadow-Mask Color Kinescope," *Proc. IRE*, Vol. 39 (Oct. 1951) pp. 1186-1194.

11. "General Description of Receivers which Employ Direct-View Tri-Color Kinescopes," *RCA Review*, Vol. 11 (June 1950) pp. 228-232.

12. Fyler, N. F.; Rowe, W. E.; and Cain, C. W.; "The CBS Colortron," *Proc. IRE*, Vol. 42 (Jan. 1954) pp. 326-334.

13. Law, H. B.; "Photographic Methods of Making Electron-Sensitive Mosaic Screens," U.S. Patent 3, 406, 068 (filed 1951, issued 1968).

14. Seelen, H. R.; Moody, H. C.; Van Ormer, D. D.; and Morrell, A. M.; "Development of a 21-inch Metal-Envelope Color Kinescope," *RCA Review*, Vol. 16 (Mar. 1955) pp. 122-139.

15. Janes, R. B.; Headrick, L. B.; and Evans, J.; "Recent Improvements in the 21AXP22 Color Kinescope," *RCA Review*, Vol. 17 (June 1956) pp. 143-167.

16. Smith, C. P.; Morrell, A. M.; and Denny, R. C.; "Design and Development of the 21CYP22, 21-inch Glass Color Picture Tube," *RCA Review*, Vol. 19, (Sept. 1958) pp. 334-348.

17. Yoshida, S. and Ohkoshi, A.; "The Trinitron — A New Color Tube," *IEEE Trans. on Broadcast and TV Receivers*, Vol. BTR-14, No. 2 (July 1968) pp. 19-27.

18. Miyaoka, S., Ohloshi, A.; and Yoshida, S.; "The Trinitron — A New Color TV Tube," *IEEE Student Jour.*, Vol. 8 (May 1970) pp. 11-15.

19. Fiore, J. P. and Kaplan, S. H.; "The Second-Generation Color Tube Providing More Than Twice The Brightness and Improved Contrast," *IEEE Trans. on Broadcast and TV Receivers*, Vol. BTR-15, No. 3 (Oct. 1969) pp. 267-275.

20. Masterton, W. D. and Barbin, R. L.; "Development and Performance of the RCA 19V and 18V 110° Color Picture Tubes and Deflection Yoke," *Electronics*, Vol. 44, No. 9 (Apr. 26, 1971) pp. 60-64.

21. Philips Product Information. No. 13; "110° Colour Television. Picture Tube and Deflection Principle," N. V. Philips Gloeilampenfabrieken, Electronic Components and Materials Division, Eindhoven, The Netherlands.

22. Thierfelder, C. W.; "RCA Large-Screen, Narrow-Neck 110° Color Television System," *IEEE Trans. on Broadcast and TV Receivers*, Vol. BTR-17, No. 3 (Aug. 1971) pp. 141-147.

23. Yoshida, S.; Ohkoshi, A.; and Miyaoka, S.; "A Wide-Deflection Angle (114°) Trinitron Color-Picture Tube," *IEEE Trans. on Broadcast and TV Receivers*, Vol. BTR-19 (Nov. 1973) pp. 231-238.

24. Barbin, R. L. and Hughes, R. H.; "A New Color Picture Tube System for Portable TV Receivers," *IEEE Trans. on Broadcast and TV Receivers*, Vol. BTR-18, No. 3 (Aug. 1972) pp. 193-200.

Table I — List of milestones in the development of the shadow-mask tube.

Year	Milestone
1950	First tube demonstrated
1953	Curved mask with phosphor on faceplate
1954	21-inch, 70° deflection tube
1954-1963	Period of manufacturing advances
1964	90° Deflection, rectangular tube
1965	Rare-earth phosphors
1968	Trinitron (3-beam gun, striped phosphor)
1969	Black matrix
1970	110° deflection
1972	Precision in-line system

9

High-voltage silicon devices open doors to electronic ignition

M.S. Reutter|J.S. Vara

A key element in the success of the electronic ignition system has been the availability of highly reliable, low-cost, high-voltage silicon power transistors in quantities commensurate with automotive production line requirements. Automotive designers have used these devices to produce systems that perform effectively and that are more reliable than electromechanical systems with point contacts.

CREDIT for the introduction to the original-equipment market of an all-electronic ignition system must go to Chrysler. The success of their optional all-silicon transistor system introduced in 1972 led to the use of a similar system as standard equipment on all of their model 1973 cars. This bold step by Chrysler has led to the "all-out"effort by all other auto makers to incorporate the electronic ignition on a "no-delay" basis on their models as well.

The beneficial effects of long-term timing accuracy coupled with the aid to emission control provided by higher firing voltages are the prime technical incentives behind adoption of the electronic ignition. By model-year 1975, what began as one car maker's revolution will have evolved into a standard feature offered by all four domestic car makers. When trucks are included, approximately 10 million original equipment ignition systems will have become solid state, for an 85% penetration by solid-state devices into the market in only a little over three years. This is a truly remarkable response, and a validation of the success and benefits of the electronic ignition system.

Evolution of ignition systems

The ignition system of an internal combustion engine must fulfill two basic functions: 1) Release energy in the form of a spark and 2) Determine when that spark is to occur. In conventional breaker-point ignition, Fig. 1, the points perform the switching function of in-

Fig. 1 — Conventional cam-point ingition system.

Fig. 2 — Block diagram of electronic ignition system.
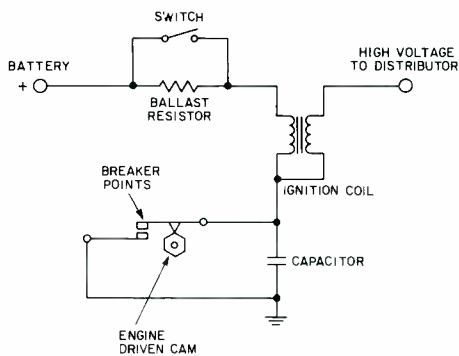
terrupting the coil current, thereby producing the high-voltage spark. The cam on the distributor shaft provides the timing function. This is the lowest cost system, but it has several major disadvantages. Inherent in all contact-triggered ignitions is timing error resulting from contact erosion and rubbing-block and distributor-shaft wear. Frequent, costly tune-ups are needed to maintain engine performance and compliance with present-day emission standards.

To overcome the disadvantages of the conventional cam-point system, several contactless systems have been developed. The pick-up elements of such systems are required to generate a signal that varies in step with the mechanical rotation of the distributor drive shaft. Contactless systems require additional electronics between the pick-up elements and the power-transistor switch to define a precise trigger point and to amplify the small signals picked up—hence, electronic ignition. Fig. 2 shows a simplified block diagram of an electronic ignition system.
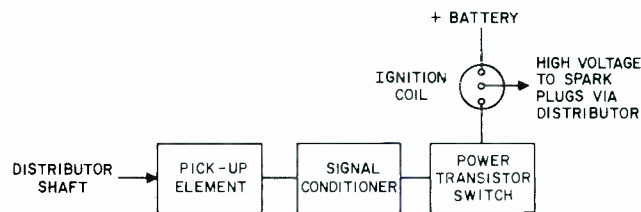
Contactless systems

Magnetic pick-up

The most common form of contactless ignition system employs a variable reluctance transducer, Fig. 3. The pickup unit

Fig. 3 — Magnetic pick-up.

magnet forms a closed magnetic path through the coil pole piece and reluctor wheel. As the distributor rotates, magnetic coupling varies, and a signal is generated in step with engine rotation. A problem encountered with this type of pick-up results from sensitivity of the output signal to speed. The transducer must produce a usable output signal at distributor speeds as low as the 15 r/min encountered during cranking. To achieve the required performance economically, the air gap between rotor and stator must be very small. Thus, the tolerances to which the distributor assembly must be built and maintained throughout service

John S. Vara, Power Transistor Applications Engineering, Solid State Division, Somerville, NJ, received the BSEE in 1965 from Fairleigh Dickinson University. He worked for Tung-Sol Electric in Rectifier and Transistor Applications prior to joining RCA in 1966 as an Applications Engineer for Power Transistors. He is currently Project Leader in the Power Transistor Applications Automotive Group. Mr. Vara received the RCA Electronic Components and Devices 1968 Engineering Team Achievement Award for Power Transistor Engineering.

Authors Vara (left) and Reutter.

life are very close. To overcome this disadvantage a trigger circuit is required that is capable of accurate triggering over a wide range of signal levels and that has a high degree of noise immunity to prevent triggering at low noise levels.

Photoelectric pick-up

Another form of triggering used to a lesser extent in the after-market employs a light-emitting diode as shown in Fig. 4. A parallel beam of radiation passes between detector and source; triggering is accomplished by means of a rotor which interrupts the beam. By arranging the

Maurice S. Reutter, Power Transistors, Vehicular Market Planning, Solid State Division, Somerville, NJ, attended Iowa State College, Ames, Iowa. He joined the RCA Service Company as a Radar Engineer in 1942. His background in commercial communications with RCA covers transmitter design, field sales and product planning for the RCA line of mobile communications equipment. This includes promotion and marketing of RCA's first transistorized portable receiver "The Personalfone". In 1959 he joined the Solid State Division in a field sales capacity in Detroit, Michigan. Since that time Mr. Reutter has witnessed and participated in the revolution that brought about the diversity of electronic applications of solid-state devices to the automobile
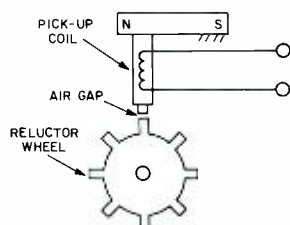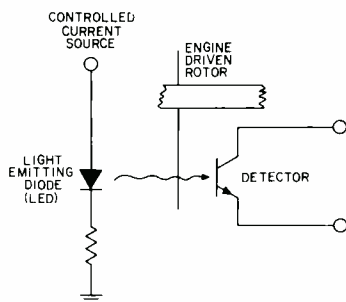
Fig. 4 — Photoelectric pick-up.

beam parallel to the distributor shaft, the effects of axial rotor movement on timing accuracy can be eliminated. Also, radial movement of the rotor will have no affect provided the rotor disc continues to cut the beam completely. With present radiation sources, the beam width may be several millimeters; this dimension represents a substantial shaft angle. Special circuit techniques are required to select a fixed trigger point within the beam.

Conductance detector

A third contactless system, shown in Fig. 5, is the conductance detector. This system works on the principle of loading the Q of a tank circuit of a tuned oscillator. The system advantages are excellent noise immunity and a signal whose amplitude is independent of speed.

Dwell

Dwell is the period of time during which battery current flows in the ignition coil before each spark, thereby providing a reference for the measurement of stored energy available for spark voltage. A system with cam and breaker points generates a fixed percent dwell independent of r/min. The dwell is a compromise between excessive current at idle and too little current at high r/min. Most of the pick-ups which replace the ignition points do not provide appropriate dwell signals; the dwell must be generated electrically. One approach is to make the electronics duplicate what the points did; another more simplified approach is to produce a constant off time.

Circuit selection — capacitive vs inductive

In selecting an ignition circuit, the

automotive manufacturer had to consider performance in terms of lower exhaust emissions, better cold weather starts, and lower maintenance. While capacitive-discharge systems were, perhaps, more desirable from a semiconductor viewpoint (lower stress levels), ignition performance was unacceptable because of the typically short spark duration inherent in these systems. Short spark durations can cause engine misfire with present-day air-fuel mixtures. (With the move toward leaner ratios, the capacitive-discharge system was just not acceptable; therefore, the remainder of this article will consider only inductive ignition systems.)

Two types of inductive ignition circuits are shown in Figs. 6 and 7. Both designs use a zener clamp from the collector-to-base to protect the output transistor from excessive voltage, and both are now in use by car manufacturers. Current in the regulated type, Fig. 7, is limited to approximately 5 amperes. The power transistor in this circuit is required to handle considerably less energy under worst-case conditions than its counterpart in the saturated switch circuit. The trade-off is cold-weather starting performance and higher dissipation in the transistor.

The hostile environment

The ambient temperature under the hood of an automobile varies widely. A low temperature of $-30°C$ ($-22°F$) can be expected in a parked vehicle. The ambient temperature rise after start-up will be slow at this temperature extreme; therefore, the low-temperature design goal which has been adopted is $-30°C$. High-temperature extremes depend on several factors, including ambient conditions and cooling-system performance. Components reasonably isolated from the exhaust manifold can be expected to reach $125°C$ ($257°F$). Mechanical shock, vibration, and exposure to chemicals are other considerations; however, a category deserving special attention is the electrical environment. From an electronic-system viewpoint, the automotive electrical environment must be rated as severe; Table 1 summarizes some of the reasons.
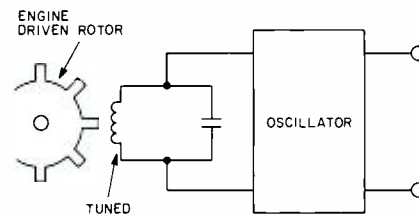
Output-transistor requirements

Operating voltages in the automobile can

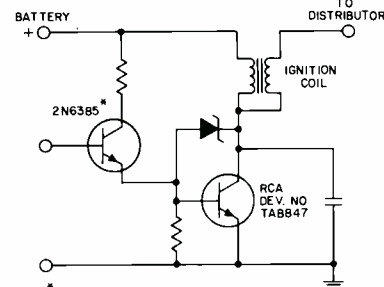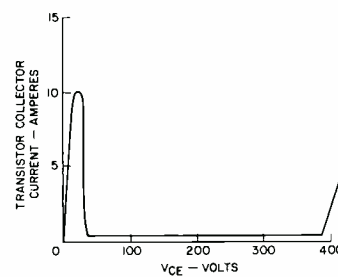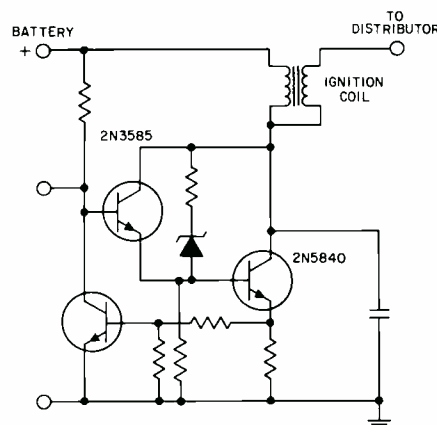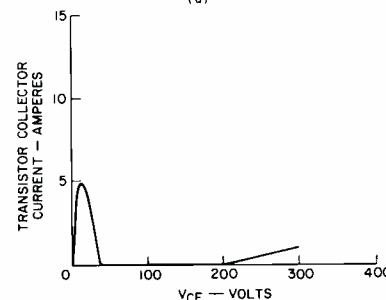**Fig. 5 — Conductance detector.**

Fig. 6 — (a) Saturated-switch inductive-ignition circuit (b) worst-case load line (open secondary, ballast resistor shorted).

Fig. 7 — (a) Current-regulated-switch inductive-ignition system; (b) worst-case load line (open secondary, ballast resistor shorted).

12

vary from 6 V during cold-weather starting to 16 V during normal running. The worst-case high-line voltage can climb to 24 V for short periods when two batteries in series are used for booster starts. The effects of this wide range of battery voltage is seen in both ignition performance and power-transistor specifications. During cold-weather starts, when high energy is needed, the battery voltage is low; thus, a low voltage drop is needed at the power stage in series with the ignition coil to get the required coil current. At the same time, base drive to the transistor is down and, to compound the problem, the forward base-emitter voltage drop is high. Good cold-weather starts require high transistor current at low battery voltage. When a 24-V boost is applied, the transistor current will rise proportionately. In a saturated-switch ignition, for example, a 5-A start requirement can result in 15-A peak currents.

The output transistor must be capable of handling high voltage and high current, simultaneously, during worst-case load condition (open spark plug). Typical requirements for the output stage of a saturated-switch ignition are shown in Table II.

Performance and reliability objectives

Based on cost alone, a change from the conventional cam-point ignition to electronic ignition is not justified. However, emission standards and service restrictions imposed on the automotive industry have made electronics more attractive. Thus, in developing an electronic ignition system, the stated goals of the automotive manufacturer are performance and reliability. For the consumer, the added cost of the solid-state ignition buys lower maintenance costs and better engine performance. Claims of up to 35% more cranking voltage for cold-weather starting are common. (In cold weather, when cranking speed is low, points in the conventional system open slowly and significantly degrade the output voltage of the ignition-coil secondary.)

The automotive manufacturer is concerned about reliability for three reasons: warranty costs, safety, and image; all specifications and validation testing focus on these important areas. To meet the reliability requirement, the car

manufacturer has developed elaborate qualification and production-validation procedures to achieve reliability goals of 0.15% replacement in warranty. Obviously, design goals must be better than this.

The components in the automobile's ignition system that are subjected to the highest stress levels are the power transistors. Thus, power transistors for automotive use must undergo a reliability test program that reflects the realistic demands of the environment in which the device is to be used. Table III outlines the type of test program designed by Solid State Division's Reliability Engineers and used to evaluate power transistors used in ignition systems. The intent of the reliability evaluation outlined is to test device design at maximum levels.

Stress, combined-environment, and reliability-sequence tests are applied to produce failures so that design margins can be determined. Once design goals have been achieved, real-time indicators are established in production to monitor capability on a lot-by-lot basis. The type of indicator used to monitor all ignition power transistors is thermal-cycling, an accelerated intermittent life test designed to produce information in three days for use in process control.

High-voltage ignition switch

The device developed by RCA for ignition-coil current switching is a multiple-epitaxial pi-nu (π-ν) power transistor. The transistor differs from

Table I — Characteristics of an automotive electrical environment.

Automotive line-voltage characteristics

Condition	Voltage
Normal running	16V max 14.4V nomial 10V min
Cold cranking −20°F (−29°C)	6V
Booster starts	24V, 3 min. or Reverse polarity

Automotive voltage transients

Condition	Max amplitude	Time constant
Load dump	125V	45 ms
Alternator field decay	−75V	30 ms

Table II — Typical specifications for a saturated-switch-ignition output transistor.

Peak collector current	15A
Peak base current	5A
V_{CER}	400V
V_{EBO}	5V
$V_{CE(sat)}$ @ I_C=5A, I_B=850mA @ T_4 = −30°C, +25°C	1.3V max
V_{BE} @ I_C = 5A, V_{CE} = 1.3V	1.5V max
I_{CER} @ V_{CE} = 390V, R=30Ω	1mA
Functional test	*

*100% functional test for 1 second in a simulated worst-case ignition circuit: i.e. 18- to 22-V battery with coil secondary open and ballast resistor shorted.

Table III — Outline of reliability evaluations performed on ignition power transistors.
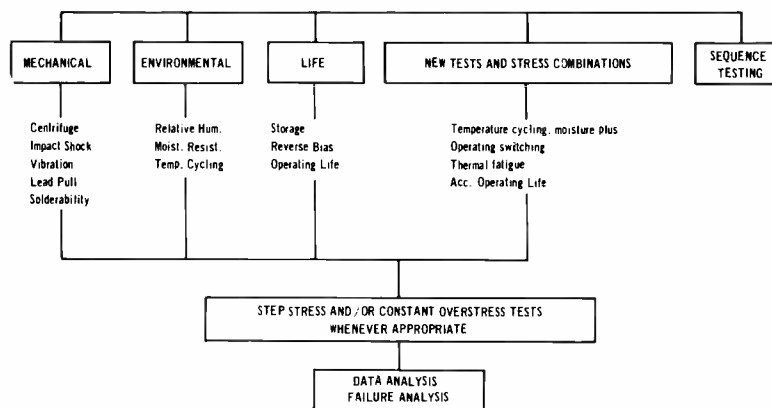
other designs in that the depletion region, which supports the electric field extends into both the n-type ν-collector region and p-type π-base region, thereby providing increased volt-ampere capability at a given current rating. Higher voltage ratings are possible because both the base and collector regions are used (instead of collector only) to support the applied voltage. Good current handling results from the lower collector resistivity needed for equivalent voltage ratings. Figs. 8 and 9 show device construction and compare electric-field distribution in conventional and π-ν epitaxial structures.

For maximum power handling capability and long life, the device pellet is mounted on a copper heat spreader in a steel TO-3 hermetic package by means of a nickel-lead metallurgical system. The clips used for the emitter-base contacts are joined to the contact areas with a high lead-content solder system. The pellet area is coated with a protective, high-purity silicon resin before the unit is sealed. An internal view of the system is shown in Fig. 10.

Future

The saturation of the ignition market by solid-state systems is a foregone conclu-

sion. Some of the new efforts in design, such as integral mounting of the electronics in the distribution housing, are leading to reduced system costs; other efforts, such as reducing component count, will lead to both cost *and* reliability advantages.

The use of a high-voltage monolithic Darlington as the output switch is both logical and cost effective. It means the use of one integrated device instead of two or three separate components, thus saving in space and mounting costs while enhancing reliability. The consolidation of all of the signal-processing portions of the system into one integrated-circuit package will yield similar advantages.

The integration of the entire system into the distributor housing, one of the greatest challenges of the future, while it provides many logistic and cost advantages, must be approached with considerable care. Overall system reliability could deteriorate as a result of exposure of the components to excessively high temperatures and the forced miniaturization of assembly methods.

Future systems certainly will have more "front end" control features to provide

for variability of timing by electronic means. These controls will be an integral part of overall engine controls for emission and fuel-management systems. The continued demand for improved reliability will remain the paramount goal in all future developments.

References

1. Gallace, L.J. and Vara, J.L; "Evaluating Reliability of Plastic - Packaged Power Transistors in Consumer Applications", *RCA Technical Publication* ST-6184 (June, 1973).
2. Denning, R. and Moe, D.A.; "Epitaxial (π-ν) NPN High-Voltage Power Transistors". *RCA Technical Publication ST-4287.*
3. Carlson, D.W. and Doelp, Jr., W.L.; "A Successful Electronic Ignition System Thru Fundamental Problem Analysis". Society of Automotive Engineers, Paper No. 140154 (February-March, 1974).
4. Moore, J.H. and Longstaff-Tyrell, J.; "Engine Position Tranducers for Electronic Ignition." Society of Automotive Engineers, Paper No. 740153 (February - March 1974).
5. Myers, R.S.; Electronic Ignition Comes of Age", RCA Reprint RE-18-6-31 (April-May 1973).
6. Baugher, D.M. and Gallace, L.J.; "Methods and Test Procedures for Achieving Various Levels of Power Transistor Reliability", *RCA Technical Publication* ST-6209 (Sept. 1973).
7. Balan, I.; VanHalteren, C.J.; and Weier, R.M.; "Performance of Electronics in the Automobile to Date at Chrysler"; Society of Automotive Engineers. Paper No. 730131 (January, 1973).
8. Bennett, W.P. and Vara, J.S.; "Power Transistors in Automotive Applications"; RCA Reprint RE-18-6-12 (April-May 1973).
9. Gallace, L.; "Quantitative Measurement of Thermal Cycling Capability of Silicon Power Transistors". *RCA Application Note AN-6163.*
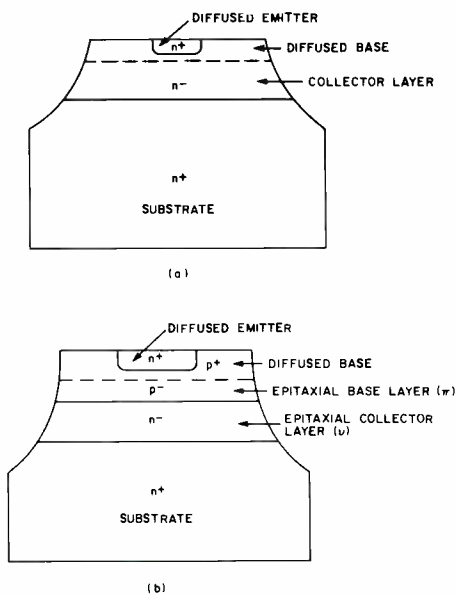
Fig. 8 (above) — Structure os a conventional n-p-n transistor. (b) the pi-nu multiple epitaxial construction.

Fig. 9 (right) — Electric field distribution in (a) an n+ pn-n+ structure, and (b) an n+ p- n- n+ structure.
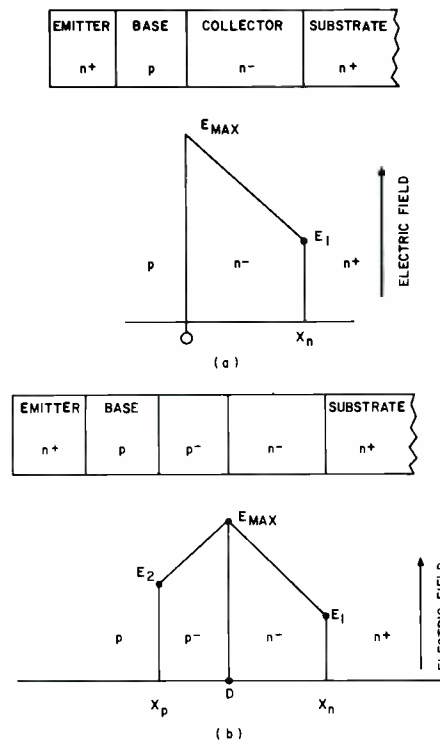

Fig. 10 — Internal view of the high-voltage ignition switch.

Surface acoustic-wave filter for television intermediate frequencies

Dr. J. A. van Raalte

In recent years, a surface acoustic-wave (SAW) i.f. filter for use in modern television receivers has been developed at RCA Laboratories; in addition to being small than the present i.f. filters, such a filter has more stable and reproducible characteristics since it requires no alignment. This paper reviews the main features of SAW tv-i.f. filters.

SHARP selective tuning in television receivers is a prerequisite for good reception; this is particularly true for cable systems which provide a multitude of available channels.

Television channel allocations determined by the FCC provide for 6-MHz bandwidth at specified frequencies, which in most instances are only 6 MHz apart — i.e., channels 2 through 4, channels 5 and 6, channels 7 through 13, and uhf channels 14 through 83. By broadcasting a vestigial-sideband signal extending from −1.5 MHz to +4.5 MHz around the picture carrier frequency, a signal bandwidth (including sound and chroma information) of approximately 4.5 MHz is achieved. This type of frequency allocation, which is conservative of total bandwidth, poses more stringent requirements on the front end of a television receiver if it is to avoid adjacent-channel interference and various types of cross modulation.

The ability of a television receiver to ignore all channels but the desired one is determined primarily by its i.f. filter response. Most of the desired selectivity is provided by the input filter, whose characteristics are shown in Fig. 1:

- The picture carrier at 45.75 MHz should be down 3 dB for proper transient response in a vestigial-sideband system.

- The color carrier at 42.17 MHz is normally 3 dB down to minimize intermodulation effects between chrominance and luminance signals.

- A deep trap (66 dB) is required where the adjacent-channel sound carrier (47.25 MHz) is located; another trap is also desirable where the adjacent-picture carrier (39.75 MHz) is located.

- The stop-band response should be as low as possible to remove adjacent-channel interference; this is especially critical in a CTV environment ($\lesssim$ − 40 dB).

- The in-channel sound located at 41.25 MHz should be ~20 dB down to minimize beats between chroma and sound.

- In addition, the filter should produce a minimum of attenuation ($\lesssim$ 10 dB) in order to achieve good signal-to-noise performance in the receiver.

The selectivity requirements shown in Fig. 1 are not easily achieved on the production line nor maintained in the presence of drift or aging. In the past, because of the FCC policy to avoid allocations of adjacent tv channels in the same metropolitan area, problems resulting from adjacent-channel interference were minimized. Even where adjacent channels could be received from different cities, the directionality of a good antenna could be used to enhance the desired signal considerably, relative to the unwanted one. However, due to rapid growth of cable television (CTV) systems with simultaneous transmission on all channels, receiver deficiencies, heretofore ignorable, have suddenly become important as studies undertaken by the National Cable Television Association are making increasingly clear.

Acoustic-wave devices

Surface acoustic waves in isotropic media were first discussed by Lord Rayleigh in 1885, but their main interest remained in the field of seismology until quite recently. In 1960 Boemmel and Dransfeld[1] demonstrated the use of coherent acoustic waves in quartz thereby stimulating the more recent interest in acoustic-wave devices for communication and signal processing applications. The slow propagation velocity of acoustic waves (typically 1.5 to 12×10^5 cm/s — about 10^5 slower than electromagnetic waves) makes them ideally suited for delay lines at vhf or uhf frequencies; thus, microsecond delays are readily obtained in small devices (~1 cm).

Dr. John A. van Raalte, Head. Displays and Device Concepts Research. RCA Laboratories. Princeton, NJ. received the BS and MS from the Massachusetts Institute of Technology in 1960. Subsequently he carried out his doctoral research under Professor A. R. von Hippel. Director of the Laboratory for Insulation Research at M.I.T. He was awarded the Engineer's Degree in 1962 and received the PhD in 1964; his doctoral thesis entitled *Conduction Phenomena in Rutile Single Crystals*. Dr. van Raalte joined the David Sarnoff Research Center of RCA, Princeton, New Jersey, in July 1964, as a Member of the Technical Staff. He has conducted research in the areas of electro-optical materials, lasers, holography, liquid crystals and their applications to display and recording functions. He was awarded a 1969 RCA Laboratories Achievement Award for the development of a novel television projection system. He assumed his present position in 1970 and is currently directing research in new displays, television rf and i.f. circuitry, acoustic surface-wave devices and tv camera tubes. He is a member of Tau Beta Pi, Eta Kappa Nu, Sigma Xi, the American Physical Society. the AAAS, and a Senior Member of the IEEE.
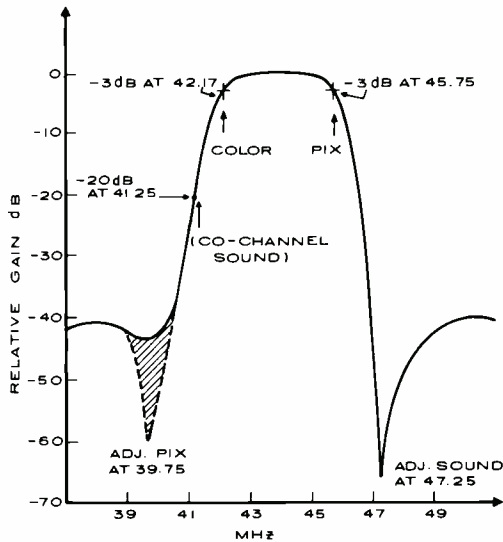
Fig. 1 — Desired response of i.f. input filters.
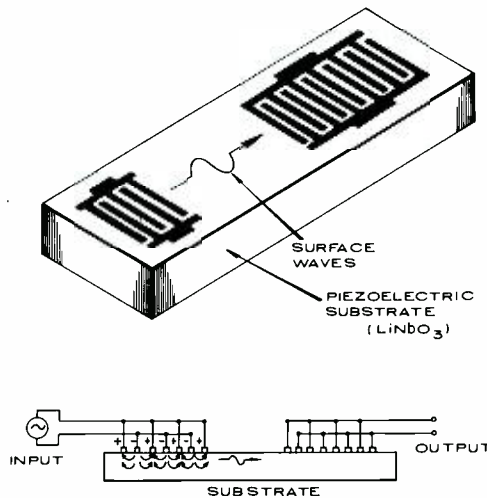
Fig. 2 — SAW filter with interdigital transducers.
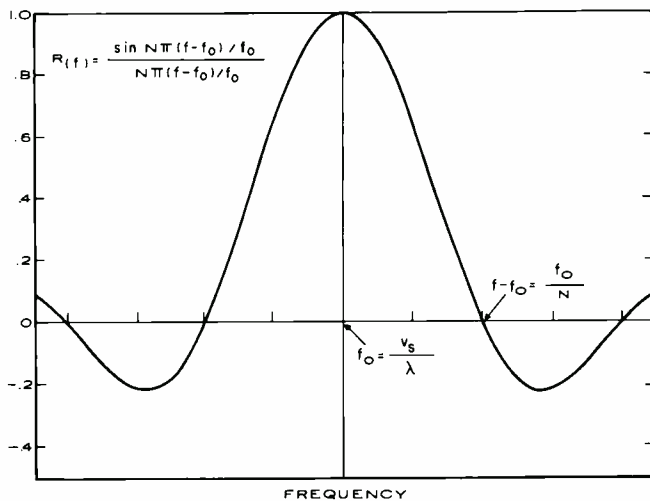
Fig. 3 — Frequency response for uniform IDT.

The interdigital transducer, an efficient means for generating and sensing surface waves in piezoelectric media,[2,3] shifted the emphasis from bulk acoustic-wave devices to surface acoustic-wave (SAW) devices. Surface waves, having lower velocities than bulk waves, do not couple to bulk waves; consequently the surface-wave energy remains confined to a thin surface layer in the substrate.

Surface waves have several advantages over bulk waves in many applications: The transducers can be fabricated by well-established planar technologies and require no bonding of the transducer to the propagating medium; the waves are continuously accessible at the surface and can be sensed at different locations — this is useful in tapped delay lines or transversal filters. Depending on the choice of substrate, the propagation losses can be negligible. An excellent review of surface waves and their potential applications was published by R. M. White.[4]

SAW filters

A typical SAW transducer is shown in Fig. 2a. This interdigital transducer (IDT) consists of a set of conducting electrode fingers alternately connected to either terminal. When a voltage signal is applied to the transducer terminals, an electric field of spatially alternating polarity appears across the surface of the substrate (Fig. 2b).

If the IDT is fabricated on a piezoelectric substrate (as the name implies, a piezoelectric material converts an electric signal into a mechanical stress, and vice versa), then an electric-field-induced stress is generated by the electrode fingers. This stress will propagate, much like ripples in a lake, along the surface of the substrate with a velocity that is characteristic of the material and its crystallographic orientation. Since stress is proportional to the electric field, the contribution from each finger pair is proportional to the applied voltage signal and inversely proportional to the finger spacing.

A SAW filter normally consists of two IDT's (Fig. 2a); the *sender* IDT converts the electrical input signal into a surface wave which is subsequently detected by the *receiver* IDT and converted again into an electrical output signal. The operation is as follows: An alternating signal of frequency ω applied to the sender produces at each electrode finger a cor-

Fig. 4 — Experimental SAW i.f. filter.

responding mechanical stress that propagates orthogonally to the finger lengths in both directions. All these stress waves are added together with a phase shift depending on the location of the originating fingers. Thus if we look at the response of the IDT, say, at some point betw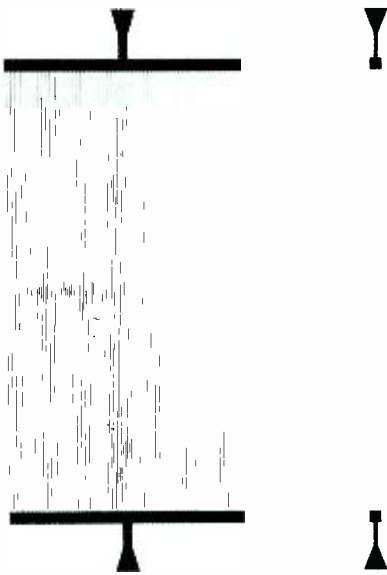een sender and receiver, we find a stress that is the sum of contributions from individual fingers with appropriate phase factors:

$$R(\omega) = \sum_{n=1}^{N} a_n \cos \phi_n \qquad (1)$$

Here the coefficients a_n are related to the magnitude of the stress produced by the nth finger, and the phase ϕ_n is determined by the distance between the nth finger and the sampling point.

In the simple case, where the IDT consists of N fingers of equal lengths, spaced equally ($\lambda/2$ center-to-center) and of equal width ($\lambda/4$), the frequency response (Eq. 1) reduces to the well-known function

$$R(\omega) = \frac{\sin \chi}{\chi} \qquad (2)$$

$$\chi = \frac{N\pi(f - f_o)}{f_o} = \frac{N\pi(\omega - \omega_o)}{\omega_o} \qquad (3)$$

The resonant frequency f_o is determined by the finger spacing:

$$f_o = \omega_o / 2\pi = V_s / \lambda \qquad (4)$$

and the bandwidth is inversely proportional to the number of fingers N (Fig. 3). This response is simply the Fourier transform of the coefficients a_n at phase ϕ_n. The coefficients a_n depend on the applied voltage and piezoelectric constants of the substrate (which do not vary from finger-to-finger and therefore do not influence the shape of the frequency response) and the finger spacings and finger lengths which can be varied depending on IDT design.

Quite generally, in fact, the frequency response of an IDT and its finger-overlap pattern are related by Fourier transformation. This is readily made plausible from a consideration of the nature of a transducer. Each pair of fingers launches an acoustic wave with amplitude proportional to the amount of overlap between the two fingers and with phase given by the location of the finger pair along the transducer. These waves are then summed in the receiver transducer. Such a sum of amplitudes and phases can be recognized as a Fourier transform.

Filter design

The previous section gives a key to the design procedure for SAW filters. Given the desired frequency response, the pattern of finger overlaps (weighting) is derived by taking the inverse Fourier transform. This is done efficiently on the computer by using the mathematical techniques of Fast Fourier Transformation.

Since both sender and receiver IDTs each have their own frequency response, their joint response must be determined. Unlike cascaded electrical filters, the response of two weighted IDTs is, in general, not equal to the product of their individual responses. This is so because the response of an IDT represents the line integral of the stress wave orthogonal to its direction of propagation. When two weighted IDTs are cascaded, the energy emitted by the sender is not uniformly received by each finger electrode of the receiver since they have different lengths. Thus, the response of two weighted transducers can only be represented as the double sum of contributions from each finger in the sender to each finger in the receiver. In practical cases where the sender and receiver may each have 50 to 100 fingers, this double summation becomes a tedious computation, especially if second-order effects such as reflections due to fingers, energy extraction from the wave as it travels under the transducer, and diffraction effects (especially severe for short fingers) have to be taken into account.

Thus, in practice, it is more convenient to combine a weighted and a uniform IDT; in this case, their joint response is indeed the product of their individual responses. The uniform transducer with a $(\sin \chi)/\chi$ response can be made broadband (few fingers) so as to have little effect on the overall filter response, and its response can be included in the computation to determine the desired response of the weighted transducer.

The desired pass band for the television i.f. is relatively rectangular, which would imply a finger overlap pattern of the form $(\sin \chi)/\chi$. However, truncation of the $(\sin \chi)/\chi$ pattern to any finite number of fingers causes ripple in the pass band and stop band (Gibb's phenomenon) with the result that overall selectivity is limited to ~21 dB. To improve the selectivity, a further weighting function is applied to the $(\sin \chi)/\chi$ pattern as shown for a typical i.f. filter design (Fig. 4) By the use of computer optimization and Fast Fourier Transform techniques, designed selectivities of 60 dB, or even greater, are possible.

Insertion loss

An important requirement for the i.f. filter is low insertion loss in the pass band: high insertion loss reduces the signal level and therefore deteriorates the signal-to-noise performance of the receiver. In addition to the obvious increase in cost, the use of amplification to overcome losses is limited by other practical considerations: amplification after the i.f. filter cannot avoid the deterioration in noise performance, while amplification before the filter is limited by the desire for low cross modulation with adjacent-channel signals. Although no precise values can be given for maximum i.f. filter loss, lumped-element filters can easily achieve insertion losses less than 10 dB; any new filter design should therefore also have the lowest possible loss, preferably less than 10 dB.

An IDT is essentially a bidirectional antenna. Its impedance can be characterized by a real component, the radiation resistance, and a shunt capacitance determined by the IDT geometry and substrate dielectric constant; this capacitance is normally tuned out by means of an inductor. The radia-

17

tion resistance is determined by the IDT geometry and is roughly inversely proportional to the IDT area — that is, the product of the number of electrode fingers, their spacings, and their lengths. Maximum power is coupled into the sender IDT when the source impedance is matched to the radiation resistance of the sender.

The power coupled into the sender divides equally into two surface waves traveling in opposite directions. Unless two receiver transducers are used, one on each side of the sender, more than half of the input energy is lost. Moreover, the amount of energy absorbed by the receiver depends on the ratio of load impedance to transducer impedance; the output power is maximized under a matched condition and, in this case, half the energy can be extracted. Thus there is an unavoidable 6-dB loss when only one sender and one receiver IDT are used. Additional losses will occur if the substrate is lossy (this is not the case for $LiNbO_3$ at television intermediate frequencies) or due to impedance mismatch. As is pointed out later, impedance mismatch at the receiver is normally used to minimize adverse reflections and the insertion loss in practical SAW i.f. filters is typically 10 to 15 dB.

Reflections

Several types of reflections that occur in microsonic filters can pose problems for the designer. One type of reflection is caused by the unavoidable surface loading and shorting that occurs under each electrode finger; the resulting acoustic mismatch produces a variation in the propagation velocity and results in reflection of some of the acoustic energy.

Since the resistivity of the electrode fingers must be low enough to avoid resistive losses, the designer is faced with a delicate tradeoff between excessive resistance and excessive mass-loading of the surface; no completely adequate solution exists.

The problem that results from finger reflections can be greatly alleviated by using a $\lambda/8$ finger width and spacing, instead of $\lambda/4$. In this design, each finger is effectively split into two fingers, which puts the reflections at twice the frequency of interest, thereby usually placing them outside the frequency range of interest.

The mass-loading of the fingers that produces small variations in propagation velocity also tends to delay the acoustic wave more in the central region of the transducer than near the edges where there are fewer finger overlaps. The net result is a diffraction or defocusing of the acoustic energy (bending of the wave front) so that the wave is no longer uniformly incident on the receiver. This problem can be largely avoided by using "dummy fingers" in between the electrically active fingers in order to produce a uniform delay over the wave front of the acoustic wave. A more current i.f. filter design incorporating the $\lambda/8$ finger pattern and "dummy fingers" is shown in Fig. 5.

Triple transit

Although we have so far talked about a sender and a receiver IDT, one can use either transducer as the sender and the other as the receiver. Both transducers, like antennae, can be used to send or receive acoustic waves by means of the piezoelectric coupling to the substrate. In

fact, any signal generated at the sender that produces a voltage signal at the receiver will cause the receiver to act as a sender and re-emit the same signal as if it were the sender IDT. It can be easily shown that the energy extracted from a traveling wave depends on the loading of the receiver: if the output load is matched to the impedance of the transducer, then a maximum fraction (50%) of the acoustic energy is extracted, one-quarter is transmitted, and one-quarter reflected.

In a microsonic filter, the signal energy that is not received should not be allowed to be reflected from the substrate edges, since it would be detected again with a considerable time delay. Consequently, the transmitted energy is usually absorbed by means of a lossy coating (wax) between the transducers and substrate edges.

The energy (25% under matched load) reflected between the IDTs, however, cannot be absorbed since it travels along the same path as the desired signal. This reflected signal can produce, at the sender, a spurious signal that is delayed twice as long as the main signal and is therefore called the double-transit signal. Its effect is usually not bothersome and can be cancelled by other means. However, part of this double-transit signal is again reflected back towards the receiver (at $\frac{1}{4} \times \frac{1}{4} = 1/16$ of the sender's original intensity) and will appear at the receiver, triply delayed and indistinguishable from the singly delayed, primary signal.

The effect of the triple-transit signal is twofold. Since the time delay is fixed by the physical spacing between the transducers and the propagation velocity of the substrate, it produces a phase delay which is directly proportional to frequen-
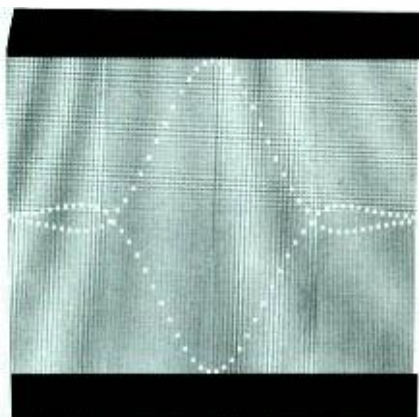

Fig. 5 — Experimental IDT design incorporating narrower finger widths and "dummy fingers".
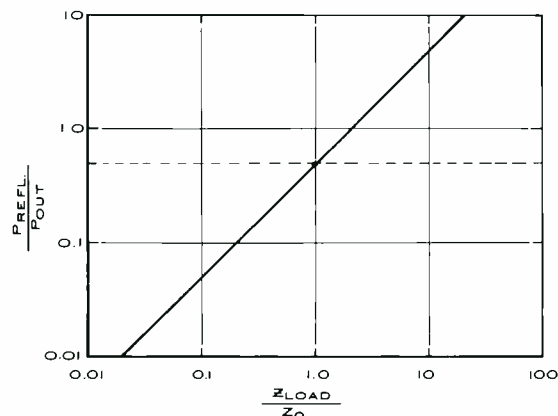

Fig. 6 — Ratio of reflected power to output power from IDT as function of load impedance.

18

cy. Thus a ripple appears on the pass band of the filter. Furthermore, the delayed signal attenuated by 12dB (1/16) being indistinguishable from the main signal, produces a ghost on the tv screen corresponding to the relative delay. For instance, a 1/8-in. spacing between transducers will cause a delay of ~2 μs, which corresponds to a ghost image separated from the main picture by ~¾ in. on a 25-in. tv screen. This condition cannot be tolerated.

Although a lossy substrate attenuates the triple-transit signal more than the main signal, this is not a cure in view of the need for low insertion loss. In fact, $LiNbO_3$ was chosen partly because of its negligible propagation loss at tv intermediate frequencies.

The output load impedance, however, can be varied to minimize reflections. In the extreme case where the output transducer is shorted, no voltage signal will appear across it to generate a re-radiated signal; all the incident energy passes under the receiver without attenuation and there is no triple-transit signal. However, no energy is absorbed by a shorted receiver and, consequently, this condition is of no practical interest.

As the load impedance is reduced from the matched condition, both the absorbed and reflected energies decrease monotonically. In this range of load impedances, the ratio of absorbed to reflected energy increases (Fig. 6), thus reducing the triple-transit problem.

A practical dilemma arises because the reduction in the primary signal is equivalent to loss in the filter's pass band, which leads to degradation of the television picture, at least under weak signal conditions. Nevertheless, the filters are normally mismatched at the output to reduce the triple-transit signal to a point where it produces no visible ghost on the screen.

Bulk waves

Surface acoustic waves remain confined in a thin surface layer of the substrate because their propagation velocity is less than that of bulk waves and consequently mode conversion does not occur. The higher propagation velocity of various types of bulk waves causes the IDTs to couple to them at somewhat higher frequencies, however, usually just above the pass band of the filter. This bulk-wave
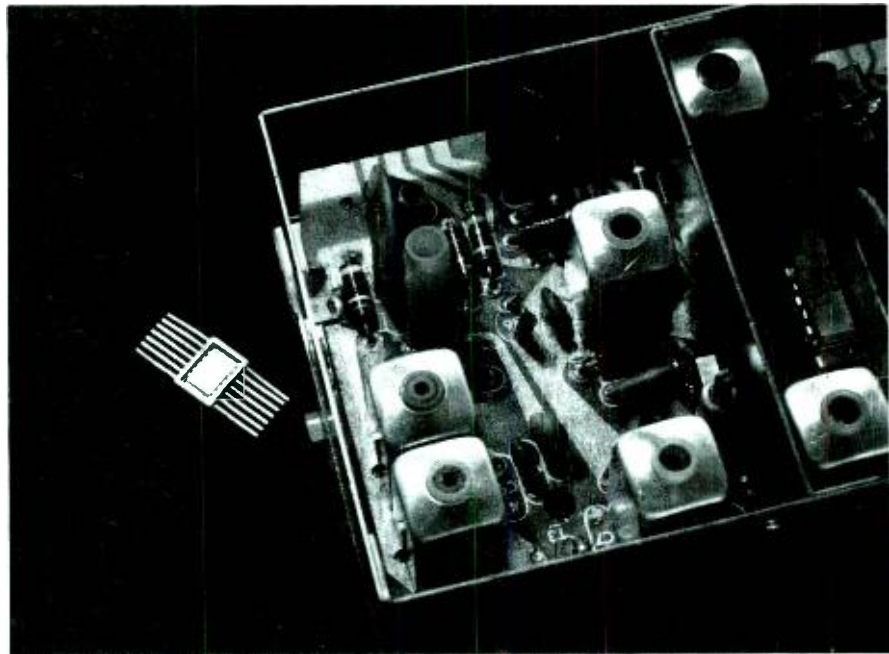

Fig. 7 — Experimental SAW tv-i.f. filter shown next to coil/capacitor filter from MAK-001 module which it replaces.

response then prevents the filter from achieving high rejection at frequencies above the pass band where the system requires good selectivity and deep traps.

Several techniques have been explored with some success to reduce the bulk-wave response in microsonic i.f. filters. These include roughening the bottom surface, bonding the substrate to a larger, lossy material, or tilting the various crystal faces at an angle to deflect the generated bulk waves; none of these techniques, however, is fully adequate. Better means have been demonstrated, such as the use of multiple transducers so that surface waves are added in phase while bulk waves cancel, or the steering of surface waves along the surface to physically separate them from the bulk waves. These techniques, however, are more costly since they require considerably larger substrates. Bulk wave suppression to 35 to 40 dB has been achieved in simple SAW filters, and this is probably adequate.

Conclusion

A SAW television i.f. filter was designed and incorporated into an RCA XL-100 television receiver. It replaced the first filter (six coils and capacitors) of the (MAK-001) i.f. module (Fig. 7). Its insertion loss (~15 dB) is somewhat higher than that of the production filter due to a deliberate impedance mismatch in order to suppress the triple-transit signal. Weak-signal performance does not suffer

as much as might be supposed, however, because of the variations in the i.f. amplifier's input impedance as a function of signal level. The integrated-circuit amplifier is designed to have an increasing input impedance Z_{in} under weak signals in order to "unload" the filter and peak up the carrier levels. This increased impedance presents a more nearly matched load to the SAW filter with a correspondingly large decrease in insertion loss. Stop bands in this filter were attenuated ~35 to 40 dB, limited by bulk-wave levels. Temperature stability proved comparable to that of the present coil-capacitor i.f. filter, and, of course, no alignment is required in production.

Acknowledgment

References

1. Boemmel, H. E.; Dransfeld, K.; "Excitation and Attenuation of Hypersonic Waves in Quartz," Phys. Rev. Vol. 117 (Mar. 1960) p. 1245.

2. White, R. M.; Voltmer, F. W.; "Direct Piezoelectric Coupling to Surface Elastic Waves," Appl. Phys. Letters, Vol. 7 (Dec 1965) p. 314.

3. Sittig, E. K., "Elastic Wave Delay Device," U.S. Patent 3,360,749 (Dec 26, 1967).

4. White, R. M.; "Surface Elastic Waves," Proc. IEEE, Vol 58. (Aug. 1970) p. 1238.

19

Very high resolution radiometer

A.I. Aronson

High-resolution radiometers are the primary sensors used today in environmental and earth-resource observation satellites to provide day and night cloud-cover pictures, geophysical observations of surface temperatures, land and water features, crop, ecological, and many other resource-study applications.

A.I. Aronson, Senior Engineer, Astro-Electronics Division, Princeton. N.J.. received the BEE from Syracuse University in 1951. He joined RCA in 1951 and transferred to AED in 1958. Since 1964, Mr. Aronson has been responsible for system and equipment engineering on infrared radiometers. horizon sensors, and spectrometers. Mr. Aronson developed a system concept for a highly reliable precision radiometer using thermopile detectors and supervised the development of a dual-channel scanning radiometer using a thermistor bolometer. Mr. Aronson originated the system design and supervised the development of the RCA Very High Resolution Radiometer for ITOS D and E from 1967 to 1971. Before the infrared assignments at AED, he worked with spacecraft command systems, including major roles in the development of command systems for SCORE, Tiros, and Stratoscope II. Before his transfer to AED. Mr. Aronson worked on one of the first magnetic tape recorder systems using solid state electronics video synchronizing generators. and various digital circuits, with special emphasis on the application of transistors as early as 1952. Mr. Aronson has taught courses at RCA in low-frequency transistor circuits, has published eight technical papers. and holds six patents in transistor circuit applications.

ELECTROMECHANICAL SCANNERS, despite the sometimes archaic scanning techniques used, have largely replaced electron-beam-scanned television cameras in environmental satellites, primarily because they produce geometrically registered multispectral images extending from the ultraviolet to wavelengths longer than 20 μm — a range not possible at present with electronic television. Other advantages of the electromechanical scanners are improved radiometric accuracy, linearity, stability, and lack of shading in the image.
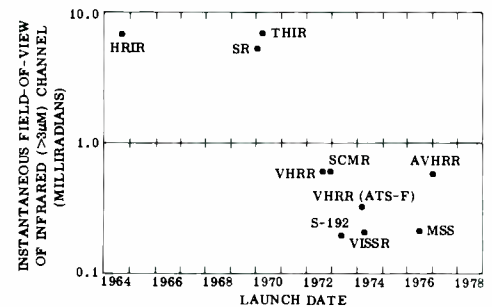
Acronym	Sensor name	Spacecraft
HRIR	High resolution infrared radiometer	Nimbus
THIR	Temperature humidity infrared radiometer	Nimbus
SR	Scanning radiometer	ITOS
VHRR	Very high resolution radiometer	ITOS
SCMR	Surface composition mapping radiometer	Nimbus
VHRR ATS-F	Very high resolution radiometer	ATS-F
VISSR	Visible-infrared scan radiometer	SMS
S-192	S-192 multispectral scanner	Skylab
AVHRR	Advanced very high resolution radiometer	TIROS-N
MSS	Multispectral scanner	ERTS

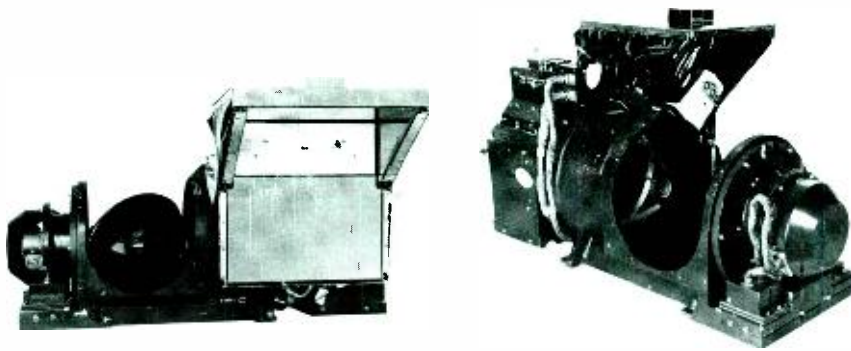Fig. 1 — Evolution of resolution capability of imaging radiometers on NASA spacecraft (for infrared channel only).

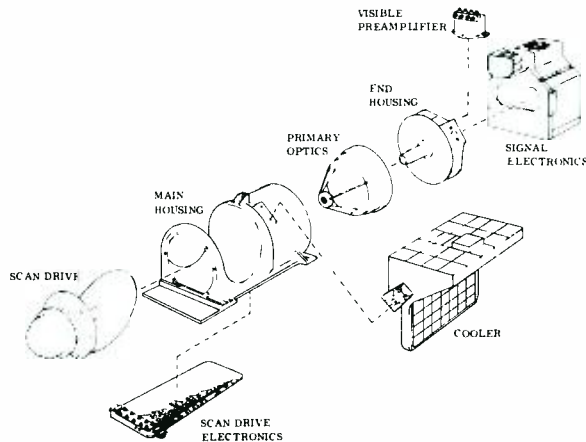Fig. 2 — Very high resoluiton radiometer, two views.

Fig. 3 — Exploded view of VHRR.

Parameter	Typical performance
Orbit altitude, nmi	790 ± 25
Resolution	
IFOV, mrad	0.6
Modulation transfer function @ 0.6 mrad (square wave)	0.4 IR, 0.5 visible
Spectral coverage, μm	
Visible	0.60 - 0.70
Infrared	10.5 - 12.5
Sensitivity	
Visible SNR (p-p/rms) @ 65 fL	4.0
IR minimum resolvable temperature (MRT) @ 315 K	0.3
Dynamic range	
Infrared, K	180 - 315
Visible, fL	65 - 10,000
Electrical bandwidth, kHz	35
Scan rate, scans/min	400
In-flight calibration	
Infrared, K	4 and 300
Visible	Sky, solar target
Scan linearity	±0.05 mrad jitter along any vertical straight line
Power, W	6.5
Size, in.	18.4 × 10.77 × 12.75
Weight, lb	21

The Very High Resolution Radiometer (VHRR) starts a second generation of high performance infrared scanning radiometers, as shown in Fig. 1. The radiometers of the 1964-1972 time frame had subpoint ground resolution in the range of four to five miles; the VHRR launched on October 15, 1972 provides 0.47-mile resolution. This performance breakthrough, in the infrared band, was made possible by the use of a mercury-cadmium-telluride detector cooled to approximately 105 K by a passive radiator cooler. The VHRR made the first operational use of this new passive radiator cryogenic technology — an important technology which represents the only practical means at present for reliable infrared detector cooling for periods of a year or more in space.

VHRR design

The VHRR shown photographically in Fig. 2 and in an exploded view in Fig. 3, is a scanning radiometer designed for use on the ITOS D series spacecraft. Two VHRR's are mounted on the earth-oriented, three-axis-stabilized sensor platform of the spacecraft. The overriding emphasis throughout the development of this sensor has been design simplicity, low power consumption, and compact size.

This two-channel instrument can provide day or night cloud-cover pictures in the 10.5- to 12.5-μm infrared band and sunlit-pictures in the 0.6- to 7-μm visible-light band. The instantaneous field of view (IFOV) of each channel is 0.6 mrad, providing a subpoint resolution of 0.47 nmi. Cross-track scanning is produced by a single 45-degree mirror, rotated at 400 r/min by a direct-drive (gearless), brushless, dc torque motor; spacecraft orbital travel provides the along-track picture component. Table I lists the key parameters of the VHRR.

The two VHRR's are operated in a right-and left-hand configuration in either a primary or backup mode. In the primary mode, both instruments are used with their mirrors phased 180 degrees apart to time multiplex infrared and visible data.

This halves the spacecraft transmission bandwidth requirement. In the backup mode, either one of the two radiometers can be used to provide two parallel channels of data in non-multiplexed fashion with some degradation of the received S/N on the ground.

The high-resolution performance of the VHRR infrared channel is obtained using a cooled mercury-cadmium-telluride detector. Cooling the infrared detector to 105 K provides the sensitivity (D*) and fast response required to achieve very high resolution. Cooling is accomplished with a unique, passive cooler which uses geometry, special surface treatment, and staging to better radiate heat to space, while rejecting thermal inputs from the earth, the sun, and the spacecraft.
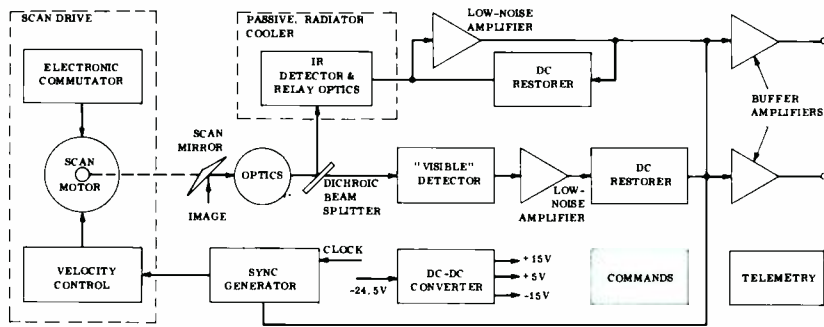
21

Fig. 4 — Simplified block diagram of VHRR.

The primary optics of the VHRR is a Dall-Kirkham 5-in.-diameter telescope. Secondary optics are used to spectrally separate the infrared and visible channels and to relay them to the respective detectors.

In-orbit radiometric calibration targets are used to monitor the sensitivity of each spectral channel for possible changes with orbital conditions and time. The orbital calibration references in the infrared band are space and the radiometer backscan black body, both of which are viewed once per revolution. A two-point calibration reference in the 0.6 to 0.7 μm band is obtained by scanning space and a sun-illuminated, diffusely transmitting target.

A block diagram of the VHRR is shown in Fig. 4.

Optical design

The VHRR optical subsystem consists of a scanning mirror, a Dall-Kirkham telescope, a dichroic beamsplitter, relay lenses, spectral filters, and detectors. The optical design stresses simplicity and a minimum of optical elements. This is particularly true in the visible-light-channel optics, where the detector is the field stop and the only image-forming element is the telescope objective. The infrared channel design minimizes the effects of cold-plate/detector movement by collimating the energy between the radiometer housing and the cooler. Fig. 5 shows the layout of the optical system.

The 5-in. Dall-Kirkham objective combines an ellipsoidal primary and a spherical secondary, and is the simplest form of a two-mirror telescope that meets the modulation transfer function (MTF) requirements. An 0.018-in.-diameter silicon photodiode located at the focal point of a 29.6-in.-focal-length objective results in an instantaneous field-of-view (θ) of 0.6 mrad. An infrared channel f-number of f/0.8 chosen to maximize the 0.89 system S/N requires a detector size of 0.0026 in. to provide a θ equal to 0.6 mrad. The infrared relay magnification is then 0.018/0.0026 or 6.92.
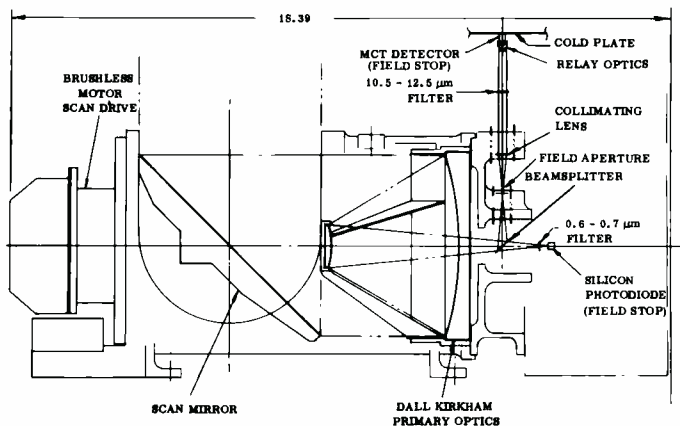
Only two interfaces in the VHRR optical system are critical with respect to dimensional stability. One is the spacing between the relay lenses and the infrared detector; the other is the spacing between the primary and secondary in the telescope. The relay/detector assembly is maintained at the detector temperature of 105 K and is inherently stable. The effects of temperature variation on the telescope are minimized by using an Invar tripod assembly to mount the secondary with respect to the primary. The variation in the spacing for a -5 to $+45°$ C temperature change, using Invar, is ±0.000167 in., resulting in a shift of the primary focus of only ±0.0075 in. This focus shift is negligible, since the depth of focus at the image plane is ±0.125 in.

A typical VHRR subsystem has a square-wave MTF of 0.5 in the visible and 0.4 in the infrared regions, with a variation of no more than 5% in MTF over a temperature range of -10 to $+40°$ C.

Detectors

The information bandwidth and sensitivity requirements of the VHRR dictate the use of a fast, high D^* ($>10^{10}$cm Hz$^{1/2}$ watt^{-1}) detector. The only commercially available infrared detectors that satisfy these requirements and can operate at temperatures (100$\pm$10 K) achievable with a passive radiative cooler, are mercury-cadmium-telluride (HgCd-Te) and lead-tin-telluride (PbSnTe). At the present, HgCd-Te is superior to PbSnTe with respect to responsivity and D^* and was chosen for the VHRR application. The characteristics of the VHRR infrared detector are summarized in Table II.

The visible channel uses a selected version of the Hewlett-Packard stock 5082 - 4204 PIN silicon photodiode.

Electronics

The VHRR signal electronics shown in the block diagram of Fig. 4 is mounted on four PC boards in the electronics assembly box. The scan-drive electronics are mounted both inside the scan drive and on a board mounted in the scanning and optics housing, as shown in Fig. 3. The visible-light preamplifier is a separate assembly, mounted near the silicon photodiode.

Fig. 5 — VHRR optics, physical locations of components.

22

Signal electronics

The signal electronics consists of the analog electronics required to amplify and condition the signals from the infrared and visible-light detectors.

The infrared detector forms one leg of a bridge circuit. The bridge resistors are selected by calculation to provide the bias required for maximum detector D^* and to balance the bridge. The bridge is followed by an amplifier whose noise figure is approximately 1.5 dB. This configuration results in a detector noise-limited condition, when used with high-responsivity detectors of the type specified for the VHRR. The amplifier is dc-coupled from detector to output and requires a dc-restore function to provide a zero radiance reference and dc stability.

The dc-restore function is provided by feeding back offset errors to balance the bridge when the radiometer views zero radiance (space) once per mirror rotation.

The visible-light channel analog electronics consists of a current-mode preamplifier. With this arrangement, the effective diode load resistor can be made very high (5 megohms in the VHRR) to provide both high S/N and good linearity of signal output vs. brightness. The dc-restore function, once per revolution when the scan mirror views space, is used to maintain low-frequency stability and a radiometric reference.

Sync generator

The sync generator electronics provides all the timing signals required by the radiometer.

Timing is initiated by the index pulse generated once per mirror rotation by the encoder in the scan drive. This analog pulse is reclocked to a 5-kHz scan reference pulse to eliminate any scan jitter from sync and all other timing signals in the video. Timing of all events is done by counting down from the 300-kHz spacecraft clock and decoding event times. The decoded events activate a multiplexer to gate a seven-level stairstep reference voltage, 0- and 6-volt levels for sync pulses, temperature telemetry, and infrared and visible video derived from on-board calibration targets.

Precursor frequency bursts, which are unique to the infrared and visible-light channels, are added to structure the complete video format.

The sync generator also provides the 5-kHz scan-drive reference and the phase-modified 5-kHz required when time-multiplexing two radiometers. In this mode, one radiometer slips phase until its index pulse is 180 degrees out of phase with the other radiometer index pulse.

Scan-drive electronics

The scan-drive electronics provides for commutation of the brushless motor winding, velocity, and phasing control. Commutation of the six motor windings, each of which is switched four times per revolution, is controlled by Hall elements mounted in the stator. The signals from three Hall elements are amplified and fed to a matrix, which decodes six states from the three inputs. The six commutation signals turn on the six motor drivers at the appropriate angular positions of the rotor.

An incremental tachometer, consisting of a 750-line encoder, provides velocity feedback for servo control of scan velocity and jitter. The encoder rotates between a gallium arsenide diode and a phototransistor, providing a sine-wave output whose frequency is proportional to velocity. The velocity signal is shaped and squared and fed to a phase detector. The phase detector saturates to provide maximum drive until the motor comes within the lock-in range of the phase detector. The phase detector output then oscillates between saturation and cut-off until frequency coincidence is obtained between the velocity track signal and the 5-kHz clock reference frequency. At the point of frequency coincidence, the velocity loop is locked in phase. After lock-in, motor jitter results in a pulse-width-modulated, 5-kHz signal at the phase-detector output, the instantaneous modulation being proportional to the scan-drive jitter. The pulse-width-modulated signal is filtered, frequency-compensated, and amplified to drive the motor.

The VHRR phasing logic will cause the scan mirrors of the master and slave radiometers to rotate 180 degrees out of phase. This phasing operation occurs automatically when both radiometers are operating, one with the IR channel enabled and the other with the visual

Table II — Infrared detector characteristics.

Characteristic	Value
Responsive element size, in.	0.0026 × ±0.0003
Detectivity, D^* (λ_{max}, 3000, 60°) cmHz$^{1/2}$W^{-1}	1.6 × 10^{10} (at 105 K)
Bias current (chosen for max $D^*\lambda$), mA	≤5
Bias power, mW	≤2 mW
Responsivity, R_λ ;V W	≥ 7500 at λ_{max} and at optimum bias current (at 105 K)
Spectral characteristics	1. 11μm ≤λ_{max}≤ 13μm
	2. R_λ ≥ 0.7Rλ_{max} for 10.5 μm ≤λ ≤ 12.5 μm
Frequency response, kHz	DC to 35; flat to 0.5 dB
Resistance; ohms	>10 at operating temperature
Stability (after 55°C soak)	Δ resistance ≤ 10% Δ signal ≤ 10% or ΔR_λ ≤10% Δ noise ≤20% or ΔD^*_λ ≤20%

channel enabled. The radiometer with IR enabled is the slave and shifts phase with respect to the other (master) radiometer. The phasing logic compares the time delay between a master once-around pulse and a slave half-around pulse, and generates an acquisition signal if the two motors are not phased within a 300 ± 100 μs acquisition window.

These two signals are used to control the 5-kHz velocity reference, which will cause the slave motor to either slow down or speed up, depending on the phasing of the two motors. A signal from the timing logic occurs at a 194-Hz rate, with a period of 3.41 ms, and is used to control the number of 150-kHz clock pulses fed to the 5-kHz velocity counter. This is accomplished once every 3.4 ms by removing one clock pulse of the 150-kHz clock if the slave is too fast or by adding one clock pulse, if the slave is too slow. This results in a modified 5-kHz pulse that is one period of the 150-kHz clock earlier or later in time. This causes the motor to slip phase ±6.6μs periodically at a 3.41-ms rate. Thus, the scan phasing changes 1.94 ms/s for a maximum phasing time of 38.7s for 180 degrees.

Scan drive

The drive mechanism is shown in Fig. 6. The scan mirror is attached to a stainless-steel shaft, which is supported on a pre-

23

loaded (5-lb) pair of 102H angular contact ball bearings. Labyrinth seals are mounted on each side of the bearings to retain lubricant. An optical encoder disc having a 750-line-pair servo track, together with a once-around pulse track, is mounted to the motor shaft. The encoder sensor and emitter module is mounted to the housing, accessible for alignment. A one-piece stainless-steel housing locates the stationary components and attaches by a flange to the scan and optics housing.

Cooler

The cooler, shown in the photograph of Fig. 2 and in the cross-section view in Fig. 7, is used to cool the infrared detector to approximately 105 K. The cooler employs a combination of geometry and special thermal surfaces to shield it from (and reject thermal input from) the spacecraft, the sun, and the earth, while simultaneously radiating heat to cold space to accomplish this completely passive cooling function.
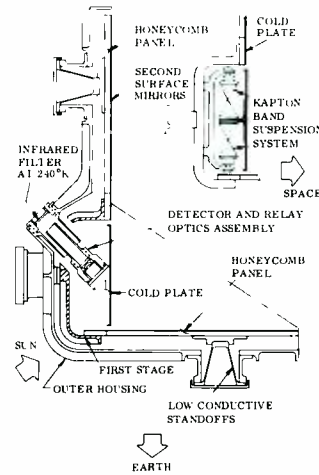

Fig. 7 — Cross section of VHRR passive radiator cooler.

The cooler consists of three main parts: 1) a cold plate, 2) a first-stage coolers, and 3) an outer frame. The cold plate is thermally isolated from the inner frame by a unique truss-type Kapton band suspension.
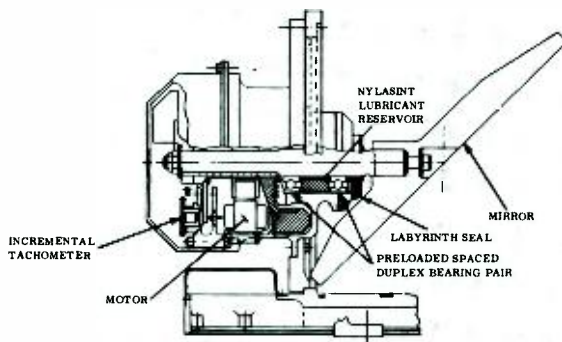

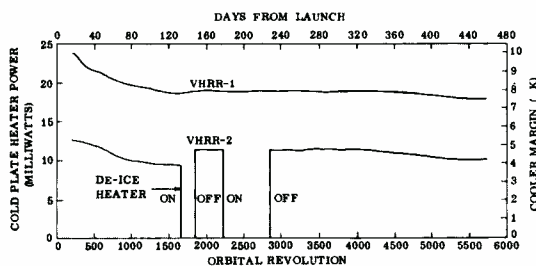
Fig. 6 — Scan drive, sectional view.

Fig. 8 — Thermal performance of cooler in orbit.

The cooler cross section is "L" shaped, with sides, to form a "scoop" type of geometry surrounding the cold plate. Both the first-stage cooler and the outer frame have this same scoop configuration. This geometry is unique among contemporary spacecraft passive cooler designs, all of which use a conical configuration to shield the cold plate. The earth-facing, or scoop part of the cooler shields the cold-plate from thermal inputs from earth albedo and self-emitted infrared energy. No additional shielding from the sun is required, because the cooler is mounted on the side of the spacecraft opposite the sun and the cold plate is shielded from the sun by the spacecraft and the sides of the scoop. The cold plate radiates heat to space. It absorbs heat from the low-emittance, vapor-deposited-gold scoop sides, thermal conduction from wires and the cold-plate support, and radiative coupling from the back of the cold plate. The thermal equilibrium of these inputs and the radiation to space result in a "natural" cold-plate temperature of approximately 95 K. The cold plate is electrically heated to 105 K with a proportional-control heater circuit in order to maintain a constant detector temperature if the natural cooler temperature should vary within the orbit or with time.

Radiative inputs to the cold plate from the first stage are minimized by maintaining the first stage at approximately 160 K. This cooling is accomplished by use of second-surface mirrors mounted on the vertical part of the first stage. Second-surface mirrors have an absorbtivity (α) of 0.07 and an emissivity (ϵ) of 0.8, which make them both good reflectors of earth albedo and good emitters to cold space.

The first stage is surrounded by the outer frame, which is thermally isolated from the radiometer housing and the spacecraft by a Delrin support bracket. The outer frame is cooled to approximately 240 K by means of second-surface mirrors mounted on its earth-facing side.

All internal cooler parts are gold-coated, and the spaces between the outer frame, inner frame, and cold plate are insulated with multilayer gold-on-Kapton thermal blankets to minimize radiative coupling losses.

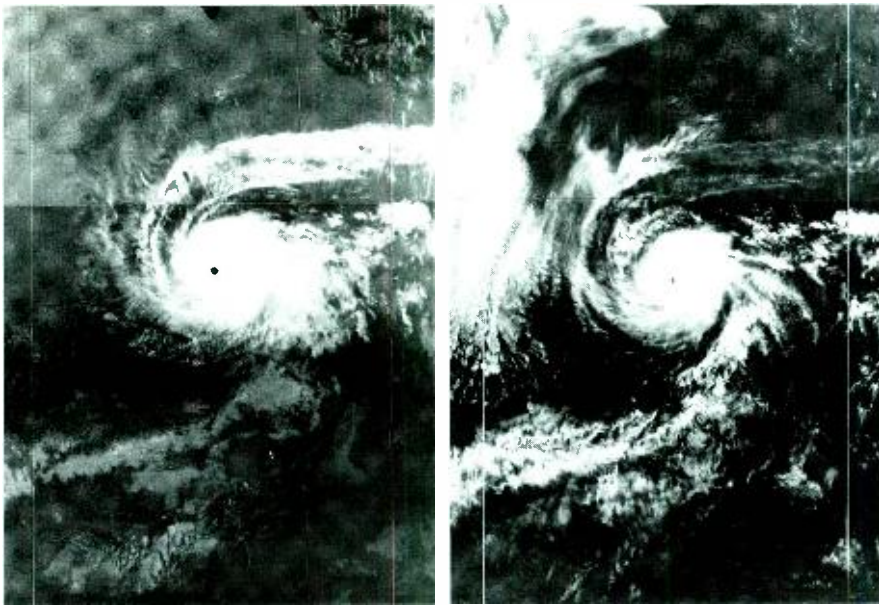Performance of the coolers on the

24

Fig. 9 — NOAA - 2 satellite VHRR pictures of Hurricane Ava taken June 1973. (Picture on left imaged by VHRR infrared channel; picture on right imaged by visible channel.)

The VHRR tracks cold and warm eddies to yield more accurate local surface thermal patterns than is obtainable with aircraft, as an aid to the Bureau of Fisheries. Using VHRR's, NOAA is currently mapping three US river basins operationally for snow-cover extent.

In meteorology, the higher resolution and multispectral capabilities of the radiometer allows improved analysis of both local and synoptic atmospheric data.

And finally, an interesting proposal for a feasibility study concerns the use of VHRR data to monitor ground temperatures and find areas conducive to the hatching of screw worms. The area would then be "seeded" with sterile male screw-worm flies to reduce the screw-worm population.

NOAA-2 meteorological satellite since launch is shown in Fig. 8.

Contamination protection

An anti-ice trap is incorporated in the cooler to prevent the contamination of cold (105 K) optics from icing or outgassing-product accretion.

The trap works by surrounding the cold inner tube, which is at detector temperature, with a 240 K outer tube to prevent direct contamination of the cold relay optics. This arrangement is shown in Fig. 7. A foreign molecule will freeze or condense at the base of the cold inner tube before it can work its way between the inner and outer tube and contaminate the cold relay optics. In addition, heaters are incorporated on the inner frame (first stage) and the cold plate to heat these parts to about 240 K, on command, to purge these elements if accretion of contaminants reduces the margin between the cold-plate control temperature and the "natural" temperature of the cold plate.

VHRR performance

The NOAA-2 (originally ITOS D) meteorological satellite, carrying two VHRR's, was launched into a circular, near-polar, 790-nautical mile orbit from the Western Test Range on October 15,

1972. As of the date of this paper, the two VHRR's, operating continuously since launch, have logged a total of 25,500 hours of successful operation.

The cooler operation has been particularly noteworthy, as shown in Fig. 8. This shows the cold-plate heater power required to maintain the detectors at 105 K. The margin above the natural cooler temperature is found by dividing the cold-plate power in milliwatts by 2.4. Degradation in 16 months of operation has been small and has leveled off, indicating a VHRR-cooler lifetime that will exceed the instrument design lifetime of one year by a large margin.

The high-resolution, low-noise, and jitter-free pictures derived from these instruments can be seen in the pictures of Hurricane Ava shown in Fig. 9.

VHRR data utilization

The improved resolution of VHRR data has already aided the scientific studies of ice, sea surface thermal patterns and current, snow, and the atmosphere.

The advantages of high-resolution viewing of ice at night has found application in ice mapping during polar nights, support for the US Navy weather operations, and ice mapping in Alaska and the Great Lakes.

Acknowledgments

Bibliography

1. Hudson, R.D., Jr., *Infrared System Engineering*, John Wiley and Sons, New York (1969).

2. Schnapf, A., "The Evolution of ITOS, the Operational Environmental Satellite of the 1970's," Ninth Space Congress, Cocoa Beach, Fla., April 19-21, 1972.

3. "Observations from the Nimbus I Meteorological Satellite," American Geophysical Union, Seattle, Washington, Dec. 29, 1964, NASA SP-89.

4. Aronson, A.L., "Application of Infrared Sensing in Meteorological Satellites," NEREM - 70 Record.

5. Tepper, M., Johnson, D.S., "Toward an Operational Weather Satellite System," *Astronautics and Aeronautics*, Vol. 3, No. 16, (June 1965).

6. Breckenridge, R.W., Gabran, F., "Cryogenic Cooling Systems for Spaceborne Experiments," Proceedings of Electro-Optical Design Conference, 1972.

25

High-capacity high-data-rate instrumentation tape recorder system

O. E. Bessette

A 240-megabit/second serial-bit-stream recording system using a longitudinal (fixed-head) magnetic recording technique called HDMR (High Density Multitrack Recording) has been developed. This system provides maximum bits per square inch of tape at reliable in-track packing densities. Unique "unitized" fabrication techniques have been used to construct single-stack magnetic heads (record/play on the same head) at track densities of over 100 tracks per inch. Commercially available tape is accommodated by the use of error detection and correction. HDMR technology, applied to the implementation of a typical ground instrumentation recording system, allows key performance parameters of 240 Mb/s serial data input, 108 in./s tape speed, a 142-track head, 240-Mb/s serial data output, and less than one bit error in one million.

Fig. 1 — 164-track high-density multichannel recording head.

SENSOR OUTPUTS — whether synchronous scan (television, radar, electro-optic) or non-formatted (i.t., rf, telemetry) — are basically analog at the data source. However, because of the relative ease of handling data in digital form, the trend is to use A/D converters to digitize data from these sensor sources for processing. Typically, a digital format 1) provides minimal performance degradation during data processing, multigeneration copying, or editing; 2) allows easy detection and correction of errors and dropouts; 3) accommodates very high data rates through parallel processing; 4) drastically reduces operational adjustments; 5) is the most easily encrypted form of data; and 6) can be computer compatible.

Until recently, A/D converters were limited to low bandwidth and/or low dynamic range applications. With the advent of A/D systems capable of adequately processing such complex signals as broadcast-quality color tv and high resolution radar, a need for recording and processing digitized data at rates in the hundreds of megabits per second has emerged.

To address this need, a longitudinal high density multitrack recording (HDMR) technique has been developed. HDMR provides maximum storage of data bits on a minimum quantity of tape (in other words, maximum bits/square inch). To achieve this goal, both the in-track packing density (or bits/inch along tape), and the track density across tape (tracks/inch) have been increased. HDMR is unique, however, in the degree of extension of track densities. This feature permits extended area packing density at reliable recorded wavelengths. An alternate approach, which has been widely promoted, uses standard inter-range instrumentation group (IRIG) track format heads with in-track densities extended up to 35,000 b/in. This approach yields an area packing density of 0.980×10^6 b/in.^{2} with an IRIG track density of 28 tracks/inch. Experience has shown that sensitivity to head-to-tape separation losses at such short wavelengths results in high bit-error rate (BER), low reliability of the head-to-tape
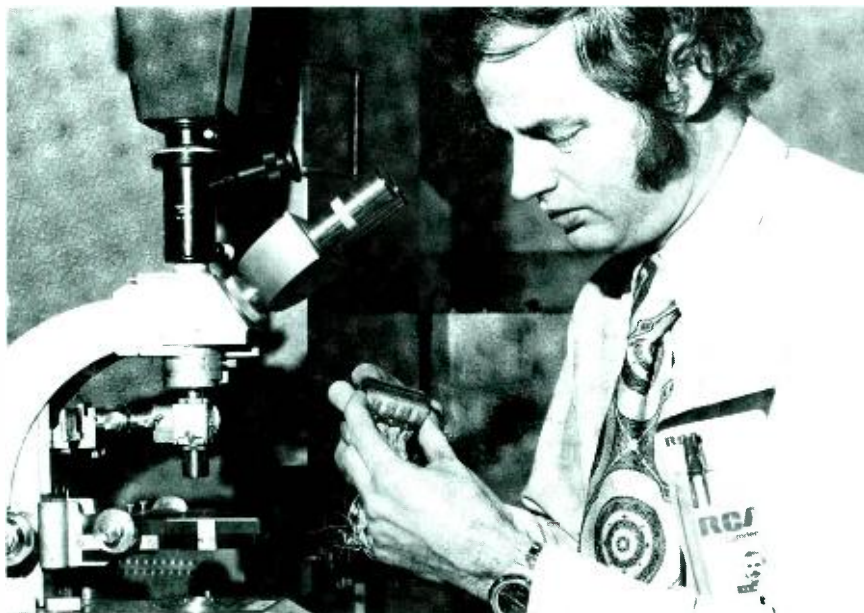
Oliver E. Bessette, Ldr. Aerospace Systems GCS Recording Systems, Government Communications and Automated Systems Division, Camden, N.J. received the BSEE in 1958 from the Worcester Polytechnic Institute. He joined the RCA Defense Communications System Division and participated in the Design and Development Training Program. In 1959, he joined the Speech Engineering section of CSD which is now the Recording System group. As a junior and then senior engineer, he participated in recording systems hardware design and development in areas such as wideband fm modulation/demodulation, phase-linear fm processing, low-noise wideband amplifiers, magnetic head design, tape-transport development, servos, rotating bandwidth, automatic time base correction (ATC) using electronically variable delay lines (EVDL) and digital encoding. In addition to circuit and subsystem design, his assignments included program management, cost control, customer liason and field support activities for many types of RCA ground based, airborne and space video and wideband instrumentation recorders. In 1969, Mr. Bessette was promoted to Engineering Leader and has since been the Principal Investigator in development of a new product line of RCA recording systems called High Density Multitrack Recording (HDMR). This IR&D activity has led to development techniques which have proven the realizeability of digital recording systems that can store digital data in magnetic tape memories at 3×10^{11} bits/reel of tape, with transfer rates up to 300 megabits/second. Mr. Bessette is a member of IEEE group on Magnetics and holds a patent on a magnetic head.
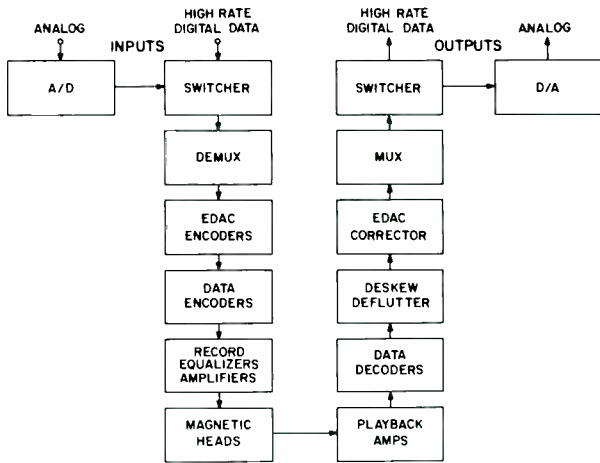
Fig. 2 — HDMR system block diagram.

interface, and compromised tape usability. Hence, in development efforts to obtain high packing densities (b/in.^{2}), maximum effort was devoted toward extending the track density while maintaining reliable in-track density.

Successful video head technology, developed by the Broadcast Engineering Group and RCA Laboratories, led directly to unique fabrication techniques for ultra-high-track-density longitudinal heads. Applications of this technique have successfully demonstrated track densities of more than 80 tracks per inch, yielding an area packing density of over 2×10^6 b/in.^{2} with an in-track density of only 25,000 b/in.

Typically, the two-inch, 164-track HDMR head (shown in Fig. 1), operating at 30 inches/second, records at the same data rate as a 28-track IRIG version operating at 120 inches/second, but the HDMR version requires only two-thirds the in-track density. This means a more reliable head/tape interface *plus* increased tape utilization, *i.e.*, less tape used, or more record time available.

For example, a requirement to record 60 Mb/s for 1 hour can be satisfied by HDMR with a 4500-ft roll of tape. IRIG format at 35,- to 40,000 b/in. requires 18,000 ft of tape (a reel greater than 16 in. diameter, with a dreaded tape splice).

Experience has also shown that 28 tracks/inch provides "overkill" in signal-to-noise ratio even at high b/in. figures. A 5-mil (0.005-inch) track operating at 25,-000 b/in. reliably produces a measured BER of less than 1×10^{-8} if tape imperfections are ignored, and 1×10^{-4} with tape imperfections included. The

latter effect is the reason wide tracks are normally used. An error detection and correction (EDAC) system for HDMR has been developed which effectively circumvents the tape dropout errors, thereby providing a BER of better than 10^{-6} at packing densities of over 2×10^6 b/in.^{2}. [The EDAC system requires very little overhead (implementation), does not require that the data be blocked or formatted, and can be utilized to correct errors generated during data processing external to the recorder.[1,2]] With this system, standard instrumentation tape can be used direct from the factory without burnishing and cleaning. The HDMR technique thus provides a tape utilization capability that allows the recording of ultra-high data rates at reasonable tape speeds by spreading the high rate signal over many parallel tracks on tape. The development of high density heads was the prime element in HDMR technology. Other important elements contribute substantially to the performance and reliability:

Heads — No gap scatter, 1000 hours life;

Head-tape interface — Commercial tape, reliable in-track packing densities, accurate tracking;

BER — Error detection and correction;

b/in.^{2} — Double density code, unique equalization, high track density, incremental operation;

Simple electronics — No equalizer to adjust, only 20 active elements per channel; and

Deskew — No overhead, no static skew, simple system

HDMR system

The major elements of a typical HDMR

system are shown in Fig. 2. Although this diagram shows an analog-to-digital converter at the system input, the digital signal to be recorded can actually be derived from various sources:

- A serial or parallel digital input
- A digitized analog input
- A "self-test" signal

The selected input data is demultiplexed to many parallel lines and parity checked by the EDAC encoder. All data and EDAC NRZ (non-return-to-zero) signals are phase encoded and equalized for optimum record bandwidth. Each channel is then amplified to a suitable record level and applied to the multitrack magnetic head.

The reproduce portion of the HDMR system utilizes the same HDMR head to read out the stored data. Each head output is amplified, filtered, and limited by analog circuitry. These circuits and the final stage of the record amplifier are the only analog circuits associated with the basic HDMR record/reproduce system. These multi-channel circuits contain only twenty active devices per channel and require only one adjustment: record current. No playback equalizer is required since this function has been replaced by a simple and unique equalizer on the record side. Thus, the normal complications associated with equalizer adjustment have been eliminated and the analog reproduce electronics are reduced to 50% of the normal requirement.

The outputs of each limiter are decoded independently of clock circuitry. During decoding, clock information is extracted from some of the data channels and used to strobe the data out of the decoders and into the de-skew/de-flutter buffers.[3] The lack of "gap scatter" in HDMR heads (no interchannel-time-displacement error between adjacent tracks) allows this minimal implementation of clock circuitry. Typically, only one clock is needed to strobe out ten tracks, the limit being determined by the amount of dynamic skew. A VCXO (voltage controlled crystal oscillator) or an external reference can be used to control the data output stability. The source selected serves as the reference for the recorder capstan and the output clock for the de-skew/de-flutter buffer. Digital time base correction is accomplished in the de-skew/de-flutter buffer with a single digital integrated

Table I — Typical specifications — HDMR-240G.

Data rate*	Record 40 to 240 Mb/s continuously variable Reproduce 40 to 240 Mb/s fixed, selectable
Data format	Serial NRZ-L in/out
Auxiliary data inputs	Up to 12 lines @ 2 Mb/s digital (or other signal formats)
Record time	23 min. @ 240 Mb/s 138 min. @ 40 Mb/s
Start time	50 ms. record 100 ms. reproduce
Error rate	2×10^{-8} maximum
Magnetic tape	2-in. on NAB reel 16-in. (12.500-ft) maximum
Tape interchangeability	Tape recorded on one HDMR-240G can be reproduced on a second HDMR-240G
Packing density	In-track density of 20,000 b/in. 1.4×10^6 b/in.^{2}
Total storage	Primary data 3.3×10^{11} bits
Capability	Auxiliary data 3.3×10^{10} bits
Head life	1.000 hrs.
Size	65 ft.^{3}
Power	115 Vac, 60 Hz, 1 phase. 2 kW
Number of tracks	112 data, 14 EDAC, 12 aux
Head stacks	One record play**
Head construction	Alfecon II Unitized HDMR
Track width spacing	0.008-in. 0.014-in.
Transport	Vertical with waist-level tape loading, vacuum bins for fast start/stop
Tape speed	107 in./s at 240 Mb/s (18 in./s at 40 Mb/s)
Cabinet	Welded EMI design on casters. transport door is pressurized to keep tape compartment clean
Special effects	Edit, auto search and other special features also available

*Also available at 120 Mb/s on 1-inch tape

**Read while write available (two head stacks, plus increased de-skew electronics)
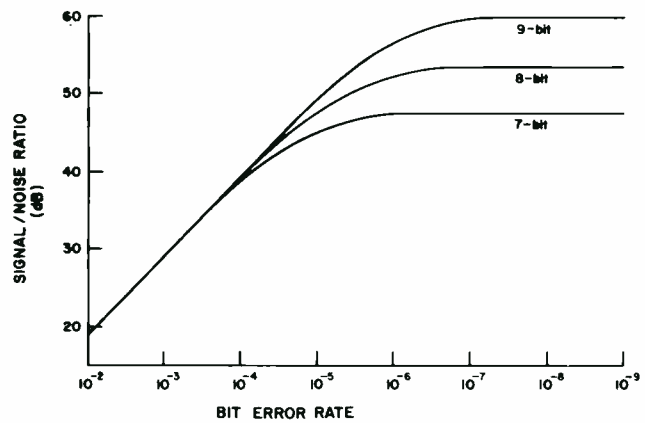

Fig. 4 — HDMR system configuration.

Fig. 3 — Signal-to-noise ratio (peak/rms) as a function of bit-error rate for 7-, 8-, and 9-bit quantization (for rms S/N subtract 5 dB).

circuit (random access memory) which replaces all the functions normally accomplished by sophisticated analog time base correctors such as MATC, CATC, and EVDL.

The coherent parallel data from the buffers are error checked and corrected by the EDAC system, and multiplexed for D/A conversion or further digital processing.

Applications

The HDMR system is available in one- and two-inch versions. Both versions use standard instrumentation tapes and have a 2:1 data rate ratio. The one-inch version has exactly half the signal processing electronics and records up to 120 Mb/s, or exactly half that of the 240 Mb/s version. HDMR applies equally well to ground, airborne and space data storage requirements. Low power, small size and weight and high reliability are accomplished by simplified channel electronics and transport design. An aerospace version of HDMR can be implemented in a configuration weighing less than 250 pounds and occupying less than 5 cubic feet, storing and producing digital data at a rate of 250 Mb/s, and requiring less than 350 watts of power.

HDMR provides *computer compatibility* for analysis of high speed and wideband data. Eight or sixteen output lines may be chosen, with output rates of 4×10^6 words/second or less, for dumping into present minicomputers or main-frame input buffers. Incremental reproduce capability is available with HDMR to allow data reduction/processing at transfer rates which are normally too high to process serially. In this mode, the HDMR system would play back a sufficient number of bits to load a memory (e.g., 1.2×10^6 bits), then stop, rewind a short distance to index the following data, and wait for another playback command. Bit error rates of 10^{-4} to 10^{-7} are typical of standard HDMR systems. This range encompasses the requirments for most system applications. For instance, NTSC broadcast video, which has been A/D converted with 8-bit quantization[4] and recorded, will produce a reconverted (D/A) video signal with a 47 dB signal-to-noise ratio (S/N) for BERs less than 10^{-5} (refer to Fig. 3). The basic HDMR system operates at 240×10^6 bits/second. This is considered a typical bit rate for today's needs.

In addition the system reflects the capabilities of present A/D converters and covers the required rates for present and near future systems. HDMR provides the capability to record a serial 240-Mb/s bit stream as might be available from a very wideband data link, or to record multiple, synchronous data outputs (typical of A/D converters) at line rates of $240/N \times 10^6$ bits/second for each of N lines. An illustration of such a 240-Mb/s recorder/reproducer is shown in Fig. 4 and typical specifications are listed in Table I.

References

1. Melas. C. M.; "A New Group of Codes for Correction of dependent Errors in Data Transmission". *IBM Journal* (Jan. 1960) pp. 58-65.

2. Griffin. J. S (RCA); "Ultra High Data Rate Digital Recording". *Proceedings of SPIE Conference* 1973, Dayton, Ohio.

3. Thompson. C. R. (RCA) and Hayes. J. M. (NASA-Goddard). "High-Data-Rate Spacecraft Recorders". *Proceedings NTC Conference*. 1972, Houston. Texas.

4. Viterbi. A. J.; *Principles of Coherent Communications* (McGraw Hill. New York; 1966) p. 257.

Linear transistor power amplifiers

Dr. E. F. Belohoubek| D. S. Jacobson

New microwave transistors using emitter ballasting provide high gain, linear operation with power outputs of 2.5 W at 2 GHz and 700 mW at 4 GHz. With suitable circuit techniques, these devices permit the development of octave bandwidth power amplifiers that are in many respects superior to present TWTs.

THERE IS a general trend today to replace existing TWT amplifiers by solid-state devices. Most solid-state amplifiers for present communications applications are relatively narrowband and operate under saturated conditions, with class-C transistor amplifiers dominating the lower microwave frequency range. Recent improvements in bipolar transistors now make it possible to develop wide-band class-A microwave power amplifiers.[1,2,3] Class-A operation has very definite advantages compared to standard class-C operation; besides a much larger dynamic range, it offers lower second-harmonic output, lower amplitude modulation/phase modulation conversion, higher gain, and a wider bandwidth capability, especially at the upper useful frequency end of a particular transistor. The drawbacks are lower overall efficiency and the requirement that the transistor must tolerate forward biasing at high cw dissipation levels without thermal runaway.

Over the last few years, transistors have been developed that include heavy emitter ballasting and thus permit class-A operation up to 4 GHz. Some of the possible applications for these devices in the communications field are very wide-band driver amplifiers with large dynamic range for laser communications links, truly linear power amplifiers for multiple carrier repeater stations, or wideband i.f. driver amplifiers for millimeter wave upconverters. Many other applications probably will open up when system designers become aware of the possibilities of class-A power amplifiers in the microwave frequency range.

In this paper we discuss the present state of the art in ballasted microwave transistors and their applications to microwave power amplifiers. Some results obtained recently with FET transistors are included to illustrate the upcoming full band coverage with linear amplifiers to X-band.

Linear microwave power transistors

The present state of the art of class-A power transistors at frequencies above 1 GHz is illustrated in Fig. 1. The TA numbers represent RCA developmental devices operating common base in

Erwin F. Belohoubek, Head. Microwave Circuits Technology. RCA Laboratories. Princeton, N.J., received the degree of Diplom-Ingenieur in 1953 and the PhD in Electrical Engineering in 1955 from the Technical University in Vienna, Austria. From 1953 to 1955, he worked as Research Assistant at the Institute for High-Frequency Techniques of the same university. He joined the RCA Tube Division in Harrison, N.J., in 1956 and transferred to the Microwave Applied Research Laboratory in Princeton, N.J., in 1957 as a Member of the Technical Staff. In this position, he worked on the development of magnetrons, electrostatically and magnetically focused traveling-wave tubes, and a crossed field microwave delay tube. In 1969, Dr. Belohoubek was put in charge of a group working on microwave hybrid integrated circuits. In this capacity, he is responsible for the development of passive and active MIC circuits which include high-power transistor amplifiers, multipliers, linear bipolar and FET amplifiers, electron-beam, semiconductor amplifiers, circulators and limiters, and small microwave subsystems. He received an Outstanding Performance Award of the RCA Electronic Components Division in 1963 and an RCA Laboratories Achievement Award in 1967. Dr. Belohoubek holds five patents and has written more than twenty papers in the areas of microwave techniques, traveling-wave tubes, and microwave integrated circuits. He is a Senior Member of the IEEE.

David S. Jacobson, Mgr., RF and Microwave Devices Design. Solid State Division. Somerville, New Jersey, received the BChE from the Polytechnic Institute of Brooklyn in 1954. He then joined the General Electric Company where he participated in the Chemical and Metallurgical Training Program. After a tour in the U.S. Navy, Mr. Jacobson joined the Semiconductor Division of Texas Instruments in 1958 and worked on processing techniques for grown-junction silicon transistors. Mr. Jacobson joined the RCA Semiconductor and Materials Division in 1961 as a device development engineer; he engaged in the development of germanium double-diffused transistors and germanium and gallium-arsenide tunnel diodes. He was promoted to Project Leader of the Varactor Device Design and Development group where his major responsibilities included the development of high-reliability varactors for the LEM program. Mr. Jacobson transferred to the RF Transistor Design group in 1965 where he worked on the 2N3866 overlay transistor. Subsequently, he was responsible for the design and development of microwave power transistors, including the 5-watt, 2-GHz 2N5921 and 2N6266 and the 2-watt, 2-GHz 2N5920 and 2N6265. Mr. Jacobson was promoted to Engineering Leader of the Microwave Transistor Design group in 1968. In that position he was responsible for the design and development of microwave power transistors, low-noise transistors, and transistors for CATV applications. He is presently responsible for the design of all RF and Microwave Transistors and Microwave Integrated Circuits.
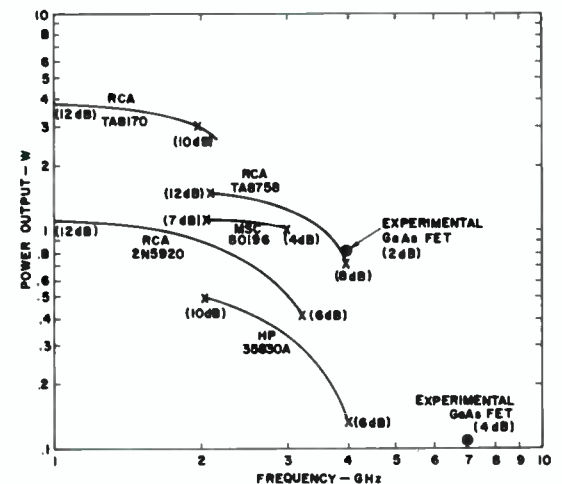
Fig. 1 — Power output curves (above 1 GHz) of several linear power transistors, including RCA developmental devices.

microstrip carriers. The results for the HP device are also for common base operation, while the MSC device performance is given for common emitter. The gain (shown in brackets) of the latter device would probably increase somewhat if used in a common base microstrip carrier. Common base is used nearly exclusively with all class-C transistors in the microwave range; it also provides higher gain performance in class-A but requires careful circuit design to avoid instabilities and makes the dc bias circuitry more complex.

The effect of ballasting on class-A transistor performance can best be understood by comparing Figs. 2a and 2b. The transistors in both cases use the same geometry, an overlay structure with broad, thick emitter metallization. The unballasted version (Fig. 2a) shows a very rapid fall-off in gain for collector currents above 200 mA. The onset of this decline is characterized by a thermal imbalance in the chip, where one part of the transistor starts hogging the current while the rest of the transistor practically is turned off. If operated at currents considerably above the point where the rapid gain decline sets in, the transistor will be destroyed by local overheating. The gain fall-off is not only influenced by ballasting but also by the magnitude of the rf drive. At high
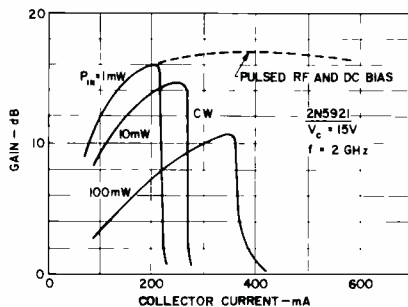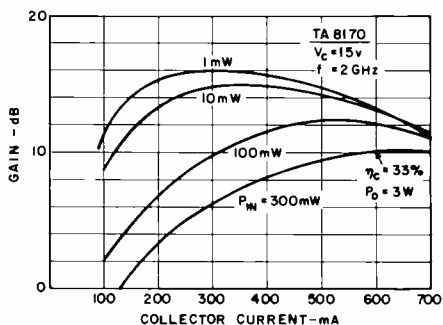
Fig. 2 — Effect of ballasting on class-A transistor performance: 2a (curve above) for unballasted transistor; and 2b (curve below) for ballasted transistor.

Fig. 3 — Cross section of ballasted overlay transistor.

drive levels, the transistor can be biased at much higher collector currents without incurring thermal runaway. In the extreme of very high drive into saturation, the average dc power dissipation capability approaches that of class-C operation, which for this particular transistor is approximately 12 watts.

The key to successful true class-A operation at high-power levels lies in heavy enough ballasting of the emitter to practically eliminate the termal imbalance within the transistor chip. Fig. 3 shows the crossection of a typical overlay transistor, which includes emitter ballasting. A polycrystalline silicon layer interspersed between the aluminum metallization and the shallow diffused emitter sites acts as the vehicle for introducing ballasting to the emitter sites. For heavy ballasting, the metallization of each emitter finger is interrupted where it normally connects to the common-emitter bond pad. The current has to pass through the polycrystalline silicon layer, which permits heavy emitter debiasing in the order of 200 mV. The debiasing provides degenerative feedback to prevent excessive current in any portion of the transistor and thereby controls the hot spotting. The effect of the emitter finger ballasting is illustrated in Fig. 2b. No rapid gain fall-off exists up to 700 mA of collector current, except for a gradual decline associated with the normally observed f_T (gain-bandwidth product) fall-off at high collector currents.[4] At 600 mA, a power output of 3 W with 33% efficiency can be obtained.

If the transistor size is rather small, hot spotting generally is less pronounced and lower levels of emitter ballasting are sufficient (e.g., 40 to 100 mV). This is particularly important if operation at higher frequencies is desired where the reduction of rf gain due to heavy

ballasting may become excessive. For high-frequency operation, a technique designated as emitter site ballasting is utilized where the contacting geometry of the metallization is designed so as to place the polycrystalline layer as ballast resistor in series with each emitter site. The TA8758 that provides linear performance at the 1-watt level at 3.4 GHz is a typical example of this type of ballasting.

Linear power amplifiers

Besides providing linear multiple-signal amplification, ballasted transistors in class-A operation generally also offer improved high-frequency response and wider bandwidth capability than their class-C counterparts.

Class-C operation is severely limited by turn-on problems at high frequencies due to the high Q of the input impedance, which makes it very difficult to match into the transistor over a wide-frequency range. Class-A operation provides more gain, and since the transistor is always biased well into forward conduction, it does not depend critically on a good input match to turn on. On the contrary, for truly wideband operation, the input impedance may be even negative over a
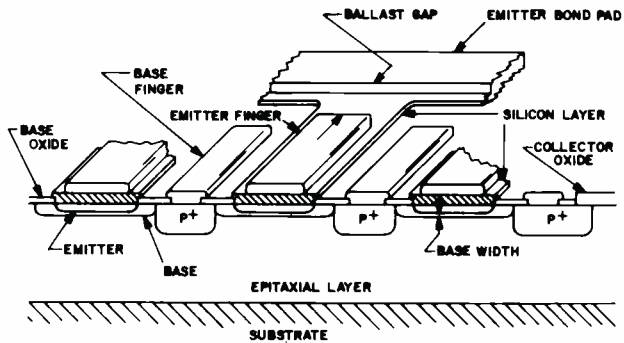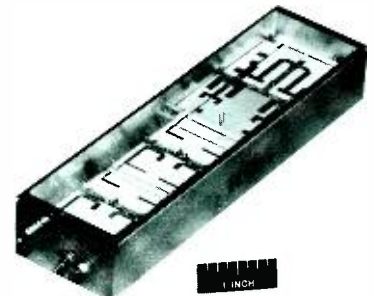
Fig. 4 — Hybrid integrated-circuit, 1-2 GHz power amplifier.

large part of the operating bandwidth. To overcome cascading problems under these conditions, two class-A amplifiers are generally combined by 3-dB hybrids in each stage, which not only provides more power but also effectively decouples the stages from each other.

The above techniques were successfully demonstrated in the octave bandwidth L-band power amplifier shown in Fig. 4. Amplifiers with 1 GHz or more bandwidth capability are required, for example, in gigabit data links. To obtain approximately 10W of cw power, two directly paralleled power transistors are employed in each arm of the balanced output stage. Power sharing is ensured by individual dc biasing of each of the four output transistors. The near-saturation performance of the three-stage amplifier, which measures 5.65 x 1.5 x 0.925 inches, is shown in Fig. 5. The overall efficiency of the amplifier including bias network losses ranges from 16% to 24% over the band. A single power supply of 17 volts drives the amplifier module.

The same technique that was used successfully to combine four transistors in the power stage of the above amplifier, if applied to the smaller high-frequency transistor TA8758, would provide a 2-W power output capability for a linear amplifier in the 3.7 to 4.2 GHz communications band. Fig. 6 shows the performance of a single-cell transistor at 4 GHz. The P_{in}/P_{out} curve shows a gain reduction at low rf drive levels, which indicates a small remaining thermal non-uniformity throughout the chip. The amount of this gain compression depends on the degree of ballasting, the location of the bias point and, since the local hot spots generally are also affected by the output loading, to some extent on the load impedance.
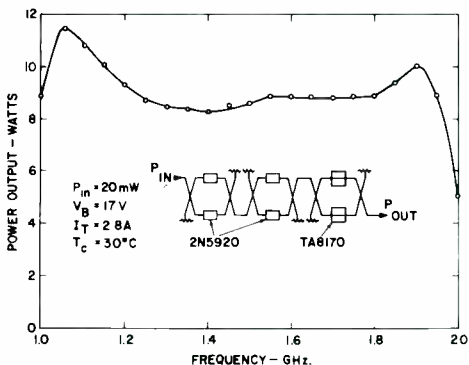

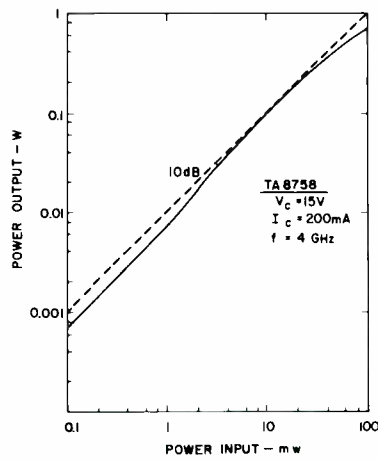Fig. 5 — Performance of 1-2 GHz power amplifier.

Fig. 6 — Performance of emitter-ballasted transistor amplifier at 4 GHz.

For frequencies above 4 GHz, *GaAs* field-effect transistors are presently being developed that have superior high-frequency capabilities and better power-sharing characteristics. The positive temperature coefficient of *GaAs* makes the FET much less susceptible to thermal runaway conditions prevalent in un-ballasted bipolar transistors; paralleling of many cells is thus possible without hot spotting. The FET has, however, a more difficult topology since all three electrodes of each cell appear on top of the chip. Interconnection of many cells without incurring excessive parasitics and feedback is thus more difficult than with bipolar transistors. Recent experimental results obtained with power FETs are included in Fig. 1. The highest power output to date is 0.8 watt at 4 GHz, which was achieved with six paralleled cells on a single *GaAs* chip.[5]

Preliminary results from a two-stage FET amplifier covering the frequency range from 4.5 to 6 GHz are shown in Fig. 7. This amplifier uses two chip-mounted, experimental, single-cell FETs in a circuit that measures only ½ × ¾ inch. Simple, combined, distributed, and lumped matching networks provide excellent gain flatness and phase linearity. FETs have the added advantage of a more linear P_{in}/P_{out} characteristics close to the saturation level compared to that of bipolar transistors. Therefore, the intermodulation distortion of FETs is generally lower at power levels a few dB below saturation.

Conclusion

The advent of well-ballasted bipolar
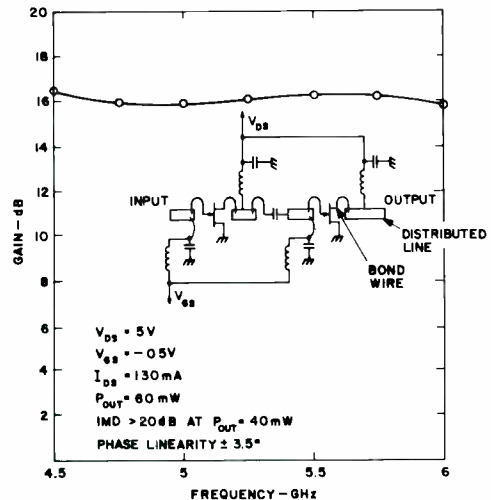
Fig. 7 — Performance of two-stage FET amplifier.

microwave power transistors makes it possible to develop wideband amplifiers that in many cases represent a superior alternate to present TWTs. Except for a lower tolerance to high-temperature operation, the solid-state amplifiers have the inherent advantages of better reliability, smaller size and weight than even the most advanced minitubes, much simpler power requirements, better gain flatness, less susceptibility to mechanical shock and vibration, and they require no warm-up time. Within the next 1 to 2 years, bipolar class-A amplifiers with 3-W output are expected to reach 4 GHz, while FETs should approach the 1-W level at 10 GHz.

Acknowledgment

References

1. Presser, A., et al. "1.5 Watt, S-band Linear Transistor Amplifier", *High-Frequency Generation and Amplification Conference*, Cornell, pp. 445-450, June 1971.

2. Presser, A., et al. "1-2 GHz High-Power Linear Transistor Amplifier", *RCA Review*, vol. 33, pp. 737-751, December 1972.

3. Renkowitz, D., "L- and S-Band MIC Power Amplifiers Come of Age", *NEREM Record*, vol. 13, 1971.

4. Muller, O., "Ultralinear UHF Power Transistors for CATV Applications", *Proc. IEEE*, vol. 58, pp. 1112-1121, July 1970.

5. Napoli, L. S., et al. "High-Power GaAs FET Amplifier - A Multigate Structure", *Digest, IEEE International Solid State Circuits Conference*, pp. 82-83, February 1973.

31

Digital image transform encoding

W. B. Schaming

The transmission and storage of continuous-tone imagery in digital form is a subject of intense investigation by a large and ever increasing number of researchers. One particular area of investigation receiving much attention is image encoding. In general, the purpose of this research is to determine ways in which an image can be encoded to reduce the total number of bits required to represent the image. Most techniques produce a small amount of degradation to achieve large reductions in the number of bits required. Obviously, the more degradation one can tolerate, the greater the bit compression ratio (BCR) that can be achieved. Two measures of this degradation are the mean-square error in the reconstructed image and subjective ranking by untrained observers, although no one asserts that either of these measures is adequate as an image quality standard. Many different approaches to image encoding have been studied, including one- and two-dimensional differential pulse-code modulation (DPCM), one- and two-dimensional transform coding, contour coding and a host of variations. The subject of this article is the research carried on in Advanced Technology Laboratories in the area of two-dimensional digital image transform coding.

W. B. Schaming, Advanced Technology Laboratories, Camden, NJ, received the BSEE in 1962 from Gannon College, where he was the recipient of the alumni award for general scholastic excellence. In 1964, he was awarded the MSEE from the University of Pennsylvania. Mr. Schaming joined the Astro-Electronics Division in 1962, where he worked on slow-scan television cameras for space-observation systems. In 1964, he transferred to the Advanced Technology Laboratories, where he has been engaged in projects requiring computer solution and simulation. The projects have included signature analysis, part retrieval systems, Monte Carlo techniques, generation and processing of magnetic anomaly signals, generation of buffered I/O systems, generation of graphical output, functional simulation of computer systems, and real-time processing. Mr. Schaming has many years of experience in computer systems and programming, with primary emphasis on the integration of digital computers into engineering systems In addition, he has conducted extensive research and development in the areas of image encoding and picture processing.

TRANSFORM coding is generally understood to mean that the picture elements in the spatial domain are mapped via some linear process into the transform domain. When the Fourier transform is used, the transform domain is the familiar frequency plane. The elements in the transform domain may then be thinned by some algorithm and quantized. This thinning and quantization leads to the reduction of the number of bits required to represent an image, since some of the transform coefficients are discarded and most of the retained coefficients may be represented by fewer bits than an original PCM sample in the spatial domain. Various transformations, including Fourier, have been compared in detail by other researchers. (For an excellent discussion of transform picture coding the reader is referred to an article by Wintz,[1] which also provides an extended bibliography on the subject.)

Image partitioning

An image represented as an $N \times M$ array of picture elements (pels) can be partitioned into $n \times n$ subpictures as shown in Fig. 1. $N \times M$ image contains NM/n^2 $(n \times n)$ subpictures.

The choice for the size of subpictures has been varied in our studies. As indicated in Ref. 1, subpicture sizes between $n = 4$ and
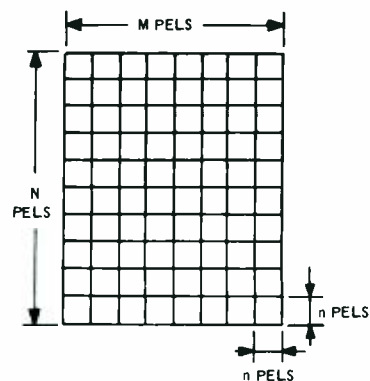
Fig. 1 — Partitioning of NxM array of pels into nxn subpictures.

$n = 16$ are adequate and yield comparable results. It is felt that 8×8 is large enough to provide flexibility in the coefficient thinning studies and yet small enough that real-time implementation is not ruled out. However, if the additional storage is acceptable, 16×16 subpictures tend to produce better results at a given bit rate.

Subpicture transformation

The Fourier transform has been the vehicle for coding studies under the current project. However, the transform is applied to image data in such a way that the input data to be transformed exhibits fixed, known symmetries.

The Fourier transform and corresponding inverse given by Eqs. 1 and 2 can be used to transform each image subpicture. This discrete transform is equivalent to a Fourier series expansion, and will therefore treat each subpicture being transformed as though it were a period of a two-dimensional periodic function as shown in Fig. 2.
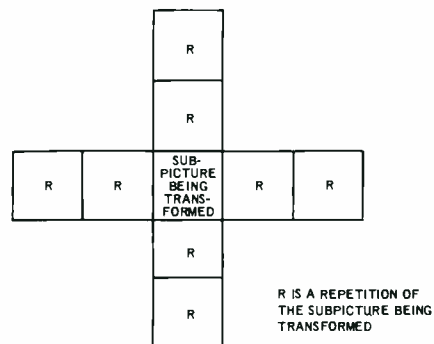
Fig. 2 — Image subpicture shown as 2-d periodic function.

Fig. 3 — 4x4 subpicture taken from image.

$$F(u,v) = \frac{1}{N} \sum_{x=0}^{N-1} \sum_{v=0}^{N-1} f(x,y)$$
$$\exp\{(-2\pi i/N)(xu+yv)\} \qquad (1)$$

$$f(x,y) = \frac{1}{N} \sum_{u=0}^{N-1} \sum_{v=0}^{N-1} F(u,v)$$
$$\exp\{(2\pi i/N)(ux+vy)\} \qquad (2)$$

Edge effects

When viewed as a periodic function, differences in brightness values on opposite edges of the subpicture create discontinuities in the periodic function. The existence of these discontinuities contributes high frequency energy in the transform domain. Anderson and Huang suggested increasing the subpicture size by one row and column whose values are the average of opposite edge subpicture samples as one way to help smooth this discontinuity.[2] They observed improvement by using this technique.

Phase considerations

The transformation of an 8×8 subpicture produces 64 complex coefficients in the Fourier domain. However, since the image samples are real, the complex coefficients exhibit conjugate symmetry through the origin. Therefore, only half of the samples are independent, and an 8×8 subpicture can be completely specified by 32 coefficients (64 numbers). Research by Andrews and Tescher of USC indicates that the phase information is extremely important.[3] In fact, when encoding the amplitude and phase of the complex coefficients, more bits were assigned to phase than to amplitude.

Symmetric transformation of subpictures

A method which has been the subject of our investigations is presented here for preventing the warped spectrum caused by discontinuities in the periodic
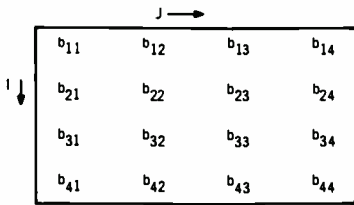
functions and at the same time guaranteeing that phase information is preserved exactly.

Given the 4×4 image subpicture shown in Fig. 3 whose elements are the brightness values b_{ij}, an 8×8-element subpicture can be constructed as shown in Fig. 4. (A 4×4 initial subpicture is used here for ease of illustration.) With the x and y axes drawn as shown in Fig. 4 (no samples on either axis) and the brightness samples assumed to be in the center of the sampling interval, the 8×8 subpicture is even

symmetric about both the x and y axes. When the original 4×4 subpicture of Fig. 3 is transformed, 16 independent numbers are required to specify the subpicture. When the 8×8 even symmetric subpicture is transformed, still only 16 independent numbers are contained in the 64 Fourier coefficients. This is because the transform of a function which is even symmetric in both directions produces coefficients which are pure real and equal in all quadrants. Since the transform of the even symmetric subpicture is pure real, the phase is zero and need not be considered.

Fig. 4 — Even symmetric 8x8 subpicture constructed from 4x4 subpicture of Fig. 3.

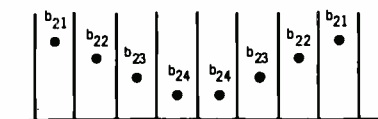

Fig. 5 — Subpicture samples from Fig. 3.

Fig. 7 — Subpicture samples as appear in the even symmetric subpicture of Fig. 4.
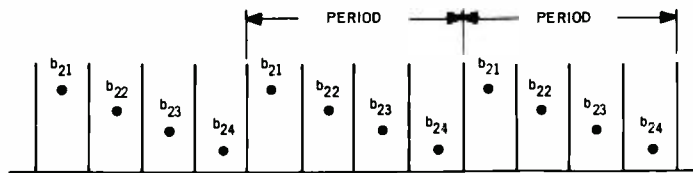

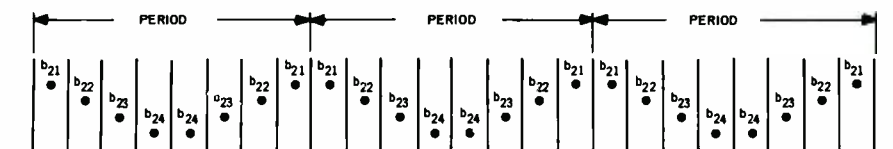Fig. 6 — Subpicture samples in the periodic representation of Fig. 5.

Fig. 8 — Subpicture samples in the periodic representation of Fig. 7.
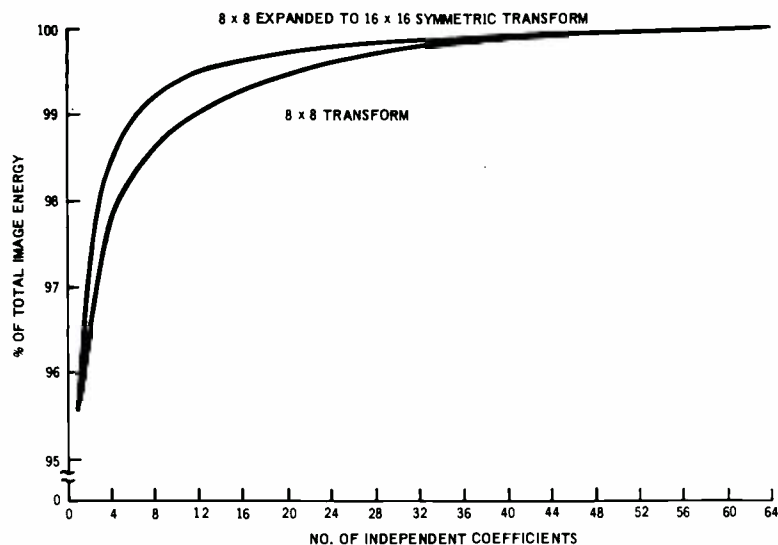
33

Fig. 9 — Convergence of two transform methods.

Furthermore, the discontinuity in the periodic function is eliminated, thereby removing extraneous high frequency energy in the spectrum. Suppose that the original samples b_{21}, b_{22}, b_{23}, b_{24} have brightness values as shown in Fig. 5. The same line of samples in the periodic function would appear as in Fig. 6 which clearly shows a discontinutiy. On the other hand, the same samples when taken from the expanded 8×8 even-symmetric subpicture of Fig. 4 appear as in Fig. 7. The periodic rendition of this same line in the symmetric subpicture appears as shown in Fig. 8 which clearly has no discontinuity. Therefore no articficial high frequency energy is inserted into the specturm.

Comparison of symmetric and nonsymmetric subpicture transformation

The series representation of the image taken from the even-symmetric transform will converge faster than that taken from the straight transformation. To illustrate this, a test picture was transformed first by directly transforming each 8×8 subpicture in the image to obtain the coefficients for each subpicture. It was also done by transforming a 16×16 symmetric subpicture derived form each 8×8 region of the image. The convergence rates for the two methods can be seen in Fig. 9.

Transform coefficient thinning and quantization

The reduction of the number of bits

required to represent an image comes about through the thinning and quantizing of the coefficients in the transform domain prior to transmission. Many differenct approaches have been investigated and reported in the literature. The approach used in our investigations is a combination of these techniques. Some of the variations introduced were dictated by our initial goal of having the encoding process useful for real time implementation. This implies that the entire image is not available prior to the encoding process.

Ordering of coefficients

Most of the reported coefficient thinning techniques require that the coefficients be ordered by the variance computed from all the subpictures in the image. Our finding in the limited experiments performed has been that this type of coefficient ordering agrees quite well with the ordering of coefficients by their distance from the dc coefficient. As shown in Fig. 10, all coefficients in a band are an equal manhattan distance from the dc coefficient $C_{o,o}$. [The *manhattan distance* is defined as the number of increments in the x and y direction from $C_{o,o}$ to $C_{i,j}$.] The variance of any coefficient taken from the subpictures in the image tends to decrease with increasing band number, since the energy content of most images decreases with increasing spatial frequency. This seems to be supported by the findings of Landau and Slepian.[4] Furthermore our observation has been that all coefficients within a band of equal manhattan distance tend to have com-

parable variances.

Thus it seems reasonable that all coefficients within a band of equal manhattan distance have equal significance, on the average, in the image reconstruction.

Thinning techniques

Some of the most popular techniques for the thinning of coefficients are the following. The simplest approach is to keep the first η coefficients (ordered by variance) in the transform plane. No additional bookkeeping is required since the same coefficients are transmitted for every subpicture in the image. η is determeined by examining the variances of the coefficients. The next approach in order of complexity is to keep the η largest coefficients (ordered by their variance) in each subpicture. This requires additional bookkeeping bits to indicate which coefficients are being transmitted. Both of these approaches can be made to adapt to local picture content by letting η vary for each subpicture by thresholding the amount of energy preserved. This requires that η be also transmitted for each subpicture.

Quantization techniques

The simplest quantizing scheme is one in which each coefficient is normalized by its standard deviation (σ) such that all coefficients can utilize the same quantizer and are assigned the same number of bits. Another approach is to normalize the coefficients by their σ, but vary the number of bits assigned to the coefficients. The number of bits assigned can be made proportional to the coefficient variance.

Strategy in current experiments

Two approaches have been used in this project, one of which is adaptive, the other is not. Both approaches use the same quantizing technique but different thinning techniques. The test image was partitioned into strips of subpictures as shown in Fig. 11. For a 256 × 256 image, there are 32 strips each having 32 8×8 subpictures. Each strip of subpictures was encoded independent of all other strips. This approach is dictated by our assumption that the entire image is not stored prior to encoding. Each 8×8 element subpicture in a strip was then expanded to an even-symmetric 16×16

subpicture and transformed. The variances of the coefficients shown in Fig. 10 from all subpictures in the strip where then computed. However a separate variance for each coefficient was not computed. Instead, one variance was computed for each band of coefficients having the same manhattan distance from $C_{0,0}$. In our investigations we never use more than the eighth band of coefficients when using 8×8 subpictures, therefore only eight σ's are computed. For example σ_3 corresponding to band 3 is computed form the values of $C_{0,2}$, $C_{1,1}$, $C_{2,0}$ taken from each of the 32 subpictures in the strip. This is justified since our observations show that coefficients in bands of equal manhattan distance tend to have comparable mean and variance. After computing the σ for each coefficient band, the coefficients are then divided by the proper σ and passed through the same 6-bit quantizer. (in the case of the dc coefficient, $C_{0,0}$ the mean is subtracted before normalization.) All six bits are not utilized for each coefficient band. A typical assignment of bits for the coefficients in the first eight bands is given in Fig. 12. When a 3-bit quantizer is desired for band 3, the three most significant bits are retained from the 6-bit quantizer.

Nonadaptive thinning has been employed by retaining the first N bands of co-efficients in each subpicture. Adaptive thinning has been used in which the number of bands varies for each subpicture. Successive bands are kept until a preset percentage of the total energy in the subpicture is exceeded. Only the determined number of bands of coefficients are then quantized and transmitted. For this adaptive approach a minimum of three bands and a maximum of eight bands are used when the subpicture size is 8×8 elements.

Overhead bits

For the nonadaptive thinning and quantizing scheme using N bands [$N(N+1)/2$ coefficients] for each subpicture, the required bookkeeping bits include those required to code the dc mean, $M_{0,0}$ as well as the value of σ for each band. This data is required for each strip of subpictures. Therefore the overhead per picture element is given by

$$Overhead = \frac{N \times 8 + 6}{32 \times 64} \quad bits/pel \quad (3)$$

assuming eight bits for each σ and six bits for the dc mean.

In the adaptive thinning and quantizing scheme, a value of σ for each of the eight bands must be transmitted for each strip of subpictures, in addition to the dc mean since that is the maximum number of bands which any subpicture might require. In addition, a 3-bit number is transmitted for each subpicture in the strip to specify the number of coefficient bands being transmitted. Therefore the required overhead for the adaptive technique assuming eight bits for each σ and six bits for $M_{0,0}$ is given by

$$Overhead = (8 \times 8 + 6)/(32 \times 64) + (3/64)$$
$$= 0.081 \quad bits/pel \quad (3)$$

Generation of 6-bit quantizer

The 6-bit quantizer used in our ex-periments assumes that each coefficient has a gaussian probability density and has been standardized prior to quantiz-ing. The cut points were generated first and the representative values for the reconstruction levels were taken as the midpoint between successive cut points. The cut points were generated using the method described by Andrews which minimizes mean-square error.[5]
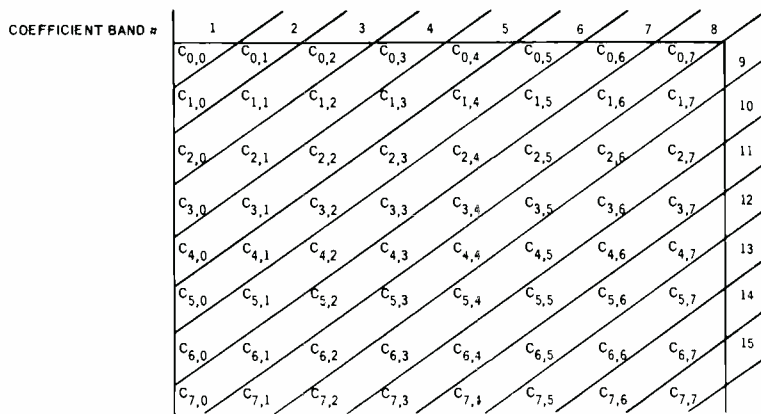

Fig. 10 — 64 independent real coefficients from transform of even-symmetric 16x16 subpicture.

Fig. 11 — Strips of subpictures from original image.

Fig. 12 — Typical bit assignment for first 36 coefficients.

Effects of bit errors

One of the concerns in any encoding process is the sensitivity of the encoded data to channel noise which results in bit errors in the received data stream. Transmission links are often characterized by specifying the probability of any bit being in error at the receiver. This probability may vary from 10^{-2} to 10^{-5}.

The effect of bit errors on the reconstructed image received over a transmission link greatly depends upon the encoding process. When transmitting an image in the spatial domain using a PCM sample for each picture element, the bit errors appear in the reconstructed image as the familiar salt-and-pepper noise. When DPCM (delta modulation) is used, the bit errors will appear as streaks in the image. When a transform encoding process is utilized, however, the results are quite different. A bit error will result in the wrong value for a coefficient in the transform domain. However, the inverse transformation operation will spread the effects of the bit error over the entire subpicture to which the coefficient belongs. The resultant degradation will depend upon the subpicture size used in the encoding process as well as the allocation of bit patterns to the reconstruction levels in the quantizer.

Simulations have been performed inserting bit errors into the transmitted data stream using both 8×8 and 16×16 subpicture sizes encoded with the same average bit rate.

Although the total number of bits required to describe each of these images is the same, and the number of bit errors inserted in each image is the same, the resulting images appear very different. Using an 8×8 element subpicture size, there are 1024 subpictures in the total image. There are only 256 subpictures in the total image when the subpicture size is 16×16 elements. As a result, when using the smaller subpicture size, the chances of getting a bit error in the most significant bits of very low frequency coefficients is four times as great.

Images were encoded using a natural ordering of the code words in a six-bit quantizer as shown in Fig. 13. When less than six bits are used for a given coefficient, the desired number of high-order bits are retained. In studying Fig. 13, one can conclude that th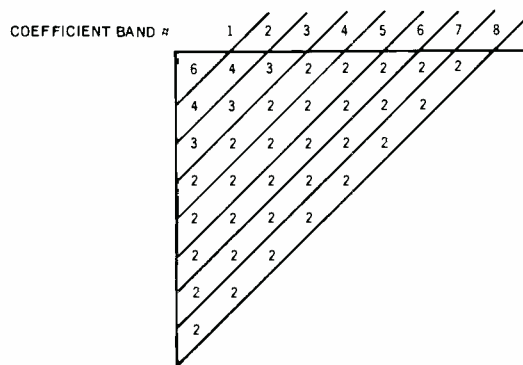e natural ordering of the code words is disadvantageous. The code words near the peak of the coefficient distribution have the highest probability of being used. However when using the natural ordering

of code words, a bit error in the most significant bit of a code word near the peak of the distribution results in a maximum shift of 32 reconstruction levels. For example, an error in the most significant bit of code word 32 results in the code word 0, which is located at the left end of the distribution. Likewise, an error in the most significant bit of code word 31 results in code word 63, which is at the right-hand end of the distribution. It appears that simply revising the order of the code words on the left half of the distribution would provide considerable reduction in error sensitivity. This results in the inverted order code words also shown in Fig. 13. For this ordering of the code words, a bit error in the most significant bit of a code word near the peak of the coefficient distribution results in a small shift in the reconstructed level. A bit error in the most significant bit of a code word on the tail of the distribution will now result in a shift to the opposite tail. However, the probability of being on the tail of the distribution is much smaller.

Experimental results

The images shown in Fig. 14 are the result of applying the techniques described
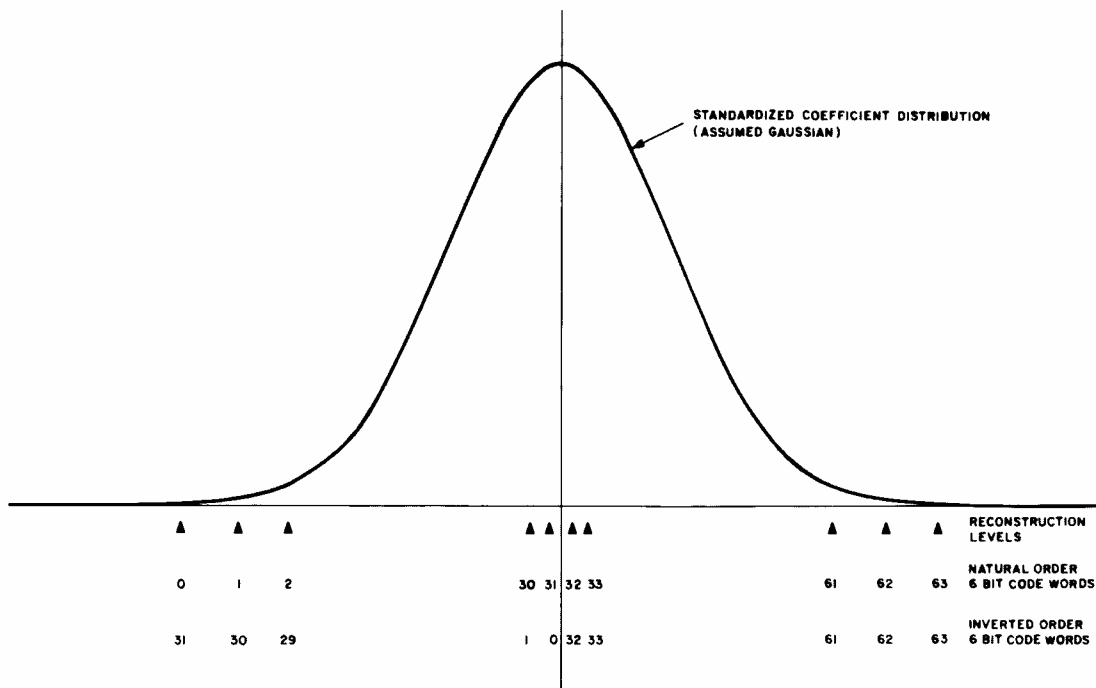

Fig. 13 — Two possible code-word assignments for 6-bit quantizer.

above to the sample image. The pertinent data applying to each picture is given in Table 1. The percent mean-square-error values in the table are computed from the reconstructed image by

$$\% \ mean \ square \ error = \frac{\dfrac{1}{N^2} \displaystyle\sum_{i=1}^{N} \sum_{j=1}^{N} (I_{ij} - I'_{ij})^2}{\dfrac{1}{N^2} \displaystyle\sum_{i=1}^{N} \sum_{j=1}^{N} (I_{ij})^2} \ 100\% \qquad (5)$$

where I'_{ij} are reconstructed image samples.

Conclusions

The results produced by these experiments indicate that a reduction of 10:1 in the number of bits required to represent an image, with only small degradation, is feasible using these techniques. The effect of a noisy transmission channel, although different from PCM or DPCM systems, is not catastrophic and, in some cases, is less disturbing to the observer.

Although no tests have been attempted, it may be possible to take an additional transform in the frame-to-frame direction to take advantage of the high frame-to-frame correlation of a tv-type signal. This would be equivalent to a three-dimensional transform.

References

1. Wintz, P.A.; "Transform Picture Coding." *Proc. IEEE*, Vol. 60 (July 1972) pp. 809-820.

2. Anderson, G.B. and Huang, T.S.; "Piecewise Fourier Transformation for Picture Bandwidth Compression," *IEEE Trans. Comm. Tech.*, Vol. COM-19, No. 2 (April 1971) pp. 133-140.

3. Tescher, A.G.; "Adaptive Intra-and Inter-Frame Image Coding Utilizing Fourier Techniques," USC Image Processing Research Semiannual Technical Report No. USCEEE 444. pp. 24-33.

4. Landau, H.J. and Slepian; "Some Computer Experiments in Picture Processing for Bandwidth Reduction," *Bell System Tech. Jour.*, (May-June 1971) pp. 1525-1540.

5. Andrews, H.C.; "Computer Techniques in Image Processing" (New York, N.Y.; Academic Press; 1970) p. 144.

Table I — Reconstructed image statistics.

Picture number	Subpicture size	No. of bands or % energy	Bit error rate	Bit/pel	Bit compression ratio	% mean square error
1	Original image	NA	0	8.0	1	0
2	8×8	5 bands	0	0.8	10.0	0.56
3	16×16	10 bands	0	0.8	10.0	0.50
4	16×16	8 bands	0	0.58	13.79	0.70
5	8×8	99.3%	0	0.77	10.4	0.54
6	8×8	99.5%	0	0.85	9.4	0.48
7	8×8	5 bands	10^{-3}	0.8	10.0	*
8	16×16	10 bands	10^{-3}	0.8	10.0	0.81
9	16×16	10 bands	10^{-2}	0.8	10.0	1.77
10	16×16	10 bands	10^{-2}	0.8	10.0	1.54

Notes:
— For 8×8 subpictures the number of bits/coeff. in successive bands in 6,5,4,3,2,
— For the apaptive images (5 and 6) the number of bits/coeff. in successive bands in 6,5,4,3,3,3,3,3,
— For 16×16 subpictures the number of bits/coeff. in successive bands is 6,6,5,5,4,4,3,3,3,3,
  Picture 10 is identical to 9 except that the inverted ordering of the code words described in Fig. 13 is used.
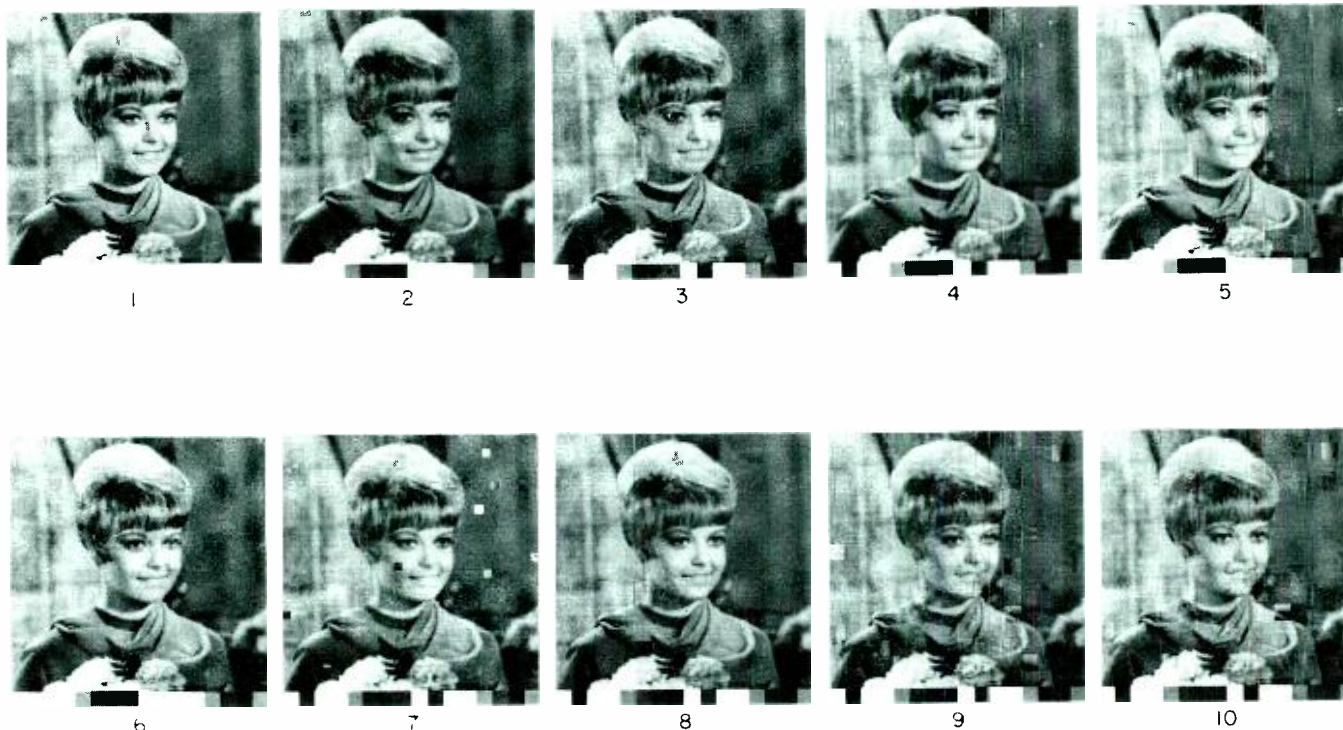* Mean square error extremely large due to large dc errors in many blocks

1 2 3 4 5

6 7 8 9 10

Fig. 14 — Images corresponding to data in Table I.

# Numerical control applications for spacecraft components

D. Charrier | M. F. Luft

RCA Limited has been involved with numerically controlled (NC) equipment since 1969. Originally, its function was to provide an in-house means of machining high-tolerance parts for Canadian communication contracts. The business has since expanded to include the fabrication of satellite components required for commercial applications. Resulting from this growth, enhancements to the in-house NC shop have doubled the value of the equipment (present value approximately $1 million) and increased capacity by 40%. This paper is divided into three sections: 1) definition of NC, 2) computer interface, and 3) present and future usage at RCA.

M. Luft, Management Information Systems, RCA Limited, Montreal, graduated from McGill University in 1968 with a B.Sc. degree in mathematics. He then entered the University of Waterloo to obtain a Masters degree in Mathematics and Computer Science. Mr. Luft spent one year as a programmer analyst with the Federal Government employed in the Marine Sciences branch of the Oceanographic Research Department. He joined RCA Limited in 1970 as an Administrator of Engineering Systems within the Management Information Systems department. His main function includes technical support for the Government and Commercial Systems Division on all aspects of computer applications.

Dan Charrier, Fabrication Model Shop, RCA Limited, Montreal, graduated from Ecole Polytechnique in 1970, obtaining his Bsc A and Mechanical Engineering degree. He then joined Canadian General Electric's technical support staff specializing in the area of NC applications. In 1972, Dan developed and programmed the G.E. post processor for the CIM-X tool changer equipment now in use at RCA Limited. In the Fall of 1972, Dan joined RCA Limited as a senior NC Project Leader within the Fabrication Model Shop.
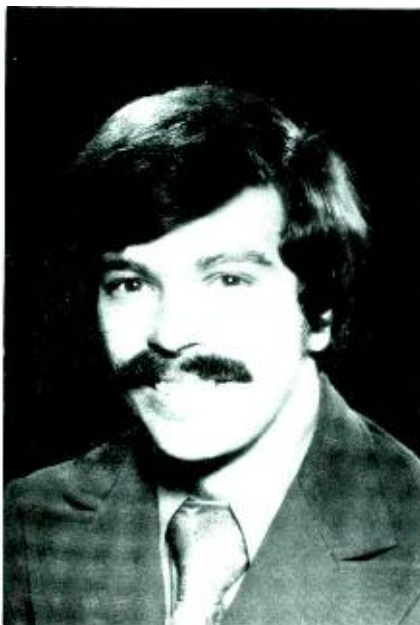
NUMERICAL CONTROL (NC) is a technique for the control of production tools by information prerecorded in symbolic form. It is a method designed to optimize in advance and then control the work of a metal-cutting machine tool.

The NC concept

The concept of NC was developed during the late 1940's by John Parson, an engineer who was preparing templates for aircraft component construction. The complex airfoil design was defined geometrically by a series of curves; this approach enabled Parson to represent integral template points with a table of X and Y coordinates. His men drilled holes in the template sheet metal which formed straight lines, tangent to all the various points on the desired curve — a complex calculating and measuring task in itself. An error in any one of thousands of measurements might ruin a template. The operators then filed the remaining cusps until a faired curve resulted. Parson conceived the idea that the dimensions could be recorded on punched cards; that the cards could be read by a machine; and, that servo-motors could move the template to the correct position under the cutting tool.

The Servo-Mechanism Laboratory at M.I.T. was commissioned to work out the details of Parson's theory. M.I.T. developed a machine control system in which the control instructions were embodied in a paper tape. The tape was punched by the manufacturing engineer to achieve the exact machine movements he wanted. The tape reader and servo-controls caused the machine to execute those instructions repeatedly and dependably. Since then NC revolutionized the metal-working art. Today, one quarter of all metal-cutting machine tools are numerically controlled and applications outside the metal-cutting field are occurring with increased frequency.

Present machines in use are a CIM-X series 20 (Fig. 1) featuring a 24-tool drum with a 3-axis contouring capability, and a jig borer (not shown) having an accuracy of 80-millionths of an inch.

Computer interface

Computerized numerical control applies computer languages and systems to the
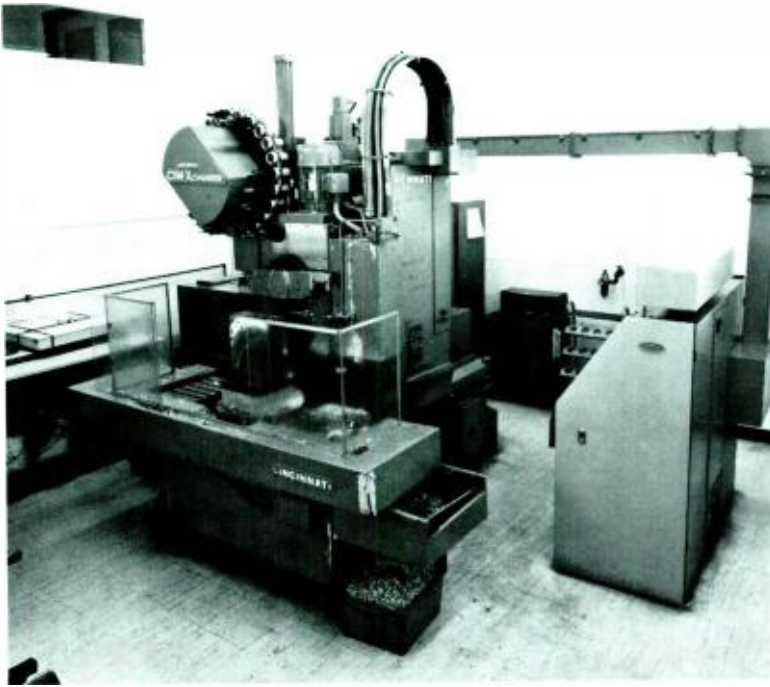
38

Fig. 1 — Photo of a CIM-X tool changer machine used in the numerical control applications at RCA Ltd.　Fig. 2 — Part programs are prepared by perforating paper tapes to be used in controlling part production.

preparation of control instructions for guiding machine tools in their production of machine parts. Automatically programmed tools (APT) is the programming system which generates these instructions. The APT process is divided into three integral steps: 1) vocabulary, 2) part program, and 3) post processors.

APT vocabulary

The APT programming language permits the user to describe the geometric properties of machine parts in simple terms. The vocabulary (consisting of over 300 words) describes the various motions of the machine tool. The large number of words allows the user to define a particular part and machine in an optimal number of instructions. As a result, a large number of NC machine tool motions is necessary to produce a complex part and can be programmed in relatively few APT statements.

APT part programs

A systematic patterned application of the APT language results in an APT part program. Such a program consists of a series of statements in symbolic and numerical form, representing the geometry of a particular tool and a description of the cutter tool.

A specific part program is used as an input for the APT general processor. APT processes the input and produces a cutter-location tape and a listing of the processed part program, including diagnostics. The cutter-location tape file contains successive cutter location coordinates and control information concerned with placing a tool. General processor computations are valid for a wide range of machine tools and their controllers.

APT post processors

APT general processor output serves as input to an APT post processor which converts the generalized coordinate values into a form compatible with a particular machine tool. Standard instructions must be interpreted and translated into correct codes that apply to a particular controller. The post processor generates a punched tape (Mylar® or paper) or a direct numerical control (DNC) file. The DNC applies to specific families of machine tools and their controllers. The post processor output tape, or DNC file, is then fed into a controller to produce the desired part.

At the computer interface facility (Fig. 2)

an operator types a part program using a 30-character/s terminal. Upon completion, a punched Mylar® tape will be generated for production of the trial part.

Present and future usage at RCA

The vital link between the computer and the NC machine is the part program. The development of a part manuscript can be divided into three basic steps: geometrical description, tool motions, and machine functions.

The first operation identifies the part for the computer. Such identification consists of geometrical equations describing the physical size and shape of the object to be machined. Dimensions are taken from the drawing specification and formulated into statements such as line, point, circle and plane definitions.

The second step outlines how the tool (punch, drill or end mill) should be located relative to the geometrical definitions previously stated. The tool is driven along these surfaces or lines to simulate the actual machine process. The choice of these motions is of great significance in producing an economical part. The motion efficiency will
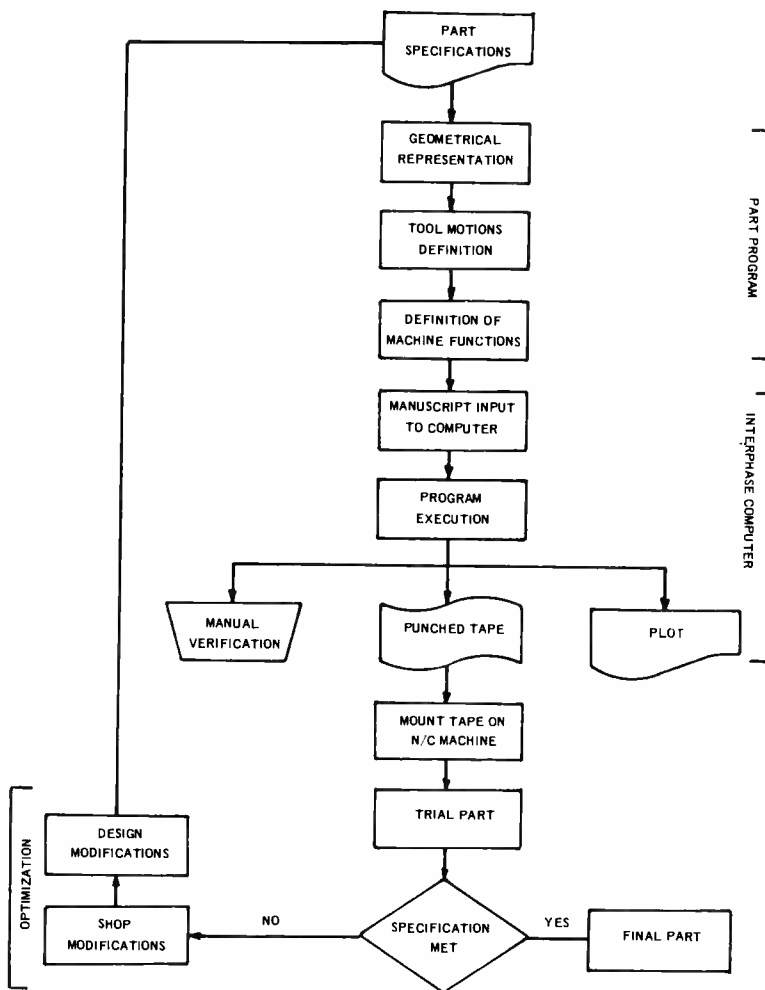
39

Fig. 3 — The three basic part production modes (part program, computer interface and optimization) are shown here in step-by-step fashion.

Fig. 4 — The speed-brake manifold above was precision machined by use of RCA Ltd's numerically controlled machine processes.

determine machining time. Routines have been developed to optimize cutter travel and programming time.

The final step is to include in the program machine functions or commands. Such functions are unique for each machine type. For example, a punch press must be instructed when to punch a hole, when to change a tool and which tool to use next. The machine function step is of primary importance, as it will govern, on most machines, the rate at which the material will be processed. Efficient feeds and speeds will increase productivity and tool life. The rate of material removal (feed) can also determine the surface finish of the part and the precision.

A complete part program is typed on a data terminal to produce a source document on paper tape. The tape is then transmitted to a computer for processing by the APT System.

The execution is performed in a time-sharing mode. This type of environment permits a program to be debugged and modified without the delays in turnaround encountered in a batch system.

A machine tape may be requested once the execution is satisfactory; this paper tape output is mounted on the NC machine for a trial run. Optimization can then be performed from this part for production use. For complex parts, a plot of the program output can be produced for detailed verification prior to producing the final machine-coded tape. Flexibility, the primary aim of the machine function procedure, allows changes to be incorporated and easily recycled in the process. It is this adaptability feature that is of prime importance to a high-variety, low-volume shop, prevailing at RCA Limited.

Prototypes and experimental models are most suited for numerical control processes. By devising a part program first, later modifications (such as design improvements and material changes) can be easily and quickly implemented. The high accuracy of NC machines is an asset in the fabrication of spacecraft components. Also in a manual system, such design would require weeks to fabricate. The steps involved in designing and producing a part from original specifications are shown in Fig. 3.

Fig. 4 illustrates a typical example of the workmanship achieved with the CIM-X tool changer in machining a speed-brake manifold from a solid block of aluminum.

Current planning

Plans are currently underway to incorporate a computer-aided design and an automated drafting system within the engineering activity. The interface between the NC shop and the new engineering facility will provide a more effective method for the fabrication of parts such as printed circuit boards, currently one of our major products.

From a series of specialized computer instructions, a drafting machine can be controlled to outline the layout of printed-circuit boards. Such instructions, with the aid of particular computer software, can be used to produce NC tapes. Resulting from this technique a parts geometry data bank could be set up to interphase with NC programming and greatly enhance productivity within the NC shop.

40

Data acquisition, control and display for Navy ORTS

T. Taylor, Jr. | M. LeVarn

Data acquisition, control and display functions for the Navy's AEGIS Operational Readiness Test System (ORTS) is described herein. ORTS provides on-line, real-time monitoring of the status of the AEGIS Naval Weapon System and is designed to: (a) determine operational readiness at system and equipment level, (b) evaluate performance degradation and recommend reconfiguration, and (c) provide centralization of maintenance functions for display and control which can be operated with minimum of personnel training. Specific goals achieved are fault detection coverage of 90-95%; false alarm probability not greater than 1%. This paper describes advanced techniques used in the development of the data acquisition, control and display systems of ORTS applied specifically to the AEGIS AN/SPY-1 phased array radar system.

Theodore Taylor, Jr. Senior Engineering Scientist, Aerospace Systems Division, Government and Commercial Systems, Burlington, Mass. received an (SB) ME degree with sub-major in electronics from MIT in 1953. He has pursued graduate studies at the University of Pennsylvania and Northeastern University. He was responsible for system analysis, integration, diagnostics, and test planning for the USAF/USMC TIPI DC/SR program and studies for application of a large-scale information processing system to Armed Forces Entrance Examination Systems. Mr. Taylor was formerly responsible for concept development and engineering design of the data acquisition display for the AEGIS Shipboard Operational Readiness Test System (ORTS). From 1967 through 1970, he managed design and development of time-shared computer controlled test systems for manufacturing test of disc storage units. He also directed test programs related to improving the acquisition and dissemination of manufacturing process information. From 1962 through 1967, Mr. Taylor was responsible for development of automatic test systems for the Apollo Lunar Module. His work involved mission simulation, automation of stimulus and measurement, and probabilistic models for checkout effectiveness and confidence levels, for S-band communications, X-band radar and transponder, and attitude propulsion control systems. Mr. Taylor has 20 years experience in developing electronic systems for DOD and NASA and has published numerous papers in this field. He is a member of IEEE and AES professional group; he is a registered professional engineer in the State of Massachusetts.

Marc F. LeVarn — Senior Project Member, Aerospace Systems Division, Government and Commercial Systems, Burlington, Mass., received the BE in Electrical Engineering from Villanova University in 1958 and the MS in Electrical Engineering from the University of Pennsylvania in 1962. His recent assignments have been as principal engineer for concept development and system design of the data acquisition and display portion of AEGIS MK-545 Operational Readiness Test System (ORTS) — and as a system engineer responsible for preparation, review, coordination, and negotiation of specifications and test procedures as well as integration of portions of the USAF TIPI DC/SR segment. He has participated in the design of a number of general and special purpose test systems including Multi-System Test Equipment (MTE), Depot Installed Maintenance Test Equipment (DIMATE), special test equipment for the Lunar Excursion Module Attitude and Translation Control Assembly (LEM/ATCA) and others. He is currently studying the transition of the AEGIS ORTS system from the engineering development model to a modified version for the DG class of ships. Mr. LeVarn is a member of IEEE and a registered engineer in the State of Massachusetts.

TODAY'S COMPLEX Naval weapons systems must be able to monitor system operability, observe performance in real time, and assess mission effectiveness. Having these resources, alternate weapon-system configurations and maintenance actions can be initiated to remedy system failure immediately.

In a multi-radar, command-and-control complex such as Aegis, system performance and effectiveness criteria are acquired from observing the following diverse parameters and sources:

1) normal system operation through the data channels and displays;
2) system response to periodic tests interleaved during normal mission activity;
3) response to dynamic target tests at specified on-line intervals; and,
4) results of on-line, continuously-scanned, test-point data from equipment locations.

On Aegis, these four functions are performed by the MK-545, Operational Readiness Test Systems (ORTS).

Of the sources identified above, item 4 is particularly important with respect to impact on hardware design, since care must be exercised to insure that data acquisition does not impair system performance. In this regard, item 4 is the main subject of this paper which addresses the data acquisition, control and display elements of ORTS.

System requirements

The basic system requirements for ORTS were derived from functional and test requirement analyses dictated by the overall Aegis Mission. Aegis (Shield of the Fleet) is a total weapon system designed to provide wavetop-to-stratosphere area defense of the fleet. It provides total integration of target detection, command and decision, and weapons deployment within the Aegis ship and the total escort force. The heart of the system is the multi function array radar (AN/SPY-1) which detects and tracks multiple targets at all ranges.[1] Illumination radars provide missile control and target illumination for guidance, homing, and kill evaluation. Overall control and display of the weapon system environment is facilitated by a complement of AN/UYK-7 computers and AN/UYA-4 display consoles located in the combat information center (CIC).

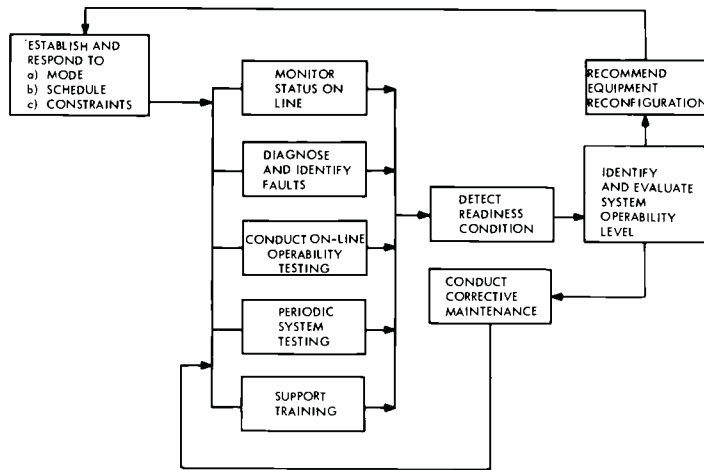The functional requirements necessary to

Fig. 1 — ORTS functional flow diagram.

support Aegis dictated that ORTS provide:

a) Determination of operational readiness at both the system and equipment levels.
b) Evaluation of system performance and reconfiguration options.
c) Centralization of maintenance functions such as display and control.
d) Control and integration of system and equipment level testing.

The functional relationships of system requirements are shown in Fig. 1; principal data-flow paths are indicated by arrows. The feedback loop (across the top in Fig. 1) provides the means for AEGIS tactical management to select the best system mode of operation to meet a particular threat under readiness conditions existing at an exact moment. Hardware elements of ORTS are mainly concentrated in the "on-line monitor status," "detect readiness," and "diagnostic identification paths"; Specific requirements imposed by

AEGIS are:

1) Fault detection coverage (90-95%)
2) Monitoring accuracy (<1%)
3) Median active repair time (<0.5 hours)
4) False alarm probability (0.005)
5) Fault isolation - to the line replaceable Unit Level (LRU).

To satisfy these design goals, large quantities of test-point data were processed and evaluated, in addition to other ORTS-derived system operability data. The amount of information dictated computer control with an automatic status-display update CRT/keyboard terminals at the operator interface.

General system description

The AEGIS functional requirements resulted in an final ORTS design that is

closely integrated into the weapon system. This was a logical conclusion in that over half the operational-readiness test information is derived from the prime equipment's normal operating data channels, utilizing ORTS computer-controlled simulation tests for mode operability and target track. The remainder of the test data and much of fault-isolation information are obtained through test-point data sources spread throughout the system and in remote ship locations.

The EDM-1/MK-545 ORTS configuration and its interface with the Aegis weapon system are shown in Fig. 2. Central control of ORTS is provided by the Test and Monitor (T&M) console. Tests are scheduled, controlled, and reported on automatically by program control from the computers, with access provided to the console operator for special display data and override control. Operability tests using stimulus, simulation, and performance data received through normal data channels are controlled directly by the appropriate computer to the subsystem in question. Test results are received from two sources:

1) The subsystem directly, via its own computer, associate ORTS data processor and,
2) Remote test points serviced by data buses controlled directly from the T&M console.

Data from both sources are computer processed and results fed back through the T&M console to "status and CRT" displays in the T&M console and to the ORTS deckhouse monitor and status cabinet. The ORTS and the prime weapon system functions are heavily interleaved; for physical locations of the equipment aboard ship, see Fig. 3.
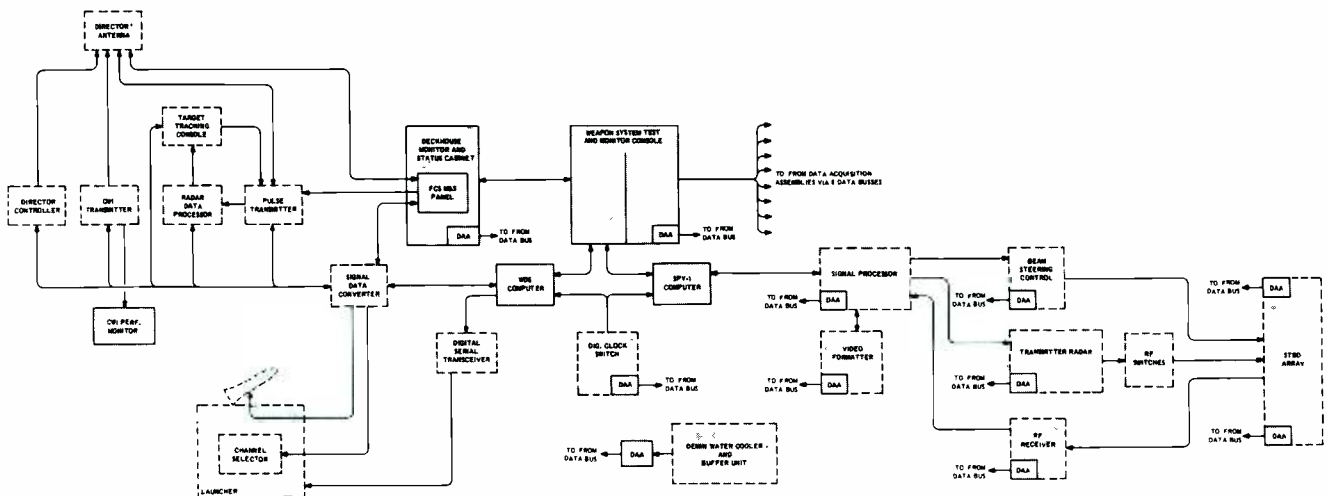

Fig. 2 — AEGIS/ORTS, EDM-I/MK-545 configuration

Retrieval of remote test-point data and the role of the T&M console are major elements of the system. Acquisition of remote test-point data is essential not only for failure detection, but as the most expedient means for reliably isolating failures to repairable levels.

The test-point data is gathered by means of data acquisition assemblies (DAA) resident in each weapon system cabinet. Each DAA is serviced by a common data bus from the T&M console. In response to sequentially received address and clock data, the DAA's transmit measured test-point data back up the bus. As many as sixteen buses with a maximum of 512 test-point addresses per bus may be used. The sequence of addresses on the bus as well as the processing of received test data are computer controlled through the T&M console.

Critical to the design of the ORTS system was the determination of data bus characteristics, data rates, methods of coding, cable immunity to noise and EMI, cable length, test-point preconditioning and fail safe provisions. A discussion of analysis, tradeoffs and design details of these areas follows.

Data gathering

Test requirements analysis

A test requirements analysis (TRA), (initiated during contract definition and later expanded during engineering development.) identified significant test parameter and measurement criteria. The analysis encompassed the following:

a) Test parameter purpose (failure detection or fault isolation;
b) Effect of system operating mode on test point function;
c) Nominal value, tolerance and measurement limits;
d) Noise, ripple and common-mode rejection;
e) Pre-conditioner and stimulus requirements;
f) Physical location.

A diagnostic flow chart for each major equipment illustrated the logical progression of the diagnostic process from fault detection to isolation of the failed replacable sub-assembly or sub-assembly group.
A significant result of the TRA was the determination that all test-point data could be preconditioned to one of three standard outputs: dc analog 0.25 to 6.67V, serial digital, and parallel digital.
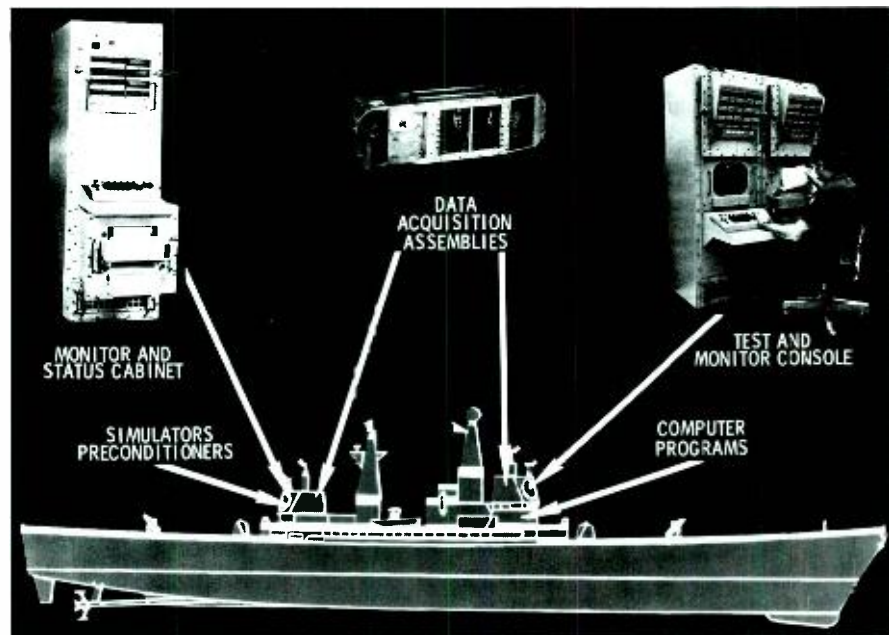
Fig. 3 — Placement of ORTS equipment aboard ship.

Transmission system

Two basic methods of data acquisition were considered. The multiplex method (Fig. 4) employs sequential switching of remote test points to a central set of signal conditioning equipment where the data is converted to a standard data processing format. The master multiplex-sub-multiplex method is a variation using two or more levels of multiplexing (e.g. a master multiplexer within the equipment room with a sub-multiplexer within each cabinet). Multiplex methods ordinarily acquire test-point data at a fixed sequence and rate, and are well suited for monitoring continuously available, slowly varying analog signals. A major shortcoming of the multiplex system is the impact of a failure at the multiplexer control or the central signal conditioning.

The data bus (Fig. 4) uses individual signal conditioners for each test point. Moreover, each test point is individually addressable. The use of individual signal conditioners has been made possible by the advent of large scale integration (LSI). This same technology allows incorporation of register storage, making it possible to acquire high-speed-digital data asynchronously to weapon system timing. The data-bus approach reduces the impact of circuit failure, and minimizes the required cabling. Sequence of test-point acquisition is completely under computer control.

Design analyses

In arriving at the data-bus design, several additional factors and tradeoffs were considered:

Binary coded transmission vs signal gated transmission.

Signal gated transmission of data was considered because of its immunity to single bit error. However, it would have required either much higher data rates, or greatly extended data transmission times to obtain analog resolution equivalent to that of a 10-bit binary code. Also, this technique would have been incompatible with the data transmitted from digital test

Fig. 4 — Data acquisition approaches showing the single multiplex and multiple signal conditioner arrangement.

Fig. 5 — The ORTS data acquisition system.

Fig. 6 — Data bus transfer timing.

points and would have complicated the processing circuitry in the T&M console.

Although the impact of a single bit error due to random noise is much greater in the binary system, it was chosen because the probability of error was calculated at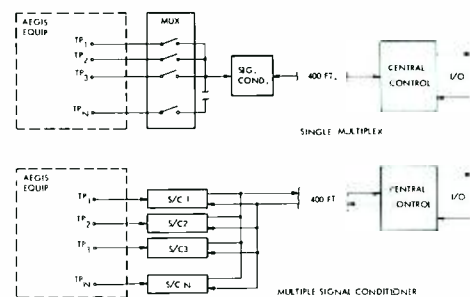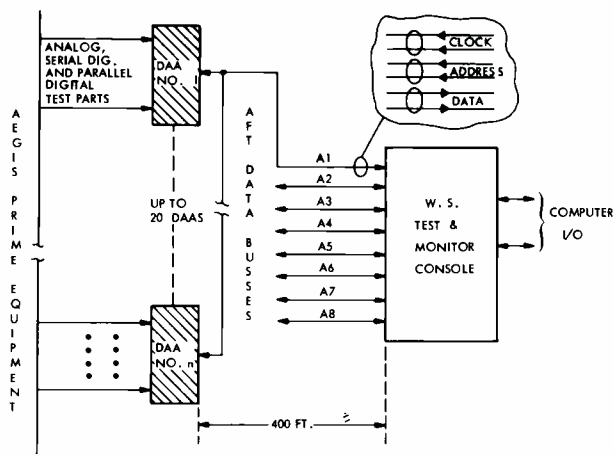 less than 1 part in 10^{10}. As an additional precaution, the software was so designed that all out-of-tolerance values are re-sampled for confirmation before any failure indication is displayed.

Biphase vs non-return-to-zero (NRZ), or pulsewidth coding

A biphase-coding scheme was adopted because the maximum pulse width is only one cycle of the clock frequency. Therefore, ac coupling is used at the drivers both in the DAA and the T&M console; thus, dc ground loops are avoided, providing a common-mode immunity that contributes to fail-safe driver design. Ac coupling would not be possible with NRZ or pulse-width transmission techniques.

Parity vs address retransmission

A positive safeguard is required to avoid acquiring data from an erroneous test point due to circuit failure or noise induced on the data bus. Use of a parity bit was considered, as was an address retransmission scheme (receiver returns to sender the address received). The chosen parity approach minimizes circuit complexity and data acquisition time, while providing protection against single-bit errors equivalent to address retransmission. Address retransmission offers superior protection against two-bit errors; however, the probability of two-bit errors was found to be negligible, and

the parity approach was adopted. Also test point addresses which differ by only one bit are avoided to preclude noise-induced addressing errors.

Data rate

A relatively conservative clock rate of 20 KHz was chosen. This permits acquisition of approximately 770 test points/s on each data bus, and 6150 test points/s with all buses operating in parallel. It is more than adequate to meet the performance monitoring needs determined by the test requirement analysis.

The 20-KHz rate also provided very wide latitude in choice of technology for the DAA design. The long multi-tapped bus structure requires use of conservative data rates, and noise immunity is enhanced by the use of a restricted bandwidth system.

Data transmission characteristics

The final transmission system design uses a data-bus approach with limited multiplexing, providing the advantages of the data bus at a reasonable cost per test point (Fig. 5 illustrates this system). Each prime equipment cabinet contains all multiplexing, test point selection circuitry, and common-signal conditioning in one data acquisition assembly (DAA). Only signal conditioning unique to each test point is exterior to the DAA. Eight data buses extend from the Weapon System Test and Monitor (T&M) console into the AEGIS equipment rooms.

Each bus may be up to 400 ft long, and up
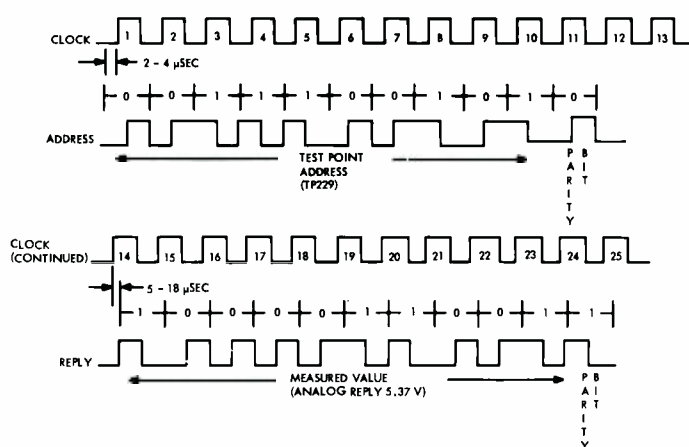
to 20 DAA's may be "daisy chained". Each data bus has three twisted shielded pairs with an overall shield and armor where required. Two of the pairs are used to transfer clock and address signals, to the DAA's and the third pair carries data reply signals from the DAA's to the T&M console.

Interrogation of a test point consists of transmitting 10 bits plus parity of address data from the T&M console to all DAA's on a data bus. The particular DAA which recognizes this address responds with 10 bits plus parity of measured value. Twenty-five 20-KHz clock pulses are transmitted from the T&M console as timing references for this data transfer (Fig. 6). Both the address and data signals are transmitted in biphase code. The address bits are weighted in binary fashion; the reply bit weighting depends upon the characteristic of the parameter being monitored.

DAA characteristics

The TRA identified three types of signals most commonly existing at test-point interfaces: analog, serial digital, and parallel digital. Standardization of three monitoring interfaces permitted development of a minimum number of new custom integrated circuits and hybrids for use in the DAA, while not creating unreasonable preconditioning problems in the prime equipment.

The DAA (block diagram Fig. 7, photograph Fig. 8) contains a quantity of test acquisition modules (TAM's) of three types corresponding to the three monitoring interfaces identified above. A single

44

DAA contains slots to accommodate up to 13 TAM's. Nine slots are capable of accepting either analog or serial digital TAM's. The remaining four slots are capable of accepting analog, serial digital or parallel digital TAM's.

Analog monitoring

Each analog TAM is capable of monitoring 16 differential inputs. Of these, 15 are used for prime equipment test points, and one connected to a calibration standard internal to the DAA. Each of the 15 analog test points monitors a voltage in the range from +0.25Vdc to +6.67Vdc; the range was established by MIL-S-1326 which was used for design guidance.

Associated with each test point is a unique test-point address established by hardwired interconnections internal to the DAA, but external to the TAM; thus, all TAM's of a given type are identical. Each TAM compares all addresses on the address bus to its set of wired -in addresses and responds when comparison is successful. Upon receipt and recognition of a test-point address, the analog TAM converts the test-point input to a serial 10-bit plus parity binary representation. All address and timing signals are received on common address and clock buses. The serial binary output is transmitted on a common reply bus.

The internal calibration standard has its own address and is measured in the same
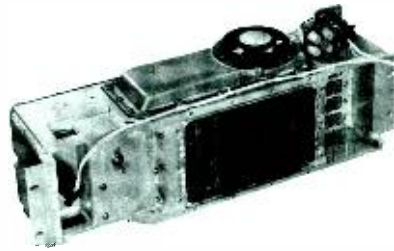

Fig. 8 — Data acquisition assembly with cover removed showing modules placement.

way as an analog test point. The results of this measurement are used by ORTS software to perform offset calibration on all other measurements from that TAM. This permits ±30-millivolt accuracy measured at the ideal switching points of the TAM analog-to-digital converter.

Analog-to-digital converter design

A tradeoff study compared the various alternative analog-to-digital conversion techniques for use in the analog TAM. Included were: voltage controlled oscillator, single ramp, up/down ramp, and successive approximation. Only the double ramp and the successive-approximation techniques appeared capable of meeting the accuracy requirements. Successive approximation was selected because:

1) it naturally generated a binary output which was most desirable for data-bus transmission,

2) its analog conversion accuracy was independent of input-clock accuracy, and

3) the critical parameters for assuring satisfactory performance were more easily identified and controlled for this approach.

Serial digital monitoring

Each serial digital TAM is capable of monitoring 16 test points. It does this in conjunction with local storage cards located within the prime equipment.

Whenever any one of the 16 addresses associated with the TAM is recognized, timing is initiated, resulting in a burst of shift pulses on the shift-pulse output line. This line is "daisy chained" to all 16 local storage registers associated with that TAM. One of these registers is enabled by the setting of the appropriate "address recognition output" line (Fig. 7). The shift pulses transfer the data stored in local storage to the TAM which generates parity and transfers data plus parity to the data bus.

Parallel digital monitoring

Each parallel digital TAM is able to monitor four groups of 10 bits of parallel data. Each group may represent data from one or more parallel digital test points. A strobe signal may be used to load 10 bits of information into the TAM, or the strobe may be permanently wired to a strobe-enable line. When the strobe is permanently enabled, the local storage will continually reflect the state of the data inputs.

Whenever one of the four addresses associated with the TAM is recognized, it will shift the associated 10-bit group plus parity in serial onto the DAA common reply bus. This output is non-destructive, and the data remains stored in the TAM for possible re-interrogation.

Each parallel digital TAM provides four address recognition outputs. These lines may be used as control inputs to the prime equipment to be available to initiate test operations.

TTL compatibility

All outputs from both the serial digital and parallel digital TAM's to local preconditioning are TTL compatible. All inputs to these TAM's from local preconditioning are TTL compatible, provided external pull-up resistors are added to the
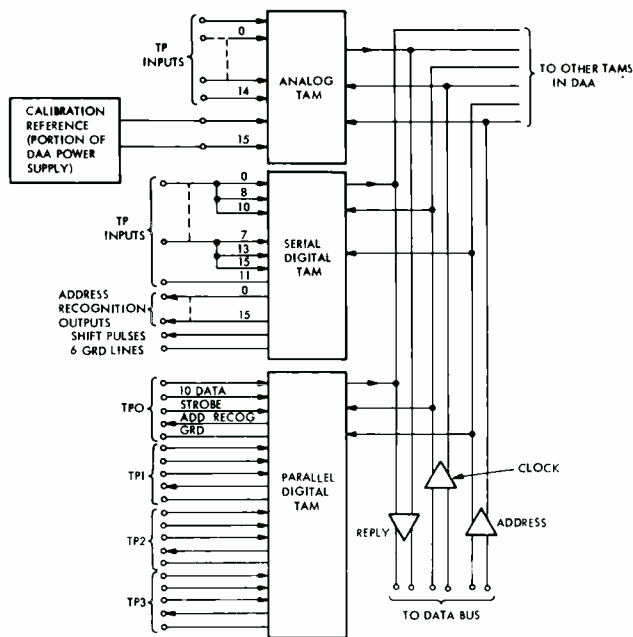

Fig. 7 — DAA block diagram.

TTL output stages in the local preconditioning.

TAM design

All Tam's are combinations of PMOS arrays and hybrid devices mounted on multilayer printed circuit cards whose dimensions are about 4.1 x 3.1 inches (Fig. 9 shows top views of an analog and a serial digital TAM).

Various combinations of LSI and hybrid technology were considered during the TAM design. PMOS, COS/MOS, and bipolar LSI using manual custom designs, computer-aided designs, and gate-universal array approaches were all appraised against these criteria; speed, power, consumption, size, reliability, cost, and delivery. At the time of the tradeoff, it was decided to use PMOS-gate universal arrays developed by RCA in Somerville to accomplish all logic functions. The PMOS approach employs standardized gate structures interconnected by a customized final metalization layer.

This provided LSI circuitry at a significantly lower non-recurring cost and promised faster initial delivery than other approaches considered. The PMOS circuitry offered adequate speed and power consumption well within the ORTS constraints. The PMOS technology was also known to be capable of performing satisfactorily under the environmental conditions of shipboard use. COS/MOS computer-aided design would be more seriously considered today because of technology advancements.

It proved possible to standardize two address and control arrays which perform the functions of interfacing the TAM's to the two DAA data buses, address comparison, test-point selection, and of parity-checking-and-generation. These arrays are identical on the serial and parallel digital TAM's, and are identical in design to the equivalent arrays on the analog TAM, but are fabricated using a different process to achieve operation at different voltage levels.

All precision analog signal switching and conditioning required for analog TAM's is performed within a hybrid circuit. Other hybrids are used to provide the high-drive levels required by the digital TAM outputs which drive TTL. Voltage regulation is also done by hybrids. All
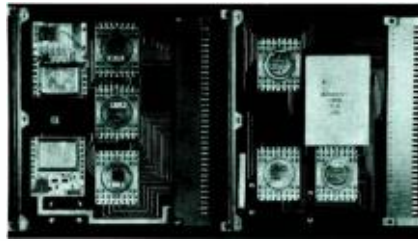

Fig. 9 — Top views of an analog TAM (left) and serial digital TAM (right).

hybrid development was initially done by the custom hybrid facility at ASD, Burlington. External second sources were later utilized for some circuitry.

Control and display

The Weapon System Test and Monitor (T&M) console provides a centralized facility in the preventive maintenance room to operate in conjunction with other ORTS equipment (and AEGIS computers) for monitoring and testing the weapon system; it provides a multilevel display of operability status and performs the following functions for the EDM-1 AEGIS system:

a) Provides summary status of the Radar, Fire Control, and Weapon Direction Segments of AEGIS.

b) Provides I/O communication with two computers.

c) Controls acquisition of sensor data.

d) Provides a 2-way data link to deckhouse monitor and status cabinet.

e) Provides a capability to initiate special test and monitoring routines (through operator interfaces).

The operation of the (EDM-1) T&M console (Fig. 3) is shown by the block diagram of Fig. 10. The console communicates with two AEGIS computers. Ordinarily, the radar computer controls all devices on the FWD-I/O bus, and the weapon direction (WD) computer controls all devices on the AFT-I/O bus. During reconfigured operating modes, either computer may access any device. The switching required is accomplished within the I/O routing circuitry.

The external interrupt electronics detects, stores, and encodes keyboard parity error, time out and power on master reset (PMR) interrupts. The interrupt electronics establishes the priority for each interrupt and initiates the transfer of an interrupt code, based on its priority, to the computer designated by the interrupt code.

Status displays

Status display panels provide indications of weapon system function status, and mode availability. Sufficient detail permits the maintenance supervisor to determine the presence of prime equipment and ORTS failures, functionally locate failures, and permit preliminary assessment of the impact on the weapon-system operational capabilities. It also provides initial display call-up guidance to the maintenance operator in the use of the interactive data display for detailed fault isolation. Display functions are implemented by using rear-projection indicators; thirty six such indicators display the status of the major hardware functional elements for the radar. Twenty-four indicators are provided to display the availability of the radar operating modes. Sixty indicators display functional status of the Fire Control and Weapon Direction Segments.

All function status and mode availability indicators employ a color code to indicate the status of the function or mode as follows:

1) *OK* (Green)

2) *FAILED* (*Red*)

3) *DEGRADED/BACK-UP* (Yellow)

4) *OFF* (White)

5) *NOT MONITORED* (indicative of ORTS failure—white with red diagonal stripe).

Summary displays of maintenance mode and mission status are also provided.

Data display and keyboard

The console contains a data display unit employing a CRT display of detailed maintenance information. The CRT displays 38 lines of 80 alphanumeric character spaces each. The upper and lower two lines are protected from keyboard data entry or erasure, and are used by the two AEGIS computers interfacing with this console. Thus, *information pending* may be called up for display by use of the keyboard. The summary-status display panels previously described also provide guidance in the call-up of detailed displays. Display call-up is accomplished by typing a code on the keyboard and entering it into the appropriate computer, using one of two "enter" keys on the console. The display-and-control characters used in operation of the data display unit and keyboard are

46

those of the ASCII code set.

The data display unit is capable of accepting data from either the forward or aft console I/O bus, but only from one at a time. It will output a "busy" status word if the second bus attempts to access it before the first bus terminates.

Data entered on the keyboard is displayed on the CRT in the position indicated by a cursor. The initial cursor position is controllable by the computer, or by the operator using special keys on the keyboard. The size and position of the screen portion protected from keyboard data entry or erasure are variable under computer control. An audible alarm is provided and sounded upon receipt of the ASCII bell code. Keyboard editing controls (in addition to those for cursor positioning) include screen erase, line erase, and cursor return which accomplishes a partial line erase.

Display formats

The display format and content is completely under software control, and is subject to continuing evaluation and updating. The following are among the display possible associated with test point data acquisition:

a) Results of periodic monitoring scan of functionally related test points with indication of measurements out of limits.
b) Results of diagnostic measurement sequence with indication of measurements out of limits.
c) Identification of failed sub-assemblies or sub-assembly groups.

d) Output of any one test point periodically updated.

Teleprinter

The T&M console contains a teleprinter providing a capability of obtaining hard copy output of any display on the data display unit. This is accomplished by depressing a print key on the keyboard causing the contents of the data display unit memory buffer, including necessary control codes, to be outputted to the teleprinter. The minimum teleprinter print speed is 50 lines per minute.

Data acquisition electronics

The T&M console includes circuitry for routing data between the radar computers, and the data acquisition buses described earlier. Each bus is controlled by an acquisition control module (ACM). The ACM's in turn are controlled by a test control module (TCM). The TCM controls eight ACM's and is designed to permit all ACM's and their associated data buses to operate in parallel.

Deckhouse interfaces

The T&M console contains deckhouse control circuitry which permits bi-directional communications between console, and the ORTS deckhouse monitor and status cabinet located up to 400 ft. away from the console. The

arrangement serves as a remote extension of the T&M console forward and aft I/O buses. Display information is outputted to the monitor and status cabinets and requests for display generation and special test initiation are received from these cabinets. A tradeoff was performed to ascertain the optimum method for data transfer. It was concluded that serial data transfer using parallel control and interrupt lines reduced the number of cable conductors greatly over parallel data transfer.

All data and continuous control signals are transmitted in biphase form, permitting ac transmitter coupling and the resultant high common-mode immunity. The data transfer rate is 150 KHz; the similarity in data transmission technique between the deckhouse interface and the data acquisition bus interface permits a common design for the T&M console drivers and receivers for these interfaces even though the data rates differ.

In addition to the signal interface between the T&M console and the deckhouse monitor and status cabinets, a remote power control interface is also provided on the T&M console. This makes it possible to apply power to a monitor and status cabinet, provided that power is available in the equipment room. Indications of power availability and application are provided on the T&M console.

Deckhouse monitor and status cabinet

The deckhouse monitor and status cabinet provides a local display and control capability in the AEGIS equipment rooms. It contains summary status displays similar to those on the T&M console. It does not contain a CRT, but does employ a printer to output detailed diagnostic information. A keyboard is used to input data requests and control information. The cabinet also contains a 14-character alphanumeric message display, using light-emitting diodes. The message display is used to compose and edit keyboard data messages before processing them in a computer. It is also used to view test-point measured values, as requested from the keyboard.

DATA ACQUISITION BUSES
TO EQUIPMENT ROOMS

Fig. 10 — Weapon system test and monitor console block diagram.

Reference

1. Bernstein, F., and Strip, J., "Aegis Engineering Model Command and Control System", RCA Engineer, Vol. 19, No. 5, Feb/March 1974.
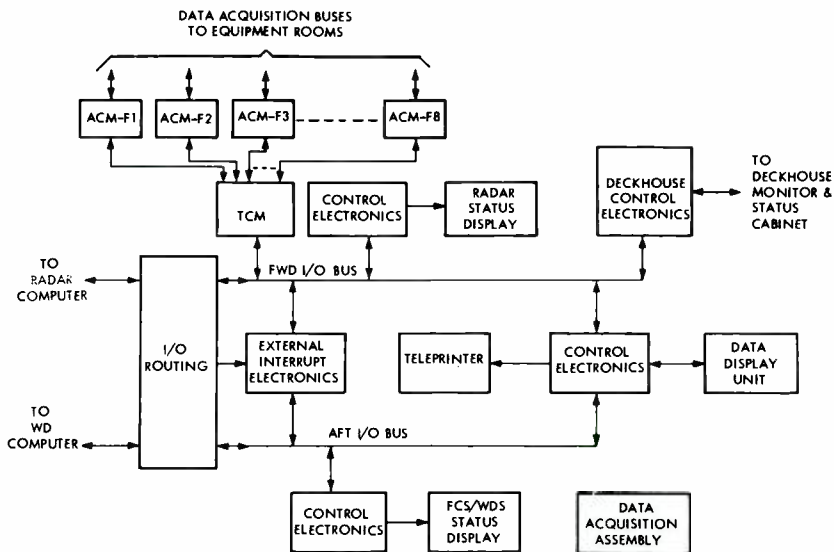
Low-cost distributed-port reflex loudspeaker enclosure

C.C. Rearick

The author discusses the design of a loudspeaker enclosure, cost competetive with existing products on the market. The loudspeaker system is optimized for the best possible sound response consistent with cost. To reduce distortion at low frequencies, the reflex concept was incorporated. The paper describes the design restrictions, theoretical restrictions, design analysis, actual results, and conclusions. Illustrations include frequency response data, impedance characteristics, and distortion data.

SMALL LOUDSPEAKER SYSTEMS have not commonly been designed using the reflex-enclosure approach. Instead, it has been easier to use the acoustical-suspension approach wherein the compression of the air inside the sealed enclosure provides the restoring force or compliance element of the speaker suspension system.

Reflex versus acoustical suspension

An acoustical suspension system is almost foolproof from a design standpoint, but the loudspeaker requires an unusually wide-displacement capability. The wide displacement need results from the mechanical relationship for constant output power, requiring that voice-coil displacement vary inversely as the square of the frequency—and increase still further near resonance. A loudspeaker capable of such large linear displacement, especially in the 5-inch-size range, becomes inordinately expensive compared to the reflex enclosure scheme where the realizable benefits are also greater.

The reflex enclosure, in contrast with the acoustical-suspension approach, can be designed to acoustically load the rear of the loudspeaker within a wide range of frequencies, and thereby contain the voice-coil motion to reasonable excursions. The bulk of the sound energy, instead of radiating from the speaker cone, now radiates from the enclosure vent or port which is not hampered with restrictions in displacement as is the acoustically suspended speaker. Since large excursions of the speaker are not needed in a reflex-enclosure design, a significant saving in loudspeaker costs results.

Reflex enclosure principles

An open-ended tube, when inserted into the side of a closed box, effectively shunts the acoustical compliance of the box with an acoustic mass equivalent to the mass of the air in the tube. The result is analogous to placing a parallel LC resonant circuit in series with the mechanical impedance network of the loudspeaker. This resonance can be effectively utilized in a loudspeaker system by tuning the box resonance to about one-half octave below the resonance of the loudspeaker. It is in

Fig. 1 — The author is shown with the model 12R-410 distributed port, reflex loudspeaker enclosure. Both the prototype and final product are pictured.

Charles C. Rearick, Engineering, New Products, Parts and Accessories, Deptford, N.J., joined RCA in 1956, having graduated that year from the University of Maine with the BSEE. He completed the engineering training program and then served two years of military service as an army lieutenant. He returned to the Home Instrument Division engineering labs at Cherry Hill, where he became responsible for the acoustical and audio performance of the TV product line. After one year with the M&SR Division, he transferred to the Camden plant where he participated in various audio, digital signal processing and magnetic recording projects. He received his MS in Engineering for Graduate Work in Electrical Engineering from the University of Pennsylvania in 1969. As Technical Publications Administrator for Parts and Accessories, Mr. Rearick is also responsible for the review and approval of technical papers; for coordinating the technical reporting program; and for promoting the preparation of papers for the RCA Engineer and other journals, both internal and external.
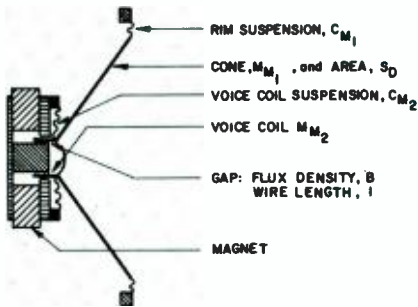
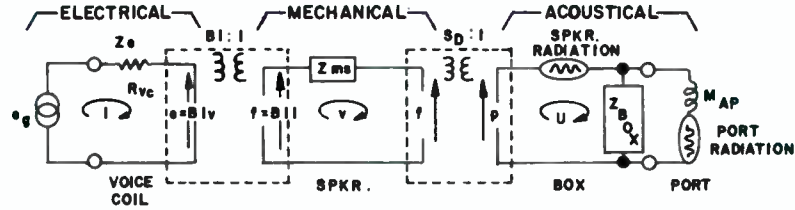Fig. 2a — Sketch of the loudspeaker component parts.

Fig. 2b — For loudspeaker design and analysis, the circuit above has an electrical analog (at left), a mechanical analog (center), and an acoustical analog (at right). The three equivalent circuits are coupled by ideal transducers.

this region where the linearity of the loudspeaker suspension is sorely strained and represents the principal source of non linear distortion in most loudspeaker systems. From an octave or so above resonance, the mass of the diaphram and voice coil limits the motion well within the linearity constraints of the suspension; below this point, the motion becomes progressively more *compliance-controlled*. The restriction of voice-coil motion caused by the loading of the resonant box on the rear of the diaphragm will obviously result in reduced acoustical output from the speaker. However, the volume velocity of the sound energy (acoustically analogous to current) circulating in the resonant box, radiates a sound pressure from the port almost totally unrestricted by non-linear suspension elements. Such radiated sound is of sufficient magnitude and phase to augment nicely any loss of the sound from the loudspeaker diaphragm.

Unfortunately, the Q of a reflex enclosure is generally quite high so that the sound-energy-conversion efficiency in the vicinity of box resonance is also high. This effect is responsible for the *juke-box-bass* so typical of the many improperly designed bass-reflex enclosures one hears all too often. By introducing a controlled amount of acoustical resistance in series with the port mass, the Q can be reduced sufficiently to reduce the peaked response and blend it in with the radiation from the loudspeaker itself. A distributed port, one consisting of a set of small holes instead of a single large one accomplishes the sound blending.

The 12R-410 loudspeaker

A loudspeaker/enclosure system has

been designed (Fig. 1) at RCA Parts and Accessories according to this premise, and is represented in our product line by model 12R-410. It was designed to complement the RCA car stereo-tape player line for use in the home with the model 12R-900 and 12R-1000 car stereo-tape player, home-converter models.

The 12R-410 utilizes a driver costing considerably less than acoustical-suspension types of drivers—and is patterned after the very successful driver used in the model 12R-400 car stereo speaker installation kit. This speaker, however, has especially tight specifications on its fundamental resonance, a cloth-rim suspension, and an oversized voice-coil suspension. The system performs very well down to frequencies nearly as low as those reached by an equivalent sized acoustical suspension system, exhibits better damping of transient signals and performs as well or better with respect to non-linear distortion.

Analysis of pertinent technology

The following is a review of the design procedure, possible alternatives, and a discussion of the performance of the final configuration. The understanding of loudspeaker enclosure design is best taken in incremental steps. Analytically, we choose to start with the loudspeaker voice-coil terminals, adding in the various mechanical and acoustical elements until the solution is either adequate or so complex as to defy solution.

Mechanical properties of a loudspeaker

Figs. 2a and b show an ideal elec-

trodynamic loudspeaker whose voice coil exhibits the usual characteristics of resistance and inductance. Our first act of simplification will be to ignore the inductance since it is insignificant at the low frequencies we are considering (30 to 1000 Hz).

Therefore, our first approximation of the system consists of an electrical resistance called R_{vc}. The ideal loudspeaker (Fig. 2a) will *move* whenever current flows through its voice coil. As soon as we get *motion*, in the mechanical circuit (Fig. 2b), we enter the realm of the mechanical world wherein the system contains a mass that must be moved, and a compliance or spring element to be stretched.

At some frequency (in loudspeakers, a low frequency is most expedient), the mass and compliance are in resonance. Since a mechanical system such as this exhibits a large displacement at resonance, electrical engineers will envision immediately an electrical analogue of a series resonant circuit (Fig. 3), and will include enough mechanical resistance to be realistic.

Acoustical properties of a closed box

At low frequencies, a box acts primarily upon the loudspeaker as a pure compliance (spring load). This load combines directly with the compliance of the loudspeaker suspension, raising its resonant frequency accordingly Fig. 4). The acoustical compliance (C_{AB}) of a box at low frequencies (below 500 Hz) is a direct function of box volume and is given[1] by the equation:
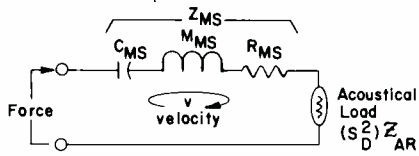
Fig. 3 — Mechanical analog of the loudspeaker without baffle (enclosure).

Fig. 4 — Mechanical analog of loudspeaker inside a closed box.

Fig. 5 — Mechanical analog of loudspeaker inside a (ported) reflex enclosure.

$$C_{AB} = V_B/\rho_o C^2 = m^5/N \qquad (1)$$

where V_B = box volume in cubic meters; ρ_o = density of air = 1.18 kg/m^3; and c = velocity of sound (in air) = 344.8 m/s.

Associated with the acoustic compliance of the box is a small acoustic mass of air which moves within the box as if the box were a closed pipe of length (l'). This acoustic mass is calculated according to the relationship[2]:

$$M_{AB} = l'\rho_o/3A_x = kg/m^4 \qquad (2)$$

where A_x = Cross-section area of box in m^2.

The complex acoustical impedance of the closed box is then the algebraic sum of the reactances of the compliance and mass relationships of equations (1) and (2); for example:

$$Z_{AB\ closed\ box} = -j(1/\omega C_{AB}) + j(\omega M_{AB})$$
$$= mks.\ acoustic\ ohms \qquad (3)$$

where $\omega = 2\pi f$.

To convert the acoustical impedance of the box, Z_{AB}, into a mechanical impedance, Z_{MB}, as seen by the loudspeaker force element, $Bl(i)$, the acoustical impedances must always be multiplied by the square of the effective area of the loudspeaker piston, S_D^2. This conversion is represented in Fig. 2b by the ideal coupling ratio between the mechanical and acoustical networks, $S_D/1$.

As mentioned previously, an open-ended tube inserted into the side of the box effectively shunts the acoustic compliance of the box with an acoustic inductance equivalent to the mass of the air in the tube. This acoustical parallel resonant circuit appears in series with the loudspeaker series resonant circuit as illustrated in Fig. 5. The possibilities for port configuration are legion, and authorities do not agree in all cases as to which is the best. Our problem, however is specific in that we desire a *lossy*
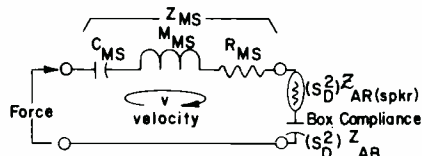
acoustical mass. The so called "distributed port" configuration, consisting of a set of small diameter holes, offers both acoustical mass and moderate resistance; and, it offers the convenient design advantage of being constructed at the rate of one hole at a time until the response is proper. The contribution of a set of N holes to the elements of *port mass* (M_{AP}) and *acoustical resistance* (R_{AP}) is calculated from the following:[3,4]

$$M_{AP} = \frac{\rho_o}{N\pi a^2}[l'+l'']$$
$$= kg/m^4$$
$$= Acoustical\ mass \qquad (4)$$

$$R_{AP} = \frac{\rho_o}{N\pi a^2}(2\omega\mu)^{1/2}[l'/a + (2)]$$
$$= Acoustical\ ohms,\ mks \qquad (5)$$

where N = number of holes; a = radius of one hole; l' = length of one hole; l'' = end correction for hole = $(2)(0.85)a$; ω = angular frequency = $2\pi f$; and μ = viscosity coefficient = $1.56 \times 10^{-5}\ m^2/s$.

The resonant frequency of the reflex-enclosure box is then found from the classical formula for parallel tuned circuits, using results of equations (1), (2), and (4):

$$f_B = 1/2\pi[(M_{AP} + M_{AB})(C_{AB})]^{1/2} = Hz \qquad (6)$$

Experimental box design

Closed box design

A box, having a volume of 656 cubic inches (0.01075m[3]) was built out of 3/8-inch-thick plywood. Computation of the acoustical impedance elements of this box from equations (1), and (2), result in the following:

Acoustical compliance: $C_{AB} = 7.66 \times 10^{-8}$
$$= m^5/N$$
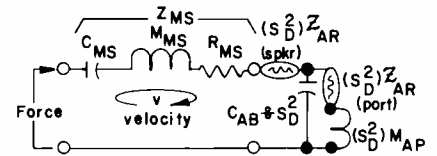
Acoustical mass: $M_{AB} = 7.83$
$$= kg/m^4$$

Measurements of the frequency response, voice-coil impedance, and distortion were taken for the closed box enclosure — and the results are illustrated in Figs. 6 and 7.

Reflex box design

Careful testing showed that about ten 1/2-inch diameter holes in the 3/8-inch-thick front panel were about right for the loudspeaker proposed for the design. Calculation of the theoretical acoustical mass (M_{AP}) and acoustical resistance (R_{AP}) of a set of ten 1/2-inch holes (3/8-inch deep) from equations (4) and (5) — results in the following:

$$M_{AP} = 18.93\ kg/m^4$$

$$R_{AP} = 45.64\ (f^{1/2}),\ acoustical\ ohms$$

Though the port is principally a mass element at this frequency, the distributed port is almost three times lower in Q than a typical open-hole vent. The lower Q is a favorable condition for reducing the *bass-boominess* referred to earlier. Vent Q, for the distributed port at the frequency of 100 Hz, is 27.33.

From these results, the acoustical resonance (f_b) of the box can be calculated to be 111.2 Hz, using equation (6). This agrees quite closely with the experimental results for the reflex enclosure, as indicated by the minimum point between the two peaks on the impedance curve of Fig. 6.

Open-back enclosure

The loudspeaker was also tested in a large open-back enclosure backed with a heavy fiberglass-lined corner. Under these conditions, the speaker performance is indicative of what the loudspeaker itself is

fundamentally capable of doing (*i.e.*, without the assistance of an enclosure). The difference between the performance of the loudspeaker under this condition and the performance when mounted in either the closed or reflex boxes is illustrated in Fig. 6. The net effect the different enclosure designs have on speaker performance is apparent.

Discussion of results

Frequency response

The improvement in frequency response gained through the use of the reflex design is evident in Fig. 6. The improvement begins at about 70 Hz, reaches a maximum at 100 Hz, and tapers off smoothly to merge with the closed box response at about 500 Hz. The result is a leveling off of the drooping response in this region. The ragged low-frequency response of the same speaker in an open back (large) baffle, shows the inability of this speaker to control its motion adequately through its own suspension elements. The mid-range and high-frequency responses of this loudspeaker are excellent. The responsibility for this however lies with the manufacturer of the speaker — and not with the design of the enclosure. Though the enclosure cannot usually improve the high-frequency response of a loudspeaker, it should be pointed out that a careless design can very well spoil that response with spurious resonances.

Distortion response

The loudspeaker used in the design of this enclosure system was selected and specified to have a free-air resonance slightly lower than that generally regarded as standard for its size (see Table I). The low resonance, however, can be accommodated to advantage with the reflex-enclosure loading technique explained earlier. Fig. 7 illustrates the effect of the enclosure on the linearity of voice-coil motion. Below box resonance, (about 100 Hz or so), the reflex enclosure reacts much as an open-back enclosure, while the closed-box compliance characteristic takes over almost completely from the loudspeaker suspension compliance. Between 90 and 500 Hz, however, the enclosure is very effective in its control of the voice-coil motion, reducing distortion within this region by as much as 5 dB over the closed-box case, and up to 3 dB over the open-baffle case. Since this is the region in which the maximum amount of fundamental program energy is concentrated (and there is actually an increase in sound output), the improvement is much more significant than the loss.

Conclusions

The enclosure utilizes only a single, five-inch (130 mm) diameter, low-cost loudspeaker in a 656-cubic-inch box with a distributed port consisting of ten, 1/2-inch diameter holes. The loudspeaker/enclosure system satisfactorily meets the requirements for an economical, quality, high-fidelity sound

reproducing unit.

The frequency response is smooth and adequate at the high end and is optimized at the low end for smoothest response and low-harmonic distortion. Table I is a list of the performance specifications of the 12R-410 loudspeaker and enclosure.

References

1. Beranek, L.L., *Acoustics*, McGraw-Hill Book Co., Inc., N.Y., 1954, page 129, equation (5.38)
2. *Ibid.*, page 123, equation (5.36).
3. *Ibid, op. cit.* page 133, equation (5.45).
4. *Ibid.*, page 137, equation (5.54)

Table I — Performance specification on 12R-410 home converter sound reproducer unit.

System

Frequency response	60 to 14,000 Hz
Sensitivity	95 dB
Power handling capability	3-1/2 W nominal
	7 W maximum

Distortion @ 78 mW input power:

@ 70 Hz	5%
@ 100 Hz	<2%
@ Second resonance	<2%

Driver

Nominal impedance	3.2 ohms
Voice-coil diameter	3/4 in.
Loudspeaker diameter	130 mm (5-1/4 in.)
Free-air resonance	120 Hz±15%
Ceramic magnet	
Weight	130 gram (4.59 oz.)
Flux density	9000 gauss

Enclosure box dimensions

Width	7-3/8 in.
Height	10-3/4 in.
Depth	9-1/4 in.
Volume	656 in.

Fig. 6 — Sound pressure response and loudspeaker terminal impedance response for three types of loudspeaker enclosures.
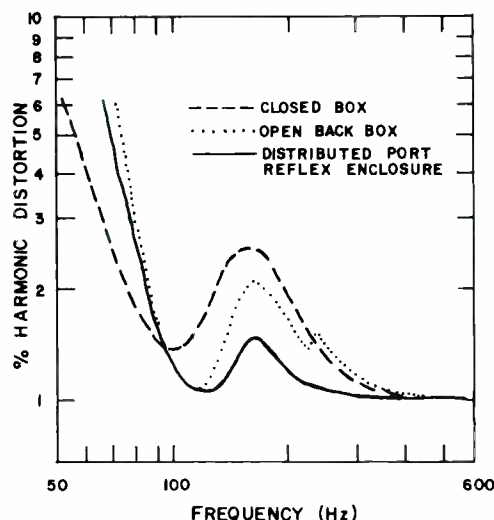
Fig. 7 — Percent total harmonic distortion versus frequency in the sound output of a small loudspeaker.
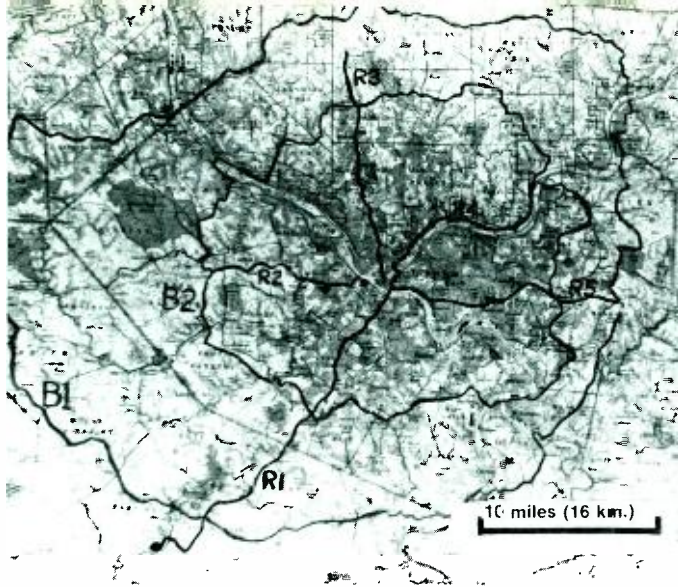
Fig. 1 — Pittsburgh area map.

Fig. 2 — View of downtown area.

Fig. 3 — View of suburban area.

Fig. 4 — Relief detail of Pittsburgh area.

900-MHz and 450-MHz mobile radio performance in urban hilly terrain

F.A. Barton | G.A. Wagner

A field-test program to compare mobile radio performance in the 900-MHz and 450-MHz bands has been carried out in the Pittsburgh, Pennsylvania, urban and suburban area. Details of the equipment used, methods of measurement with preliminary results and conclusions are given.

IN THE NEAR FUTURE mobile communication systems will be operating in the 806-947-MHz band, and a number of studies of such systems have been made. In cities such as Chicago, Washington, D.C., Philadelphia, and New York—the viability of practicable 900-MHz systems has been well-established.[1-4] Since the terrain in these studies was relatively flat, it is important to find out how such systems behave in more hilly areas.

The rolling hills, deep valleys and thick tree cover characteristic of Pittsburgh make it an appropriate region for additional study of 900-MHz performance. Comparison with the existing 450-MHz mobile band was desirable as a general yardstick of performance. The basis of this comparison should also be made in terms of:

a) Voice modulation performance (qualitative only),

b) Field strength variation (quantitative), and

c) Data message transmission (quantitative).

To obtain a fair comparison of propagation between the two bands, it was necessary to develop 900-MHz transmitters, receivers and antenna with performance equal to those already available in the 450-MHz band. A brief

description of this experimental equipment is included.

Topography of the Pittsburgh area

Fig. 1 is a map of the Pittsburgh area. The average terrain elevation is 1000 feet (312m) with peak-to-peak variations of 500 feet (156m). The three rivers are bordered over much of their length by steep 300- to 400-foot cliffs (94 to 125m). Fig. 4 is a relief detail of a typical deep valley in the area. Because of this rough terrain, there is essentially no line of sight operation once outside the downtown area, and multipath propagation is the rule for the majority of the area. The concept of open radials and cross streets has no significance here, as terrain eliminates the possibility of any grid work of streets.

Fig. 5 — Overall test system.

Test plan and equipment

Tests and measurements were accomplished with the use of a base station transmitting site and a mobile receiving, control, and instrumentation van (Figs. 5, 6, and 9). Located on a large apartment building on a 400-foot (125m) bluff overlooking the city, the test base station site was an availble site already in use by several other radio systems.

Transmitting and receiving equipment

Both the 862- and 450-MHz transmitters at the base station site were operated unattended and were remotely controlled from the mobile van. A 150-MHz control link equipped with subaudible tone equipment provided control of transmitter *carrier on/off* and *modulation on/off* functions. Audio for the test signal was on a broadcast type cartridge tape player fed to both base test transmitters.

A standard-product base station was used as the foundation for the 862-MHz transmitter (Fig. 7) using the low-level, 150-MHz multiplier output to drive a 450-MHz tripler stage. The 150 milliwatt (21.8 dBm) output from the tripler drives a parametric transistor doubler to an output of 250 milliwatts (24 dBm) at 862 MHz. The doubler uses an inexpensive CATV transistor and is built with etched inductors on teflon board. Output from the doubler is fed to a three-stage thin-film hybrid amplifier module which

Frederick A. Barton, Leader, Advanced Development, Mobile Communications Systems, Meadowlands, Pa., received an HNCEE degree from the Borough Polytechnic London, England in 1944. He served as a Radar Officer with the Royal Indian Navy from 1945 to 1947. From 1948 until 1955, he was a development engineer in the Communications Department of Redifon Ltd., London. After two years with Central Redifusion Services as a CATV Systems Engineer in the field, he rejoined Redifon Ltd. as Section Leader in charge of HF Transmitter Design. In 1960, he joined the Mobile Communications Engineering Department of RCA and has had design and management responsibility for a variety of mobile products. A Senior Engineer in the Advanced Development Department, Mr. Barton became leader of this group in April 1974. He is also Technical Publications Administrator for Mobile Communications Systems, Meadowlands.

Greg A. Wagner, Mobile Communications Product Engineering, Meadowlands. Pa., graduated from Point Park College, Pittsburgh, Pennsylvania, in 1970 with a BSET. He joined RCA in 1972 in the Product Design Group and is a member of the engineering staff at Meadowlands. In January, 1973 he was transferred to the Advanced Development Engineering Group to design and construct the RF and control hardware used in this 900 MHz study. A 12 year background in VHF-UHF amateur radio activity, including moon-bounce communication provided useful experience for this program.

Authors Barton (left) and Wagner.
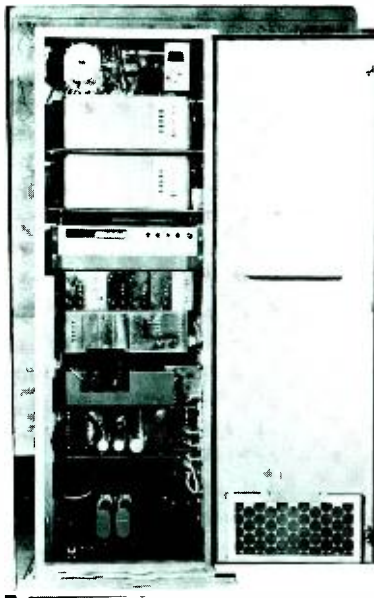
Fig. 6 — Base station used for test.

produces the 10 watts (40 dBm) necessary to drive the final-amplifier tube. This multiplication and amplification arrangement eliminates the need for a high-level varactor multiplier with its undesirable spurious products. Operating at 100 watts (50 dBm) output, the tube-type cavity amplifier feeds an 8.5 dB omnidirectional vertical colinear antenna, and including feedline losses produces an effective radiated power of 560 watts (57.5 dBm).

Using inexpensive and commercially available components, a standard-product 450-MHz receiver was modified for 862-MHz operation for use in the mobile van (Fig. 8). The addition of a hot-carrier diode mixer, bipolar rf stage and 862-MHz rf selectivity produced a basic triple-conversion receiver with a sensitivity of 0.4 μV (−116 dBm) for 20-dB quieting. By using the local oscillator multiplier output for two conversions, only one multiplier chain was needed. A single-stage rf preamplifier was added to improve the sensitivity to 0.25 μV (−119
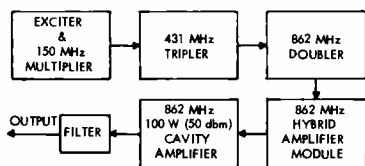
dBm) for 20-dB quieting.

The 450-MHz receiver for the van was a standard-product unit with an optional rf preamplifier, producing a sensitivity of 0.25 μV (−119 dBm) for 20 dB quieting. Mobile receiving antennas for both 450 and 862 MHz had 5-dB gain.

Signal-strength data was recorded on a strip chart recorder for immediate monitoring and on magnetic tape for more detailed analysis later (see Fig: 10).

Signal strength measurement system

The output level of the first stage of the 455-kHz amplifier in the receiver is linear with rf level inputs between 0.1 μV (−127 dBm) and 10 μV (−87 dBm).

After linear amplification, the 455-kHz signal is rectified in a full-wave detector. A logarithmic amplifier converts the dc output from the detector into a linear dB scale with a 40-dB dynamic range.

The pen chart recorder can be connected either directly to the logarithmic amplifier output or to the playback head of the corresponding fm record channel on the tape recorder. The pen recorder was normally operated in the latter mode so as to provide continuous monitoring of the tape recorder performance. Initial calibration of the complete system was provided by a signal generator connected to the receiver input.

In areas where signal strength exceeded 10 μV (−87 dBm) a switchable attenuator was connected in series with the antenna, and the attenuation required to operate the receivers within the basic 40-dB dynamic range noted both on the pen chart and the 450-MHz voice channel of the tape recorder.

The initial linearity of the logarithmic scale was within about 1 dB for calibration at 0.1 μV (−127 dBm) and 10 μV (−87

Fig. 9 — Test van.

dBm) points.

At the end of a run, calibration was rechecked. Maximum error even after several days operation was two dB. The stability of the system is due to the normal voltage regulation of the receiver rf and i.f. stages, and the use of voltage regulated IC operation amplifiers with high feed-back ratios in the remainder of the system.

Chart records of the output from signal measurement system are particularly difficult to interpret in a raw form because of:

1) Receiver internal noise at signal levels below 0.25 μV (−119 dBm), and

2) The rapid multipath variations typically resulting in amplitude changes of 20 - 30 dB at cyclic rates up to 100 times a second.

To provide a more readable chart recording, a 10-Hz low-pass filter is normally switched in series with the chart recorder input to dampen the pen movement. The chart therefore records signal levels averaged over periods of approximately 100 milliseconds (Fig. 11).

Distance measurement system

Real time sampling of a signal level data would not be suitable for statistical analysis as the speed of the truck must vary according to local traffic and road conditions. This would cause a false

Fig. 7 — 862-MHz transmitter.

Fig. 8 — 862-MHz receiver.

Fig. 10 — Signal strength measurement system.

54
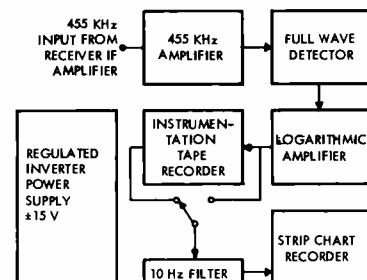
Table I — Tape Recorder Channel Assignments.

Channel	Type	Information
1	Direct	450 MHz receiver audio output or tape recorded notes
2	Direct	862 MHz receiver audio output
3	fm	450 MHz signal strength
4	fm	862 MHz signal strength
5	fm	Distance marker signal

weighting of the data, as the time spent in high traffic or on poor roads would be longer than that for other portions of the run. These areas may or may not be high- or low-signal areas, and would introduce an unpredictable uncertainty into the data. Real distance information, however, is quite appropriate for use as a sampling mode. A commercial distance measurement unit which produces output pulses at programmable intervals of driven distance was used to provide sampling triggers for analysis. Normally programmed to provide an output at 50-foot (15.6m) intervals, the distance information was recorded on one event channel of the chart recorder and on a separate channel of the tape recorder. After an analog-to-digital conversion over a 50-foot (15.6m) sample — and with hold intervals triggered from the distance channel of the tape recorder, the varying dc outputs from the logarithmic amplifiers can be statistically analyzed. This analysis is still in progress.

Antenna beam width

Calculations of the effects of antenna vertical beam width on signals received at various elevations encountered in the area of measurement show that these should not be significant. This has been confirmed in the test measurements. One area, Saw Mill Run Boulevard, which is only 0.6 mile (967m) from the base station and is in the shadow of a 400-foot (125m) cliff shows a relatively low but still usable signal at 862 MHz. This is the combined result of vertical beam width and shadow loss and is an extreme example not likely to be encountered in more level terrain.

Multipath propagation effects

Owing to the limited elevation of the base-station antenna site and the uneven terrain, the received signal (in both bands) in nearly all locations is the vector sum of a large number of reflected wavefronts of differing path lengths. As the vehicle travels through the composite field the resultant amplitude at the receiver varies cyclically at a rate related to the wavelength of the signal and the angle of motion of the vehicle relative to the field.

This phenomenon results in the well-known *picket fence* interference effect. Fig. 12 shows the signal strength variation in both bands when the truck was driven at slow speeds alongside the RCA plant in Meadow Lands. The variation in both cases ranges from 20 to 30 dB in amplitude with the frequency of variation of the 862-MHz signal being approximately twice that at 454.55 MHz.

At 30 mi/h (48.km/h) the frequency of the fade rate is approximately 44 times/s at 454.55 MHz, and 88 times/s at 862-MHz. The deep fade duration is only a small fraction of the fade cycle, and the average signal strength is only slightly lower than the peak level.

Effects on voice communications

When the average signal strength was 1 μV (−107 dBm) or greater, the *picket fence* interference effect was almost negligible. With an average signal of 0.25 μV (−119 dBm), the interference was at an annoying level but with little effect on intelligibility. As the signal fell below 0.25 μV (−119 dBm), there was a rapid degradation in intelligibility due to the increased length of the bursts of receiver noise.

Effects on data reception

The data-signalling waveform consists of a 1200-Hz burst of tone. Data encoding is achieved by phase shift modulation of the tone as shown in Fig. 13.

In both bands it was found that correct data messages were consistently received if the average signal strength was 1 μV (−107 dBm or greater). Further detailed analysis of data system performance results is underway.

Signal strength prediction

Meadow Lands Plant

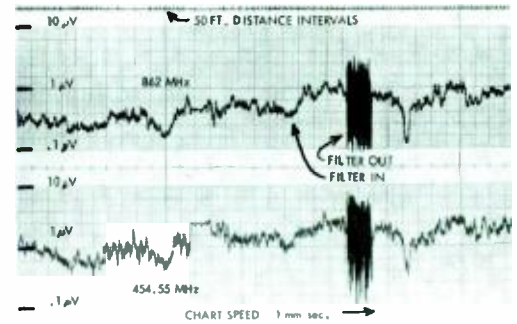An elevation profile of the 19-mile (30.4

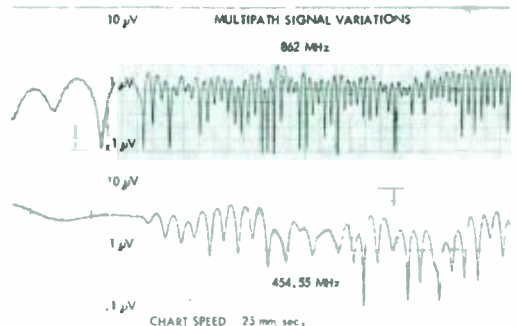Fig. 11 — Typical received signal chart.

Fig. 12 — Picket-fence signal variations.

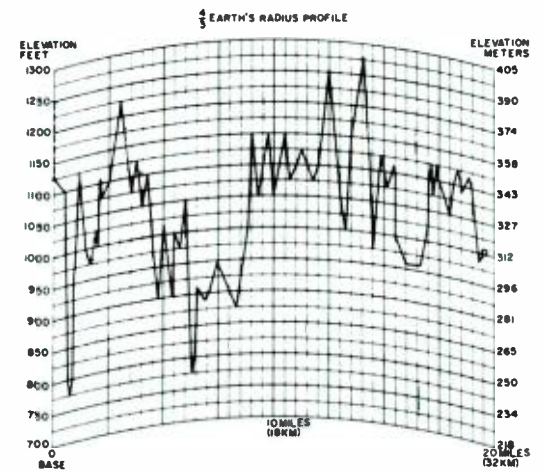Fig. 13 — Message format of test data.

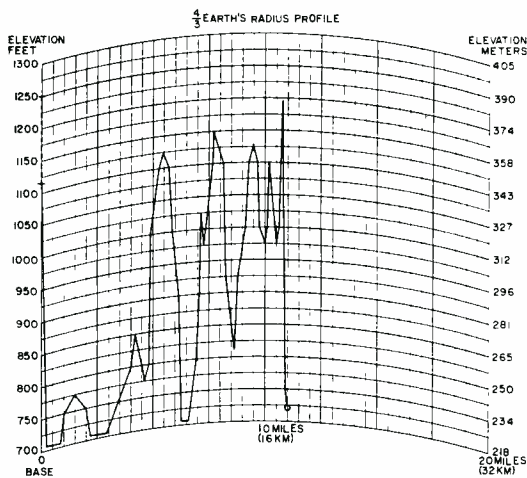Fig. 14 — Pittsburgh-Meadow Lands elevation profile.

55

Fig. 15 — Pittsburgh-Harmarville elevation profile.

km) path from the base station to the Meadow Lands plant is shown in Fig. 14.

Table II compares Bullington[5] and Okumura[6] predictions with measured median signal strength:

Table II — Compares Bullington[5] and Okumura[6] predictions with measured median signal strength.

Freq.	Bullington Prediction	Okumura Prediction	Measurement
454.55 MHz	1.6 μV (−103 dBm)	1.9 μV (−101.5 dBm)	3 μV (−97.5 dBm)
862 MHz	1.1 μV (−106 dBm)	1.5 μV (−103.5 dBm)	1 μV (−107 dBm)

Allegheny river at Harmarville

Fig. 15 shows the elevation profile of the 11-mile path from the base station to Harmarville alongside the Allegheny River. The predicted and measured signals are shown in Table III. In both locations reasonable agreement with the prediction methods is demonstrated.

Area signal coverage

Base-to-mobile

The two belt measurement runs shown in Fig. 1 traversed the full gamut of terrain features that are characteristic of the Pittsburgh area; and, it has assumed that a signal-quality analysis of these belts will provide a conservative estimate of the signal variation pattern to be expected in the area enclosed within the belts.

The analysis method consisted of dividing the belts into four equal quadrants, and in turn, dividing the quadrants into approximately 50 equal intervals. The results of this analysis are shown in Table IV. The minimum average signal strength in each interval was classified as being in one of three categories.

1) Good: greater than the average signal level of 1.0 μV (−107 dBm).
1) Usable: between 0.25 μV (−119 dBm) and the average signal level of 1.0 μV (−107 dBm).
3) Not Usable: less than the average signal level of 0.25 μV (−119dBm).

The S.E. quadrant has more steeply sided valleys than the rest of the area and has resulted in worse coverage in both bands; the inner belt (B₂) travelled over the narrowest valleys of all (being worse than the outer belt, B₁). The shadowing effect is dependent on rate of change of elevation rather than the absolute changes involved; the latter changes are in fact fairly uniform over the whole area.

Table III — Predicted and measured signals — base station to Harmarville.

Freq.	Bullington Prediction	Okumura Prediction	Measurement
454.55 MHz	4.5 μV (−94 dBm)	2.7 μV (−98.4 dBm)	5 μV (−93 dBm)
862 MHz	3.2 μV (−97 dBm)	2.1 μV (−100.6 dBm)	3 μV −97.5 dBm)

Mobile-to-base prediction

Predictions of 862-MHz coverage to be expected on the inner belt (B₂) using mobile transmitter powers of 10 watts (40 dBm) and 33 watts (45 dBm) are given in Table V. The classification of signal quality was revised for reductions in signal strength of 10 dB and 5 dB respectively.

Reducing the power level from 100 watts (50 dBm) to 33 watts (45 dBm) has changed coverage from 96% to 90%: whereas a further reduction to 10 watts (40 dBm) results in a drop to only 63% coverage. For reasonable mobile-to-base coverage, a minimum mobile power of 30 watts (44.5 dBm) would be desirable for systems in this type of terrain.

Tunnel propagation

There are three major highway tunnels in Pittsburgh as shown in Table VI.

It can be seen that a solid usable 862-MHz signal was present throughout the length of these three quite differently located tunnel systems. The 450 MHz-signal was as much as 15 dB lower than the 862 MHz-signal.

By rapid changing of the 150-MHz control signalling functions, loss of communication was shown within 500-1000 feet (156 - 312m) of entering and leaving the Fort Pitt tunnels.

The remarkable improvement in tunnel propagation at 862 MHz is attributed to a more highly scattered signal illumination at the tunnel entrance and multiple reflections along the tunnel walls.

Wind effects

On still days when parked at the Meadow Lands plant in an area with no other traffic movement, the received signal

Table IV — Base-to-mobile measurements.

OUTER BELT (B1)

	PERCENT OF QUADRANT READINGS								PERCENT OF BELT READINGS	
	N.E.		S.E.		S.W.		N.W.			
	450 MHz	862 MHz	450 MHz	862 MHz	450 MHz	862 MHz	450 MHz	862 MHz	450 MHz	862 MHz
Good	73	54	83	52	Measurements		80	55	79	54
Usable	21	30	15	42	not		18	32	18	35
Not Usable	.6	16	2	6	completed		2	13	3	11

INNER BELT (B2)

	PERCENT OF QUADRANT READINGS								PERCENT OF BELT READINGS	
	N.E.		S.E.		S.W.		N.W.			
	450 MHz	862 MHz	450 MHz	862 MHz	450 MHz	862 MHz	450 MHz	862 MHz	450 MHz	862 MHz
Good	94	58	70	46	Measurements		100	85	85	62
Usable	6	42	28	43	not		0	15	14	34
Not Usable	0	0	2	10	completed		0	0	1	4

Table V — Mobile-to-base predictions.

10 WATT (40 dbm) MOBILE AT 862 MHz – INNER BELT (B2)

	PERCENT OF QUADRANT READINGS				PERCENT OF BELT READINGS
	N.E.	S.E.	S.W.	N.W.	
Good	29	8	Measurements	47	25
Usable	29	42	not	38	38
Not Usable	42	50	completed	15	37

33 WATT (45 dbm) MOBILE AT 862 MHz – INNER BELT (B2)

	PERCENT OF QUADRANT READINGS				PERCENT OF BELT READINGS
	N.E.	S.E.	S.W.	N.W.	
Good	42	12	Measurements	0	34
Usable	48	70	not	42	56
Not Usable	10	18	completed	58	10

strength on both channels over a period of several minutes showed little variation.

However, on days with high gusty winds in excess of 20 mi/h, variations of ±3 dB at 862 MHz—and ±1 dB at 450 MHz were observed at roughly half a second cyclic rate. Base station and/or mobile antenna motion under these wind conditions does not appear to be great enough to account for the magnitude of the signal variation, and it is believed that the phenomenon may be due to patterns of foliage movement with wind gusts.

Interference

During the course of hundreds of miles of measurements, degradation of audio output in weak signal areas due to ignition inteference from either our own or other vehicles could not be positively identified on either the 459.55-MHz or 862-MHz channel. This is due to the fact that when in motion the multipath fade effects closely resemble impulse noise. To obtain a better quantitative picture the test van was in a busy downtown street for an hour.

The rf inputs to the receivers were initially terminated in 50 ohms with signal generator inputs provided by a high attenuation T coupler. The signal generators were adjusted to provide a 10-dB quieting input corresponding to ap-proximately 0.15 μV (−125.5 dBm) signal. The antennas were then substituted for the 50-ohm load and degradation in quieting observed as various vehicles drove by.

Significant quieting degradation at 450 MHz was observed with some vehicles (particularly certain motor-cycles). This degradation typically reduced quieting to 8-dB. At 862 MHz, although no measureable effects were observed on a Ballantine meter, some mild audible clicks were observed.

The Test Van which had its motor running at all times had no measurable or audible effect. Observation of the noise spectrum appearing on a spectrum analyzer connected in turn to both 450-MHz and 862-MHz antennas confirmed that vehicle interference frequency components could be identified up to approximately 600 MHz but not above.

Conclusions

Our preliminary measurements have confirmed findings of previous investigators that:

1) 900 MHz city-wide mobile dispatch systems will be practicable in the near future, not only in level areas but also in more undulating terrain such as Pittsburgh.

2) The propagation effects of changes in elevation due to either natural or man-made obstructions will closely follow those already experienced in existing 450-MHz systems with approximately 8-dB increased propagation loss.

3) 900-MHz multipath effects on both voice and data communiction will also be comparable to those in the 450-MHz band.

In addition, it appears that the 900-MHz band may offer some significant coverage advantages over the existing band in city areas such as long tunnels and under elevated roads and railroads. Another marked improvement in coverage in the heavily noise-polluted downtown areas should result from the uniquely low-noise levels generated in this band.

Owing to the wide range of propagation losses in terrain similar to Pittsburgh, the channel reuse pattern in cellular systems will require extreme care in design to avoid intolerable interference between cells sharing common channels.

Looking ahead to the hardware requirements for the new band, recent component tehcnology developments have made practicable the design of mobile and base stations comparable in performance to existing 450-MHz equipment.

Acknowledgments

References

1. Black, D.M. and Reudink, D.O., "Some characteristics of mobile radio propagation at 836 MHz in the Philadelphia area," *IEEE Transactions on Vehicular Technology* - May, 1972.

2. "Examination of the feasibility of conventional land mobile operation at 950 MHz", *FCC Research Division Report R-7102*.

3. Lynk, Charles N., "Multi-user dispatch system "*IEEE Vehicular Technology 23rd Annual Conference* - December, 1972.

4. Shefer, J., RCA Labs, Princeton, New Jersey, "Private Correspondence," May 2, 1973.

5. Bullington, K., "Radio propagation at frequencies above 30 Mc", *Proceedings of the IRE*, 35 (October, 1947)

6. Okumura, Y., Ohmori, E., Kawano, T., and Fukuda, K., "Field Strength and Its Variability in VHF and UHF Land-Mobile Radio Service, *Review of the Electrical Communication Laboratory*, Vol. 16, pp. 825-873, Sept.-Oct., 1968.

Table VI — Tunnel propagation.

Tunnel	Distance From Base Station	Length (Yds.)	Minimum 450 MHz Signal	Minimum 862 MHz Signal
Fort Pitt	400 ft. (125m) underneath	1200 (1097m)	0.5 μV (−113dBm)	1.0 μV (−107dBm)
Liberty	1.4 miles (2.25 km)	2000 (1829m)	0.8 μV (−109dBm)	0.5 μV (−113dBm)
Squirrel Hill	5.5 miles (8.85 km)	1370 (1253m)	0.3 μV (−117.5dBm)	1.5 μV (1−103.5dBm)

Computer program architectural design for weapon system radar control

T. Mehling

This paper presents an example of the methods used in developing the structure of large-scale Command and Control programs. First a description is presented of the basic elements or building blocks used in such programs; then the methods used in developing the AEGIS AN/SPY-1 radar control program architecture are described in terms of these building blocks, with examples of the factors influencing the architecture. Finally, the tools of the computer program architect are discussed with examples of their use. The processes described will vary somewhat as a function of the tasks to be performed by the program, but will generally be similar to those described in this paper.

PREEMPTION LEVEL	PRIORITY WITHIN PREEMPTION LEVEL	TASKS
1	1	F
	2	I
	3	
	4	
	5	
	6	
	⋮	
	16	
2	1	
	2	
	3	
	4	
	5	H
	6	
	⋮	
	16	
3	1	
	2	B
	3	
	4	
	5	D,G
	6	
	⋮	
	16	
4	1	
	2	
	3	
	4	
	5	
	6	C
	⋮	
	16	

Fig. 1 — Executive priority structure.

FOR LARGE command and control computer programs, the development process has only begun when the functions to be performed have been identified and defined. The next critical step is the translation of the functional design into the computer program system structure — that is, the computer program architecture. Thorough software architectural development is especially important for multi-computer

Thomas H. Mehling, Signal and Data Processing Engineering. MSRD, Moorestown, NJ, received the BEE and MEE from the University of Louisville in 1961 and 1962 and has taken additional graduate work in systems engineering at the University of Pennsylvania. On joining RCA in 1962. he was a member of the BMEWS Systems Engineering Department. developing requirements for automatic operability testing of the BMEWS radars. Since then his responsibilities have been in the specification of requirements for real time computer programs, as well as their implementation and testing. Since the late 1960's he has been assigned to the AEGIS Program; he participated in the development of specifications for the AN/SPY-1 programs within AEGIS at the AEGIS Land Based Test Site; he is currently responsible for AN/SPY-1 control program integration and testing aboard the USS Norton Sound. He received Chief Engineer's Technical Excellence Awards for his work on the SAM-D guidance system flight tests. and for his work on integration and test of AN/SPY-1 control programs in 1967 and 1974, respectively.

programs performing complex functions within stringent timing requirements. An example of this complexity is the AN/SPY-1 radar control program package for the AEGIS Weapon System. The architectural development process for such a complex system can best be understood by a study of the basic building blocks.

For large, complicated computer programs, a modular program design approach is used with three basic classes of elements: 1) the task-performing subprograms (or modules), 2) the executive, and 3) the data base. In the simplest terms, the executive controls the flow of tasks between the program modules, which in turn communicate with each other and the outside world via the data base.

A modular program approach permits partitioning of the job into manageable work packages for implementation of the program and ease of program maintenance. Thus, the performance requirements for the individual program components must be developed along with the interfacing definitions, a process common to development of complex hardware implememented functions. As with complex hardware, the mere satisfaction of program module performance requirements does not guarantee the performance of the entire system unless these requirements are carefully considered in the context of interface requirements and total system performance.

Task-performing module

The first of the three building blocks in the modular program design are the task subprograms (modules). In general, a module performs several functionally related tasks. The module itself may be further subdivided into procedures (subroutines) to perform specific tasks at one or more points within the module. In addition, the module may be entered at

Table I — Module entries.

Entry	Purpose
Initialization	Initialize module data and input output devices.
Error	Process module-related errors.
Successor	Process a request from another module.
Message	Process a request from another module with input data in temporary storage.
Periodic	Perform periodic functions.
Buffer complete	Processing due to termination of input output
Channel complete	functions related to the module.

more than one point to perform a specific task. This is accomplished either through procedures independent of those for other entries, or by sharing some or all procedures from other entries. In AEGIS, for example, each module has seven classes of entries (Table I) which are called via the AEGIS Tactical Executive Program (ATEP).

All modules have access to common subroutines as well as to their individual procedures. The common subroutine is a special class of subroutine usable by more than one task-performing module; typically, it is used to compute trigonometric functions, logarithms, and other mathematical functions. Since these subroutines are common to several modules, care must be taken to prevent inadvertent interference between the user modules through these subroutines. If one task module is allowed to interrupt operation of another task module using a common subroutine, errors are likely in the resulting output from the subroutine to the interrupted module. If the subroutine uses the same memory to store intermediate results within its computations, these intermediate results will be overwritten if the subroutine is interrupted and reentered prior to finishing the original computation. Such subroutines are called non-reentrant in that they may not be successfully reentered during the performance of computations.

The subroutine may be successfully used by modules which interrupt each other only if care is taken either to store all intermediate data in memory individually assigned for a particular subroutine call, or to keep this data in registers which the executive saves and restores during these interruptions. Such subroutines are referred to as reentrant subroutines because of their ability to be interrupted and subsequently reentered without causing erroneous outputs to the interrupted module.

Executive program

In general, the executive allocates computer processor time, memory, and input/output facilities for use by the task-performing modules. The degree to which this is done depends largely on the computer design. In AEGIS, all computers used are Univac AN/UYK-7's which have features that tend to dictate requirements for the executive program. This computer has a set of privileged instructions that may be executed only when it is in its executive state. Among these are instructions which use memory protection facilities to exercise direct control over memory access by task module.

In this process, the executive must allocate processor time to task modules for timely execution of the tasks required. This implies a means of scheduling and executing task module entries based on task priority and individual task reaction time. Reaction time is categorized in two classes of requirements, preemptive and non-preemptive. The most critical time requirements demand that tasks in process be temporarily suspended until the short-reaction-time task is performed. At the termination of this time-critical task, the suspended task is picked up at the point of suspension. This preemption process is referred to throughout the remainder of the discussion.

The second general class of time criticality is referred to as nonpreemptive, in which tasks in progress are completed prior to execution of a new task. The execution of the new task, then, will occur upon completion of all higher priority tasks and any tasks of the same priority requested earlier.

In AEGIS, both classes of time criticality are present. To handle such requirements, a priority system has been implemented which allows preemption as needed and provides a priority structure for non-preemptive tasks. The executive structure contains two levels of task priority—one for the preemption level, and another for its execution within that preemption level. Fig. 1 shows a representative priority structure where four preemption level. Fig. 1 shows a representative priority structure where four preemption levels exist with sixteen of priority represent the higher priority values. The tasks listed at right are shown at the preemption level and priority within that level at which they are to be executed. Fig. 2 is an example of the operation of this priority scheme.

The top line of this time-line diagram shows the occurrence of events which result in request for use of the computer's central processor unit (CPU). The next line shows the content of the priority queues as a function of time for tasks awaiting CPU time. The third line shows usage of the CPU at any given time. The last line shows which tasks are suspended at any time, awaiting resumption of CPU availability. At $t=0$, task A is being performed by the CPU with tasks B,D, and C awaiting service. Prior to completion of task A, a request for task E occurs at a higher preemption level, causing suspension of task A. Shortly after this event, task F occurs, with the same preemptive priority as E but with higher priority within that preemptive level. By the rules, the preemptive priority is not higher than that of the task being executed; therefore task F is placed in the priority scheduling queue, in this case at the top of the queue. When task E is complete, task F is begun and deleted from the priority queue since it is also at a higher preemptive priority than the suspended task A. When task G is requested, it is placed third in the priority queue since it is not preemptive. Also, since it occurred after the request for D and is of the same overall priority, it is scheduled after D in first-in first-out (FIFO) fashion. At completion of task F, task A is resumed since the queue contains no other requests of higher preemptive priority.
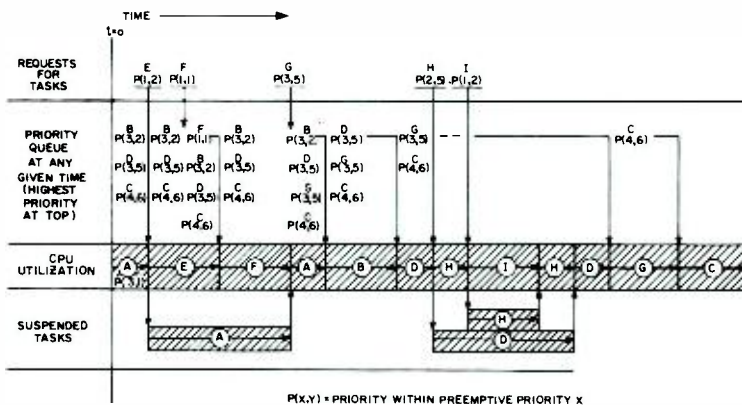
When task A is finally completed, tasks B

Fig. 2 — Examples of AEGIS executive priority structure operation.

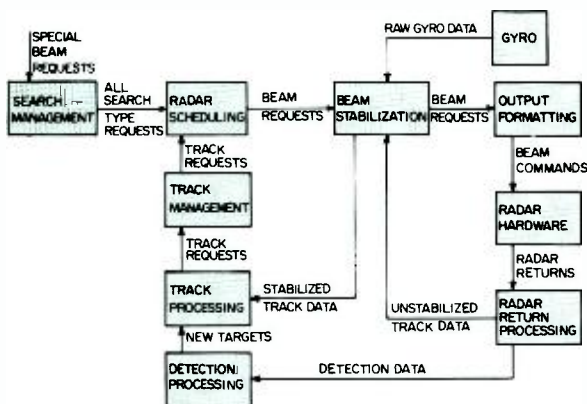P(X,Y) = PRIORITY WITHIN PREEMPTIVE PRIORITY X

Fig. 3 — Primary radar control loop functions.

and D are given use of the CPU. Prior to completion of task D, task H is requested. This again causes preemption of task D because of the higher preemptive priority of H. This time, however, a new higher preemptive priority, task I, occurs prior to completion of H, and H is also preempted. When task I is complete, task H then task D are completed, and task G begun.

In some computers, a multi-level hardware interrupt system is used with separate registers for each level of task to be performed. This can greatly simplify the role of the executive, sometimes to the point that the executive function is almost entirely assumed by the hardware interrupt system. In this case, the executive program is effectively implemented in the computer hardware. In AEGIS, on the other hand, the executive function is nearly all implemented in computer software. The AN/UYK-7 computer has four interrupt levels, but these are used strictly to perform executive functions and are not available for use by the task-performing modules. The interrupt levels are 1) hardware-detected hardware faults, 2) hardware-detected software errors and periodic clock interrupts, 3) input/output-related interrupts, and 4) program-requested interrupts by which the task modules request service of the executive program. Although this represents a priority interrupt structure, the priority is related strictly to those priorities of importance to the execution of the executive; it is in no way directly usable for task-module priority scheduling.

Data base

The data base consists of all data with which the programs must operate. This data includes doctrine and rules defining operating constraints, and system data such as target tracking data, coordinate conversion matrices, and display data.

In the context of AEGIS software, there are three general classifications of core-resident data: common data, private data, and temporary data. Common data consists of that data shared by two or more task-performing modules. Generally this implies that any of these modules sharing the data may both read and modify the data; although in many cases, modification of some portions of the common data base is restricted by design to only one of the modules. Private data, in contrast, is only accessible by the module with which it is related. It is used to maintain constraints and working data needed within the module, whereas common data is used for passing data between modules. Temporary data (or storage) is generally used to pass data from module to module as a message without requiring a permanent allocation of memory to hold the specific data passed. This is done by dynamic allocation of storage locations by the executive program upon request of a module. This module in turn places data in the allocated memory area and then, via the executive, passes the data to another module, requesting it to do the required tasks as determined by the contents of the temporary data passed to it.

In this case, the data is accessible to the sending module only up to the point of sending the message, and by the receiving module only after it has been requested to process the request. Upon completion of this processing, the temporary storage is generally returned to the pool of temporary storage locations and is not accessible to any module until the process is repeated. Temporary storage can also be used as a temporary work area within a module which is released upon exit from the module. This is generally not done because of the overhead times that the executive would take in allocation and deallocation of the temporary storage; instead private data is generally used.

Another whole class of data remains and this is the non-core-resident data base. The non-core-resident data base normally is required whenever the overall database size is too large to contain in on-line core memory and is also amenable to lower-speed access usually available from the off-line storage devices such as disk, drums, and magnetic tape. In AEGIS, this form of data includes Operational Readiness Test System (ORTS) data which includes test data and evaluation criteria as well as display messages for maintenance action. Since ORTS and SPY-1 software share the same two computers, the use of the non-core-resident data base is a factor in the architecture of the AN/SPY-1 software even though the normal SPY-1 functions do not require this form of data base.

Development of the AN/SPY-1 program architecture

At this point, the development of the architecture for the AN/SPY-1 radar control program will be discussed. This radar system, developed for the Navy as part of the AEGIS Weapon System, is a multi-function array radar capable of maintaining track on a large number of simultaneous targets as well as surveillance of the radar volume for appearance of new targets. In this system, the radar receives commands from the radar control software, directing the transmitted energy relative to the array antenna and the required waveform, and then processes the returning signal to determine the instantaneous measured position of a target or targets within the beam in the presence of noise, interference, or clutter. The programs in the radar control computers generate commands to the radar equipment within the constraints of the capabilities of that equipment and user requirements. These programs also initiate and maintain tracks on targets reported by the radar equipment, and provide the users with requested track and detection data and other display information. The primary functions of the radar control software are listed below, with a brief description of each. (See Fig. 3).

1) *Radar scheduling* — the process by which radar time is allocated on a priority basis within the constraints imposed by the radar equipment, such as transmitter average power and phase shifter switching-rate constraints. This process must also meet system reaction times required to initiate and maintain track for the various classes of track.

2) *Search management* — the process by which search and special beam requests to the radar scheduler are generated. The generation of search requests includes the search beam pattern generation within the constraints of the requested search coverage defined by the radar operator.

The special beam requests, such as acquisition and ORTS special test beams, will result in generation of a request(s) to the scheduler if the requests are allowed.

3) *Track management* — the process by which request for track dwells are made to the scheduler, including determination of priority of individual dwells and the sequence of the requests.

4) *Output formatting* — the process by which dwell requests from the scheduling function are converted to commands to the radar equipment.

5) *Radar return processing* — the process by which return data from the radar equipment is pre-processed to determine presence of valid data; resulting track and search data are then forwarded to the track and detection processing functions.

6) *Beam stabilization*—the process required to account for the heading, pitch, and roll motion of the ship in generating beam-steering commands and computing stabilized tracking-error data derived from radar returns.

7) *Track processing* — the process by which track-return data is used to update target tracking data (smoothes position and velocity), track look-rate, and waveform determination. The process also includes initiation of new target-track data based on the output of the detection processing function.

8) *Detection processing* — the process by which firm detections derived from search dwells are correlated with existing tracks using a process called crossgating to determine if the detection is a valid new detection or a redetection of an existing track. If it is a valid new detection, track processing is requested to initiate track on the new target. If correlation with an existing track occurs, the new detection is dropped from further consideration.

9) *Track association* — the process by which redundant tracks, which occur as results of merged tracks and crossing tracks, are removed from the track data files. This is a low priority frunction accomplished at a low rate.

10) *Switch aciton/display processing* — the process by which radar-control operator requests are processed and displays are generated for the operator, including various symbolic displays, raw video displays, and alphanumeric readouts.

11) *User service* — the process by which radar data (including raw radar track data) is sent to users such as the command and control weapons segments. This function also includes reporting results of all other requests by these segments and general status reporting.

12) *Recording* — the function by which data is extracted and recorded on magnetic tape for post analysis of radar performance (primarily for purposes of testing).

13) *Load evaluation* — the process which maintains radar and computer load parameter information for the system operators.

14) *Operational Readiness Test System (ORTS)* — though not specifically part of the radar control program, ORTS monitors operation of the radar equipment. Since it shares the computers used by the radar control programs, the needs of the ORTS programs must be considered in the architecture of the AN/SPY-1 control program.

15) *Background self test* — the process performed in spare computer time, used to verify proper operation of the computers.

An examination of this set of functions shows that the first eight are the primary functions in the radar control loop and impose the most severe time requirements and timing restrictions on the total program; obviously these functions will tend to dictate the design. Fig. 3 shows the interrelationships between these functions and related equipment, including the radar equipment and gyro.

A preliminary analysis of the search requirements and track capacities for the AEGIS Engineering Development Model (EDM-1) indicated that two AN/UYK-7 computers would be required to perform all required tasks for both ORTS and radar control programs. This version of the radar uses one array antenna covering one quadrant of space about the radar, and is used to demonstrate the radar performance. The AN/SPY-1 radar to be used aboard ship for anti aircraft defense will make use of four array antennas covering the full volume about the ship and will require additional computers. All further discussions of the architectural development presented will be based on the Engineering Development Model which requires two computers. It was found that the radar-control loop itself could not be implemented solely within one computer because these function require more processing time than a single computer can provide.

Two-computer configuration

Development of the software architecture within the two-computer configuration requires allocation of tasks between the computers and then to the individual task-performing modules. The allocation criteria include the ability to perform the required tasks within timing and capacity constraints, plus several other factors which determine the efficiency of the design and possible growth capability. In such a two-computer configuration it is desirable to partition tasks between the computers to minimize the amount of

redundant data needed, minimize the amount of intercomputer input/output traffic and delays, and maintain a reasonable balance of computer load and memory utilization between them. At this point, it should be stressed that there should be reasonable memory and timing estimates for the individual functions (and in many cases subfunctions) before this allocation process can reasonably be made. In many cases this estimation process may require detailed algorithm develoment of particularly critical tasks (*i.e.*, those that could require large amounts of computer time or memory) to guarantee the feasibility of performing the tasks within the available computer resources.

A good example of such a task is the cross-gating process, a part of the detection processing function. This process requires correlation of a new detection report with existing track data to verify that the detection is not an existing track. In the brute-force approach of correlating the detection with every track in the system, the required processing time would tax the capacity of several computers, assuming normal search under a full load. The process can be greatly simplified by segmenting the volume about the radar into bins of given azimuth and elevation, and then maintaining a range-ordered list of all targets within each of these bins. In this way, only targets in the bins in the near vicinity of the detection need be examined for possible correlation.

By use of the optimum bin size for the maximum target motion expected and for ease of computation, the time required for this process was reduced approximately 30-fold to a quite acceptable load of computer usage — even when considering the additional processing required for maintaining the lists of targets in each bin. In this case, the additional memory required for both the program and related cross-gate bin tables was very acceptable, making this an effective time/memory tradeoff.

Program efficiency

As in most modular programs, program efficiency is enhanced if as much processing is done within a module as practical prior to giving control back to the executive. This fact leads to two different actions. The first of these is to
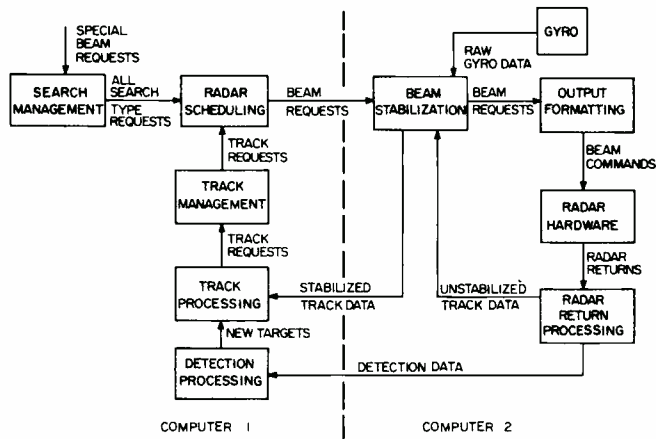
Fig. 4 — Primary radar control loop functions by computer.

combine functions assigned to the modules; the second is to lower the rate at which modules are entered by having the module process data in batches on each call rather than a single data item. This batch processing of data is particularly advantageous in the radar loop where hundreds of beams must be generated and processed each second; however, there are drawbacks to this approach. The prime concern with the radar control loop is the ability to close the radar tracking loop in the software for the maximum tracking rate required. The next major step, then, is to determine the size of the data batch to be processed in these control loop modules, and the makeup of these modules.

Fig. 5 shows the modules that comprise the radar control loop. The radar scheduler module basically performs the radar scheduling function, passing all required request data to the output-formatting module. This module performs the output formatting function and that portion of the beam stabilization function required to generate steering

commands to the radar equipment (using gyro data provided by the gyro-data-update module which periodically samples the ship's heading, pitch, and roll). When formatting these commands, the output-formatting module passes sufficient data to the radar-return-processing module to identify the purpose of each beam, plus control data to enable the radar-return-processing module to control both the radar input and output channels. The radar-return-processing module performs its assigned function as well as beam stabilization for track return data. It uses matrices generated by output formatting in the generation of commands for these track beams.

Track and detection data are forwarded to the track-processing module, and returns from special ORTS dwells are passed on to the appropriate ORTS module. The track-processing module performs the track processing, detection processing, and track management functions, passing priority-oriented requests for track beams to the scheduler module via data tables. It also extracts
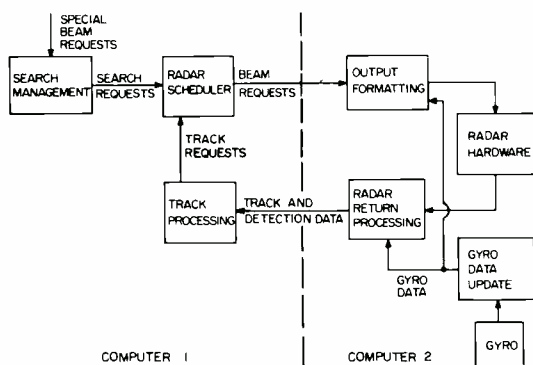
data for other radar data users, but not for the actual communication of this data (which is accomplished by other modules). The search-management module generates search beam requests and other special beam requests whenever the scheduler is capable of processing them. The four modules that make up the critical part of this radar control loop are radar scheduler, output formatting, radar return processing, and track processing. The other two, gyro data update and search management, are of lower importance on the short-term basis although both are necessary for the overall operation of the radar.

The four critical modules are designed to operate on an amount of data equivalent to an amount of radar time called a scheduling interval which has a nominal value T_S. Every T_S milliseconds, the scheduler is called by the executive to generate a variable number of radar beam requests for a time span $2T_S$ to $3T_S$ in the future. The number of beams is limited by the number of dwells the radar is capable of executing within its hardware constraints and by the amount of time required by the four modules to process that number of beams without software overloads on the the short-term basis. Subsequently, output formatting will format that number of requests as a batch. Only when the return from the last beam of this group is available in memory will the radar-return-processing module be called by the executive to process those returns. Track processing will, in turn, process all return data derived from that interval. The restriction on the number of beams in any interval based on module run time should be such that the combined execution time of the critical loop modules in each computer is less than T_S; otherwise short-term overload (if not long-term overload) would be possible.

Other modules in the radar control portions of the program have been restricted in execution time so that they need not be preempted by critical loop modules. This restriction implies that the amount of processing per call is limited to this maximum value. If necessary, the module may call itself to complete the rest of the required task after the higher priority modules are executed. Although preemption will give quicker response times to the critical loop modules, there would be a heavy penalty in executive

Fig. 5 — Primary control loop modules.

62

overhead for the use of the preemption feature, as well as possible complexities caused by data being changed by one module that preempts another. Based on these constraints, Fig. 6 shows the timing relationships that could exist in both computers for the execution of these critical loop modules.

This diagram represents a time history of the events occurring in each of the computers and in the radar equipment. For example, at time = t_o a periodic request is made to the scheduler in computer 1, but since another module is being executed at the present time, the radar-scheduler module is delayed until the area labeled RS/A (radar scheduler/interval A) is shown. At the end of the required processing in the scheduler. a request is sent to computer 2 where an I/O delay is encountered. In computer 2, there is a further delay — again to await execution of another module labeled OF/A (output formatting/interval A). Output formatting generates commands to the radar for the interval labeled A on the bottom line starting at $t_o + 2T_s$. At the end of this interval ($t_o + 3T_s$) is computer 2, the radar-return processing module will process the return data from interval A (labeled RR/A).

When processing is complete, it will send the return data to C1 where the track-processing module will process the return data again after a delay to complete another module's execution. As shown, track processing for interval A is always completed prior to execution of the radar scheduler for interval E. It is then possible, for example, for a track scheduled in interval A to be rescheduled in interval E after updating the track and a delay of four intervals ($4 T_s$). By allowing another interval T_s for possible scheduling conflicts, it can be seen that a loop closure time of $5 T_s$ is easily to be expected, provided the priority rules for the required high data rate track support this short scheduling delay. Although the scheduling priorities are not discussed here, this condition is also met. Therefore if a loop closure time of T is required, the scheduling interval (T_s) should ideally be $T/5$ or less. For sake of efficienty the $T/5$ value is approximately the value used for T_s.

If, as a hypothetical example, a 2/second closure rate is the maximum required, the loop closure time of 500 ms would then be

satisfied by selecting a scheduling interval of 100 ms. Though not specifically stated, the priority of these modules within the same preemptive priority level as the other radar control modules is higher than that for any of the remaining modules with the possible exception of the user-service modules for the command and control interface and weapons interface (which both have the same priority as the critical loop modules). This is required to ensure the required reaction times for new high priority tracks and to prevent problems with a staleness of data when using it as part of the launch/intercept requirements of the weapons segment. Since the processing time required by these modules is very short relative to the critical loop modules, the example of Fig. 6 is still valid.

In computer 1 (where the scheduler and track-processing modules reside along with the shared track file and related tables) the track association function, switch action/display processing function, and user service function are then to be implemented as well if time and memory permit. Since there is adequate time and memory to do this, these functions are implemented there because of the availability of the track file and related data in the common data portion of the data base in that computer. The modules are called track association, switch action/display processing, command and control user services, and weapon control user services.

Track association module

The track-association module makes use of the cross-gate bin lists mentioned earlier to speed up the correlation process required to eliminate redundant tracks which occur when track targets merge.

Even so, if the entire process for all tracks is performed in one pass, the execution time could be in excess of that allowed for modules not in the critical loop and not preemptable. This module is called periodically at a very low rate to perform this function. If it cannot be completed in the allotted time, processing is broken off prior to exceeding this time, and the module calls itself at the same lower priority to continue processing where it left off, thereby allowing the higher priority critical loop modules to be executed without undue delay.

Switch-action/display processing module

In the switch-action/display-processing module, the most time-consuming requirement is the updating of the target symbology for all tracks at a minimum rate of once every two seconds. By use of a 16/s periodic entry to this module to update approximately $1/32^{nd}$ of the track symbology and any other indicators as they require it, the peak execution time is held to an acceptable value. Entries resulting from operator actions are infrequent and require processing time in amounts well within these limits as well.

Other modules

Of the remaining radar control-related functions, recording modules exist in both computers, as well as background self-test modules performing the functions of the same names for both computers. Physical extraction of the data is performed by a common service routine which does the required extraction of data upon request of the individual user modules processing the required data. The recording modules are physically responsible for control of the
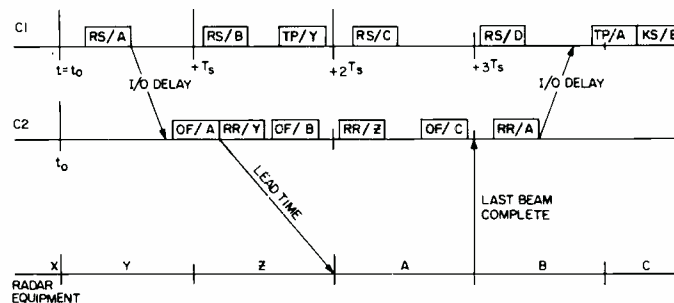

Fig. 8 — Critical loop timing.

actual recording of the data on magnetic tape. The load-evaluation module resides in computer 1 and periodically computes load status (radar load, computer load, number of tracks, etc.) based on data provided by other modules.

Operational readiness test system

The only remaining function to be implemented is ORTS. This, in fact, is not just a single function but includes many test-related functions required to monitor the operation of the radar and notify the maintenance operator of failures. By nature of the function, it is difficult to partition some of these tasks to fit the execution time limits for non-preemptable modules. Also, these modules require a relatively large amount of memory for data and program, but on the average require a small amount of computer time (although sometimes in relatively long periods). Because of the core requirement, all ORTS functions are implemented in computer 2 which has relatively light memory usage from the other modules there. In those ORTS modules where execution times could cause problems with the critical radar control modules, the priority is such that these modules may be preempted by any other module except possibly other ORTS modules or the background self-test module (which by its nature must be the lowest priority module in the computer).

Those ORTS modules that interface with the radar control modules are for the most part non-preemptable, but of lower priority than the non-preemptable radar control modules. This avoids the problem of data being changed by the higher priority module which would otherwise preempt the ORTS module, creating unnecessary problems if preemption is not really required. Those modules that are preemptable must be designed to prevent this type of problem. If common subroutines were used by both non-preemptable and preemptable modules, it would be possible for a subroutine being used by the preemptable module to be called by the other module. The likely result would be for the common subroutine to lose its intermediate data as well as its interrupt point. As mentioned earlier, the solution to this problem is either to use reentrant subroutines or make the modules nonpreemptable prior

to execution of these subroutines and again preemptable upon their completion.

With the final set of modules briefly outlined, the requirements for both the radar control program and the ORTS programs are met and a reasonably good balance of memory and timing is achieved in both computers. This discussion is only representative of the total architectural task; many details have been omitted. For example, as mentioned in the executive discussion, most modules have several entry points although those mentioned in the architectural development are the most important ones.

Tools of the software architect

So far in this discussion the basic tools used have been computer load and memory estimates, input/output traffic analysis, and elementary loop-closure timing verification. As in any other systems engineering task, the development of a viable software architecture is usually the result of an iterative process in which the interactions resulting from proposed changes in the design can be evaluated. One of the most useful tools available to the software architect is simulation. The forms of simulation available can be used to evaluate the detailed algorithms used within the program, as well as queueing delays and the general operation of the priority structure for the modules. Using either type of simulation, a model of the program and its environment must be developed. If this model is not developed carefully, the end result of the simulation may be nearly useless. For this reason, great care should be taken to include all relevant characteristics in the simulation model without including unnecessary details which greatly affect the amount of work required but do not affect the results.

In the AN/SPY-1 radar program development, a good example is the use of target motion parameters in simulation. For simulating target tracking algorithms, the target velocities and accelerations and radar measurement noise are of primary importance. On the other hand, target-related parameters may be neglected in simulating the AN/SPY-1 control program for pur-

poses of determining queueing delays and computer load; the need here is for the arrival rate of targets and the computer processing times to perform the detailed algorithms.

It is the simulation of queueing delays and reaction time that will prove to be most useful, especially when the amount of computer processing required is high relative to computer capacity, or where peak-load conditions exist which would create possible overload situations. Using this simulation, the priority structure of the program can be evaluated under expected operating conditions. In some cases where the detailed algorithms of the simulated modules affect the amount of processing performed by other modules, these algorithms must be included in the simulation. The radar scheduler module is such a case since it determines the type and number of radar beams to be generated. In developing timing estimates, those functions which are most frequently used and of higher priority should be done most carefully. As the development process continues, the estimates should be updated to reflect latest timing values as detailed algorithms are derived. If necessary, the priority structure should be modified to meet reaction time requirements and queueing problems. Excessive peak loads may well point out the need to develop algorithms that will permit the modules to limit the peaks, thereby preventing failure of the program and the overall system of which it is a part.

Conclusion

The software architecture developed using the techniques and tools described in this paper has been successfully demonstrated for the AN/SPY-1 radar control programs in a series of rigorous tests. This testing has included extensive land-based AN/SPY-1 radar performance testing as well as AEGIS system-level tests, including the Weapons Control Systems and Command and Control. The final days of this testing included a 48-hour "fast cruise" during which continuous operation was maintained with a large number of attacking aircraft. All raids during this operational test were successfully dealt with. The system is now undergoing shipboard testing aboard the *USS Norton Sound* on the Pacific Test Range for further evaluation.

Toll switching plan for Alaska

V. Batra | E.F. McGill

In its three years of operation as Alaska's certified long-lines carrier, RCA Alaska Communications (RCA Alascom) has invested over $100 million in plant and facilities to improve the state's commercial long-lines network. During 1973, RCA Alascom completed over eight-million long-distance calls — and with a growth rate of 25 to 30 percent per year. It is important that a long-range plan be formulated to provide the most efficient service at the least cost. The toll-switching plan described here is a step in this direction.

Alaska represents 1/5 the size of contiguous United States.

RCA ALASCOM took over operation of the commercial long-lines network of the Alaska Communications System (ACS) from the Air Force in January, 1971. In purchasing this system, RCA Alascom set its sights on creating a dynamic new communications system for the State of Alaska. All long-distance calls, prior to take over, were handled via Western Electric 3CL cord-type operator boards. RCA Alascom's immediate priority was to establish direct-distance dialing (DDD), comparable to that provided in the contiguous United States. By February 1972, a North Electric NX-1D with NT-500 ticketing system was installed in Anchorage, and in May 1972 another such system was placed in service in Fairbanks.

Customer reaction to DDD in Anchorage and Fairbanks toll centers, which together handle about 80 percent of the state's long distance traffic, was far beyond expectation and a series of rapid additions was initiated to meet the traffic volume. Maintenance during these additions was difficult and in some cases the service suffered. By August 1972, based on this new experience in DDD, a decision was made to re-evaluate growth projections.

Vinod Batra, Project Engineer, RCA Alascom, received the B. Tech in electrical engineering from the Indian Institute of Technology, Madras, India in 1964 and his M.S. degree from the University of Ottawa, Canada in 1967. From 1967 to 1969, he was with the R&D Labs, Northern Electric Company where he worked on various aspects of crossbar and electronic switching systems. From 1969 to 1971 he worked on the Mallard, all-digital switching system. From 1971 to 1973, he worked on various aspects of toll-ticketing and switching design at Stromberg-Carlson in Rochester, New York. He is presently the project engineer for the new principal switching center at Anchorage, Alaska.

E.F. McGill, Mgr., Engineering Planning, RCA Alascom, received his AA degree from Clark College, and his BSEE degree from the University of Washington. He was the Central Office Superintendent providing central office and transmission planning and operational direction for Pacific Power and Light Telephone Company for over a period of ten years. Mr. McGill became Switching Engineering Manager for RCA Alaska Communications in 1973 and Planning Engineering Manager in 1974.

Vinod Batra (left) and E.F. McGill.

A team of technical consultants in cooperation with RCA Alascom developed a modified plan, portions of which are discussed in this article.

Objectives of the switching plan

The objectives of the modified plan were:

a) To provide a backbone toll-switching network to provide the best and most up-to-date DDD service consistent with good management practices (*i.e.* the best service at the least cost) for all areas of Alaska.

b) To stimulate additional revenue, not only by increasing completion rates but also through influencing customer's calling habits.

c) To provide for growth capability in the range of 20% per year up to 1990.

d) To provide for additional customer service *e.g.* wide area telephone service, international direct-distance dialing and other functions required in Alaska's communicaitons needs.

e) To meet and improve established nationwide DDD service standards throughout Alaska.

f) To provide capability to accomodate future technical developments *e.g.* satellite transmission and switching.

Development of the switching plan

Fig. 1 represents the Alaskan long-lines network as it exists today. There are four class-4 toll centers: Anchorage, Fairbanks, Juneau, and Ketchikan. Each toll center provides a high usage and final route to the outside world. Presently, the control switching point for Alaska (907 area code) is Seattle. Calls travelling thousands of miles from the lower 48 have only two chances to complete in this last link. AT&T studies show that over half of such incompleted calls are never attempted a second time. Besides loss of immediate revenue, the future calling patterns are affected.

Based on these observations and objectives, the modified plan established the
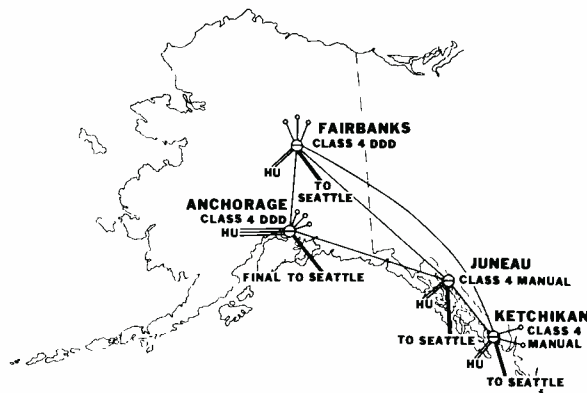
Fig. 1 — Toll switching in Alaska 1973.

following priorities (Fig. 2):

a) Establish DDD in Southeast Alaska.
b) Establish a control switching point (CSP) for the 907 area code in Alaska.
c) Establish guidelines for the orderly growth of the switching machines to meet growth projections.
d) Improve transmission on long-haul circuits through use of 4-wire, end-to-end switching and transmission, if possible.

To establish DDD in Southeast Alaska, it was agreed that a new switching machine would be required. It was decided to locate this switch-center at Lena Point, approximately eight miles from Juneau, the capital city. Lena Point is the transmission hub of Southeast Alaska, thus an obvious choice of location. However, Lena Point is far from being a population center, hence a traffic operating system would have to be remoted from this switch to the town of Juneau, the site of existing 3CL, cord-type operating boards.

Anchorage, due to its central location and accessibility was selected as the site for the new primary center. The existing switching machine at Anchorage was found to be deficient in meeting the CSP requirements. In Phase II, therefore, a second switch-center will be installed at

Anchorage. This switch will function primarily as a control switching point for the 907 area code and will work in conjunction with the existing 2-wire NX-1D, NT-500 system in a two-office (toll-center/primary-center) configuration.

Studies showed that Ketchikan is not large enough to economically support a toll center. In Phase III Ketchikan will cease to be a toll center and all tributaries will be homed on Lena Point switch-center via a new microwave system.

Phase IV of the switching plan addresses the Fairbanks Toll Center. A switch addition will be made to the existing equipment to meet the 1975 busy-season traffic forecast. Future growth direction will be studied as more data becomes available.

During the development phase of the plan, it became evident that any new switching machine should be a 4-wire system with a high degree of flexibility built in (which in turn implied a stored-program control) — and should have the ability to be used at any level of the DDD Network hierarchy as the Alaskan network develops. The system must have low and easy maintenance, a high degree of reliability, and a short installation time for initial set up and future ex-
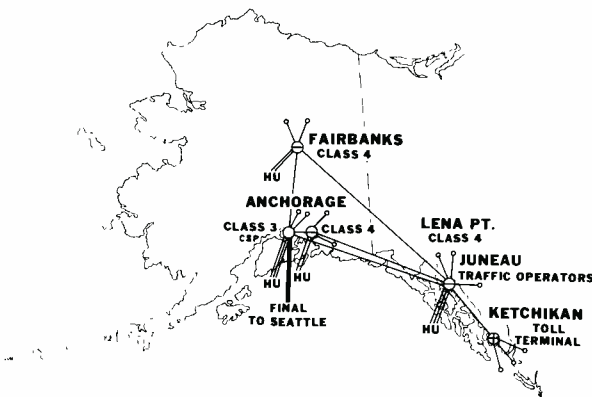
tensions. Above all, it should be economical.

Implementation of the switching plan

Implementation of the Switching Plan consisted of three major milestones:

1) Study of present machine capabilities.
2) Selection of switching machines, and
3) Installation and cut-over of switching machines.

The switching machines presently operating at Juneau and Ketchikan are Western Electric step-by-step, 2-wire systems. They cannot be adapted to provide the growth, features, and requirements of the statewide DDD network. Therefore, a new machine is required.

Anchorage toll center on the other hand, is a modern 2-wire cross-bar machine. It could, with sufficient capital, be modified to 4-wire switching but is deficient in meeting the new service demands and the control switching-point functions. It was therefore decided to freeze the growth of this machine and investigate switching machines capable of meeting all requirements.

The selection of switching machines was accomplished, using twenty-year forecasts on traffic, revenue, and costs inserted into a *present worth of annual charges computer program*. Competitive bids were evaluated on the basis of both the present worth of annual charges (PWAC), technical requirements and ultimate growth capability. Based on this study, Northern Electric's "SP-1, 4-wire ESS" distributed by Northern Telecom was selected for Lena Point and Anchorage.

The SP-1, 4-wire ESS (Fig. 3) is a stored program machine using a minibar switching matrix and a duplicated central processor. The solid-state, wired-logic and plug-in connectorized modules permit a compact package that is easily specified for initial installations and any extension thereafter. This machine is fully compatible with the North American switching network, is designed for Class 1, 2, 3, or 4 applications, and will accommodate the Alaskan network as it continues to expand.

The machine features up to 10-digit translation, code conversion, digit deletion, digit prefixing, unlimited alternate

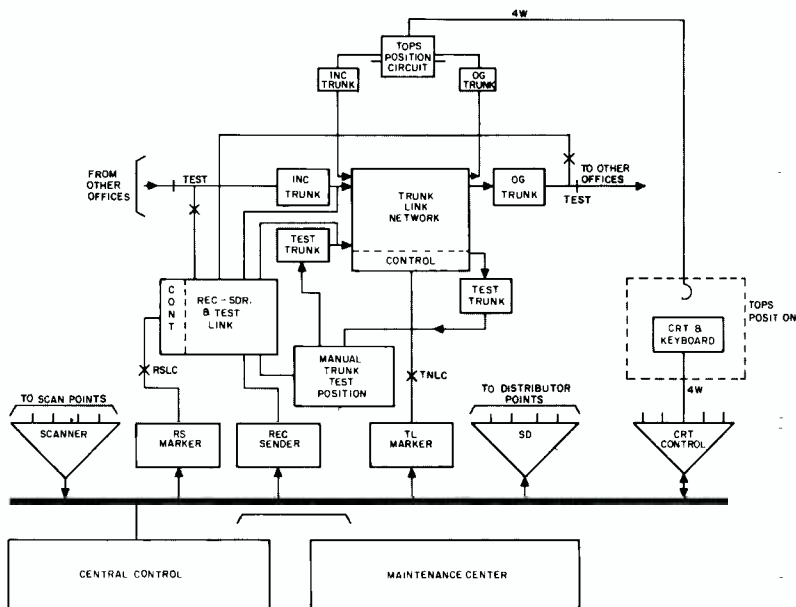Fig. 2 — Toll switching in Alaska 1975 — all DDD.

66

Fig. 3 — SP-1, 4-wire toll-switching system with TOPS

routing, dynamic overload control, traffic and plant measurements, routine and demand testing — and a whole range of other features which may be required in the future. Each SP-1, 4-wire ESS has a maximum traffic capacity of 100,000 ccs (call seconds) and the machine can be used in a multi-unit configuration to meet Alaska's network demands through the 1980's.

The traffic operating position system (TOPS) will be introduced as part of the SP-1 ESS package. Automation of operator functions and subsequent reduction in work effort has always been a prime goal of telephone administrations. Introduction of direct-distance dialing and the elimination of manual tickets are but two steps in this direction. In addition, improvement in the working environment of telephone operators is becoming more important both for job satisfaction and improved efficiency. SP-1 with TOPS will allow this to be realized for the first time in Southeast Alaska. The fully stored program capabilities of the SP-1 system will be used in the incorporation of the TOPS System.

TOPS positions will consist of voice access to the SP-1, 4-wire trunk network plus a video-display computer terminal tied directly to the central processor. All pertinent details of the call are displayed on the operator's screen for the duration of the involvement in setting up a particular call. The operator can modify, delete or add information through a teletype keyboard access. The keys will be arranged in functional groupings and color coded. The view screen can be adjusted in the horizontal and vertical plane to allow each operator to work comfortably.

Besides the regular TOPS positions, auxiliary positions will be provided to assist operators, monitor operators, restrict types of calls to certain positions and receive force administration data. The operators will be able to dial trouble codes for various types of incompleted subscriber dialed or operator assisted calls. This data will be compiled, analyzed and outputted to the RCA DDD Service Bureau. All billing information will be recorded on a magnetic tape and transmitted to the data center for subscriber billing.

All TOPS hardware will be maintained via the standard SP-1, 4-wire techniques of fault detection. The diagnostic tests will be performed on a demand basis as well as on a scheduled periodic basis.

Switch status

Lena Point switch will be housed in a new 14,000 sq. ft. air conditioned, single-story building. Besides the switching equipment, the building will house the satellite earth-station, power plant, administrative, and support facilities. The initial switch installation will consist of 1200 incoming and 1200 outgoing trunk appearances and 38 traffic-operating positions. The traffic operating system will be remoted to the RCA building in downtown Juneau. An in-service date of March 1975 is planned.

The Anchorage primary center will be housed in a new three-story, 60,000 sq. ft., air-conditioned building. Foundations have been provided for additional floors, as future growth demands. The building will house switching equipment, a network management center, a traffic-operating system and administrative and support facilities. The initial switch installation will consist of 1,920 incoming, 1,920 outgoing trunk appearances and 39 traffic operating positions. An inservice date of February 1976 is scheduled. Work on both switch centers in approximately 90% complete.

Conclusion

The population of Alaska has increased by about 40% since 1960. Alaska represents about one-fifth the total area of the continental United States. This growth in population, linked with Alaska's untapped resources, reflects the vital need for a superior communication system. During 1972, RCA Alascom completed 7-million long-distance calls. Current projections call for 35-million originated calls in 1980. The new switching configuration will help RCA Alascom to meet this growth by introducing principal city functions in Anchorage, provide direct-distance dialing in Southeast Alaska, provide 4-wire switched transmission, provide a futuristic traffic operating position system, introduce standard toll-dialing throughout the State of Alaska, introduce the dial rate in the State of Alaska, introduce international direct-distance dialing, and provide a communication system equal to in capabilities or greater than those provided by other systems in the rest of the North American Continent.

Acknowledgment

Bibliography

McGill, E.F. and Batra, Vinod.: RCA Alaska Communications, Inc., "Toll Switching Plan For Alaska." Presentations to *Alaska Telephone Convention, Anchorage, Alaska*, August 1973 and *Alaska independent connecting companies* on an individual basis throughout the year of 1973.

TTUE-4A uhf television exciter

J.B. Bullock

The TTUE-4A is the exciter now used to drive all current transmitters in the RCA uhf transmitter product line. It produces, from temperature-compensated crystal-oscillator sources, an amplitude-modulated visual carrier with much of the lower sideband removed, and, 4.5 MHz above that, a linearly modulated fm aural carrier. In the visual channel. the modulation is predistorted to compensate for phase and amplitude nonlinearities that will inevitably take place in the power-amplifier stages to follow. In the aural channel, a choice of 50 or 75 microseconds pre-emphasis is provided, to be used as required in the given broadcast system.

VISUAL and aural modulation are accomplished at intermediate frequencies. These i.f. signals, at 45.75 and 50.25 MHz respectively, are heterodyned against a common "pump" signal and "up-converted" to the desired uhf tv-channel frequency. Channel frequency is thus dependent on only pump frequency, which makes much of the exciter independent of the tv channel and thus expedites both production and the stocking of spare parts.

Visual signal

The generation of the visual signal is indicated in the functional block diagram of Fig. I. Each block on the diagram generally represents a plug-in "baby" board in the exciter.

The incoming video signal is looped through a differential input amplifier to provide for cancellation of common-mode inputs. The video signal then goes to the motor-driven (for front-panel remote operation) video level control, and to the clamp-pulse generator.

The clamp pulse is centered in time within the "back porch" at blanking level following each horizontal sync pulse. The clamp pulse activates a sample-and-hold circuit which samples the voltage level of the back porch at the input to the video amplifier preceding the modulator and closes, for the moment, a high-gain negative feedback path to the input of the differential gain driver. This restores the back porch to its preset level and establishes a blanking level at the input to the video amplifier which will be maintained by the clamp, independent of picture or sync amplitude. This clamped level is variable by an adjustable dc inserted into the feedback loop in the clamp amplifier. From the point of clamping forward, all video circuitry is dc coupled (or clamping would be lost).

At the modulator, the back-porch level becomes a reference i.f. power level from which sync will modulate upward, producing greater power output, and picture content will modulate downward, producing lesser power output.

A positive-and-negative clipper follows the output of the final video amplifier to limit video peaks which might otherwise overmodulate.

An adjustable unclamped reference level is provided via the clamp *on off* switch. In the *off* position, this adjustable reference level provides a means of setting the video signal and the resulting i.f. carrier to any desired point in their operating regions for test purposes.

Linearity correction

The rf output of the transmitter (which usually employs a klystron power amplifier) must be a linear reproduction of the exciter's video input. Fig. 2 shows a typical saturation (power output *vs* drive power) curve for a VA-890 type klystron. This non-linear performance as saturation is approached is typical of all power klystrons.

This 35-kW klystron is used only up to the 32-kW level, which is to say that the rf power output at peak of sync will be 32 kW. The transfer characteristic of Fig. 2 is replotted in Fig. 3 on a voltage basis with 100% output voltage representing the 32-kW output. It is seen from this curve that at blanking (back-porch) level, where the output voltage must be 75% of that at peak of sync, the input drive to the klystron must be 59% of the drive at sync peak. Similarly, the drive at mid-characteristic (midway between blanking and reference white level) must be 33% of the drive at sync peak.
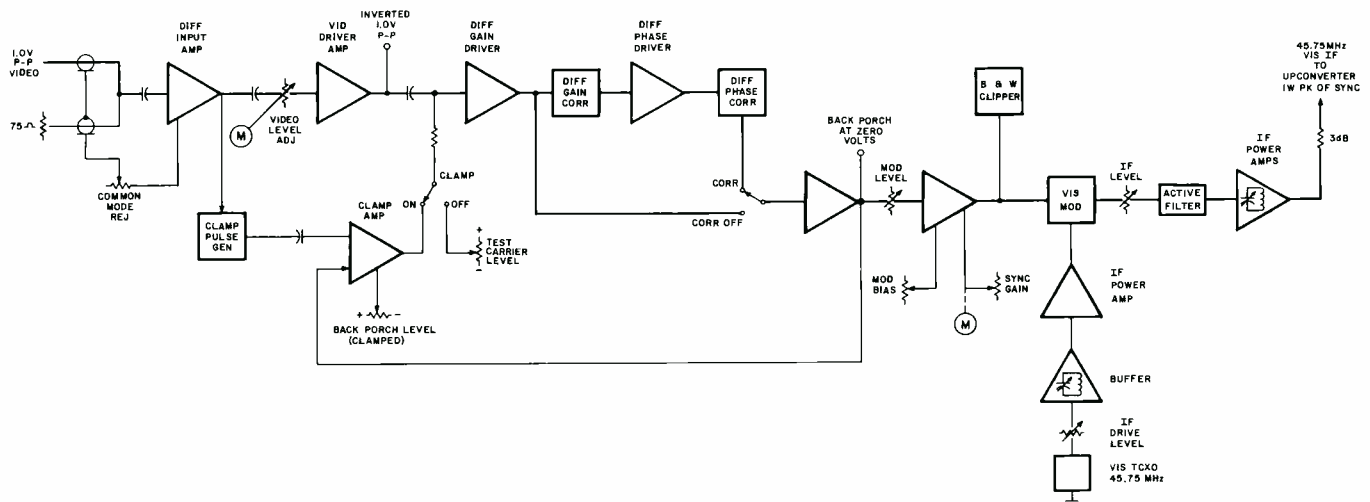
Fig. 1 — TTUE-4A exciter video — visual i.f. functional block diagram.

John B. Bullock UHF-TV Broadcast Engineering, Communications Systems Division, Meadowlands, Pa. received the EE from North Carolina State University. He served in the U. S. Army Signal Corps during WW Iı principally as an instructor at the Army Electronics Training Center at Harvard University, emerging with the rank of Captain. Mr. Bullock has taken graduate studies at Yale and at the University of Pennsylvania. Joining RCA in 1952, he became a mainstay in RCA's Microwave Relay activity in Camden and played a major part in system and circuit design of the TVM-1/3 and TVM-6/13 tv microwave relay equipment. In 1970, with the combining of tv relay and uhf transmitter engineering activities, he transferred to the Meadowlands plant where he participated in the final design stages of the TTUE-4A uhf tv exciter. Mr. Bullock was chairman of the EIA committee on tv relays from 1960 through 1970, and is a member of the IEEE and a licensed professional engineer in the State of New Jersey.

If the required klystron rf input amplitudes of Fig. 3 are plotted against the video signal to be transmitted, the necessary exciter transfer characteristic results, shown in Fig. 4. (This characteristic excludes the ac-coupled stages at the exciter input, where the video signal is inverted and its level set).

The exciter's rf output with staircase video modulation, rectified by a diode, and observed on an oscilloscope, will appear as shown in Fig. 5b. Step risers and subcarrier amplitudes here would be noted as up to 20% greater at blanking level, tapering to a constant value as reference white is approached. The 3.58-MHz subcarrier in Figs. 5b and 5c is approximately half-amplitude due to elimination of most of the lower sideband at higher frequencies. At the modulator stage the signal is double sideband; hence modulation with the signal shown does reach reference white level.

Fig. 4 shows that the only obviously required non-linearity predistortion is sync and black stretch; however, white stretch and white compression are also provided in the exciter to perfect system
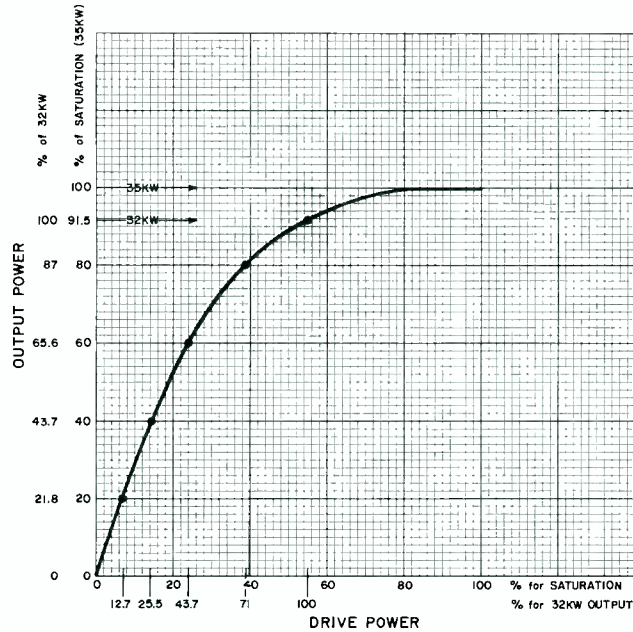
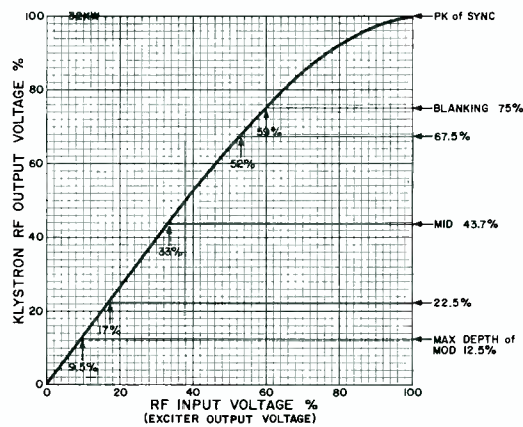

Fig. 2 — Typical saturation curve for a VA-890 klystron.

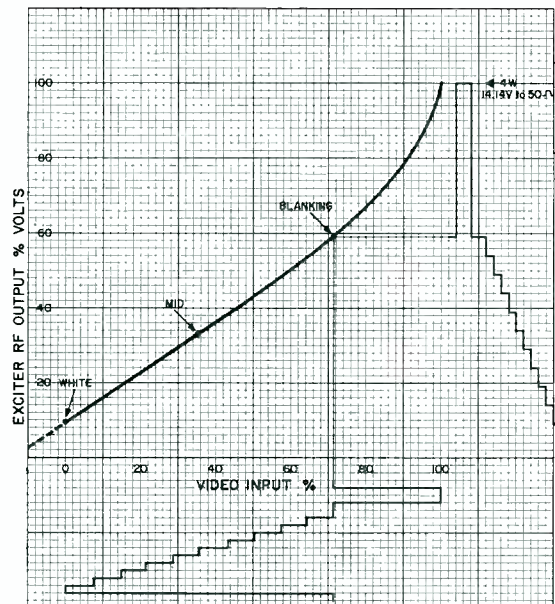

Fig. 3 — VA 890 klystron voltage transfer characteristic.

Fig. 4 — Required exciter voltage transfer characteristic.

69

linearity. Some of the white stretch is required in improving the exciter's own modulation linearity, which tends towards compression at modulation depths.

The linearity correction, or predistortion, is principally accomplished as indicated in the voltage divider of Fig. 6. Supplementary sync stretch is also provided just prior to the modulator stage.

The voltage-dropping portion of the divider is shunted via gated diodes to produce sync/black stretch or white stretch (or both) as determined by adjustment of diode bias. Similarly, the terminating portion of the divider is shunted via gated diodes to produce white compression.

Four black-stretch shunts are provided, with gating bias adjustments starting at the tip of sync. Similarly, there are six white-stretch adjustments and four white-compression adjustments. All adjustments simply set gating bias levels.

A transfer characteristic for the entire exciter is plotted in Fig. 7. Since the correctors are set to optimize linearity for the entire transmitter system, some predistortion is required from all the correctors, including an approximate 2:1 sync stretch. This transfer characteristic curve, if replotted on a percentage basis, should closely coincide with the curve of Fig. 4 between reference white and tip of sync.
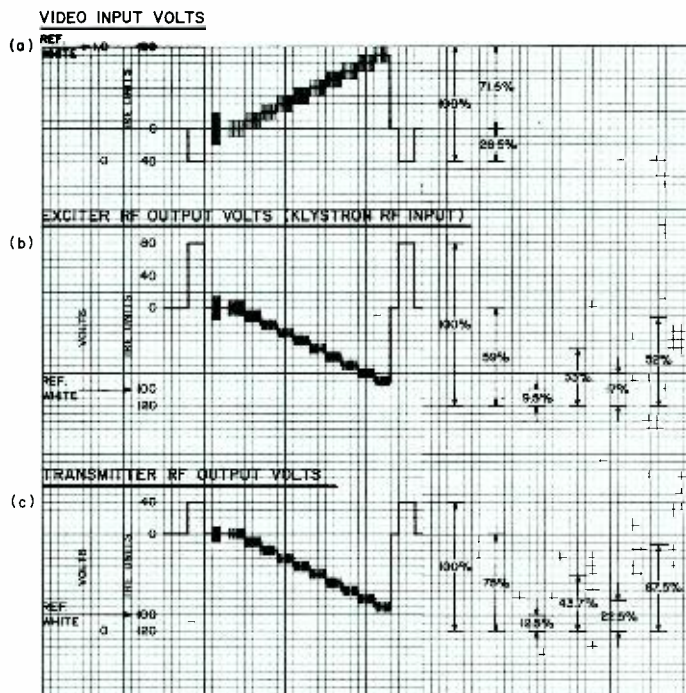

Fig. 5 — Staircase modulation waveforms.

Differential phase

Just as the above compensating distortion is required to correct expected gain changes with level (differential gain), so a compensating distortion is required to correct for phase changes with level (or differential phase) to provide overall phase linearity, without which the video waveform would be distorted in the time domain. This compensation is provided by the differential phase correctors illustrated in Fig. 8.

Differential phase correction is accomplished by gating, into the video line, an out-of-phase video signal at the level where predistortion is required. In Fig. 8, VID 2 is the main video signal, while VID 1 and VID 3 are signals identical to VID 2 which are superimposed on dc levels of 6 and −6 V, respectively. This arrangement makes it possible to apply an adjustable gating bias to the diode. When the diode is gated *on*, the opposite-phase video signal is added to the video line through the 7 pF capacitance, shifting the phase of the resultant video while the diode conducts. An approximate phase shift of 3° is obtained at 3.58 MHz. This provides a differential phase that can be adjusted to cancel differential phase of opposite sense occuring elsewhere in the system.

Fig. 6 — Linearity (differential gain) predistortion.

This type of phase-correction circuitry has the advantage that virtually no resistive loading is added to the video

70

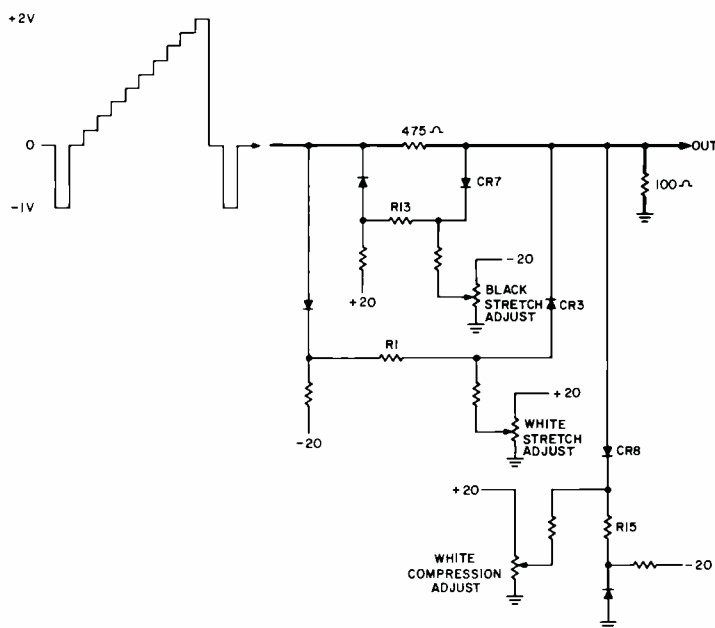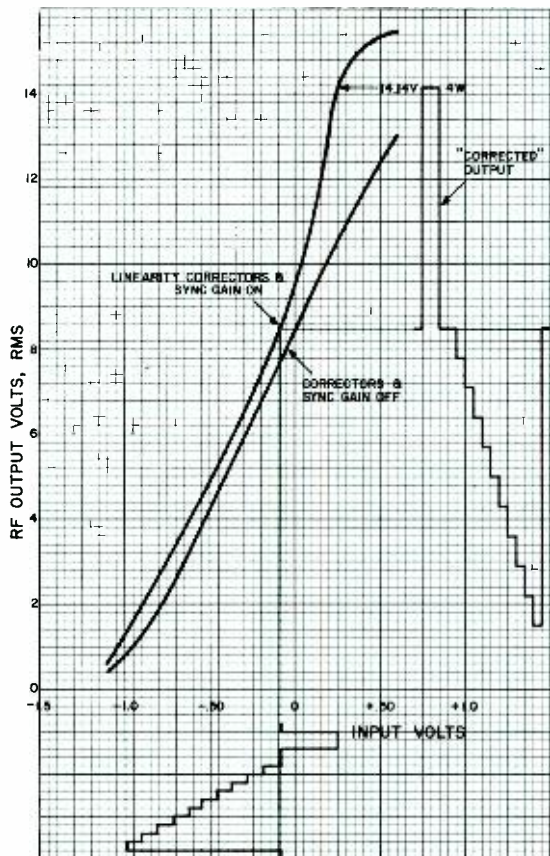Fig. 7 Exciter voltage transfer characteristic, clamped input to rf output.
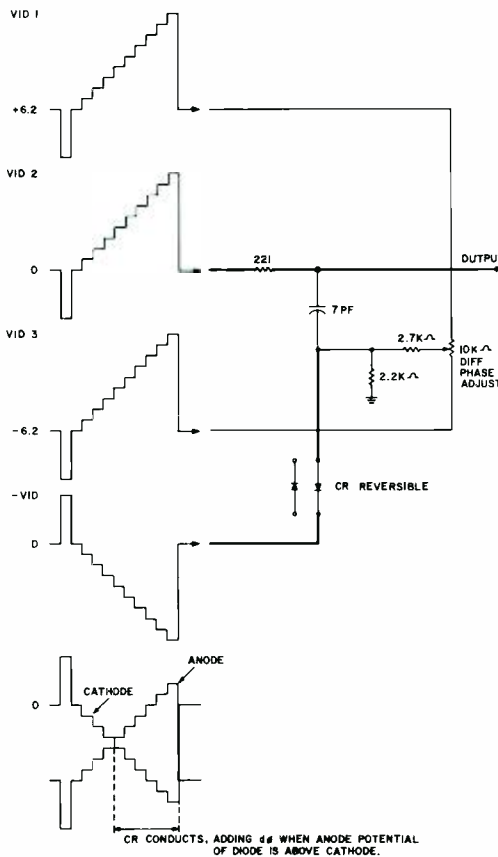

Fig. 8 — Differential phase correction.

line, thus the phase correction may be set without affecting differential gain.

Seven sets of differential phase correction are provided, with a phase-correcting (predistorting) capability of about ± 20°. A phase correction in the white region may be shifted to the black region by reversing the gated diode.

Modulation

Following the corrector circuitry, a reference test point is provided, and at this point the "back porch", or blanking level of the video signal is adjusted to a dc zero voltage level (Fig. 1). This level is maintained by the clamp circuitry. A

video-level control sets the amplitude of the video drive to the final video amplifier. The output of this amplifier, plus an added (adjustable) dc bias voltage drives the modulator.

The modulator is illustrated in Fig. 9 together with a portion of the final video
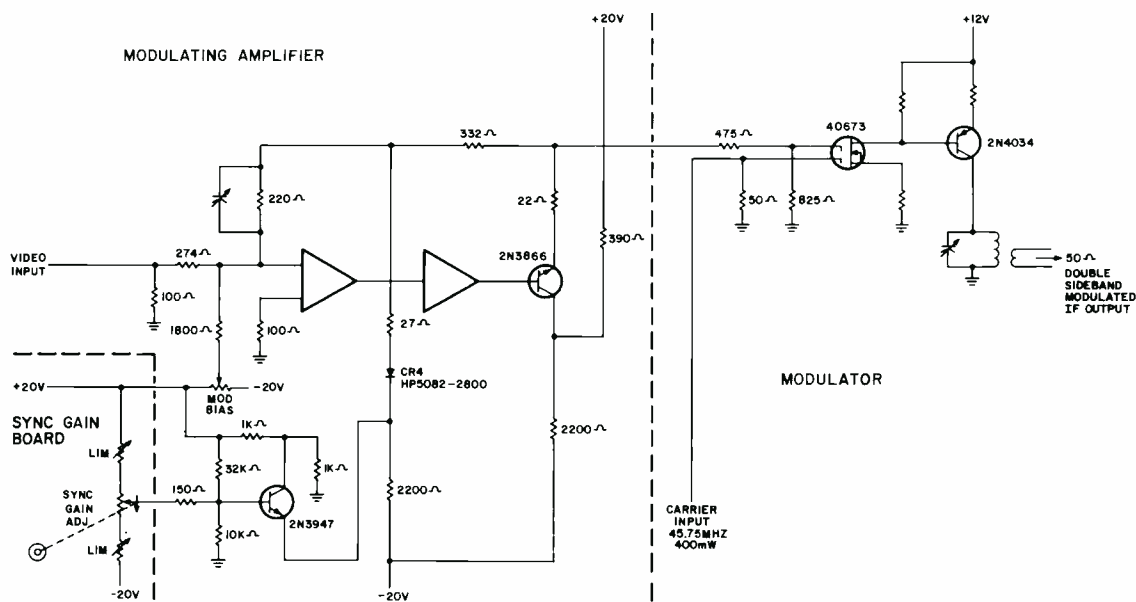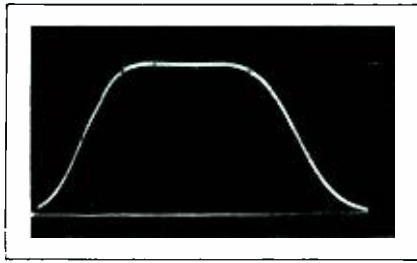

Fig. 9 — Visual modulation.

Fig. 10 — Active filter response (spectrum analyzer display). Horizontal scale: 2-MHz/division; Vertical scale: linear.

amplifier and the motor-driven sync gain control. The latter adjustment can increase the gain of the modulating amplifier in the sync region by reducing the negative feedback around the amplifier to provide additional sync stretch. About 40% of the stretch usually required in operation is obtained from this control. The feedback is reduced when bias to the CR4 diode allows it to be gated *on* as the video signal nears sync level.

Modulation of the 45.75-MHz visual i.f. signal is accomplished by the FET-transistor combination: the video signal on gate 1 of the FET varying the gate-2 transconductance. In operation, the gate-1 (MOD) bias is set such that the full amplitude of sync is preserved, allowing some white compression, which is then corrected by the white stretch available

from the differential-gain-corrector circuitry.

Sideband filtering

The modulator produces a double-sideband amplitude-modulated signal. The signal is then fed to an active bandpass filter where much of the lower sideband is removed. The swept response of the active filter is indicated in Fig. 10. Note that the lower 3.58-MHz sideband is attenuated about 6dB, leaving the bulk of sideband shaping to be done by the sideband filter following the power amplifier in the transmitter.

Following the active filter, the visual i.f. signal is taken through a series of three power amplifiers (Fig. 1). These bandpass units are adjusted to be flat from 44 to 51 MHz leaving band shaping in control of the active filter. The i.f. signal is raised to a level of 2 watts at peak of sync by these stages, and is then fed to the visual upconverter.

Aural signal

Origination of the aural i.f. signal is indicated in the functional block diagram of Fig. 11. As in the visual portion each block generally indicates a plug-in "baby"

board in the exciter.

The carrier originates with a 418.75-kHz temperature-compensated crystal oscillator. This frequency is multiplied by 120 after modulation to reach the aural i.f. of 50.25 MHz and to provide a deviation capability of better than ±50 kHz at that frequency.

Separate baseband audio and SCA (Subsidiary Communications, such as telemetering) inputs are provided. The former passes through a choice of 50 or 75 μs pre-emphasis and then both are fed to a series of five serrasoid modulators. In this type of modulation, each modulator produces a pulse whose time position is advanced or retarded from the pulse at its input in proportion to the modulating voltage at the time of its occurrence. Each modulator operates on the output pulses of the preceding modulator; thus the total phase displacement produced is the sum of the displacements produced by the five modulators. The resulting signal would be a phase modulation of the carrier. However, as is well known, a frequency-modulated signal can be produced by a phase-modulation process if the modulating signal is retarded 90° and attenuated in proportion to its frequency prior to modulation. A network for accomplishing this is incorporated with the pre-emphasis in the processing circuitry preceding the modulators.
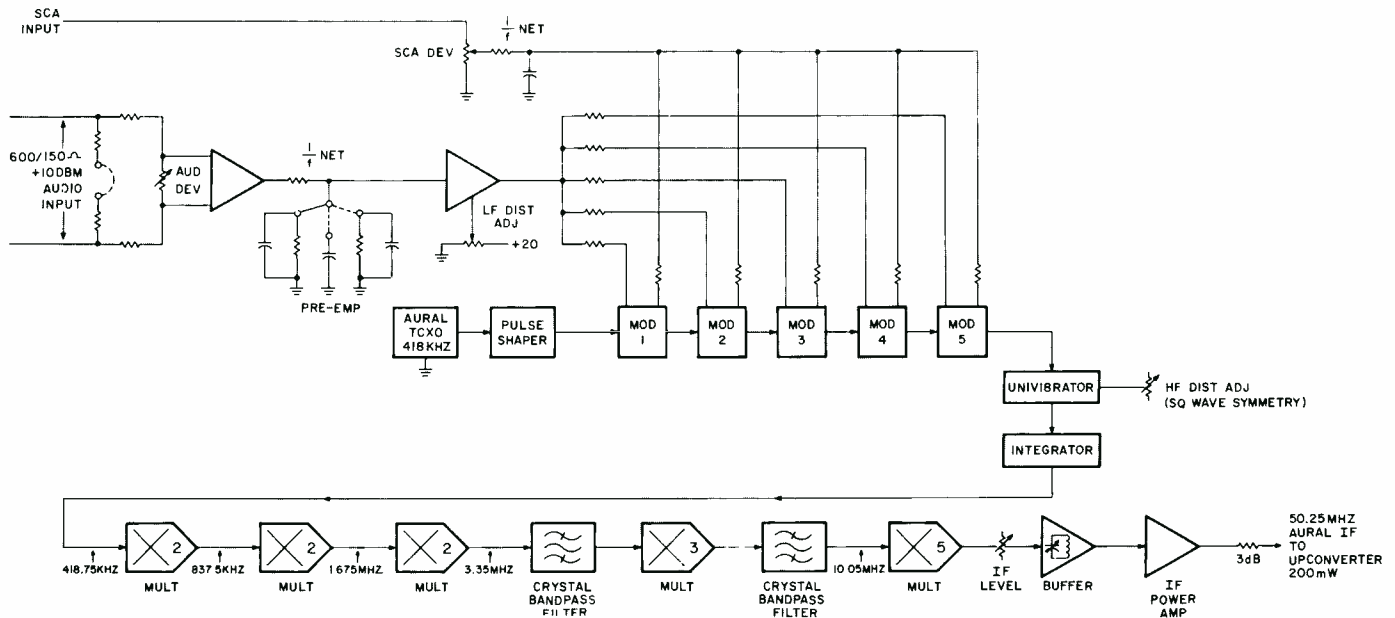

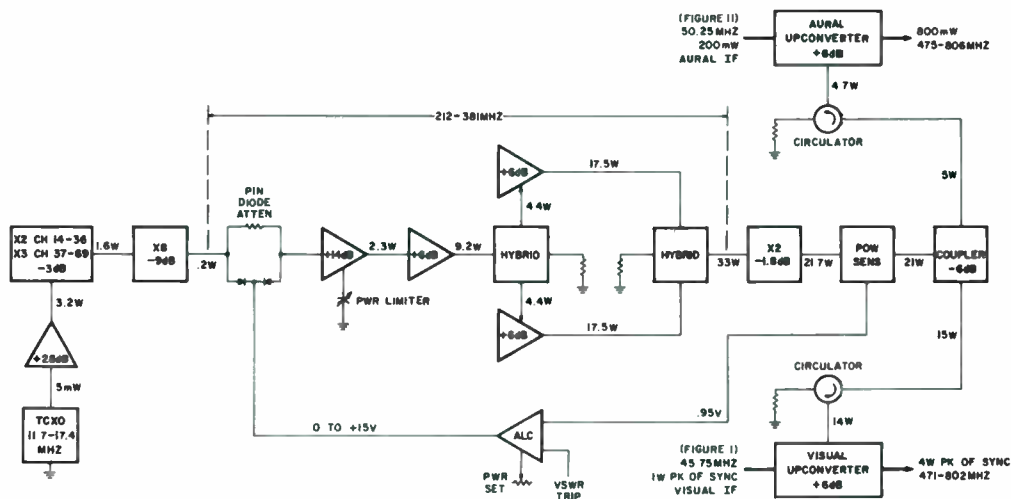Fig. 11 — TTUE-4A exciter audio — aural i.f. functional block diagram.

Fig. 12 — TTUE-4A pump power rf generation block diagram.

Frequency multipliers

The modulated signal at 418.75 kHz, at the output of the last modulator, is a series of positive pulses with the modulation information in the position of the leading edge. These pulses then key a monostable multivibrator to produce a square wave that is integrated to produce a back-to-back sawtooth waveform, still at 418.75 kHz. The multiplication process then begins by applying the back-to-back sawtooth to a series of three full-wave rectifiers, each preceded by an amplifier with a nominal 2:1 gain to restore the amplitude. Each amplifier, plus full-wave rectifier, constitutes a frequency doubler. with no tuning adjustments being required[1] Symmetry of the driving square wave is carefully maintained to assure the symmetry of the back-to-back sawtooth waveforms. Departure from this symmetry introduces distortion, and the symmetry adjustment is used as a distortion nulling control.

A tripler employing crystal filters at input and output, and a harmonic multiplier tuned to the fifth harmonic complete the multiplier chain, raising the signal to the final aural i.f. of 50.25 MHz. A tuned buffer amplifier and broadband power amplifier then provide the required power output of 400 mW. These two amplifiers are identical to stages used in raising the visual TCXO output at 45.75 MHz to a 400-mW level prior to the visual modulator (Fig. 1).

Each of the aural modulators is capable of a phase shift of nearly ±2 radians. so that the five cascaded modulators can produce about a phase shift of ±10 radians. At a modulating frequency of 50 Hz, this amounts to a frequency change of ±500 Hz from the 418.75 kHz fundamental. The multiplication by 120 raises this deviation to ±60 kHz, adequate for European standards. Operation to US standards (±25 kHz) is possible using only three modulators but with a minor increase in distortion.

Pump-power generation

The visual and aural i.f. signals created at 45.75 and 50.25 MHz, respectively, are hetrodyned up to any desired channel in the 470 thru 806 MHz frequency range (channels 14 thru 69) in two separate upconverters driven from the common pump source. The generation of pump power is illustrated in Fig. 12.

The pump signal originates with a TCXO in the 11.7-to 17.4-MHz frequency range. A specified TCXO is used for each of the uhf channel frequencies including those requiring 10kHz or −10kHz offsets. For channels between 14 and 36, the total multiplication is 32; for channels 37 thru 69, the factor is 48. Typical power levels at each stage in the chain are shown on the block diagram. The final pump signal has a 2nd harmonic about 55 dB below the fundamental, and no close-in signal higher than 70 dB down. (This data was taken from a pump chain at channel 31, TXCO frequency at 16.484375 MHz, and

final pump frequency at 527.5 MHz).

The three 6-dB power amplifiers (PA) are identical units. The two paralleled units are matched in power output by upsetting the input VSWR of the higher-gain unit via a small trimmer capacitor. The matching is done to minimize losses to the adding hybrid reject port, since available pump power is limited by the dissipation ability of the transistors in these paralleled PAs. A power limiting adjustment in the 14-dB PA is set to limit the drive to the higher of the paralleled PAs to that producing a 22-W output. This avoids PA transistor burn-out in event of an automatic level control (ALC) malfunction.

The adding hybrid following the PAs is identical to the splitting hybrid but used "in reverse."

An ALC loop surrounds the amplifiers and multiplier following the X8 multiplier. This loop permits setting the pump-power level and acts to maintain the level of power out of the power sensor constant at the required 21 W. The ALC is needed primarily to compensate for changes in amplifier gains with temperature.

Incorporated in the ALC amplifier is an input which will reduce the output of the ALC circuit to zero upon application of a −2 V to that input. Zero output from the ALC amplifier causes maximum attenuation in the pin-diode attenuator

following the X8 multiplier and thus reduces the pump-power output to zero. This feature is used to remove drive power from the transmitter klystrons in the event of a vswr fault in the output line of any klystron. The vswr fault circuitry furnishes the −2 V to the ALC. This feature saves the klystron and its output line from further damage if a VSWR fault should occur.

Upconverters

The visual upconverter and aural upconverter are identical units, however, the alignment of the former is much more painstaking in view of its linearity and bandwidth requirements.

The upconverters use a Varian VAB802 varactor diode in the circuit arrangement shown in Fig. 13. All inputs and outputs are at 50 ohms. Nominal maximum test power levels are shown on the diagram. Gain of the upconverter from i.f.-in to rf-out is 6 dB, with a 7-MHz passband.

Initial alignment is done using a swept 44-to 51-MHz i.f. input, with a pump power of about 7 W. For alignment, the reflected pump and i.f.-input powers must be minimized and power output at the pump+i.f. frequency be maximized. Initial alignment is done at reduced pump power to avoid developing excessively high rf voltage across the (initially) unloaded pump tank circuit.

It is easily seen from the circuit of Fig. 13 that there will be much interdependence in the various tuning adjustments. The varactor bias which sets the initial value

Fig. 14 — Exciter (visual upconverter) final broadbanding response test block diagram.

of the varactor junction capacitance affects tuning of both the pump tank and the first section of the output filter, and to a lesser degree, the i.f. input impedance.

As the output filter is tuned, CR1 must be "worked into" the pump and filter circuits by patient adjustment of the C7/CR1 and C8/CR1 ratios; the pump tank must be kept resonated; and the i.f. and pump inputs must be matched to 50 ohms.

When an rf output of 2 W has been achieved at the 7 W pump level, pump power is raised to 14 W and alignment is continued until the 4:1-gain, the 4-W output, and 7-MHz bandwidth are achieved with no more than 0.5 dB of compression at the 4-W output level.

Alignment to this point also includes the requirement that the pump signal at the rf output be at least 30 dB below the 4-W level, that no spurious signals are

generated by the upconverter itself, and that no added dc be drawn from the varactor bias supply due to the presence of i.f. drive.

Final stages of visual upconverter alignment are done with the upconverter installed in the exciter. The exciter is then modulated by the video sweep output of a sideband analyzer with sync and blanking added. Using this arrangement, as shown in Fig. 14, the power level at peak of sync can be held at 4 W by observing the diode; unwanted spectrum components can be held at proper levels by observing the spectrum analyzer; and the desired passband achieved by observing the sideband analyzer. The alignment will be considered complete when the swept response does not "tilt" by more than ±0.5 dB as picture brightness is varied through those levels which would produce 22% thru 67% of final transmitter-output voltage. (Referring to
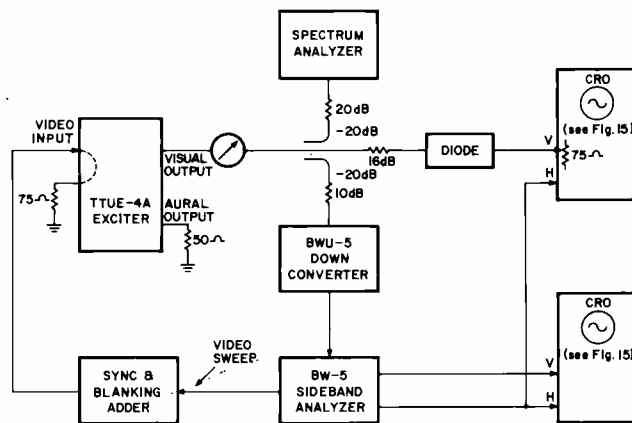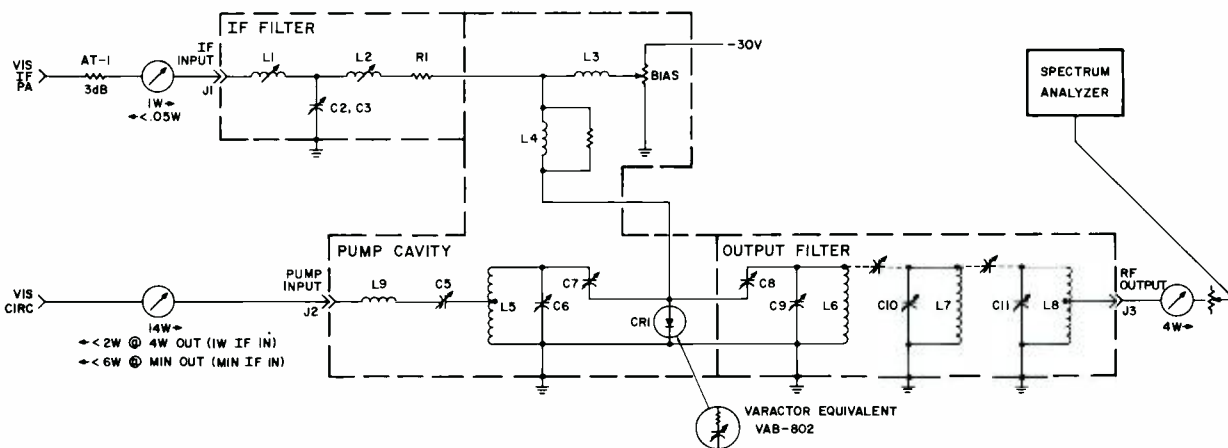

Fig. 13 — Upconverter — simplified schematic with test metering.

Fig. 3, this is seen to be a variation of from 17% thru 52% of the exciter's output voltage at sync peak).

The diode and sideband analyzer responses obtained from a properly operating exciter upconverter) in the test setup of Fig. 14 are shown in Fig. 15. The response shown on the sideband analyzer is virtually identical to that of the active filter (Fig. 10). The roll-off in diode response shows the elimination of the lower sideband at higher modulation frequencies. Tip of sync in this photo is at the 4-W level.

Packaging

The exciter is contained in one horizontal and four vertical drawers in the 28-in.-high rack-mountable frame pictured in Fig. 16. The horizontal drawer at the top of the frame contains metering and controls. The four vertical drawers contain (from left to right) the aural i.f., visual i.f., video processing and low-level pump stages, and higher level pump chain plus upconverters.

The exciter frame is mountable in the control cabinet of any of the current product line of RCA uhf transmitters, or, alternatively it may be mounted in a separate cabinet for service as a spare exciter.

The circuit packaging in three of the vertical drawers is as displayed in Fig. 16,

OUTPUT VOLTS
—0
—33%(MID)
—59%
—100%(SYNC TIP) 4W

0   4MHZ

DIODE DISPLAY
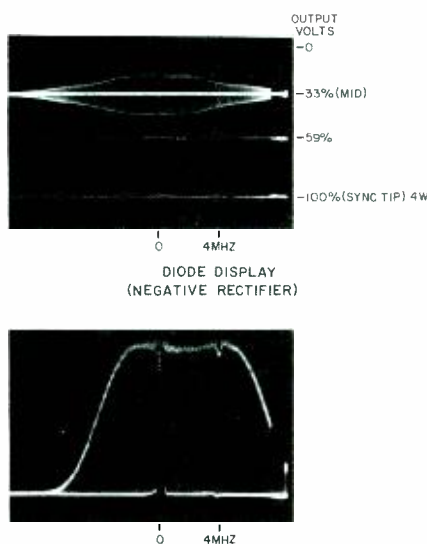(NEGATIVE RECTIFIER)

0   4MHZ

Fig. 15 — Diode and BW-5 sideband analyzer displays test setup of Fig. 14.

which shows a view of the exciter with the visual i.f. drawer open. All drawers slide forward in this manner. Each vertical circuit board seen in the figure carries circuitry of one of the blocks in the diagram of Fig. 1. The bottom row, for example, from front to back contains the visual i.f. TCXO, buffer amp, and i.f. power amp. These vertical boards plug into sockets on "mother" boards which are also vertical but run from front to rear of their respective drawer. These mother boards provide interconnection between the "baby" boards via printed circuitry and also mate with the cable harness connector. The cable harness then provides interconnection between mother boards in this and the other drawers.

The right-hand vertical drawer in Fig. 16 is the pump drawer. In it are mounted the circuit stages illustrated in Fig. 12, starting with the X8 multiplier. These stages, because of the frequency and power levels involved, are built in tightly shielded chassis with heat radiating fins and/or heat sinks to the chassis of the drawer.

Metering

Each stage in every area of the exciter has a dc metering lead brought to the front panel meter with a reading indicative of normal operation. In this manner, trouble can quickly be isolated to the stage involved. The front metering panel also includes controls for setting video modulation level and sync gain (stretch) plus jacks for connection of a counter to make direct measurement of visual, aural, and pump crystal oscillator frequencies.

Power supply

The exciter is powered by a separate dc voltage supply which operates from 200- to 250V, 50- to 60-Hz power. Four dc voltages are supplied to the exciter as follows: +45 V, −25 V, −30 V for upconverter bias, and ±24 V for control motors.

In the exciter itself are eight positive regulators and two negative regulators. All are plug-in "baby" boards and each provides a required voltage to some subdivision of the exciter. Three regulators may be seen in the upper compartment of Fig. 16. All positive regulators are interchangeable regardless
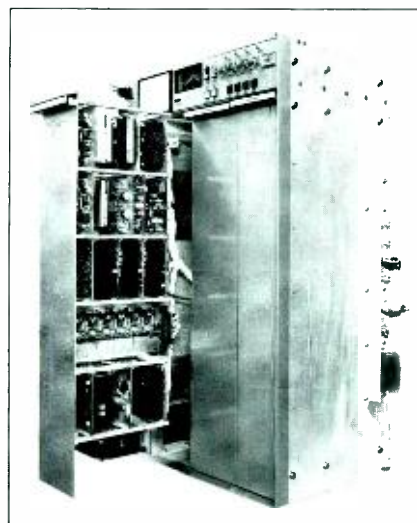
Fig. 16 — TTUE-4A exciter photograph — visual i.f. drawer open.

of their output voltage, the programming resistors which set the output voltage being mounted on the mother boards and wired via socket connections. Negative regulators are also interchangeable. Both types of regulators incorporate overload and overvoltage protection, thus protecting themselves from damage by load fault and protecting their loads from damage by an overvoltage fault.

Acknowledgment

Reference

1. Reference US patent 3596208, D. L. Yerzley

# Laser scanning as a tool for testing integrated circuits

Dr. R. Williams|P.V. Goedertier|Dr. J.D. Knox

Laser scanning can be used to test integrated circuits for defects. This paper describes the method and shows some results for a simple circuit.

GREATER RELIABILITY in the manufacture of integrated circuits means that new testing methods must be invented to keep up with advances in circuit design and fabrication. At RCA Laboratories, we are exploring a new way to look at integrated circuits. Each functioning element is probed by sequentially scanning the entire circuit with the focused spot from a laser beam. This is done at some stage of fabrication before the circuit is encapsulated. At those
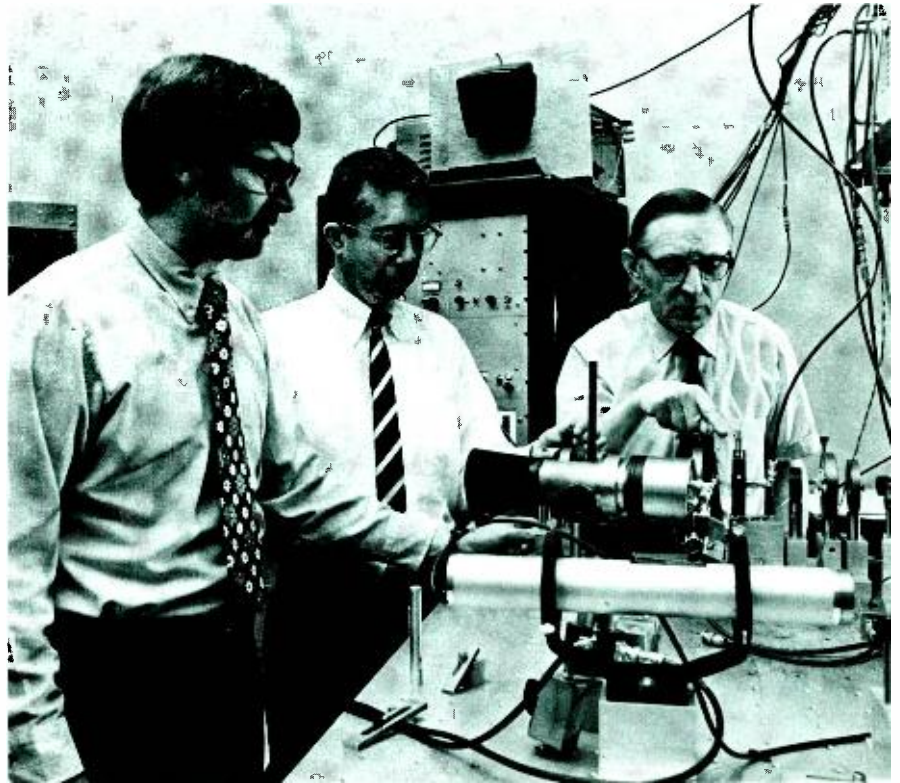
Left to right: authors Knox, Williams, and Goedertier.

Dr. **Richard Williams**, Physical Electronics Research Laboratory, RCA Laboratories, Princeton, NJ, received the AB in chemistry from Miami University and the PhD in physical chemistry from Harvard University. He joined the laboratories in 1958. He has worked in several areas, including semiconductor-electrolyte interfaces, liquid crystals, internal photoemission, and insulator physics. He was group leader in Insulator Physics from 1967 to 1970 and in Quantum Electronics from 1970 to 1972, when he was made a Fellow. He has received several achievement awards and shared in the David Sarnoff Team Award in Science in 1969. He was a visiting scientist at the RCA Zurich laboratory in 1963 and has been a Fulbright Lecturer in Sao Carlos, Brazil, a summer school lecturer at *Instituto Politecnico Nacional* in Mexico and a visiting lecturer at Princeton University.

Peter V. Goedertier, Physical Electronics Research Laboratory, RCA Laboratories, Princeton, NJ obtained the MA in 1941 from the University of Louvain, majoring in theoretical physics. He held various positions in teaching and research field at the Philosophical College of Louvain, The University of Louvain, and Duke University. At RCA Laboratories, which he joined in 1959, he has been engaged in early work on optical masers, with both gaseous and solid-state materials. He was the co-discoverer of the *He-Ne* "cascade" laser, and in 1965 was given an Achievement Award for his contributions to the development of the cross-pumped *YAG:Nd:Cr* laser. For the last three years, he has been working on the development of various optical systems, relating to the processing and the displaying of video information. He is the author of more than a dozen scientific papers, and holds three U.S. patents.

places where there is no lead metalliza-tion, the light enters the underlying silicon. Here it is absorbed to produce free holes and electrons. Wherever there is a pn junction, these move in opposite directions. This transient charge flow gives a signal that can be detected at various points in the circuit as the spot passes over the junctions. We take out this signal and use it as a video input for display on a kinescope, which shows a "picture" generated by the actual functioning of the active circuit elements. A bad transistor gives itself away by its pathological response to the laser spot. This gives us a rapid test for malfunctions: a direct visual indication of the bad spot and where it is on the chip.

The laser scanner[1] (shown in Fig. 1) uses a 1-W argon laser (4880Å) with a combina-tion of deflectors, one acousto-optic and the other a scanning-mirror galvano-meter. These generate a 525-line video-raster scan at tv frame rates. We can focus the laser spot to a small size, 3 μm if
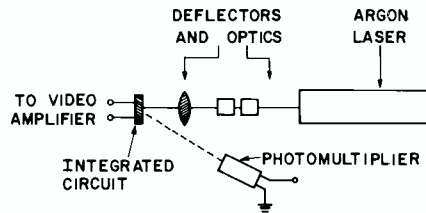

Fig. 1 — Schematic drawing of laser-scanning ap-paratus. The video signal can come either from the circuit itself, or from the photomultiplier.

necessary, and compress the scanned area so that it just covers the surface of an integrated circuit chip. To get a general picture of the circuit by reflected light, we use the apparatus simply as a flying-spot scanner: The reflected light is picked up by a photomultiplier and the photocurrent is used as a video-input signal. This gives a magnified picture by reflected light. The picture does not show defects that are not evident under an optical microscope, but it can be used to align the chip rapidly and to identify different parts of the circuit.

We chose the simple COS/MOS circuit, CD-4007, to demonstrate the method. The CD-4007 is a dual complementary pair plus inverter, with three-n-channel and three p-channel enhancement-type MOS transistors, connected as shown in Fig. 2(a). The optical microscope picture of Fig. 3 shows the layout on the chip. To emphasize the symmetry of the circuit we connected some of the leads together as shown by the dotted lines of Fig. 2(b). Leads 14 and 7 then go to the input of the video amplifier, and the circuit is scanned with the laser beam. To bring out different effects, we can apply a small dc voltage, + or −, to the input gate, terminal 6. Alternatively, we can leave it floating.

We first use the scanner as a flying-spot scanning microscope to produce a picture of the circuit by reflected light (Fig. 4). This helps with optical alignment. Then we take the electrical output generated by the circuit itself to generate pictures such as 5(a), 5(b), and 5(c). These are the kinescope displays when we use the cir-

Dr. Joseph D. Knox, Physical Electronics Research Laboratory, RCA Laboratories, Princeton, NJ, received the BSEE from the University of Dayton in Dayton, Ohio, in 1966, the MSEE from Case Institute of Technology in Cleveland, Ohio, in January 1970 and the PhD also from Case Institute in September of 1970. In September of 1970 he joined RCA where he has taken part in the design and development of a laser-deflection display system where he has worked mainly on the development of a large aperture and compact optical system incorporated within the deflection system. To date, he has designed and developed three large-aperture compact optical systems. He has also submitted a number of joint patent disclosures dealing with the applications of the laser address system. He is continuing his work with the further refinement of the optical systems. His other activities include the design and fabrication of acousto-optic deflectors, modulators and cavity dumpers for visible and infrared lasers. The tellurium dioxide deflec-tors and latest lead molybdate deflector incorporated within the laser deflection system were of his design and fabrication techniques.

TERMINAL NO. 14 = V_{DD}
TERMINAL NO. 7 = V_{SS}

(a)

TERMINAL NO. 14 = V_{DD}
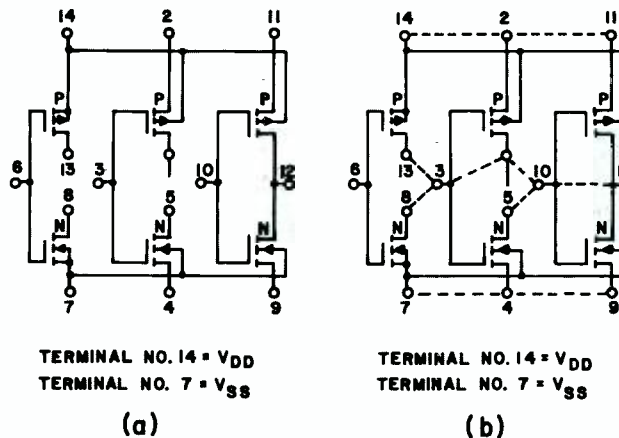TERMINAL NO. 7 = V_{SS}

(b)

Fig. 2 — (a) Circuit diagram for COS/MOS CD-4007. (b) Connections for displaying circuit output during laser scanning. The video signal generated by the circuit is taken from leads 7 and 14. A dc voltage may be applied to the input gate, 6, or it may be left floating.
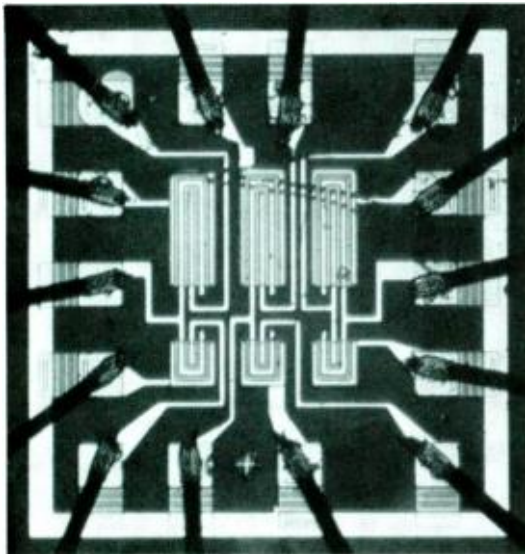
Fig. 3 — Optical microscope photograph of circuit, COS/MOS CD-4007. The three p-channel transistors are in the top row and the three n-channel transistors are in the bottom row.
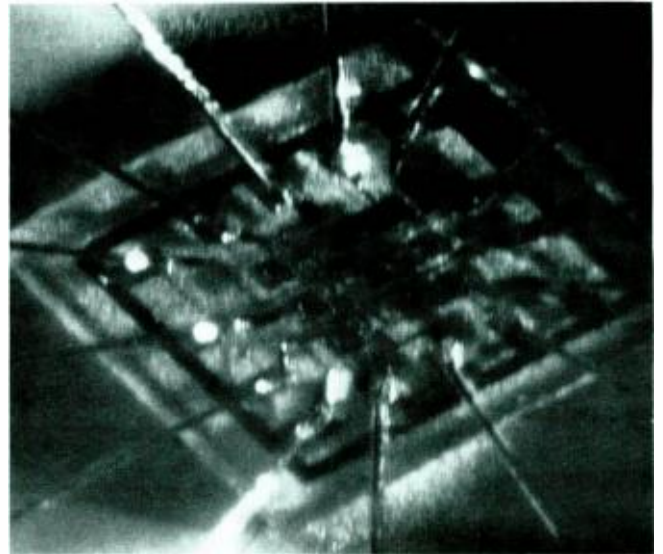

Fig. 4 — Kinescope display of circuit as viewed when the laser scanner is used as a flying spot scanner. The light reflected from the chip is picked up by a photomultiplier and the resulting photocurrent used as the video input signal.

cuit output as the video signal. They show the responses of the n-channel and p-channel transistors and how an input voltage on the gate enhances one or the other of these. In a properly functioning circuit, all the n-channel transistors behave alike and all the p-channel transistors behave alike. When one of these is bad, it is immediately obvious from the laser scan. For example, in Fig. 6 the middle p-channel transistor is visibly different. (The middle transistors on the chip are actually those at the left on the circuit diagram (Fig. 2); the bad one is that connected to the terminals 13,6, and 14.) Tests on a circuit tracer showed that the gate insulation on this transistor was faulty. Under the optical microscope, we could see no defects in the bad transistor.

but the scanner identified the problem immediately.

How generally useful is this method going to be? The results will depend a lot on the circuit. The test has to be done before encapsulation. Any circuit will generate a picture showing the functioning elements. Effective testing will require maximum use of the symmetry of the circuit and of its layout on the chip. The easiest case is one where many elements respond alike in a perfect circuit. You simply look for one that is different in the chip you are testing. What the laser scanner does is give a new look at the circuit — a "picture" generated directly by the functioning elements. This in-

dicates a bad element visually; it is different from a good one. We believe that the information from this new test will be a useful addition to that from existing methods.

Acknowledgment

We are indebted to A.C. Ipri, W. C. Schneider, and J.H. Scott, Jr., for valuable discussions and help with the experiments.

Reference

1 Gorog, I.; Knox, J. D.; and Goedertier, P. V.; "A Television Rate Laser Scanner   I. General Considerations," RCA Review Vol. 33, No. 4 (1972) p. 623.

(a)   (b)   (c)
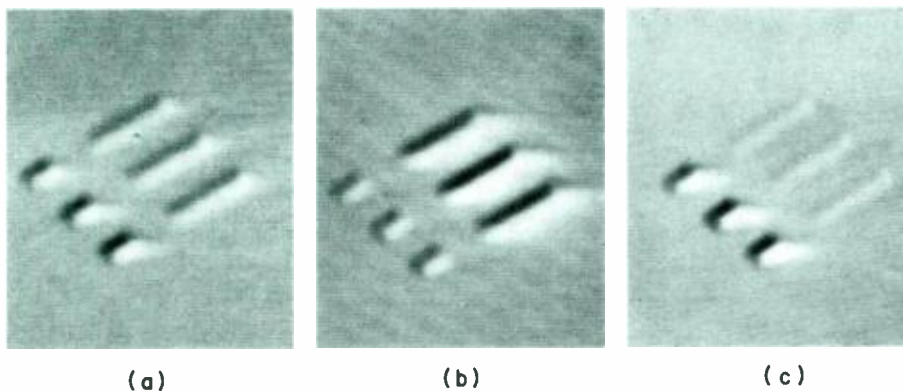
Fig. 5 — Kinescope display generated by using the signal from the active circuit elements as the laser spot passes over the circuit. (a) input gate floating. (b) +3 volts on the input gate. (c) -3 volts on the input gate. A positive voltage on the input gate enhances the signal from the p-channel transistors and a negative voltage enhances that from the n-channel transistors. Connections as in Fig. 2 (b).
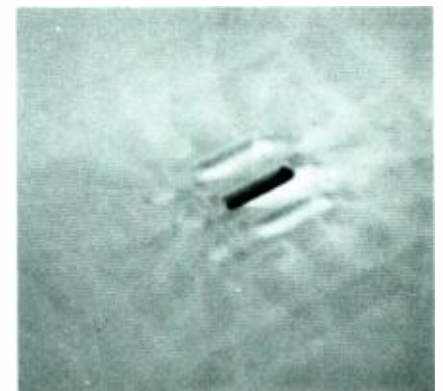
Fig. 6 — Kinescope display generated by a defective circuit. The central p-channel transistor gives an anomalous response. Conventional testing showed that the gate insulator on this transistor was shorted out.

Charge-coupled imager for 525-line television

R.L. Rodgers, III

The operation and performance parameters are described for a CCD image sensor having 512x320 elements (163,840 individual storage sites). The device is designed and fabricated for use in the standard 525-line television system. This solid-state imager is capable of performance superior to that of camera tubes with regard to signal-to-noise ratio, freedom from lag, and absence of microphonics. Additional features include its small size, light weight, low power, and precision image characteristics.

CONSIDERABLE EFFORT went into the development of a tv system that would make an acceptable picture utilizing all of the eye-brain visual perception principles. Factors such as the visual acuity of the eye and critical flicker frequency effects were considered. This effort led to the development of the U.S. Standard 525-line television system. For a solid-state image sensor to obtain its greatest market potential it should be compatible with and meet the minimum performance parameters of this standard system. Many approaches have been taken toward achieving this goal. The most promising approach thus far is a charge-coupled imager which has the potential for meeting both performance and manufacturing requirements. The production experience with silicon vidicon targets will provide a base for the manufacture of solid-state charge-coupled image sensors[1].

A 512 × 320 element CCD imager containing 163,840 individual analog storage sites has been designed and fabricated for the requirements of the standard 525-line television system. In this paper, the requirements for this system are defined and the resultant imager performance is described. Several smaller size vertical frame transfer CCD imagers were developed prior to the 512 × 320 imager[2,3,4]. These devices demonstrated that the required device performance parameters could be obtained.

Image sensor requirements for 525-line tv compatibility

The television system used for almost all broadcast and closed circuit television in the United States is the system described by the National Television System Committee (NTSC). This standard is described in EIA standards RS-170 for broadcast and RS-330 for closed circuit industrial applications. For the purpose of the following discussion, the requirements are the same.

The standard RS-170 system consists of two 262.5 line fields each 1/60 second long (1/59.939 second for color), interlaced 2:1 to form one complete frame every 1/30 second. Approximately 23% of each frame is devoted to blanking time for the display. This time is used to transfer charge from one register to another in a CCD.

Vertical cell count

The RS-170 vertical blanking interval is .075 ± .005 of the field interval yielding 241.5 to 244.125 (243 nominal) active display lines per field. This places a requirement of a minimum of 242 lines to be generated by the imager for *each* field. The maximum number of lines in each field is 262 to enable all of the cells for that field to be read out before the next field starts. One row of cells is required for each line in the display. The RS-170 sync pulses cause the display to interlace each field with the preceding field. This causes a display with approximately 486 active lines per frame. The same 243 line positions generated on one field may be repeated on the next field giving a 486 active line display, with the resolution of 243 lines, or a new interlaced set of 243 elements may be supplied by the sensor

R.L. **Rodgers III**, Manager, CCD Manufacturing and Engineering, Electro-Optic Products, Lancaster, Pa., received his training in physics and electrical engineering at the Polytechnic Institute of Brooklyn. He has been working on electro-optic imaging devices since joining RCA at RCA Laboratories in 1964. He was instrumental in the conception and design of RCA's Silicon Vidicon and Silicon Intensifier Target (SIT) camera tubes. He transferred to the Electro-Optic Products Advanced Technology area in Lancaster in 1969 to continue work on silicon camera tubes and LLLTV cameras using these tubes, resulting in the development of a photoelectron noise limited I-SIT camera. He was responsible for the development of an effective non-blooming silicon target design and new lower cost fabrication techniques for silicon targets. Most recently he has been involved with Charge Coupled Devices (CCDs) for imaging and memory applications. He was promoted to his present position early in 1974. Mr. Rodgers has presented many technical papers and received an RCA Laboratories Achievement Award in 1968.

(each field) for a total of 486 lines of vertical resolution per frame.

Horizontal cell count

The RS-170 standards call for a horizontal line frequency of 15,750 lines/s (15,734 lines/s for color). The line time is therefore 63.49 microseconds. The nominal horizontal blanking interval is 17% of the horizontal line time leaving 52.7 microseconds active display time. In closed circuit applications, the horizontal video bandwidth is unlimited. In monochrome and color broadcast, the luminance bandwidth is 4.2 MHz. Filling this bandwidth requires approximately 450 cells. A composite color signal has the color information modulated on a 3.58 MHz subcarrier. Unless the video monitor or receiver uses an expensive comb filter to remove the chroma information from the luminance signal (not commercially used), the color subcarrier beats with the luminance signal causing an annoying *edge creep*. It is therefore common practice to limit the luminance video bandwidth to 3 MHz. Most present-day video tape recorders are also limited to 3 MHz video bandwidths for luminance information. This leads to a practical minimum number of cells for the 3 MHz bandwidth of 320 cells. The corresponding video data rate is 6 MHz. Table I summarizes the 525-line system requirements.

Picture format considerations

There are several factors affecting the choice of picture format. Table II lists the most popular formats used in television,

Table I — Summary of 525-line television system requirements (RS-170).

Vertical Parameters

Frame Time (1/30 Second)
2 Interlaced Fields (1/60 Second Each)
Total Number of Lines Per Field (262.5)
Vertical Blanking Interval (.075 ± .005 V)
Active Scan Lines Per Field (Nominal/243)

Required Vertical Cell Count:
242-262 Each Field (Repeated or Interlaced)

Horizontal Parameters

Luminance Electrical Bandwidth (4.2 MHz)
Color Receiver and VTR Practice (3 MHz Bandwidth)

Required Cell Count:
4.2 MHz (Approx. 450 Cells)
3 MHz (Approx. 320 Cells)

Format Parameters

Picture Aspect Ratio (4:3)

movie film, and still photography. Most movie film and tv formats have the 4:3 aspect ratio which is required for the standard tv system. There has been a general trend towards smaller formats through the years in all three media. This has been the result of improvements in the resolution of lenses and photosurfaces as well as the need for more compact and lightweight equipment. The most popular lenses are the "C-mount" variety. There are two basic subdivisions of C-mount lenses. These are the designs for the 16 mm format of one inch vidicons and 16 mm movie film. Any of the 16 mm vidicon lenses can however be used for the smaller formats. The 11-12 mm formats seem very attractive because of their small size and ready availability of inexpensive interchangeable lenses. Lenses for 8 mm and Super 8 mm have low MTF's in the tv line ranges of interest and the small format requires extremely small CCD cell dimensions—beyond the state of the art for fabrication and device operation considerations to achieve standard tv resolution (240 television lines per picture height). An additional drawback of very small formats is the inability to achieve selective focus special effects with normal fields of view due to the inherent very large depth of focus.

512x320 CCD imager performance parameters

A 512 × 320 element CCD array has been designed and fabricated for the standard 525-line tv system as described above. It is capable of generating the full resolution requirements of broadcast color receivers and tape recorders. Fig. 1 shows the layout of this vertical frame transfer imager. The imager is composed of three sections. The lower section contains 256 × 320 cells which can be interlaced on alternate fields to generate 512 × 320 picture elements per frame[5]. In actual use, only 486 lines (243 per field) are displayed as described above. The extra elements are provided to allow variations in system blanking and timing and to avoid non-uniformities at the picture edges. The middle section contains a 256 × 320 cell storage area to provide format conversion to a sequential horizontal readout. The top section shows the 320-element readout register which shifts the video out at 6 MHz data rate. The cell size is 1.2 × 1.2 mils resulting in a 12-mm image format. The overall chip size is 500 mils × 750 mils.

Table II — Popular image formats.

Movie Film	Format (Diag.)	Aspect Ratio
8 MM	5.46 MM	4:3
Super 8 MM	6.68 MM	4:3
16 MM	12.0 MM	4:3
35 MM	25.5 MM	4:3
Television		
2/3" Vidicon	11.0 MM	4:3
1" Vidicon	15.9 MM	4:3
1.2" Vidicon	21.2 MM	4:3
1.5" Vidicon	25.0 MM	4:3
Still Film		
110	21.2 MM	4:3
126	39.2 MM	1:1
135	43.3 MM	3:2

Spectral response

The spectral response of a CCD is similar to the spectral response of a silicon vidicon. The spectral response extends from a .4μm to 1.1μm. Fig. 2 shows the spectral response for a thinned area imager test device. Absorption of light in the transfer electrodes reduces the available light to the substrate when an image is formed on the electrode side. When the light is incident on the backside (side opposite transfer electrodes), the deviation in sensivity from 100% quantum efficiency is caused primarily by reflection losses and incomplete absorption in the infrared. The magnitude of light loss in electrode side imaging varies with process variations and wavelengths, and can differ somewhat from that shown in Fig. 2, particularly in the blue end of the spectrum. The backside illumination is basically independent of electrode details.

SIT-CCD

A vertical frame-transfer CCD imager processed for backside illumination that has good blue response may be fabricated into a new type of high-sensitivity CCD imager. This device is the CCD version of the Silicon Intensifier Target (SIT) Camera Tube[6]. The SIT-CCD imager consists of a photoemissive cathode, electron-optical focusing section, and CCD imager in an evacuated envelope. The photoelectron image is injected into the silicon at high energy, forming many secondary hole-electron pairs. This current gain greatly increases the sensitivity of a CCD by raising the output signal above background signal variation limitations. Interline-transfer CCD imagers cannot use this method of low-light-level sensitivity enhancement.

Resolution

The most basic limitation on limiting resolution is the number of cells contained in the imager. In the horizontal direction, the number of cells is determined by the number of channels formed by the channel stop diffusions (320 for the 512×320 device). In the vertical, the number of resolution elements is determined by the number of different storage cell configurations formed by the transfer electrodes in the image area (256 actual cells electronically interlaced 2:1 to achieve 512 sample positions in the vertical direction).

Resolution is usually defined in terms of Television Lines/Picture Height (tvl/ph). In the horizontal direction, this number is 3/4 of the horizontal cell count or 240 tvl/ph due to the 4:3 aspect ratio. In the vertical direction, only 486 resolution samples are displayed out of the 512 possible, and the finite line structure in the display is often quoted as reducing the effective useful resolution to approximately 350 tvl/ph due to the *kell factor* even though actual resolution may be seen to the 486 sample limit with proper pattern phasing. In the horizontal, the video is smoothed into a continuous waveform and the finite cell (moire) effects are not as severe.

Another factor affecting picture sharpness is the reduction of MTF (sine wave response) due to resolution loss mechanisms in the image formation and readout processes. These losses are tabulated in Table III for a 1.2 mil cell dimension. The lens is the first contributor to the loss of resolution in image formation. The lateral diffusion of electrons in the imager before collection is the second mechanism. It is a *Sech* function of the optical spatial frequency and field-free diffusion length in the bulk. The numbers shown are representative of typical geometries. The third loss is the *Sin X/X* loss due to the finite cell sampling process. All of these effects are also present in silicon vidicons[1]. The resolution losses in the readout process are given by the equation in Table III. N_ϵ is the transfer loss and f_o is the frequency of one cell. This resolution loss mechanism is analogous to the resolution loss of a scanning electron beam in a silicon vidicon. The overall *MTF* is the product of the image formation *MTF* and the readout *MTF*. The squarewave response *CTF* is larger than the sine-wave response *MTF*. The actual measured

responses depend on the phasing of the light pattern with respect to the cell pattern. If the black-and-white bars are lined up with the cells in an in-phase condition, the response is greatest. If the bars are lined up with half a white bar and half a black bar contained in each cell, the response at the cell limit will be zero.

Transient response

In the vertical frame transfer design, the picture is integrated for one field (16.66 milliseconds). The picture is then read out completely each field. There are therefore no smearing effects due to *lag* during panning except for resolution loss due to image motion during exposure as in any movie film camera. Some other types of solid-state sensors integrate for a full frame (33.3 milliseconds) and have twice the panning resolution loss because of the longer exposure time.

Dark current

During the operation of a CCD imager, a two-dimensional charge pattern replica of the light pattern is formed inside the CCD. Thermally generated charge partially fills the potential wells and generates a background signal known as dark current. There are three basic dark-current generating mechanisms[1]. These sources are illustrated in Fig. 3. The first source is diffusion current from the substrate. This current source can be neglected. The second source of dark current is from the depleted layer between the SiO_2 interface and the substrate. A simplified equation for this current density is $J_{Dep} = eN_iD/2\tau$, where τ is the effective lifetime and N_i is the intrinsic carrier concentration. The effective lifetime is a complex function of the actual hole and electron lifetimes and the energy level of the generation centers. If CCD's are processed to remove most of the generation centers near the center of the bandgap, this component of dark current is less than the third dark-current source.

The third dark-current source is generation current from surface states at the silicon $Si\,O_2$ interface. A simplified equation for the surface-generation current density is $J_s = e\,N_iS/2$. S is the effective surface generation velocity and is proportional to the surface-state density N_{ss} near the middle of the bandgap. The value of N_{ss} near the center of the band
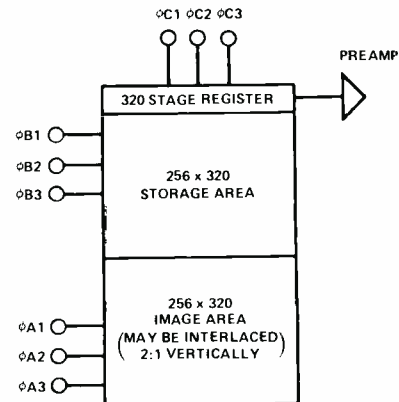
Fig. 1 — Layout of 512x320 element CCD imager.
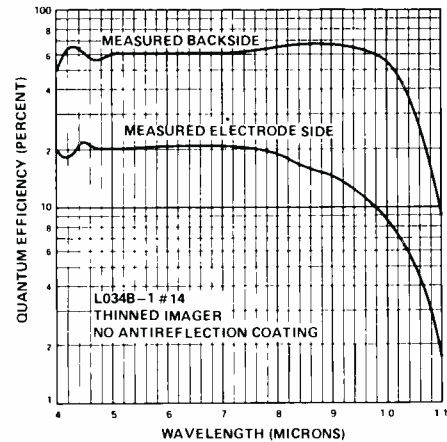

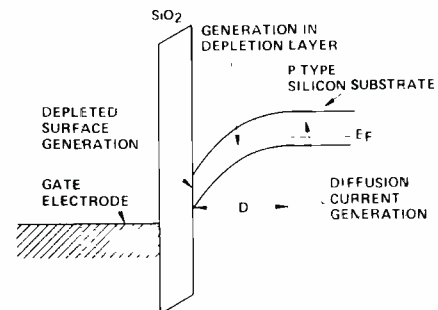**Fig. 2 — Spectral response of CCD imager; wavelength is in micrometers.**

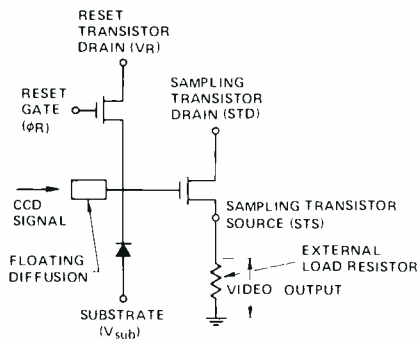**Fig. 3 — Dark current sources in CCD imagers.**

81

Fig. 4 — On-chip video processing.

may differ significantly from the density of surface states nearer the band edges which affect transfer efficiency. Actual dark current measurements have yielded dark current densities of 5 nA/cm^2. This results in a dark current of about 4 nA in the image sensing area of a 512×320 cell device.

The second and third dark-current sources depend on the temperature variation of N_t. This results in the standard silicon dark-current variation of a factor of 2 for every 9° – 10°C temperature change around room temperature.

Blooming

CCD's exhibit unique problems of charge containment when overloaded with light. Charge is fairly well confined from spreading sideways by the channel stop diffusions. However, excess charge can spill up and down the channel. A special mode of operation has been developed to greatly reduce the spreading of charge down the channel under overload conditions. This low-blooming mode is accomplished by maaintaining the phase fingers adjacent to a charge integrating phase finger at a voltage that maintains the surface under these fingers in light

accumulation. This forms a temporary extension of the channel stop around each charge intergration collecting site minimizing charge spread down the channel.

On-chip video processing

The charge signal in a CCD is manipulated around without touching a finite electrode until it is extracted at the output. A floating diffusion is used as a charge detector. The voltage on the floating diffusion is reset to a fixed potential once each clock period by a reset transistor. When each charge packet reaches the floating diffusion, the charge changes the voltage on the capacity at that node. This voltage is sampled by a sampling transistor operating as a source follower. These circuits are shown in Fig. 4. The very low node capacity of the floating diffusion results in a significant improvement in signal-to-noise ratio over a silicon vidicon operating at the same light level. In fact, at normal signal levels, no noise is visible in a displayed picture generated by the CCD imager.

Developmental camera

A developmental black-and-white camera has been fabricated for the 512 × 320 CCD imager. Fig. 5 shows a picture of this camera. The camera is approximately the size of a pack of cigarettes and has a C-mount for lens interchangeability. Fig. 6 and Fig. 7 show 525-line monitor pictures made by this camera with a 512 × 320 CCD imager.

Summary and conclusions

A CCD imager has been developed that will offer an attractive alternative to

Table IV — Summary of developmental 512x320 CCD imager performance parameters.

(1) Spectral Response Similar to Silicon Vidicon
(2) Operable in SIT-CCD Mode
(3) 500 Nanoamp DC Maximum Signal
(4) 4 Nanoamp DC Dark Current at 25º C
(5) Compatable With Standard 525 Line TV
(6) Supplies Full Resolution of Color TV (240 TVL/PH)
(7) No Lag – Picture Erased in One Field

Notes:

3ϕ, N-Channel Vertical Frame Transfer
163, 840 1.2 x 1.2 Mil Cells
6 MHz Data Rate, 16.66 ms Integration
12 MM Image Format
500 x 750 Mil Chip Size

camera tubes for many 525-line television applications. It is capable of supplying the full resolution of color tv (240 tvl/ph). The features of CCD imagers that are superior to camera tubes are signal-to-noise ratio, freedom from lag, and absence of microphonics. The small size, light weight, low-power consumption, and precision image characteristics are additional benefits. Table IV summarizes the performance parameters for this developmental 512 × 320 CCD imager.

References

1. Rodgers, III, R.L., "Beam Scanned Silicon Targets for Camera Tubes," Paper presented at IEEE Intercon, New York, NY, March 1973.

2. Weimer, P.K., Pike, W.S., Kovac, M.G., AND Shallcross, F.V., "The Design and Operation of Charge-Coupled Image Sensors," Paper presented at IEEE Solid State Circuit Conference, Philadelphia, Pa., February 1973.

3. Kovac, M.F., Shallcross, F.V., Pike, W.S., and Weimer, P.K., "Design, Fabrication, and Performance of a 128 × 160 Element Charge Coupled Image Sensor," Paper presented at CCD Applications Conference, San Diego, California, September 1973.

4. Tompsett, M.F., Amelio, G.F., Bertram, W.S., Buckley, R.R., McNamara, W.J., Mikkelsen, Jr., J.C., and Sealer, D.A., "Charge-Coupled Imaging Devices: Experimental Results," IEEE Trans. Electron Devices, Vol. ED-18, pp.992-996, November 1971.

5. Sequin, C.H., "Interlacing in Charge-Coupled Imaging Devices," IEEE Trans. Electron Devices, Vol. ED-20, pp. 535-541, June 1973.

6. Rodgers, 3rd, R.L., et al, "Silicon Intensifier Target Camera Tube," Paper presented at IEEE International Solid State Circuits Conference, Philadelphia, Pa.

Fig. 5 — View of the black-and-white camera for the 512x320 CCD imager.

Fig. 6 — A 525-line picture made with the 512x320 CCD imager.

Fig. 7 — A 525-line picture made by the 512x320 CCD imager.

82

Power switching using solid-state relays

T. C. McNulty

Solid-state relays make use of a semiconductor device for control of ac or dc power. Since, in most ac applications, the semiconductor element chosen for power control is the triac, this paper describes the triac as a power-switching element. Advantages and disadvantages of the active element over the electro-mechanical relay are discussed in general terms. Basic parameters, such as surge in-rush capability, transient-voltage ratings, suppression networks, turn-off consideration and the different modes of triac gating are also discussed. Various circuit designs for on/off control, zero-voltage switching, and line-voltage isolation are described which demonstrate ac power control.

Fig. 1 — The seven basic steps required in the fabrication of a standard, glass-passivated triac.

POWER SWITCHING using electromechanical relays is probably as old as the electrical industry itself. The electromechanical relay comes in many forms (general purpose, telephone type, TO-5, reed, mercury wetted, *etc.*) and has various contact configurations. It is probably fair to say that most electronic engineers have, at some time, used or designed circuits employing electro-mechanical relays. During the past few years, the electromechanical device has been challenged by a new breed of relay which has no moving parts, is capable of handling large amounts of power for relatively low input power, and comes in many package and circuit configurations. This new solid-state relay (or SSR) uses transistors for dc power control or triacs for ac power control.

Tom McNulty, Manager, Applications Engineering, Solid State Division, Somerville, NJ. received the BSEE in 1966 from Newark College of Engineering. Prior to joining RCA in 1966, he gained extensive experience in digital logic-system design at Burroughs Corporation. His first assignment with RCA was in Mountaintop as an Applications Engineer with Thyristor/Rectifier Engineering. In 1967 he transferred to Somerville where he is now engaged in the devleopment of circuits for ac power-control. Mr. McNulty hold a U.S. patent and has written several papers on the use of SCR's and triacs in ac power-control and appliance-control applictions.

Perhaps, the SSR is to the electromechanical relay as the transistor was to the electron tube. That is to say, there will not be an immediate widespread conversion to SSRs, but rather a gradual adoption of the new device, particularly for applications in which increased reliability is required and shock or mechanical fatigue impose severe limitations on the electromechanical relay; some movement has already been made in this direction. Probably the major limitations to SSR use are cost, line isolation, immunity from line transients, and the need for multiple-pole arrangements. However, with solid-state technology advancing at such a rapid rate, lower-cost triacs with improved voltage ratings will become increasingly available, and economical methods of line isolation will be developed. With these innovations, the disadvantages of SSRs may begin to fade. If so, we may begin to see an increase in the use of SSRs, and the need for a better understanding of triacs as the power element in ac applications will become a must.

TRIAC construction

Thyristors (silicon controlled rectifiers and triacs) are semiconductor switches whose bistable state depends upon the regenerative feedback associated with a pnpn structure. The SCR is a unidirectional device used primarily for dc and ac functions, whereas the triac is a bidirectional device used primarily for control of ac power.

The fabrication of a standard, glass-passivated triac requires the seven basic steps illustrated in Fig. 1 and delineated
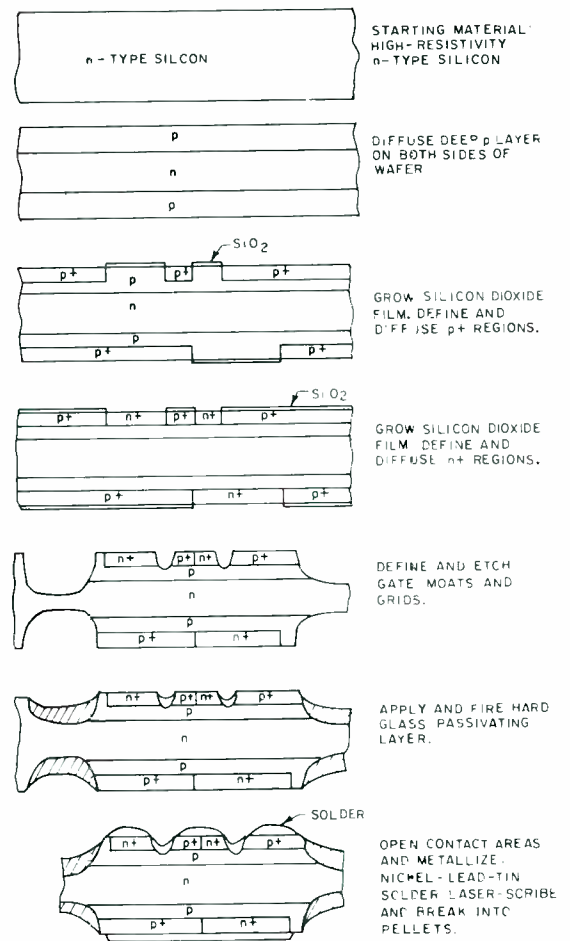

Fig. 2 — An isometric view of a completed triac and dimensions of three devices now available or in the design stage.
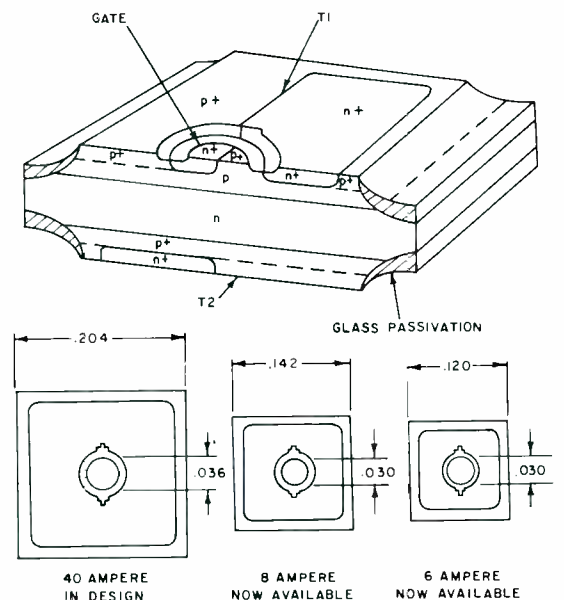
83

below.

1) The process begins with an n-type, high-resistivity, silicon wafer;

2) p layers are diffused deeply into noth sides;

3) Silicon-dioxide diffusion masks are grown, and p^+ regions are defined and diffused into the wafer;

4) A second oxide diffusion mask is grown, and n^+ regions are defined and diffused into the wafer;

5) A silicon-dioxide etch mask is grown and defined. Grids and gate moats are etched into the wafer;

6) A hard glass-passivated layer is applied in the grids and gate moat;

7) Contact areas are opened on the wafer and nickel-lead-tin solder metallization is applied. The wafer is then laser-scribed and separated into pellets.

Fig. 2 contains an isometric view of a completed triac and dimensions of three devices now available or in the design stage.

Voltage and temperature ratings

The effects of voltage and temperature are important in thyristors because of the regenerative action of these devices, and because they are often required to support high voltages under high temperature conditions. The imposed voltages create a field at the junction interface, and the increased temperature releases additional surface ions. Should the field concentrate the additional surface charge and allow it to migrate into the gate region, non-gated turn-on may occur. Most manufacturers realize that the gate region must be terminated for high voltage/temperature operation, and a shunt resistance is built into the triac pellet during fabrication. This shunt reduces the immunity of the triac to non-gated turn-on. Additional reliability can be gained by operating the triac under less severe voltage/temperature conditions.

In-rush currents

One of the features that has made thyristors the work-horses of the power semiconductor industry is their ability to absorb in-rush currents many times in excess of their steady-state ratings. This unique feature results from the regenerative action of the thyristor, an action which maintains the internal beta at a level such that, under in-rush conditions, the charge density is equally distributed over the entire triac pellet. The equal charge distribution assures the presentation of a low impedance to the in-rush current. Each manufacturer clearly

rates device surge capability from single cycle to multiple cycles. Since this rating cannot be exceeded repeatedly, care should be exercised in the actual application to provide a sufficient safety margin between the published ratings and the actual circuit in-rush currents.

Another important parameter associated with a triac is its di/dt rating, a parameter most significant during turn-on. With the initiation of a gate signal, the active area closest to the gate region is, essentially, turned on, and, for a few microseconds, the instantaneous power dissipation is a function of the rate of rise of the on-state current. This power dissipation may cause localized heating and result in silicon-lattice destruction and triac degradation. The di/dt ratings are a function of triac geometry and pellet size, and ratings of 100 A/μs are easily achieved. In most circuit applications, stray or actual-load inductance is present, and for the condition of $di/dt = E_{pk}/L$, it is easily seen that a few microhenries of inductance are all that are required to limit circuit di/dt to within the maximum rating. When di/dt ratings are exceeded, it is usually because of the RC snubber network in parallel with the triac. In such networks, stray inductance is essentially zero, and the magnitude of discharge current is limited by the snubber resistance. The di/dt in the snubber is not affected by the inductance added to qwell the di/dt caused by the stray or actual-load inductance; only careful selection of RC-snubber-network components will eliminate this second source of di/dt and minimize triac failures.

Transient voltages

It is well known that triacs are susceptible to non-gated turn-on and possible damage as a result of transient voltages. Transients are generally caused in a triac by the switching of inductive loads on adjacent lines or in proximity to the device. If the transient voltage generated exceeds the critical rate-of-rise of the off-state voltage (dv/dt) then a displacement current ($i = C \cdot dv/dt$) is generated which causes non-gated turn-on. Non-gated turn-on is not destructive if the energy transfer is within the maximum rating of the device; however, if the transient voltage does not exceed the off-state dv/dt rating, but does exceed the maximum voltage rating, then triac breakover occurs. Whether triac degradation occurs depends on whether the energy transfer is within the bulk silicon or the edge avalanche.

Although the transient-voltage problem may seem critical, there are precautions that can be taken to minimize it. The use of RC snubbers in parallel with the triac can reduce the rate of imposed transients. This arrangement is most effective for fast-rising, short-duration line disturbances. For critical applications, the use of a voltage-clipping device in addition to an RC snubber effectively suppresses both the rate of rise and magnitude of line-generated transients.

Another type of transient particularly prevalent in the area of inductive loads, and often overlooked, is the circuit-induced transient. Consider an inductive load in series with a triac and RC snubber network which also includes a switch for line-voltage interruption. With the triac in the off state, a leakage current flows which is a function of the characteristics of the load, the RC snubber network, and triac leakage. If the switch is momentarily opened when the triac is off, then a voltage transient ($E = L \cdot di/dt$) is generated which can exceed the voltage rating of the triac; cause non-gated turn-on and abrupt energy transfer; and may result in damage to the triac. Again, the proper selection of RC-network components and voltage-clipping device will suppress the circuit-induced transient to a level compatible with the voltage rating of the triac.

Commutating dv/dt

The term *turn-off time* is not associated with triacs since triacs are bidirectional, and reverse voltage is nothing more than a forward voltage to one-half of the triac chip. A new term — *critical-rate-of-rise-of-commutation-voltage* — is used with triacs. The term describes the ability of the triac to turn *off* as the current passes through zero, or commutates. One must remember that the triac is a current-dependent device: Current is injected into the gate to turn the device *on*, and current must be removed or allowed to pass through zero for turn-off regardless of the source-voltage polarity. Commutating dv/dt is less critical with resistive loads and most important with inductive loads. Consider an inductive load in which the load current lags the source voltage by a phase angle θ. As pointed out, triac commutation occurs at zero current, whereas the source voltage has some magnitude E. As the load current crosses the zero point, a small reverse current is established as a result of the charge in the n-type region. This charge, plus a displacement current ($i = C \cdot dv/dt$) resulting

84

from the reapplied source voltage, can cause the triac to turn *on* in the absence of a proper gate signal. A minimum commutating dv/dt at rated current and at a specific operating case temperature should be defined in all triac applications; the circuit designer can use these specifications to choose an RC snubber network that will limit the reapplied dv/dt to within ratings. Loss of triac control as a result of commutating dv/dt does not degrade the characteristics of the triac. Proper RC snubber network selections for worst-case conditions of load power factor, current, and voltage are easily made by use of the charts shown in Fig. 3.

Advantages of SSRs

Before the advantages of SSRs are discussed, the types available should be reviewed.

Two types of SSR are available: all solid-state and hybrids. The solid-state class employs solid-state devices for both logic and triac gating. Hybrids generally use a reed relay for triac gating for ac power control and so combine the electro-mechanical with solid state. In either class, the triac is used as the solid-state element for ac power control. A comparison of SSRs with electromechanical relays is given below:

Life: An EMR physically makes and breaks load current, and the relay contacts deteriote with life.

SSRs: They have no moving parts, and may be designed to make and break at zero current. Regardless of the design, the triac always breaks at zero current.

Contact bounce: Inherent with an EMR — zero for SSRs.

RFI: Inherent with EMRs – dependent on SSR design.

AFI ("audio-frequency" interference). Terrible with EMRs particularly when many relays are clacking about. Not noticeable with SSRs.

Environment: High humidity, corrosion, and explosive atmospheres usually dictates a sealed relay. SSRs may easily be potted.

Shock: The SSR is far superior.

Input logic: EMRs can be operated from low-level logic. SSRs are design dependent, but offer complete versatility.

General control circuits

A simple triac control circuit, an *on/off* circuit, is shown in Fig. 4. With switch S1 open, the triac is *off* and essentially zero

current is applied to the load. Actually, there will be leakage-current flow to the load; the amount of current is dependent on the applied voltage and triac case temperature. However, because the current is very small (less than one milliampere) compared to the load current, it can be neglected in this and the following circuits. (In specific applications in which leakage current may affect the control unit, it would have to be considered.)

To apply power to the load in Fig. 4, switch S1 is closed to provide gate drive to the triac. Bias-resistor R1 is of the order of 68 to 100 ohms and provides the initial gate drive during every half cycle of applied voltage. The power consumption of R1 is very low (¼ to ½ W) because, when the triac is in the *on* state, R1 is in parallel with the *on*-state voltage of approximately 1.5 V. This method of triac triggering, called anode firing, is an effective way of triggering because it uses the source voltage as a source of gate-current drive. Maximum gate current is available for triac turn-on at peak line voltage until the device goes to the low-impedance state. In this state, the current in R1 is reduced by the forward voltage drop. In effect, bias resistor R1 is utilized only during the initial turn-on of the triac, or for approximately two microseconds. In a typical application, switch S1 would be replaced by a relay, and power control would be transferred by means of low-level-current relay contacts.

For control applications which require that variable power be delivered to a load, an inexpensive RC phase-control circuit is best. Fig. 5 shows the basic triac-diac control circuit with the triac connected in series with the load. During the beginning of each half cycle, the triac is in the *off* state; as a result, the entire line voltage is impressed across it. Because the triac is in parallel with the potentiometer and capacitor, the voltage across the triac drives the current through the potentiometer and charges the capacitor. When the capacitor voltage reaches the breakover voltage of the diac, V_{BO}, the capacitor discharges through the triac gate and turns it *on*. The line voltage is then transferred from the triac to the load for the remainder of that half cycle. This sequence is repeated for every half cycle of either polarity. If the potentiometer resistance is reduced, the capacitor charges more rapidly, the V_{BO} of the diac is reached earlier in the cycle, and the power applied to the load is increased. If
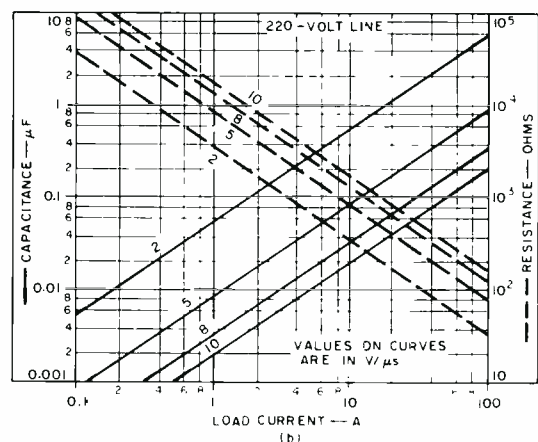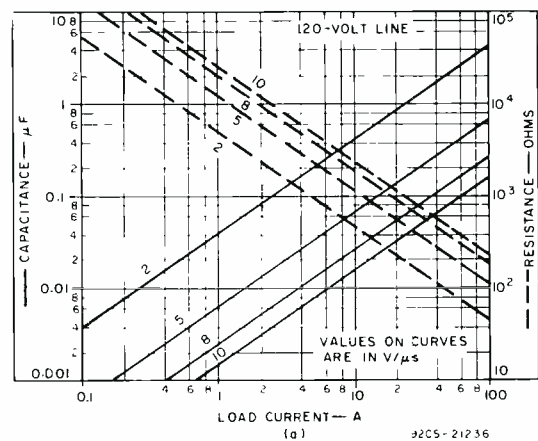

Fig. 3 — (a) Snubber components for 200-V peak on 120-V line; (b) Snubber components for 400-V peak on 220-V line.
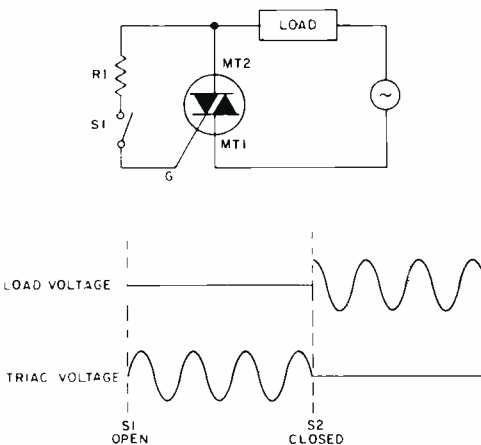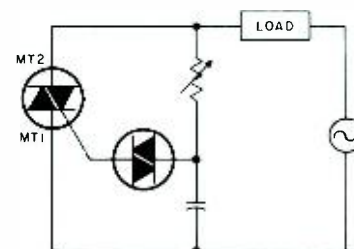

Fig. 5 — RC phase control, variable power.

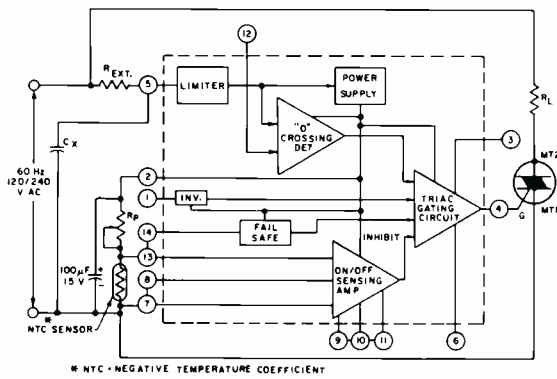Fig. 4 — ON/OFF control, non-synchronized.

85

Fig. 6 — block diagram of the integrated-circuit zero-voltage switch, CA3059.

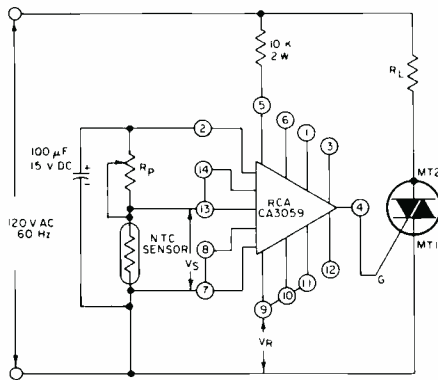* NTC - NEGATIVE TEMPERATURE COEFFICIENT

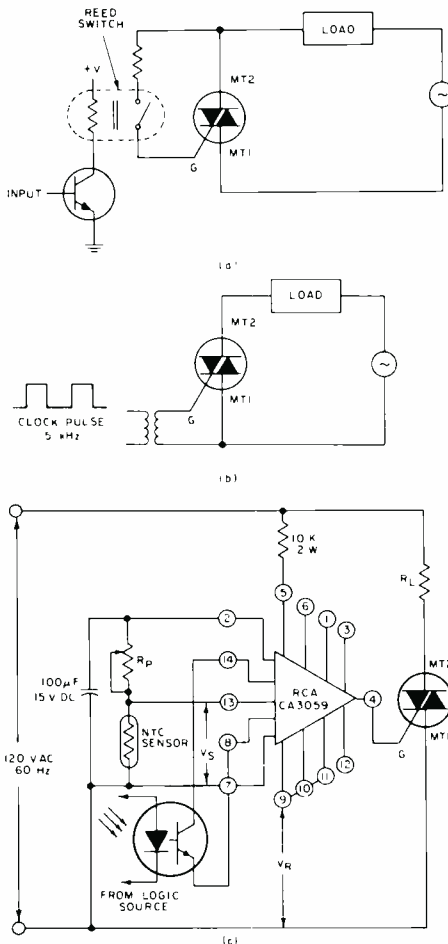Fig. 7 — CA3059 ON/OFF temperature controller.

Fig. 8 — (a) Isolation with reed relay; (b) isolation with pulse transformer; (c) isolation with light-activated devices.

the potentiometer resistance is increased, triggering occurs later and load power is reduced. The main disadvantage of this circuit is that it produces RFI.

Although the basic light-control circuit operates with the component arrangement shown in Fig. 5, additional components and sections are usually added to reduce hysteresis effects, extend the effective range of power control, and suppress radiofrequency interference.

Temperature-control circuits

A zero-voltage switch, Fig. 6, synchronized for line-pulse generation, in combination with a triac, is particularly well suited for temperature-control applications. The zero-voltage-switch/triac circuit may be used with an on/off-type control or as a proportional control depending on the degree of regulation required. A simple, inexpensive, on/off temperature controller is shown in Fig. 7; a review of the functional block diagram of the zero-voltage-switch, Fig. 6, will help in understanding the circuit. For every zero-voltage crossing, a zero crossing pulse is generated and directed to the triac gating circuit. If there is a demand for heat, the differential amplifier is in the open state, the triac gating circuit is open, and the triac is turned on at every zero-voltage crossing. When the demand for heat is satisfied, the differential amplifier is in the closed state; this inhibits the triac gating circuit and removes any further gate drive to the triac. Therefore, the key to the operation of this circuit is in the state of the differential amplifier. One side of the differential amplifier is biased to a reference voltage V_R, and the other side is biased to a voltage V_S which is dependent on a variable potentiometer setting and sensing resistor. As a result, whenever the bias voltage V_S exceeds the reference voltage V_R, the gating circuit is open and the triac is turned on for each zero-voltage crossing. The characteristics of an on/off controller are well known; i.e., there are significant thermal overshoots and undershoots which result in a differential temperature above and below the reference temperature. The magnitude of the differential temperature is dependent on the mass of the heater and the time constant of the sensing element.

For precise temperature control, the technique of proportional control with synchronous switching is introduced. The

proportional control differs from the on/off control in that it allows a specified percentage of power (duty cycle) to be supplied to the load with a finite off time that, in turn, allows the heating element to "catch up" as a result of thermal lag. In effect, this scheme provides "anticipator control." Again, the key to circuit operation is in the state of the differential amplifier.

AC-line isolation

The design engineer often must provide dc-to-ac isolation. Complete isolation can be achieved by reed relays, pulse transformers, and light-activated devices. Selection of any one of these three approaches depends on the dc logic design and component economics. Fig. 8(a) shows a reed relay and transistor drive circuit which is effective in triac gating, although it does have moving parts. Fig. 8(b) uses a pulse transformer for isolation, and requires a form of clock pulse that can be transferred to the triac gate. In some applications, clock pulses may already be available; therefore, the pulse-transformer approach is economical. This approach requires more components than that of Fig. 8(a), but it has no moving parts. The last approach, and, at present, probably the most expensive one, uses a light-activated device, such as the GaAs infrared emitter, to initiate triac gating. The light-activated device is coupled to a photosensitive transistor which, when turned on, provides inhibit logic for additional integrated circuits or, as in Fig. 8(c), for a zero-voltage-switch application.
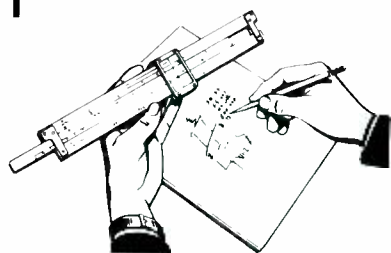
Conclusion

The designer who thoroughly understands the characteristics and limitations, but most of all the advantages, of triacs will have at his disposal a device that he can use to design power controllers that operate satisfactorily not only in normal applications, but also in severe physical and electrical environments. The triac has already proven to be a true power-semiconductor device, and is widely used in both commercial and industrial applications; restrictions on triac use in military applications, particularly in 400-Hz power systems, are gradually being lifted. It is inevitable, then, that the triac will evolve as the basic building block for ac power control in power-controller systems.

Engineering and Research Notes

Adhesive bonding of semiconductors to substrates

Robert D. Larrabee
Advanced Technology Laboratories
Somerville, NJ

When fabricating infrared imaging arrays, we were faced with the problem of attaching a delicate $(Hg\text{-}Cd)Te$ semiconductor wafer to a sapphire substrate with a thin adhesive layer that had to be both uniform in thickness and bubble-free. Our solution to this problem may prove to be a useful technique for a variety of unrelated applications.

The most effective procedure involved coating the polished sapphire substrate with a thin (several μm) layer of epoxy resin, gently pressing the polished $(Hg\text{-}Cd)$ Te wafer into the epoxy layer under vacuum, and holding it together at room temperature until the epoxy was sufficiently cured to permit removal from the vacuum apparatus without disrupting the bond. The epoxy layer was produced by mixing Eccobond 45LV Resin[1] and its hardener, Catalyst 15LV,[2] with acetone in such a concentration that when a few drops of the mixture were applied to the sapphire substrate, the desired thickness of adhesive was left after the acetone diluent evaporated.

It was found that the sapphire substrate had to be very carefully cleaned and had to have a lyophilic reaction to acetone. If these conditions weren't effected, the resin mixture would ball-up before all of the acetone was evaporated, and a series of epoxy "islands" would result instead of a thin uniform layer. A rough (*i.e.*, forepump) vacuum was necessary to eliminate any trapped air pockets that would otherwise inhibit the epoxy flow into, or out of, any irregularities in the substrate, adhesive layer, or semiconductor wafer.

Since the thin adhesive layer is so very transparent, it proved difficult to optically judge the uniformity of its thickness. Therefore, a fluorescent dye[3] was incorporated into the original diluted epoxy mixture to allow for inspection of the thin resin layer under ultraviolet light (366-nm Hg line). Uniformity was subjectively judged by the intensity and uniformity of the fluorescence emission from the epoxy layer.

The recipe for the actual mixture used is:

Acetone	200 cc
Epoxy resin[1]	5 cc
Hardener[2]	5 cc
Fluorescent dye[3]	25 mg

This mixture has a shelf life of several months when stored in a brown bottle at room temperature. After the diluent evaporates, the undiluted epoxy layer requires about 24 hours to cure at room temperature (less time, of course, at elevated temperatures). This slow room-temperature cure permits sufficient time for any flow of epoxy that might be required to fill in voids and thin regions created when the wafer is pressed into the layer. However, the curing rate is fast enough to produce sufficient bond strength for further processing after an overnight room temperature cure. After the overnight cure, the wafer and substrate are sufficiently bonded to permit removal of excess adhesive. After cleaning, the device can be put in an oven to quickly effect a complete cure.

This process has routinely yielded 2- to 3-μm epoxy layers that are bubble-free over the entire $(Hg\text{-}Cd)Te$ wafer surface area of approximately 1 cm². They have bond strengths exceeding the strength of the $(Hg\text{-}Cd)$ Te itself. Since this process is not dependent on any particular property of either sapphire or $(Hg\text{-}Cd)Te$, it should be applicable whenever two flat, polished surfaces are to be bonded together by a thin adhesive layer.

Material References

1. Eccobond 45LV (clear), Emerson and Cuming, Inc., Canton, Mass.

2. Catalyst 15LV (clear), Emerson and Cuming, Inc., Canton, Mass.

3. Azosol Brilliant Yellow, GAF Corp., 140 West 51st Street, New York, New York. (There is nothing unique about this dye other than its intense fluorescence when dissolved in the epoxy resin. A number of other dyes will serve the purpose equally well.)

Millivolt source for temperature programming of laboratory furnaces

R. Fehlmann | A.E. Widmer
Laboratories RCA Ltd.
Zurich, Switzerland

Fehlman   Widmer

A simple, inexpensive programmable millivolt source can be used for linear rate-controlled raising or lowering of a laboratory furnace temperature. Two versions of such a source have been designed and are described in this note.

The output of either programmer is set for typical applications such as the controlled growth of III-V compounds ($GaAs$, GaP, etc.) by liquid-phase epitaxy for which $Pt\text{-}Pt$ 10% Rh sensing thermocouples are used. The ranges are as follows:

1) 5 to 50 μV/min. or 0.45 to 4.5°C/min. (950 to 1000°C)

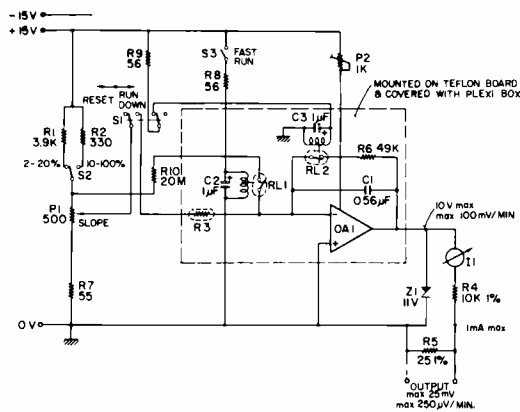2) 25 to 250 μV/min. or 2.2 to 22°C/min. (950 to 1000°C)

Fig. 1 — Circuit diagram for a programmable millivolt source for rate-controlled cool-down processes. (OA1 — Zeltex ZA 801 M1; R3 — Glass encapsulated resistor 10^{10} ohms.)
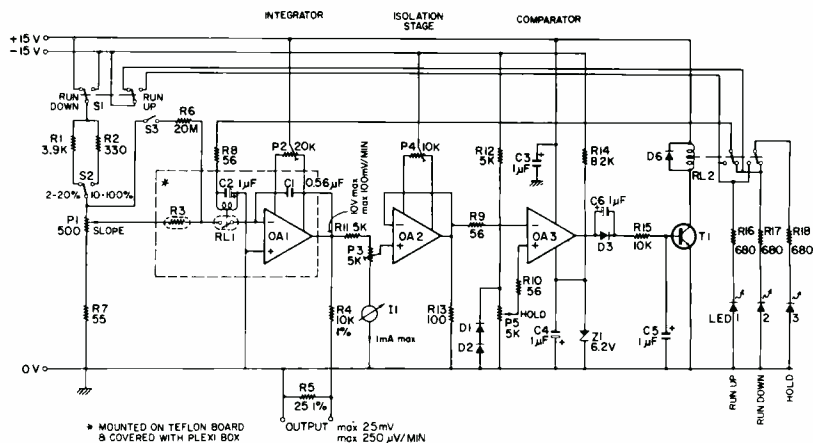

Fig. 2 — Circuit diagram for a programmable millivolt source for rate-controlled heat-up, hold, and cool-down processes. (OA1 — Analog Devices 41 K; OA2 — Texas Instrum, SN 72741; OA3 — Texas Instrum, SN 72810; R3 — Glass encapsulated resistor 10^{10} ohms.)

The simpler version is for application where only a rate-controlled lowering of the temperature is required, while the more versatile version allows a rate-controlled raising and lowering of the temperature, and in addition has a preset hold control that can be set to maintain constant temperature.

As shown in Fig. 1, the simpler version has only one FET-operational amplifier which can be used where only rate-controlled cool-down of the temperature is required. A more versatile version for rate-controlled heat-up, hold, and cool-down with three operational amplifiers is shown in Fig. 2. Both circuits can be built with readily available low-priced operational amplifiers and a few passive components. The material cost for the programmer shown in Fig. 1 is about $ 50 and for a more versatile version (Fig. 2) about $ 100.

Both circuits contain a ramp generator for the rate controlling process. The output voltage versus time for such an integrator with a constant input voltage is

$$V_2 = -\frac{1}{RC}\int_0^t V_{1(t)}\,dt = -\frac{V_1 t}{RC}$$

High accuracy for long ramp periods requires that the capacitor be a low-leakage type, that the operational amplifier have a high input impedance, and that the leakage currents of the other passive components and switches of this circuit be less than 10 pA. We used a high-quality metallized polycarbonate capacitor for C1 and an FET operational amplifier for OA-1.

The ramp rates are set on the potentiometer P1. Both programmers have the same ranges: a low one from about 5 to 50 μV/min and a high one from about 25 to 250 μV/min. For a Pt-Pt 10 % Rh thermocouple between 950 and 1000°C, this corresponds to heating rates of about 0.45 to 4.5°C/min. and 2.2 to 22°C/min., respectively. The maximum ramp rate of the integrator itself is given by the voltage from the potentiometer P1 and by the values of the resistor R3 and the capacitor C1. The maximum ramp rate set with P1 corresponds to 100 mV/min. at the integrator output. This rate is reduced by the ratio of the voltage divider (R4, R5), which leads to a maximum ramp rate at the output terminals of 250 μV/min. (100 %) and a minimum value for 2% of 5 μV/min. Small corrections of R1 and R2 may be necessary to account for the allowed deviations of the resistor value of R3 and the capacitance of C1.

The maximum output voltage, or span, is given by the voltage across the resistor R5 and is set for 25 mV. Other span voltages can be set by changing the value of R5, keeping in mind that this will also affect the ramp rates.

The additional circuit sections of Fig. 2 consist of an isolation stage, a comparator for setting the hold temperature, and a relay switching circuit. A hold temperature below the maximum processing temperature set at the temperature controller can be chosen with the potentiometer P5. The hold voltage from this potentiometer and the ramp voltage from P3 are compared at the comparator OA-3. The comparator switches its output voltage from 0 to + 3.2V when the ramp voltage is equal to the preset hold voltage. This actuates a switching circuit with the transistor T1 and the relay RL2. An isolation stage (OA-2) is required between the ramp generator and the comparator to prevent loading of the ramp generator by the switching current of the comparator.

Other circuit components are: RL1,2, reed relays with an isolation resistance of 10^{15} ohms; R3, glass encapsulated resistor (e.g. Welwyn or Victoreen); R4,5,7, metal film resistors; P2,3,4, trimpots, 20 turn. The programmers require a regulated ± 15 V power supply with 100 mA output for circuit 1 and 250 mA for circuit 2.
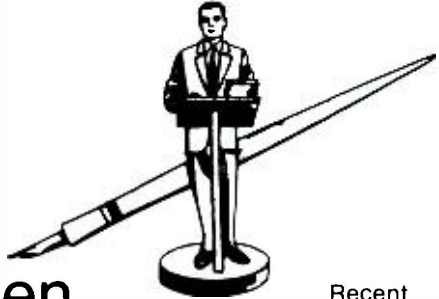
Special attention must be given to the wiring of the integrator and its associated components. Any isolation losses will affect the long-term stability. All these components are mounted separately on a Teflon board and are encased in a Plexiglas box.

The front panel controls for the simpler version include the ramp voltage potentiometer P1, the range switch S2, the percentage span meter I1, and switches S3 for normal and fast run and S1 for run-down and reset. The slope potentiometer P1 on these programmers can in addition be coupled to a synchronous motor which allows the ramp rate to increase or decrease linearly. For circuit 2, the front panel controls are the same as above except that S1 is for run-up and run-down and that the hold potentiometer P5 and the indicating lights LED1,2,3 are included.

The linearity of the ramp voltage versus time over the whole voltage span for both programmers shows no deviations or ripples and is within the linearity of the recorder used for monitoring. The same was found if the temperature of a furnace versus time was recorded. For the programmer with the hold feature (Fig. 2) the most critical requirement is the stability of the hold voltage with time. Any drift in this voltage will result in a drift of the furnace temperature. A drift measurement was made over 75 hours with a hold setting of 50% of the voltage span. Only a small, linearly increasing, positive drift voltage of 3 μV/hour was found which can be neglected for most practical applications.

We have used these controllers in our laboratory for programming the temperature of liquid phase epitaxial growth of GaP-(GaAl)P heterostructures. We found them very simple to build and to operate. These programmers can be easily added to any existing furnace controller circuitry since they have to be only connected in series with the thermocouple sensing element.

Pen and Podium

Recent RCA technical papers and presentations

Both published papers and verbal presentations are indexed. To obtain a published paper borrow the journal in which it appears from your library or write or call the author for a reprint. For information on unpublished verbal presentations write or call the author. (The author's RCA Division appears parenthetically after his name in the subject-index entry.) For additional assistance in locating RCA technical literature contact **RCA Technical Communications, Bldg. 204-2, Cherry Hill, N.J. (Ext. PC-4256).**

This index is prepared from listings provided bimonthly by RCA Division Technical Publications Administrators and Editorial Representatives—who should be contacted concerning errors or omissions (see inside back cover).

Subject index categories are based upon standard announcement categories used by Technical Information Systems. Bldg. 204-2, Cherry Hill, N.J.

Subject Index

Titles of papers are permuted where necessary to bring significant keyword(s) to the left for easier scanning. Author's division appears parenthetically after his name.

SERIES 100
BASIC THEORY & METHODOLOGY

105 Chemistry
organic, inorganic, and physical.

CHEMICAL POLISHING of sapphire and spinel — P.H. Robinson. R.O. Wance (Labs,Pr) *RCA Review*. Vol. 34, No. 4, pp. 616-622; 12/73

125 Physics
electromagnetic field theory, quantum mechanics, basic particles, plasmas, solid state, optics, thermodynamics, solid mechanics, fluid mechanics, acoustics.

ELECTROGYRATORY EFFECTS, Magnitude of — A. Miller (Labs,Pr) *Phys. Rev. B 15, Vol. 8, No. 12, pp. 5902-5908*; 12/73

IONIC CHARGE at room temperature through the interface of air with SiO_2, Injection and removal of — M.H. Woods. R. Williams (Labs,Pr) *J. Appl. Phys.*, Vol. 44, No. 12,; 12/73 pp. 5506-5510

RAMAN SCATTERING from a nematic liquid crystal: orientation studies — E.B. Priestly (Labs,Pr) *Phys. Rev. Lett.*, Vol. 31, No. 26, pp. 1552-1556; 12/24/73

TURBULENT ARCS, Voltage gradients in — I.P. Shkarofsky (RCA Ltd,Mont) *Canadian J. of Physics*, Vol. 52, No. 1, 1974; pp. 68-79

130 Mathematics
basic and applied mathematical methods.

MULTIVARIATE STATISTICAL ANALYSIS, Use of computerized techniques in — B.B. Bocciarelli (ATL,Cam) IEEE Coll. RCA Burlington, Mass.; 2/21/74

RYTOV'S method and large fluctuations, Comments on — D.A. deWolf (Labs,Pr) *J. of Acoust. So. Am.* No. 53; 1973; pp. 1109

160 Laboratory Techniques and Equipment
experimental methods and equipment, lab facilities, testing, data measurement, spectroscopy, electron microscopy, dosimeters.

FURNACE, A simple 2100°C 600-Watt tube — G.W. Webb, R.E. Miller (Labs,Pr) *Rev. Sci. Instrum.*, No. 10, Vol. 44, 10/73; pp 1542-1543

SPECTROMETRY below 10 keV, Ion scattering — R.E. Honig. W.L. Harrington (Labs,Pr) *Thin Solid Films*. 1973; pp. 43-56

175 Reliability, Quality Control and Standardization
value analysis, reliability analysis, standards for design and production.

INTERCONNECTIONS — B.R. Schwartz (MSRD,Mrstn) *Electromechanical Design*

MANUFACTURING, Electronic equipment — D.H. Mercer (MSRD,Mrstn) *Proc. of the Discrete Manufacturing Industries Workshop*. Report No. 3, 2/74

RESIDUE FLUXES in historical perspective, water soluble — O.D. Black (ATL,Cam) NEPCON West '74. Anaheim, Calif.; 2/29/74; Proc.

SEMITRANSPARENT MASKS, Fabrication of — N. Feldstein. J.A. Weiner (Labs,Pr) *J. Electrochem. Soc.*, Vol. 120, No. 12,; 12/73 pp. 1654-1657

PRODUCT INTEGRITY through design — A.C. Spear (GCASD,Mass) 12th Annual Spring Reliability Seminar: IEEE Boston Section; 4/25/74

RELIABILITY PREDICTION modelling using multivariate data analysis methods — F.R. Freiman (ATL,Cam) IEEE Boston Section Spring Seminar; Boston. Mass.; 4/25/74

180 Management and Business Operations
organization, scheduling, marketing, personnel.

BLANKET ORDERS: A solution to purchasing problems — J.A. Lyons, Jr. (EC,Har) 65th Annual SLA Conf., Toronto, Canada; 6/9-13/74

DESIGN-TO-COST Activities, The role of parametric cost estimating in — F.R. Freiman (ATL,Cam) AIIE Seminar Design-to-a-cost, Washington, D.C.; 3/27-29/74

DESIGN-TO-COST contracting guidelines, Summary of American Preparedness Association Report on — C.D. Fisher (GCASD,Cam) Mtg. Proc., ADPA, p. 10-1 thru 10-15; 10/15-16/73

PROJECT MANAGEMENT — planning, scheduling, and control — M.W. Buckley (MSRD,Mrstn) Canadian Management Centre of the American Management Associations, Toronto, Canada; 4/22-25/74

PROJECT MANAGEMENT — planning, scheduling and control — M.W. Buckley (MSRD,Mrstn) AMA Management Center, Chicago, Ill.; 4/29-5/2/74

SERIES 200
MATERIALS, DEVICES, & COMPONENTS

205 Materials (Electronic)
preparation and properties of conductors, semi-conductors, dielectrics, magnetic, electro-optical, recording, and electro-magnetic materials.

Bi_2, On the existence of bielectrons in — W. Czaja, G. Harbeke. L. Krausbauer, E Meier, B.J. Curtis, H. Brunner (Labs,Pr) *Sol. St. Comm.*. Vol. 13, pp. 1445-1450; 1973

$CdCr_2Se_4$, Composition of — R. Okamoto. K. Ametani. T. Oka (Labs,Pr) *Japan J. Appl. Phys.*. Vol. 13, p. 187-188; 1/74

DILUTE COSPUTTERED MULTICOMPONENT FILMS, Calculation of composition of — J J. Hanak, B.F.T. Bolker (Labs,Pr) *J. of Appl. Phys.*. Vol. 4, No. 11, 11/73 pp. 5142-5147

ELECTRONIC MATERIALS, Chemical vapor deposition of — J.J. Tietjen (Labs,Pr) *Ann. Rev. of Mat. Sci.*, Vol. 3, 1973; pp 317-326

EPITAXIAL InAs, Carrier lifetime in — V.L. Dalal, W.A. Hicinbothem, H. Kressel (Labs,Pr) *Appl. Phys. Lett.*. Vol. 24, No. 4, 2/15/74

GaAs:Cs-O surfaces, Calculated energy distributions of electrons emitted from negative electron affinity — J.S. Escher, H. Schade (Labs,Pr) *J. Appl. Phys.*,Vol. 44, No. 12, 12/73; pp. 5309-5313

LANTHANIDES: some lanthanide tungstate-chlorides, Observation of the crystal chemistry of — P.N. Yocom, R.T. Smith (Labs,Pr) *Materials Research Bulletin*. Vol. 8, No. 11; 11/73; pp. 1287-1294

LIQUID He, Effect of electron cooling on the lifetime of — R.S. Crandall (Labs,Pr) *Physics Letters*. Vol. 46A, No. 6, pp. 385-386; 1/28/74

PHOTOCHROMIC $LiNbO_3$, Hologram storage in — D.L. Staebler, W. Phillips (Labs,Pr) *Appl. Phys. Letters*. Vol. 24. No. 6; 3/15/74; pp. 268-270

SEMICONDUCTORS, Avalanche multiplication in — J. Conradi (RCA Ltd,Mont) Univ. of Sherbrokke; 4/4/74

SILVER AND GOLD FILMS, Optical properties of — R.W. Cohen. G.D. Cody, M.D. Coutts, B. Abeles (Labs,Pr) *Physical Review B*, Vol. 8, No. 8; pp. 3689-3701; 10/15/73

$SrCl_2$, Reduced 4f-5d electrostatic interaction of Sm^{2+} in — R.C. Alig, R.C. Duncan, B.J. Mokross (Labs,Pr) *J. of Chem. Phys.*, Vol. 59. No. 11. 12/1/73 pp. 5837-5841

STOICHIOMETRIC IRON SULFIDE SINGLE CRYSTALS near the alpha transition temperature, Magnetic properties of — T. Takahashi (Labs,Pr) *Sol. St. Comm.*, Vol. 13. 1973, pp. 1335-1337

SULFO-SPINELS containing iron-group transition metals, Some new — S. Harada (Labs,Pr) *Mat. Res. Bull.*, Vol. 8; 1973; 1361-1370

SURFACE POLARITONS at metal surfaces, Dispersion of — R.C. Alig (Labs,Pr) *Solid State Comm.*. Vol. 13; 1973

SURFACE POLARITONS at metal surfaces, Dispersion of — R.C. Alig (Labs,Pr) *Solid State Comm.*. Vol. 1, 1973

SULFO-SPINELS containing iron-group transition metals, Some new — S. Harada (Labs,Pr) *Mat. Res. Bull.*, Vol. 8; 1973; 1361-1370

VAPOR-DEPOSITED Nb_3Sn alloys, Preparation and high-field superconducting properties of — R.E. Enstrom. J.R. Appert (Labs,Pr) *J. Appl. Phys.*, Vol. 45, No. 1, 1/74; pp. 421-427

VAPOR-GROWN $InGaAs$ Epitaxial Films on GaAs and $InGaP$ substrate, Optical properties of — R.E. Enstrom. P.J. Zanzucchi, J.R. Appert (Labs,Pr) *J. Appl. Phys.*, Vol. 45, No. 1, 1/74

YTTRIUM IRON GARNET, Light scattering from thermal acoustic magnons — J.R. Sandercock, W. Wettling (Labs,Pr) *Sol. St. Comm.*. Vol. 13. 1973

Zn-IMPLANTED GaN, Photoluminescence of — J.I. Pankove, J.A. Hutchby (Labs,Pr) *Applied Physics Letters*. Vol. 24, No. 6, 3/15/74

210 Circuit Devices and Microcircuits
electron tubes and solid-state devices (active and passive); integrated, array and hybrid microcircuits, field-effect devices, resistors and capacitors, modular and printed circuits, circuit interconnection, waveguides and transmission lines.

AVALANCHE DIODES, Temperature effects in silicon — J. Conradi (RCA Ltd,Mont) *Solid State Electronics*. Vol. 17. 1974; pp. 99-106

CHARGE-COUPLED DEVICES, Experimental measurements of noise in — J.E. Carnes, W.F. Kosonocky, P.A. Levine (Labs,Pr) *RCA Review*. Vol. 34, No. 4, 12/73' pp. 553-565

COLOR PICTURE TUBES, Three-filter colorimetry of — G.M. Eheman, Jr. (EC,Har) Electrochemical Soc., San Francisco. Calif.; 5/12/74

GaAs FET for high power amplifiers at microwave frequencies — L.S. Napoli, J.J. Hughes, W.F. Reichert, S. Jolly (Labs,Pr) RCA Review, Vol. 34, No. 4, 12/73; pp. 608-615

HETEROJUNCTION DIODES for optical communications, High radiance, high speed AlGaAs — M. Ettenberg, H.F. Lockwood. J.P. Wittke, H. Kressel (Labs,Pr) IEDM Tech. Digest, 1973

LiNbO₃ transducer for microwave acoustic (bulks) delay lines, Fabrication of sub-micron — H.C. Huang, J.D. Knox, Z. Turski, R. Wargo, J.J. Hanak (Labs,Pr) Appl. Phys. Lett., Vol. 2, No. 3, 2/1/74

PHOTOMULTIPLIER TUBES in nuclear medicine, The role of — D.E. Persyk, W.D. Lindley (EC,Har) Soc. of Nuclear Medicine 12th Int'l Annual Mtg., Munich, Germany; 9/11-14/74

SCHOTTKY BARRIERS, Granular metal-semiconductor — C.R. Wronski, B. Abeles, R.E. Daniel, Y. Arie (Labs,Pr) J. Appl. Phys., Vol. 45, No. 1, 1/74

SUPERCONDUCTING TUNNEL JUNCTIONS, Current-voltage characteristics of — W.C. Stewart (Labs,Pr) J. Appl. Phys., Vol. 45, No. 1, 1/74

TRAPATT CIRCUITS, Lumped-element high-power — A.S. Clorfeine, H.J. Prager, R.D. Hughes (Labs,Pr) RCA Review, Vol. 34, No. 4, 12/73

TWO-PHASE CHARGE-COUPLED DEVICES with overlapping polysilicon and aluminum gates, Design and performance of — W.F. Kosonocky, J.E. Carnes (Labs,Pr) IEDM Tech. Digest, 1973;pp. 123-125

215 Circuit and Network Designs

analog and digital functions in electronic equipment; amplifiers, filters, modulators, microwave circuits. A-D converters, encoders, oscillators, switches, masers, logic networks, timing and control functions, fluidic circuits.

ACOUSTIC DELAY LINES utilizing LiNbO₃, Bulk — H.C. Huang, J.D. Knox, Z. Turski (Labs,Pr) 1973 IEDM Tech. Dig., 1973; pp. 263-265

D/A Subsystem Development, Radiation hardened — L. Dillon (ATL,Cam) Hardened Guidance & Weapon Delivery Technology Mtg.; Culver City, Calif. 3/26-28/74

DIGITAL INTERPOLATION FILTERS for increasing the sampling rate, Parallel realizations of — H. Urkowitz (MSRD,Mrstn) 1974 Int'l Symp. on Circuits and Systems Theory, San Francisco, Calif; 4/22/74

FREQUENCY DIVIDERS, Microwave — L.C. Uphadhyayula, S.Y. Narayan (Labs,Pr) RCA Review, Vol. 34, No. 4; 12/73; pp. 595-607

PHASE-LOCKED LOOPS, Burst synchronization of — L. Schiff (Labs,Pr) IEEE, Communications Tech. Vol. COM-21 No. 10; 10/73

SILICON IMPATT OSCILLATORS, FM noise measurements on p-type and n-type — G.A. Swartz. Y.S. Chiang, C.P. Wen, A. Young (Labs,Pr) Electronics Letters, Vol. 9, No. 25; 12/13/73

THRESHOLD LOGIC techniques — D. Hampel (GCASD,Som) IEEE Intercon 1974, New York, Conf. Record. Alternatives to random logic Session 29/3; 3/26-29/74

225 Antennas and Propagation

antenna design and performance;

feeds and couplers, phased arrays; randomes and antenna structures; electromagnetic wave propagation, scatter. effects of noise.

ANTENNA installations and circularly polarized TV, Multiple — M.S. Siukola (CCSD,Cam) Soc. of Broadcast Engineers Mtg., Phila Pa.; 2/25/74

CIRCULAR POLARIZATION for fm and tv broadcasting, Some aspects of — O.Ben-Dov (CCSD,Cam) Soc. of Broadcast Engineers, New York; 2/14/74

CIRCULAR POLARIZATION in fm and tv broadcasting, Advantages of — M. Siukola (CCSD,Cam) Soc. of Broadcast Engineers, Chicago; 2/20/74

REFLECTIONS, Another look at — W. Maxwell (AED,Pr) QST, Vol 57, No. 4 (April 1973) and in subsequent issues in several installments.

240 Lasers, Electro-Optical and Optical Devices

design and characteristics of lasers, components used with lasers, electro-optical systems, lenses, etc. (excludes: masers).

ELECTROLUMINESCENT JUNCTIONS on GaAs, Vapor-Grown in InGaP — C.J. Nuese, A.G. Sigai, J.J. Gannon, T. Zaeromowdki (Labs,Pr) J. of Electr. Mat., Vol. 3, No. 1, 2/74

GaP:N, The effect of hydrostatic pressure on the photoconductivity and electroluminescence of — H. Kressel, M.I. Wolfe, T. Halpern, P.N. Raccah (Labs,Pr) Applied Physics Letters, Vol. 24, No. 6; 3/15/74

InGaAs for 1.06 micrometre emission, CW laser diodes and high-power arrays of — C.J. Nuese, M. Ettenberg, R.E. Enstrom, H. Kressel (Labs,Pr) Appl. Phys. Lett., Vol. 2, No. 5, 3/1/74

InGaAs pn junctions, Room-temperature laser operation of — C.J. Nuese, R.E. Enstrom. M. Ettenberg (Labs,Pr) Appl. Phys. Lett., Vol. 24, No. 2, 1/15/74

INJECTION LASERS: V. Strong polarization, Experimental properties of — H.S. Sommers, Jr. (Labs,Pr) J. Appl. Phys., Vol. 45, No. 1, 1/74

LASER DIODES, of InGaAs for 1.06 micrometre emission, Efficient — C.J. Nuese, M. Ettenberg, R.E. Enstrom, H.Kressel (Labs,Pr) 1973 IEDM Tech. Digest; 1973

OPTICAL PRECURSOR detection, Laser — W. Shubert, L. O'Hara, E. Lea, L. Hansen (ATL,Cam) DoD laser conf., Colorado Springs, Col.; 3/28/74; Proc.

RELIEF PHASE HOLOGRAMS recorded in photoresists, Characteristics of — R.A. Bartolini (Labs,Pr) Appl. Opt. Vol. 13, No. 1; 1/74

SCATTERING OF LIGHT by phonons in absorbing materials — R.K. Wehner (Labs,Pr) Opt. Comm., Vol. 6, No. 2; 10/72

245 Displays

equipment for the display of graphic, alphanumeric. and other data in communications, computer, military, and other systems, CRT devices. solid state displays, holographic displays, etc.

MOVING MAP display, Holographic — B.R. Clay (ATL,Cam) SPIE Conf. on Coherent

Optics in mapping; Rochester, N.Y.; 3/28/74

250 Recording Components and Equipment

disk, drum, tape, film, holographic and other assemblies for audio, image, and data systems.

LASER RECORDING on black and white film, Multispectral — S.L. Corsover (ATL,Cam) Second European Electro-Optic Conf., Montreau, Switzerland; 4/5/74

QUADRUPLEX VIDEO RECORDING, Recent developments in — K. Sadashige (CCSD,Cam) SMPTE 115th Conf., Los Angeles, Calif.; 4/25/74

RE-RECORDING, A high speed interlock system for — L.A. ..Briel, R.S. Dickinson (CCSD,Cam) SMPTE 115th Conf., Los Angeles, Calif.; 4/23/74

VIDEO TAPE PERFORMANCE, Biased tape guidance for improved — J.D. Bick (CCSD,Cam) SMPTE 115th Conf., Los Angeles. Calif.; 4/22/74

280 Thermal Components and Equipment

heating and cooling components and equipment, thermal measurement devices, heat sinks.

AIR CONDITIONING using solar energy, Regenerative gas cycle — B. Shelpuk (ATL,Cam) National Science Foundation Solar Cooling Workshop; 1/31/74. Washington, D.C.; Proposal to National Science Foundation

---

SERIES 300
SYSTEMS, EQUIPMENT, & APPLICATIONS

---

312 Land and Water Transportation

navigation systems, automotive electronics, etc.

COLLISION AVOIDANCE, A new kind of radar for — J. Shefer. R.J. Klensch, HC. Johnson, G.S. Kaplan (Labs,Pr) Soc. of Auto Eng., Automatic Engineering Congress, Detroit, Mic., 2/24-3/1; 1974

VEHICLE-IDENTIFICATION system, A microwave automatic — R.J. Klensch, J. Rosen, H. Staras (Labs,Pr) RCA Review, Vol. 34, No. 4, 12/73; pp. 566-579

315 Military Weapons and Logistics

missiles. command and control.

AEGIS weapon system — F.G. Adams (MSRD,Mrstn) Naval Reserve Group Command 4-3(m) Camden, N.J.; 4/6/74

325 Checkout, Maintenance, and User Support

automatic test equipment, (ATE). maintenance and repair methods.

JET ENGINE ACCESSORIES, Automatic test system — G.E. Kelly. Jr. (GCASD,Mass) Automatic Testing Conf.. — International 74, Brighton, England; 11/5/74

340 Communications

industrial, military, commercial systems, telephony. telegraphy and telemetry, (excludes: television, and broadcast radio).

MICROWAVE TRANSMISSION study, Digital/analog — K. Feher (RCA Ltd,Mont) Doctorate Thesis presented at the Univ. of Sherbrooke; 3/74

345 Television and Broadcast

television and radio broadcasting, receivers. transmitters. and systems. television cameras, recorders. studio equipment.

HOLOTAPE: A low-cost prerecorded television system using holographic storage — W.J Hanna, R.E. Flory, M. Lurie, R.J. Ryan (Labs,Pr) Soc. of Motion Pic & Telev. Engineers Vol. 82, No. 11, 11/73; pp. 905-915

TV TRANSMITTING SYSTEMS for unattended operation — T.M. Gluyas (CCSD,Cam) 28th NAB engineering conf., Houston, Texas; 3/17-20/74

VIDEO RECORDING, A comparison of quadruplex and helical scan — J.L. Grever (CCSD,Cam) SECA Mtg., in Galt House, Louisville, Ky; 5/14/74

360 Computer Equipment

processors. memories, and peripherals.

MNOS MEMORY development — J. Richards (ATL,Cam) Hardened Guidance & Weapon Delivery Technology Mtg., Culver City, Calif.; 3/26-27/74

READ-WRITE HOLOGRAPHIC MEMORIES, Heterodyne readout for — R.S. Mezrich. W.C. Stewart (Labs,Pr) Applied Optics, Vol. 12, No. 11, 11/73 pp.2677-2682

365 Computer Programming and Applications

languages. software systems, and general applications (excluding: specific programs for scientific use).

CASPER (Comprehensive APL system for the preparation and execution of reports) — W.A. Rux, E. Baelen (EC,Har) APL 6 Int'l User's Conf., Anaheim. Calif.; 5/14-17/74

DESIGN AUTOMATION: Make it work in a drafting environment — A.T. Farrell (GCASD,Mass) 1974 American Institute for Design & Drafting Conf., Chicago 4/3/74

SOFTWARE COST performance, Automatic test equipment — H.L. Fischer (GCASD,Mass) Aeronautical Systems Software Workshop, Dayton, Ohio; 4/3/74

SOFTWARE DEVELOPMENT approach, Real-time — J.C. Kulp (MSRD,Mrstn) AFSC Workshop on aeronautical systems software, Dayton, Ohio; 4/3/74

NETWORK OPTIMIZATION program, Cascaded — V.K. Jha (RCA Ltd,Mont) Trans. IEEE, Microwave Theory & Techniques. Vol. 22, No. 3; 3/74

Patents Granted

to RCA Engineers
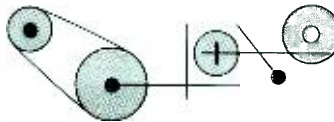
Consumer Electronics

Brightness Control — J. Avins (CE, Som.) U.S. Pat. 3804981. April 16, 1974

Information Playback System — S. E. Hilliker (CE, Indpls.) U.S. Pat. 3806668. April 23, 1974

Static Convergence Device for Electron Beams — I. F. Thompson and J. L. Smith (CE, Indpls.) U.S. Pat. 3808570. April 30, 1974

Television Receiver Using Synchronous Video Detection — J. Avins (CE, Som.) U.S. Pat. 3812289. May 21, 1974

Independent Electron Gun Bias Control — J. C. Marsh, Jr. (CE, Indpls.) U.S. Pat. 3812397, May 21, 1974

High Voltage Protection Circuit — M. N. Norman (CE, Indpls.) U.S. Pat. 3813580, May 28, 1974

Palm Beach Division

Hinged Drum System — J. P. Watson (PBD, Palm Beach Gardens) U.S. Pat. 3813678, May 28, 1974

Astro-Electronics Division

Dual Thrust Level Monopropellant Spacecraft Propulsion System — Y. C. Brill (AED, Pr.) U.S. Pat. 3807657, April 30, 1974

Rotary Solenoid Shutter Drive Assembly and Rotary Inertia Damper and Stop Plate Assembly — W. L. Cable and H. B. Dougherty (AED, Pr.) U.S. Pat. 3804506, April 16, 1974; Assigned to U.S. Government

Government Communication & Automated Systems Division

Broad Band Single Frequency Generator — F. U. Everhard, Jr. (GCASD, Burl.) U.S. Pat. 3808548, April 30, 1974; Assigned to U.S. Government

Processor Synchronization Scheme — R. M. Zieve, C. L. Maginniss and M. Kleidermacher (GCASD, Cam.) U.S. Pat. 3810119, May 7, 1974; Assigned to U.S. Government

Automatic Positioning Device Exhibiting High Accuracy and Repeatability — P. F. Minghella (GCASD, Burl.) U.S. Pat. 3811083, May 14, 1974; Assigned to U.S. Government

High-Speed Signal Following Circuit — N. R. Scheinberg (GCASD, Som.) U.S. Pat. 3812383, May 21, 1974

Magnetic Reed Sensor Suitable for Use in Ignition Timing Systems — L. R. Hulls (GCASD, Burl.) U.S. Pat. 3813596, May 28, 1974

Government Engineering

Transition Detector — G. J. Dusheck, Jr. (ATL, Cam.) U.S. Pat. 3805170, April 16, 1974; Assigned to U.S. Government

Commercial Communications Systems Division

Automatic Squelch Tail Eliminator for Tone Coded Squelch Systems — L. F. Crowley, A. M. Missenda, and D. R. Presky (CCSD, Meadowlands) U.S. Pat. 3810023, May 7, 1974

RCA Laboratories

Low Berefringent Orthoferrites — R. B. Clover, Jr. (Labs. Pr.) U.S. Pat. 3804766, April 16, 1974

Semiconductor Memory Element — F. Sterzer (Labs. Pr.) U.S. Pat. 3805125, April 16, 1974

Adaptive Surface Wave Devices — A. Miller (Labs. Pr.) U.S. Pat. 3805195, April 16, 1974

Least Recently Used Location Indicator — J. A. Weisbecker (Labs. Pr.) U.S. Pat. 3806883, April 23, 1974

Method of Polishing Sapphire and Spinel — P. H. Robinson and R. O. Wance (Labs. Pr.) U.S. Pat. 3808065, April 30, 1974

Charge Transfer Fan-in Circuitry — P. K. Weimer (Labs. Pr.) U.S. Pat. 3811055, May 14, 1974

Aluminum Oxide Films for Electronic Devices — M. T. Duffy and J. E. Carnes (Labs. Pr.) U.S. Pat. 3809574, May 7, 1974

Corona Discharge Device — R. A. Gange and C. C. Steinmetz (Labs. Pr.) U.S. Pat. 3809974, May 7, 1974

Method of Treating a Glass Body to Provide an Ion-Depleted Region Therein — D. E. Carlson, K. W. Hang, and G. F. Stockdale (Labs. Pr.) U.S. Pat. 3811855, May 21, 1974

Method of Epitaxially Depositing Gallium Nitride from the Liquid Phase — F. Z. Hawrylo and J. I. Pankove (Labs. Pr.) U.S. Pat. 3811963, May 21, 1974

Two Color Medium for Full Color TV Film System — R. E. Flory (Labs. Pr.) U.S. Pat. 3812528. May 21, 1974

Video Stripper — J. D. Cavett and R. S. Hopkins, Jr. (Labs. Pr.) U.S. Pat. 3813488, May 28, 1974

Electronic Components

Correcting Lens — A. M. Morrell and F. Van Hekken (EC, Lanc.) U.S. Pat. 3811754, May 21, 1974

Method for Coating only the Convex Major Surface of an Apertured Mask for a Cathode-Ray Tube — B. K. Smith (EC, Lanc.) U.S. Pat. 3811926, May 21, 1974

Impedance Control Using Transferred Electron Devices — R. E. Marx (EC, Pr.) U.S. Pat. 3812437, May 21, 1974

Method for Making a Negative Effective Electron-Affinity Silicon Electron Emitter — A. H. Sommer (EC, Pr.) U.S. Pat. 3806372, April 23, 1974

Method of Installing a Mount Assembly in a Multibeam Cathode-Ray Tube — J. F. Segro and G. L. Fassett (EC, Lanc.) U.S. Pat. 3807006, April 30, 1974

Method of Fabricating a Dark Heater — J. R. Hale and G. I. Merritt (EC. Lanc.) U.S. Pat. 3808043. April 30, 1974

Solid State Division

Hybrid Electron Device Containing Semiconductor Chips — E. T. Hausman (SSD. Som.) U.S. Pat. 3805117, April 16, 1974

Gated Astable Multivibrator — A. J. Visioli, Jr. and H. A. Wittlinger (SSD. Som.) U.S. Pat. 3805184. April 16, 1974

Method for Making a Radio Frequency Transistor Structure — D. S. Jacobson and R. A Duclos (SSD. Som.) U.S. Pat. 3807039, April 30. 1974

Method of Closing a Liquid Crystal Device — H. A. Stern (SSD. Som.) U.S. Pat. 3807127, April 30. 1974

Capacitive-Discharge Timing Circuit Using Comparator Transistor Base Current to Determine Discharge Rate — L. R. Campbell (SSD. Som.) U.S. Pat. 3808466, April 30, 1974

Liquid Crystal Device Closure Method — A. N Gardiner and H. A. Stern (SSD. Som.) U.S. Pat 3808769, May 7. 1974

Liquid Crystal Display — R. C. Heuner and S. J. Niemiec (SSD. Som.) U.S. Pat. 3809458, May 7. 1974

Window Detector Circuit — A. W. Young (SSD. Som.) U.S. Pat. 3809926. May 7. 1974

Set-Reset Flip-Flop — G. E. Skorup (SSD, Cam.) U.S. Pat. 3812384, May 21. 1974

Series Regulated Power Supply for Arc Discharge Lamps Utilizing Incandescent Lamps — F. Caprari (SSD. Som.) U.S. Pat. 3 3813576. May 28. 1974

Current Source — A. C. N. Sheng (SSD. Som.) U.S. Pat. 3813595, May 28. 1974

Record Division

Tape Cartridge Player Cartridge Magazine — B. A. Grae and D. R. Andrews (Record Div., Indpls.) U.S. Pat. 3812537, May 21. 1974
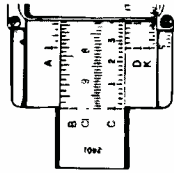
Engineering News and Highlights

Dr. Alfred N. Goldsmith
(September 15, 1888—July 1, 1974)

Dr. Alfred N. Goldsmith, a world-renowned scientist, engineer and inventor, died July 1, in St. Petersburg, Fla., where he had resided for the past 16 months. He was 86.

Dr. Goldsmith was an Honorary Vice President of RCA and its Senior Technical Advisor at the time of his death. A prolific inventor, he was a pioneer in the development of radio and television, sound motion pictures, medical electronics and other areas of electronics.

When RCA was formed in 1919, the late General David Sarnoff named Dr. Goldsmith to head the new company's research and development activities. Dr. Goldsmith served as Director of Research and later as Vice President and General Engineer of RCA from 1919 to 1931, when he resigned to become an independent consultant. He remained as Senior Technical Consultant to RCA.

Born in New York City, September 15, 1888, Dr. Goldsmith began his career as an instructor at the College of the City of New York in 1907, when he also received the BS from that college. He remained with CCNY until 1919 and, in the meantime, received

the PhD from Columbia University in 1911. He was given a lifetime appointment at CCNY as Associate Professor of Electrical Engineering. He was also granted an Honorary Doctor of Science degree by Lawrence College in 1935.

Dr. Goldsmith was consulting engineer for the General Electric Company from 1915 to 1917, and Director of Research for Marconi Wireless Telegraph Company of America from 1917 to 1919. Dr. Goldsmith joined RCA in 1919 when it acquired the Marconi Company. At the start, Dr. Goldsmith and his staff conducted their research and engineering efforts at the Electrical Engineering Laboratory of CCNY. As the work load increased RCA established a Technical and Test Department at Van Cortlandt Park, in New York City, which became the Company's first research laboratory.

In 1920, Dr. Goldsmith's work made possible the first commercial radio with only two control knobs and a built-in speaker; and also the first commercial radio-phonograph. He also made vital contributions to the development of the first color television tube to find commercial and worldwide use. He proposed a color television picture tube employing a screen of color phosphor dots and a perforated plate. In its simplest terms this was the basic idea of the shadow-mask color picture tube now in widespread commercial use throughout the world.

Dr. Goldsmith was a Co-Founder, Fellow. Director, and Life Member of the Institute of Radio Engineers, was its President in 1928; and had served as Editor, Editor Emeritus, and Anniversary Editor since its founding in 1912. He was Secretary of the IRE from 1918 to 1927. He was also a Fellow of the American Institute of Electrical Engineers. In 1963, the IRE and AIEE merged to form the IEEE, and Dr. Goldsmith became a Fellow, and Director and Editor Emeritus of the IEEE.

In addition, Dr. Goldsmith was a Fellow of the American Physical Society, the American Association for the Advancement of Science, the Acoustical Society of

America, the Optical Society of America, and the International College of Surgeons.

Among his many honors, Dr. Goldsmith was the recipient of the IRE Medal of Honor in 1941, and the IRE Founders Award in 1954. In March 1962, he was honored with a scroll of tribute by the IRE at its Golden Anniversary Celebration. Dr. Goldsmith also received the Progress Medal Award of the Society of Motion Picture and Television Engineers; Modern Pioneer Award (1940); Townsend Harris Medal (1942).

Dr. Goldsmith was elected President of the Society of Motion Picture and Television Engineers in 1932, and had been chairman and member of various sectional committees of the American Standards Association. In 1966, he became Vice President (Electronics) of the Pan-American Medical Association. He was an Honorary member of the Radio Society of Great Britain, the Royal Society of Arts (Great Britain), the International Committee of Radio Telegraphy (France), the Academy of Motion Picture Arts and Sciences, the Society of Motion Picture and Television Engineers, and of the Institution of Radio Engineers (Australia). He was also an eminent member of Eta Kappa Nu Association, and a member of the New York Medico-Surgical Society.

Jellinek receives Thurlow Navigation Award

Ernest Jellinek was honored by the Institute of Navigation for making the most outstanding contribution to the science of navigation during 1973.

Mr. Jellinek receieved the Thomas L. Thurlow Navigation Award at a banquet held during the Institute's annual meeting in San Diego, Cal. Mr. Jellinek is Staff Systems Manager, Navigation and Traffic Control, Government Plans and Systems Development, for RCA Government and Commercial Systems, Camden, N.J.

Mr. Jellinek was cited for his exceptional

ingenuity and engineering skill in conceiving and designing RCA's Harbor Traffic Ranging, Identification and Communication (HATRIC) System. (This system was described in the April-May 1973 issue of the *RCA Engineer*.)

Mr. Jellinek joined RCA in 1958 as a Project Engineer with the company's Communications Systems Division. He was a leader in programs to develop integrated navigation and communications systems for advanced aircraft such as the B-1 and AWACS.

In 1968, he joined the Systems Development Group where he is technical director for advanced systems development in the area of navigation and traffic control for aircraft and ships. Prior to joining RCA, Mr. Jellinek worked for General Electric and the Electronics Corporation of America.

Mr. Jellinek earned the BEE from the Polytechnic Institute of New York in 1941. He is a senior member of IEEE and holds memberships in the Institute of Navigation and the American Institute of Aeronautics and Astronautics. He is a Licensed Professional Engineer in the state of New York.

Volpe named Chief Engineer at MSRD

Max Lehrer, Division Vice President and General Manager, Missile and Surface Radar Division, Moorestown, N.J., recently appointed **Joseph C. Volpe** as Chief Engineer.

In his new post, Mr. Volpe will act as the principal engineering executive of the Missile and Surface Radar Division with responsibility for all engineering activities. He also will be responsible for development of advanced techniques needed for future systems.

Mr. Volpe received the BS in physics from St. Joseph's College and completed graduate courses at Temple University and the University of Pennsylvania in physics and servomechanisms. He is a member of Sigma, the honorary physics fraternity.

Prior to his promotion, Mr. Volpe was Project Manager for the AEGIS Weapon System being developed by RCA for the Naval Ordance Systems Command.

Since joining RCA in 1958, Mr. Volpe has held increasingly responsible managerial posts in various radar development programs at the Moorestown facility.

Cottler on G&CS Staff

Dr. Harry J. Woll, Vice President, Government Engineering announced the appointment of **Dudley M. Cottler** as Staff Technical Advisor. Mr. Cottler's primary responsibility in his new position is the Independent Research and Development

Program for all of the Government and Commercial Systems Divisions involved in government contracts — administering the fields of investigation and the allocations of funds for the program.

During Mr. Cottler's tenure as Chief Engineer of the Missile and Surface Radar Division (1967-1974), the Division made important advances in radar and systems technology, ranging from such major systems developments as AEGIS and AN/FPS-95 to such critical concept developments as ultra-high-speed digital logic design for advanced data/signal processing systems.

Mr. Cottler received the BChE from the College of the City of New York in 1942 and later took graduate courses in electrical engineering at Polytechnic Institute of Brooklyn as well as management courses while with the Government and RCA.

Mr. Cottler was Project Manager for the BMEWS Tracking Radar (AN/FPS-49) during its design, development, production, and test and later became the BMEWS engineering manager during implementation of the United Kingdom site. He joined RCA in 1956 where his initial responsibility was Project Leader for tracking-radar development and field evaluation in the Talos Land-Based Missile Program. Previous to this he spent eight years at White Sands Proving Ground beginning in 1948. He was also a charter member of the Electronic Trajectory Measurements Working Group of the Inter-Range Instrumentation Group (IRIG).

He is a member of the AIAA, American Ordnance Association and Air Force Association.

Rabinowitz appointed Principal Scientist

Max Lehrer, Division Vice President and General Manager, Missile and Surface Radar Division, Moorestown, N.J., appointed **Dr. Samuel J. Rabinowitz** as Principal Scientist.

In the newly-created post, Dr. Rabinowitz will act as a technical adviser to Mr. Lehrer on the various radar, data processing and related systems under development at the Division. He also will perform special assignments.

Prior to his promotion, Dr. Rabinowitz, as Manager of Systems Engineering, was responsible for directing the Division's efforts to develop new systems to meet customer needs.

Dave Shore elected President, National Association for Remotely Piloted Vehicles

David Shore, Division Vice President, Government Plans and Systems Development, Government and Commercial Systems, has been elected President of the

National Association for Remotely Piloted Vehicles (RPVs).

The Association, with headquarters in Dayton, Ohio, was organized in 1972 for the "advancement of remotely employed air power to complement manned aircraft forces."

Mr. Shore earned the BS in Aeronautical Engineering from the University of Michigan in 1941 and the MS in Physics from Ohio State University in 1950.

Mr. Shore has been with the company since 1954. Presently, he directs the planning activities for G&CS and the development of major new weapons systems concepts. Mr. Shore has led G&CS' multi-divisional efforts in several RCA and Air Force programs involving RPVs, including the Multi-Mission RPV and Drone Control and Data Relay System.

Presently, Mr. Shore is Chairman of the NSIA Command, Control and Communications Advisory Committee and was Chairman of the IEEE International Conference on Communications in 1967. He is a member of several professional associations and holds a Professional Engineering License for the state of New Jersey.

Amantea and Held named David Sarnoff Fellows

Dr. William M. Webster, Vice President, RCA Laboratories, Princeton, N.J., recently announced that two Solid State Technology Center scientists have been awarded David Sarnoff Fellowships for graduate study in the 1974-75 academic year.

One of the Fellows, **Robert Amantea,** plans to attend the Massachusetts Insitute of Technology and work toward the PhD in Electrical Engineering. **Gerald D. Held,** who is working toward the PhD in Computer Science, will start his second year as a Sarnoff Fellow at the University of California, Berkeley.

The David Sarnoff Fellowships, established in 1956 to commemorate the late General Sarnoff's fifty years in radio, television and electronics, are awarded annually to outstanding employees of RCA. The Fellowships are the top educational awards available to RCA employees.

Mr. Amantea has worked for RCA since receiving the BEE in 1965 from the City University of New York. He was awarded the MS in Electrophysics in 1969 from the Polytechnic Institute of New York.
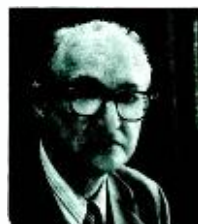
Mr. Held, an RCA employee since 1970, received the BS in Electrical Engineering from Purdue University in 1970, and the MSE in 1972 from the University of Pennsylvania

Jellinek

Volpe

Cottler

Shore

Amantea

Held

New appointments at Consumer Electronics

Loren R. Kirkwood, Division Vice President, Television Engineering and Strategic Planning, announced the organization of Television Engineering and Strategic Planning as follows: **Thornley C. Jobe,** Chief Product Development Engineer - Color Television; **Robert J. Lewis,** Chief Engineer, Black and White Television Product Design and Safety Engineering; **James A. McDonald,** Manager, Technology and Services; and **John M. Wright,** Chief Product Design Engineer - Color Television.

Thornley Jobe received the BSEE from Georgia Institute of Technology. He joined RCA in 1953 as Liaison Engineer at the Home Instruments Division (now Consumer Electronics) television receiver manufacturing plant Bloomington, Indiana. In 1961, he became Leader in the Color Television Design section at Indianapolis, Indiana. In 1966, he became Manager of Resident Engineering at the Memphis, Tennessee, television receiver plant. In 1971, he became Manager of Product Analysis and Control at Indianapolis. He assumed his present position in 1973. He is a member of Eta Kappa Nu and Tau Beta Pi. He has been awarded five U.S. patents.

Robert Lewis received the BSEE from Drexel Institute of Technology. He started with RCA at Camden, N.J. in 1941 as an electrical engineer. When the RCA Home Instruments Division moved to Indianapolis, Ind. from New Jersey, to become RCA Consumer Electronics he was responsible for organizing and training an engineering group at the new home office of the division. He was named Manager, Black-and-White TV Engineering in 1969 and in 1973 became Chief Engineer with engineering design responsibility for all RCA black-and-white tv receivers made in domestic and foreign plants.

James McDonald received the BSC (honors) from Glasgow University in 1955 and the MS from Purdue University in 1968. He worked for Associated Electrical Industries in England for seven years, mainly on signal processing for radar. In 1962, Mr. McDonald joined RCA Consumer Electronics and designed deflection circuits for Black and White Television for which he received twelve patents. In 1968 he was promoted to Leader in Advanced Development, and his assignments included a video tape player, a holographic player, and a single-tube color camera. In 1973 he was made manager of Video Disc Engineering.

John Wright received the BA in Math and Physics from Wabash College in 1938 and later attended both George Washington University and Indiana University. Prior to joining RCA in Camden in 1946, Mr. Wright was engaged in radio receiver design with the Navy Department, Bureau of Ships. Mr. Wright was transferred from the Radio Design Group to Resident Engineering at the Bloomington Plant and became Resident Engineer in 1951. He was responsible for the coordination of Engineering activities with the Manufacturing Plant in the areas for radio, black and white tv, color tv and Selectavision.

Williams invited to serve on Scientific Advisory Committee

Dr. John C. Williams Staff Engineer, Government Plans and Systems Development, Camden, N.J., has been invited to serve as an Associate Member of the Defense Intelligence Agency's Scientific Advisory Committee.

The Scientific Advisory Committee provides a valuable link between the Defense Intelligence Agency and the scientific and industrial communities of the nation. Dr. Williams was nominated by Vice Admiral V.P. dePoix, USN, Director, Defense Intelligence Agency, and subsequently approved by the Office of the Secretary of Defense for appointment as an Associate Member for a one-year term beginning July 1, 1974, subject to possible extension.

Dr Williams received the BS in Electrical Engineering from Pennsylvania State College in 1941; the MS in Engineering Science and Applied Physics from Harvard in 1948; and the PhD in Applied Physics from Harvard in 1959. He joined Government Plans and Systems Development in 1968 where he has provided technical direction and management for a number of electromagnetic systems programs.

Dr. Williams is a member of the American Physical Society, American Geophysical Union, New York Academy of Sciences, and the American Association for Advancement of Science.

Scott appointed Director of IC Technology Research

Gerald B. Herzog, Staff Vice President, Technology Centers, at RCA Laboratories in Princeton, N.J., recently appointed **Joseph H. Scott, Jr.,** as Director of Integrated Circuit Technology.

Mr. Scott received the AB in Chemistry from Lincoln University in 1957. The following year he attended the Graduate School of Chemistry at Howard University. He also did graduate work in Electrical Engineering at Howard after joining RCA.

Mr. Scott has been with RCA since 1959. He started with Electronic Components and Devices in Somerville, N.J., doing research and development work on semiconductor devices. He transferred to RCA Laboratories in 1967. In 1970, he was named Head of the Integrated Circuit Technology and Applications Research Group, the position he held until his promotion.

He received an RCA Laboratories Outstanding Achievement Award in 1967. Two years later, he became the first person in the history of RCA Laboratories to receive two Outstanding Achievement Awards in one year for work on separate research tems.

In 1973, he was given RCA's highest technical honor, the David Sarnoff Award, "for outstanding team research leading to a new class of integrated semiconductor arrays."

He is a member of Sigma Xi and the Electrochemical Society as well as being a senior member of the IEEE. Mr. Scott has been issued 14 U.S. Patents and has written about 25 technical papers.

Schindler to head IEEE Section

Dr. Max J. Schindler of the Microwave Device Operations Department, Electronic Components, Harrison, N.J., has been elected Chairman of the North Jersey Section of the Institute of Electrical and Electronics Engineers. The IEEE is the world's largest Engineering Society, with a world-wide membership of over 170,000, of which 4,500 reside in the North Jersey area.

Dr. Schindler received the MSEE and the Doctor of Technical Sciences from the Technical University in Vienna, Austria. He joined RCA in 1958 and has worked on a number of basic technical problems related to the design of traveling-wave tubes, magnetrons, crossed-field devices, and solid state devices. Dr. Schindler has published and presented numerous papers and holds three patents. He is a senior member of IEEE. In accepting his new post, Dr. Schindler commented, "Our Section will endeavor to establish closer ties to the local communities. Engineers have developed the technology which nas made this country the richest in the world, and they are able and anxious to solve the environmental and socio-economic side effects of this high technology."

Degress granted

Steven M. Vaughan of Electronic Recording Equipment Engineering, Commercial Communications Systems Division, Camden, N.J., received the Master of Science in Systems Engineering from the University of Pennsylvania.

Edward Goldman, Manager of Microwave Purchasing, Electronic Components, Harrison, N.J. received the Master of Science in Business Administration from Rutgers University. He also was elected to the the Beta Gamma Sigma Honorary Business Fraternity.

Thomas L. Nevue of the Solid State Production Engineering Group, Microwave Devices Operating Department, Electronic Components, Harrison, N.J., received the Bachelor of Science in Electrical Engineering from Newark

Jobe

Lewis

McDonald

Wright

Williams

Scott

Schindler

College of Engineering.

Frank J. Strobl, Administrator, Technical Communications, Engineering Professional Programs, received the Bachelor of Science in Management from Rutgers University.

William Shibler of Aural Broadcast Engineering, Communications Systems Division, Meadow Lands, Pa., received the Master of Science in Electrical Engineering from the University of Pittsburgh.

Andrew C. Billie, Jr., of Aural and TV Broadcast Publications, Communications Systems Division, Meadow Lands, Pa., received the Bachelor of Arts in Mathematics from Washington and Jefferson College.

Paul Rappaport, Director of the Process and Applied Materials Research Laboratory at RCA Laboratories was awarded an Honorary Doctor of Science Degree from Arizona State University in recognition of his pioneering research on solar energy and development of the solar cell.

Professional activities

RCA Laboratories

Dr. Jan A. Rajchman, Staff Vice President, Information Sciences was elected a Fellow of the American Physical Society.

Tom Cook, DSRC photographer, was cited by *Industrial Photography* magazine for his photo of a holographic image, "considered to demonstrate the most outstanding level of technical achievement of all photographs submitted" in the *Industrial Photography* 1974 *Annual.*

Missile and Surface Radar Division

Howard Wintling, Manager, Material Quality Control, was elected Second Vice Chairman of the Philadelphia Section American Society for Quality Control (ASQC). **George J. Brannin,** Manager, Product Assurance, served as moderator of the ASQC May dinner meeting — over 100 attended. **Fulvio Olivetto** and **Robert**

Killion delivered papers at the Fifth Annual Reliability Technology Seminar. **Menzo A. Christman,** Manager, Assembly Quality Control, is Editor of the monthly *ASQC Newsletter.*

Government Communications and Automated Systems Division Burlington Operations

Veronica Hsu was elected Secretary of the Aerospace Division of the Special Libraries Association. Also, she served as Chairman of the Sci Tech Committee, Boston Chapter, for two years.

Bill Curtis was elected by the Board of Directors of the Electrical Engineering Alumni Association of the University of Illinois, Urbana, Ill., as one of three recipients of the Distinguished Alumnus Award in recognition of his outstanding contributions to the Electrical Engineering profession and for his long-standing loyal support of Electrical Engineering at Illinois.

Promotions

Global Communications, Inc.

A. Annibell from Mgr., Computer Systems Sales to Mgr., Videovoice (P. Schneider, New York)

J. Christopher from Mgr., Spacecraft Engineering to Dir., Satcom Project (P. Schneider, New York)

J. J. Dietz from Engrg. Ldr. to Mgr., Digital/Voice Design Engineering (A. A. Avanessians, New York)

B. Maier from Engr. to Group Ldr., Overseas Telex Projects (R. Shaver, New York)

M. Rosenthal from Mgr., Engineering Services, to Mgr., Administration and Planning (P. Schneider, New York)

S. Schadoff from Mgr., Commercial Leased Channels to Dir., Commercial Leased Channels Engineering (V. Arbogast, New York)

L. J. Wilson from Mgr, Computer Systems to Dir., Computer Systems (P. Schneider, New York)

M. ChaFong from Mgr., Message Switching Engineering to Mgr., Computer Engineering (L. J. Wilson, New York)

Dr. Armand DilPare from Mgr., Launch Vehicle and Mission Reports to Mgr., Launch Vehicle (J. Christopher, New York)

C. Lundstedt from Mgr., Earth Station and Data Subsystems to Mgr., TTC and Mis-

sion Operations (J. Christopher, New York)

Jack L. Ray from Mgr., Data Networks to Mgr., Applications Engineering (A. W. Brook, New York)

A. A. Avanessians from Dir., Computer Engineering Projects to Dir., Advanced Switching Projects (P. Schneider, New York)

L. Correard from Mgr., Computer Switching Engineering to Mgr., Advanced Telex Engineering (A. A. Avanessians, New York)

J. Cuddihy from Mgr., Satellite Engrg. to Mgr., Earth Station Engrg. (J. JM. Walsh, New York)

J. Gleitman from Mgr., Computer Systems Engrg. to Mgr., Telex Switching Marketing (A. A. Avanessians, New York)

D. L. Lundgren from Mgr., Project Administration to Mgr., Program Control (A. W. Brook, New York)

L. Ottenberg from Mgr., Telecommunications Systems to Mgr., Communications Systems Engrg. (A. W. Brook, New York)

D. Mandato from Mgr., Special Equipment Engineering to Mgr., Special Equipment Design Engineering (A. A. Avanessians, New York)

J. McDonald from Mgr., Telex Engineering to Mgr., Services Engrg. (R. J. Angliss, New York)

W. W. Schaefer from Mgr., Telex Quality Control & Planning to Mgr., Traffic Engineering (R. J. Angliss, New York)

R. Shaver from Mgr., Overseas Telex Projects to Mgr., Iran TCI Project (A. A. Avanessians, New York)

Electronic Components

C. E. Doner from Sr. Eng. Prod. Dev. to Eng. Ldr. Prod. Dev. (T. E. Yingst, Lancaster)

K. Wright from Engr., Mfg. to Mgr., Production Engrg. (N. Meena, Marion)

D. N. Herd from Engr., Mfg. to Mgr., Production Engrg. (N. Meena, Marion)

E. L. Batz from Ldr., Liaison Engr., Resident Engrg. to Mgr., Resident Engineering (J. M. Wright, Bloomington)

Solid State Division

R. Rhodes from Member, Tech. Staff to Ldr., Tech. Staff (E. P. Zlock, Som.)

A. Dingwall from Sr. Member, Tech. Staff to Ldr., Tech. Staff (I. H. Kalish, Som.)

RCA Alaska Communications, Inc.

E. R. Leavens from Real Estate Specialist to Mgr., Real Estate (K. J. Rourke, Anchorage)

G. V. Bartley from Mgr., Logistics Coordination to Mgr., Engineering Administration (G. P. Roberts, Anchorage)

Astro-Electronics Division

J. J. Hawley from Sr. Engr. to Mgr. Communications Systems (A. Aukstikalnis, AED, Pr.)

95

Beckmann appointed to Corporate Engineering Staff

Howard Rosenthal, Staff Vice President, Engineering, at the RCA David Sarnoff Research Center, Princeton, N.J., appointed **Gerald K. Beckmann** to the RCA Corporate Engineering Staff.

Mr. Beckmann was graduated from the Virginia Polytechnic Institute with the BS in Electrical Engineering in 1964. He has done graduate work in Engineering Management at Northeastern University. Mr. Beckmann worked for the Honeywell and the IBM Corporations prior to joining RCA. In 1973 Mr. Beckmann received Honorable Mention in the Eta Kappa Nu Outstanding Young Engineer competition. He was cited for "his notable accomplishments in computer software and his involvement in his community."

Staff announcements

President and Chief Operating Officer

Anthony L. Conrad, President and Chief Operating Officer has announced the election of **Joseph W. Curran** as Vice President of the Corporation.

New Business Programs Corporate Development

Richard W. Sonnenfeldt, Acting General Manager, Electronic Industrial Engineering Division has announced the organization as follows: **Henry Duszak,** Operations Manager; **Henry Duszak,** Acting Marketing; **John L. Ovnick,** Chief Engineer; **Robert L. Schoenbeck,** Staff Technical Advisor; **Peter A. Weston,** Director, Finance; and **James F. Wiard,** Plant Manager.

Astro-Electronics Division

Mark Sasso, Manager, Plant Operations has announced the apointment of **Leo Weinreb** as Manager, Manufacturing.

Missile and Surface Radar Division

Max Lehrer, Division Vice President and General Manager has announced the appointment of **Lewis Nelson** as Manager, Strategic Systems Department.

Government Communications and Automated Systems Division

James M. Osborne, Division Vice President and General Manager has announced the appointment of **Charles G. Arnold** as Manager, Commercial Telecommunications Systems and announces the organization as follows: **Philip A. Gehman,** Manager, Telex Equipment and Systems; **Raymond J. Kowalski,** Manager, PABX Equipment and Systems; and **William G. Herold,** Administrator, Project Control.

Service Company

Julius Koppelman, President, RCA Service Company has announced the appointment of **George G. Ray** as Managing Director, Service Division, RCA Limited (U.K.)

Parts and Accessories

William B. Buchanan, Manager, Product Operations has announced the appointment of **Robert A. Famiglietti** as Manager, Product Handling.

Electronic Components

Richard H. Hynicka, Plant Manager, Lancaster Color, Picture Tube Plant has announced the appointment of **William J. Harrington** as Manager, Manufacturing.

Eugene D. Savoye, Manager, Electro-Optics Product Development Engineering, Industrial Tube Division, has announced the Electro-Optics Product Development organization as follows: **Thomas W. Edwards,** Manager, Material & Process Development; **Fred A. Helvy,** Manager, Product Development Engineering; **Frederick R. Hughes,** Manager, Solid State Emitters Development; and **Donal C. Reed,** Manager, Custom Product Engineering.

Robert C. Demmy, Manager, Product Engineering, Scranton Plant, has announced the organization as follows: **George T. Aschenbrenner,** Engineering Leader, Applications Lab.; **Louis J. DiMattio,** Engineering Leader, Design Lab.; and **Robert J. Murray;** Engineering Leader, Chemical & Physical Lab.

Solid State Division

Bernard V. Vonderschmitt, Vice President and General Manager has announced the organization of the Solid State Division: **Robert M. Cohen,** Director, Quality and Reliability Assurance; **Walter B. Dennen,** Manager, News and Information; **D. Joseph Donahue,** Division Vice President, Solid State International Operations; **Edward K. Garrett,** Division Vice President, Finance; **Ben A. Jacoby,** Division Vice President, Solid State Marketing; **Donald W. Ponturo,** Division Vice President, Industrial Relations; **Richard A. Santilli,** Division Vice President, Solid State Bipolar Integrated Circuits and Special Products; **Edward M. Troy,** Division Vice President, Solid State Services and Offshore Manufacturing; **Carl R. Turner,** Division Vice President, Solid State Power Devices; and **Harry Weisberg,** Division Vice President, State MOS Integrated Circuits.

D. Joseph Donahue, Division Vice President, Solid State—International Operations has announced the International Operations organization as follows: **Joseph W. Karoly,** Division Vice President, Solid State — Europe; **Robert L. Klem,** Manager, International Sales; and **Robert E. O'Brien,** Administrator, European Operations Support.

Barton   Birmingham

Barton is new TPA for Mobile Communications

Frederick A. Barton has been appointed Technical Publications Administrator for Mobile Communications Systems, Commercial Communications Systems Division, Meadowlands, Pa. In this capacity, Mr. Barton is responsible for the review and approval of technical papers; for coordinating the technical reporting program; and for promoting the preparation of papers for the RCA Engineer and other journals, both internal and external.

Mr. Barton received an HNCEE degree from the Borough Polytechnic, London, England in 1944. He served as Radar Officer with the Royal Indian Navy from 1945 to 1947. From 1948 until 1955 he was a development engineer in the Communications Department of Redifon Ltd., London. After two years with Central Rediffusion Services as a CATV Systems Engineer in the field, he rejoined Redifon Ltd. as Section Leader in charge of HF Transmitter Design. In 1960, he joined the Mobile Communications Engineering Department of RCA and has had design and management responsibility for a variety of mobile products. A Senior Engineer in the Advanced Development Department, Mr. Barton became leader of this group in April, 1974.

Birmingham is new TPA for GPSD

James T. Birmingham has been appointed Technical Publications Administrator for Government Plans and Systems Development, Camden, N.J. In this capacity, Mr. Birmingham is responsible for the review and approval of technical papers; for coordinating the technical reporting program; and for promoting the preparation of papers for the RCA Engineer and other journals, both internal and external.

Mr. Birmingham received the BS in Industrial Management from LaSalle College in 1960 and has completed specialized courses in Government Contract Administration at Harbridge House Inc. and William and Mary College. In 1962, he joined the Missile and Surface Radar Division, as an administrator on the BMEWS Program and in 1964 transferred to the Government Plans and Systems Development activity where he is presently Administrator, Engineering Administration. Mr. Birmingham, in his current assignment, is responsible for all phases of program administration.

Editorial Representatives

The Editorial Representative in your group is the one you should contact in scheduling technical papers and announcements of your professional activities

Government and Commercial Systems

Astro-Electronics Division
I. M. SEIDEMAN* Engineering, Princeton, N.J.
S. WEISBERGER Advanced Development and Research, Princeton, N.J.

Commercial Communications Systems Division
Broadcast Systems
R. N. HURST* Broadcast Systems Advanced Development, Camden, N.J.
R. E. WINN Broadcast Systems Antenna Equip. Eng., Gibbsboro, N J.
A. C. BILLIE Broadcast Engineering, Meadowlands, Pa.
Mobile Communications Systems
F. A. BARTON* Advanced Development, Meadow Lands, Pa.

Electromagnetic and Aviation Systems Division
C. S. METCHETTE* Engineering, Van Nuys, Calif.
J. McDONOUGH Aviation Equipment Engineering, Van Nuys, Calif.

Government Communications and Automated Systems Division
A. LIGUORI* Engineering, Camden, N.J.
K. E. PALM* Engineering, Burlington, Mass.

Government Engineering
M. G. PIETZ* Advanced Technology Laboratories, Camden, N.J.
J. E. FRIEDMAN Advanced Technology Laboratories, Camden, N.J.
J. L. KRAGER Central Engineering, Camden, N.J.

Government Plans and Systems Development
E. J. PODELL* Eng. Information and Communications, Camden, N.J.

Missile and Surface Radar Division
D. R. HIGGS* Engineering, Moorestown, N.J.

Palm Beach Division
B. B. BALLARD* Palm Beach Gardens, Fla.

Research and Engineering

Laboratories
C. W. SALL* Research, Princeton, N.J.
I. H. KALISH Solid State Technology Center, Somerville, N.J.
M. R. SHERMAN Solid State Technology Center, Somerville, N.J.

Electronic Components

C.A. MEYER* Chairman, Editorial Board, Harrison, N.J.

Entertainment Tube Division
J. KOFF Receiving Tube Operations, Woodbridge, N.J.
J. H. LIPSCOMBE Television Picture Tube Operations, Marion, Ind.
E. K. MADENFORD Engineering, Lancaster, Pa.

Industrial Tube Division
J. M. FORMAN Industrial Tube Operations, Lancaster, Pa.
H. J. WOLKSTEIN Solid State Product Development Engineering, Harrison, N.J

Consumer and Solid State Electronics

Solid State Division
E. M. McELWEE* Chairman, Editorial Board, Somerville, N.J.
J. E. SCHOEN Solid State Division, Somerville, N.J.
J. DiMAURO Solid State Division, Mountaintop, Pa.
S. SILVERSTEIN Power Transistors, Somerville, N.J.
H. A. UHL Integrated Circuits, Somerville, N.J.
J. D. YOUNG Solid State Division, Findlay, Ohio

Consumer Electronics
C. W. HOYT* Chairman, Editorial Board, Indianapolis, Ind.
R. BUTH Engineering, Indianapolis, Ind.
R. C. GRAHAM Audio Products Engineering. Indianapolis, Ind.
F. HOLT Advanced Development, Indianapolis, Ind.
E. E. JANSON Black and White TV Engineering, Indianapolis, Ind.
J. STARK Color TV Engineering, Indianapolis, Ind.
P. HUANG Engineering, RCA Taiwan Ltd., Taipei, Taiwan

Services

RCA Service Company
M. G. GANDER* Consumer Services Administration, Cherry Hill, N.J.
W. W. COOK Consumer Service Field Operations, Cherry Hill, N.J.
R. M. DOMBROSKY Technical Support, Cherry Hill, N.J.
R. I. COGHILL Missile Test Project, Cape Kennedy, Fla.

Parts and Accessories
C. C. REARICK* Product Development Engineering, Deptford, N.J.

RCA Global Communications, Inc.
W. S. LEIS* RCA Global Communications, Inc., New York, N.Y.
P. WEST* RCA Alaska Communications. Inc., Anchorage, Alaska

NBC, Inc.
W. A. HOWARD* Staff Eng., Technical Development, New York, N.Y.

RCA Records
M. L. WHITEHURST* Record Eng., Indianapolis, Ind.

Corporate Development
C. A. PASSAVANT* International Planning, New York, N.Y.

RCA Ltd
W. A. CHISHOLM* Research & Eng. Montreal, Canada

Patent Operations
M. S. WINTERS Patent Plans and Services, Princeton, N.J.

*Technical Publications Administrators (asterisked * above) are responsible for review and approval of papers and presentations